STUDIES OF THE ELECTROCHEMISTRY AND APPLICATIONS OF CONDUCTING POLYMERS

HUAN HUANG

INFORMATION TO USERS

This manuscript has been reproduced from the microfilm master. UMI films the text directly from the original or copy submitted. Thus, some thesis and dissertation copies are in typewriter face, while others may be from any type of computer printer.

The quality of this reproduction is dependent upon the quality of the copy submitted. Broken or indistinct print, colored or poor quality illustrations and photographs, print bleedthrough, substandard margins, and improper alignment can adversely affect reproduction.

In the unlikely event that the author did not send UMI a complete manuscript and there are missing pages, these will be noted. Also, if unauthorized copyright material had to be removed, a note will indicate the deletion.

Oversize materials (e.g., maps, drawings, charts) are reproduced by sectioning the original, beginning at the upper left-hand corner and continuing from left to right in equal sections with small overlaps. Each original is also photographed in one exposure and is included in reduced form at the back of the book.

Photographs included in the original manuscript have been reproduced xerographically in this copy. Higher quality 6" x 9" black and white photographic prints are available for any photographs or illustrations appearing in this copy for an additional charge. Contact UMI directly to order.

UMI

A Bell & Howell Information Company
300 North Zeeb Road, Ann Arbor MI 48106-1346 USA
313/761-4700 800/521-0600

Studies on the Electrochemistry and Applications of Conducting Polymers

by

Huan Huang

A thesis submitted to the School of Graduate Studies in partial fulfilment of the requirements for the degree of Master of Science

Department of Chemistry
Memorial University of Newfoundland
St. John's, Newfoundland, Canada A1B 3X7

July, 1998

ACKNOWLEDMENTS

My most sincere gratitude goes to my supervisors Dr. P. G. Pickup (Memorial University) and Dr. S. Gottesfeld (Los Alamos National Laboratory) for their guidance, advice and encouragement throughout my M. Sc. studies. I have greatly benefited and been influenced by their devout research attitude, critical judgment and boundless knowledge.

I am very grateful to Dr. F. R. Smith, who taught my courses. I would also like to thank Dr. X. Ren, Dr. S. Shi, Mr. J. Davey, and Ms. C. Emerson for their great help and fruitful collaboration. I appreciate very much the friendly help from the staff in the Chemistry Department of Memorial University of Newfoundland and the Electronic and Electrochemical Materials and Devices Group at Los Alamos National Laboratory.

Financial support in the form of a Graduate Fellowship from the School of Graduate Studies, Teaching Assistantships from the Chemistry Department, supplements from an NSERC grant, a Graduate Research Assistantship from Los Alamos National Laboratory, and the Beryl Truscott Scholarship are gratefully acknowledged.

CONTENTS

LIST OF FIGURES

LIST OF TABLES

GLOSSARY

Symbol	Meaning	Unit
A	electrode area	cm^2
An	aniline	
BTh	bithiophene	
C	concentration of charge carriers	M
C_F	capacitance of a polymer film	F
C_{max}	maximum capacitance	F
CDT	cyclopenta[2,1-*b*: 3,4-*b*']-dithiophen-4-one	
CDM	4-dicyanomethylene-4*H*-cyclopenta[2,1-*b*:3,4-*b*'] dithiophene	
CV	cyclic voltammogram	
d	film thickness	μm
D	diffusion coefficient	cm^2/s
E	potential	V
$E^{o'}$	apparent formal potential	V
E_g	band-gap	eV
$E_{intrinsic}$	intrinsic conductivity potential	V
E_{min}	minimum conductivity potential	V
E_{pa}	anodic peak potential	V
E_{pc}	cathodic peak potential	V
$\Delta E_{Pt\text{-}Au}$	Potential difference between the polymer coated Pt electrode and the overlying gold film	mV
EDOT	3, 4-ethylenedioxythiophene	
f	frequency	Hz
F	Faraday constant	96485 C/mol
HOMO	the highest occupied molecular orbital	
i or I	current	A
i_{pa}	anodic peak current	A
i_{pc}	cathodic peak current	A
ITN	isothianaphthene	
ITO	indium tin oxide coated glass electrode	
k	Boltzmann constant	1.38×10^{-23} J/K

LUMO	the lowest unoccupied molecular orbital	
MTh	methylthiophene	
n	the number of electrons	
N	conjugation length	
PA	polyacetylene	
PFPT	3-(p-fluorophenyl)thiophene	
Py	pyrrole	
Q	charge	C
RC	time constant for a capacitor	s
R_E	electronic resistance	Ω
R_I	ionic resistance	Ω
R_S	solution resistance	Ω
R_Σ	sum of R_E and R_I	
R_∞	resistance intercept at high frequency on real axis minus R_s	
SCE	Saturated potassium chloride calomel electrode	
SEM	scanning electron microscope	
t	time	s
T	absolute temperature	K
Th	thiophene	
TTh	terthiophene	
UV-Vis-NIR	ultraviolet, visible, and near infrared	
v	scan rate	mV/s
Z'	real impedance	Ω
Z"	imaginary impedance	Ω
σ	conductivity	$S\ cm^{-1}$
σ_E	electronic conductivity	$S\ cm^{-1}$
σ_I	ionic conductivity	$S\ cm^{-1}$
$\sigma_{intrinsic}$	intrinsic conductivity	$S\ cm^{-1}$
τ	experimental time scale	s
λ	absorption wavelength	nm
μ	mobility of charge carriers	

Chapter 1

Band-Gaps and Conductivities of Polythiophene-Based Conducting Polymers

1.1 Introduction

Polymers and metals are two of the four most important solid materials (the other two are semiconductors and ceramics). Most polymers are excellent electrical insulators (conductivity < 10^{-10} S cm^{-1}), whereas metals show good conductivity (e.g. the conductivity of copper is ca. 10^{5} S cm^{-1}). It is desirable to achieve materials having a combination of the high conductivity of metals and the processability, corrosion resistance and low density of polymers, that is, conducting polymers or synthetic metals. A breakthrough in the development of conducting polymers came in 1977, when MacDiarmid and Heeger discovered the fact that doping of polyacetylene (PA) with Lewis acids or bases led to a dramatic increase in conductivity of over 10 orders of magnitude [1, 2], endowing the polymer with metallic properties. The PA polymer was synthesized according to the Shirakawa method [3, 4]. Another important step followed in 1979 when it was shown that highly conducting films of polypyrrole (poly-Py) could be produced by oxidative

electrochemical polymerization of pyrrole [5]. These pioneering works stimulated rapid discoveries and extensive studies of various conducting polymers, such as poly-Pys [6-10], polythiophenes (poly-Ths) [11-13], polyanilines (poly-Ans) [14-16], and other polymers [16-18].

In the meantime, a large amount of work has been directed towards finding applications of conducting polymers in a wide range of fields covering battery materials [19-21], electrochromic displays [22, 23], antistatic coatings [24, 25], electrocatalysts [26], sensor technology [27-29], separation membranes [30], and molecular electronics [31-33]. However, few conducting polymers have yet seen wide commercial success. The reason for this is that most of these materials are either environmentally unstable or not sufficiently processable. In addition, the conductivity of these materials is orders of magnitude lower than metals. To overcome these disadvantages of the present conducting polymers, a key approach suddenly co-emerged among researchers in recent years: conducting polymers with low band-gaps may be an optimization.

First of all, reduction of the band-gap (E_g) will favour the thermal excitation of charge carriers to the conduction band in the neutral state of the conducting polymer, and thus increase the intrinsic electrical conductivity. In the long term, it may lead to true organic metals or even superconductors without the necessity of oxidative (p-) or reductive (n-) doping. Secondly, the lower p-doping potential and less negative n-doping potential associated with narrow gaps is likely to stabilize the corresponding doped state. In addition, the low or zero doping level required for low band-gap conducting polymers will maintain

their processibility. Moreover, the red shift of the absorption and emission spectra resulting from a decrease of E_g will make available conducting polymers transparent in the visible spectral range and potentially useful for the fabrication of LEDs operating in the IR.

Among the numerous conducting polymers, poly-Th has most often been chosen as the model system for the synthesis and design of small band-gap conducting polymers [34], due to its high environmental stability and structural versatility [35]. This introduction, therefore, will focus on poly-Th based low band-gap conducting polymers.

1.2 Background

The electrical properties of a material are determined largely by its electronic structure. Classical band theory for solid state materials is modified and adjusted to explain the electronic structure of conducting polymers [36-38]. The band structures of a monomer and its polymer in different states of doping are shown in **Fig. 1.1** [39]. Corresponding to the states illustrated in **Fig. 1.1**, the structure of thiophene (Th, structure **1**) and its polymer are shown in **Fig. 1.2**.

Polymerization of a monomer to form a polymer causes the highest occupied molecular orbital (HOMO) and the lowest unoccupied molecular orbital (LUMO) to split, forming two separated energy bands called the valence band and conduction band, respectively. The energy difference between the two bands is termed the band-gap (E_g).

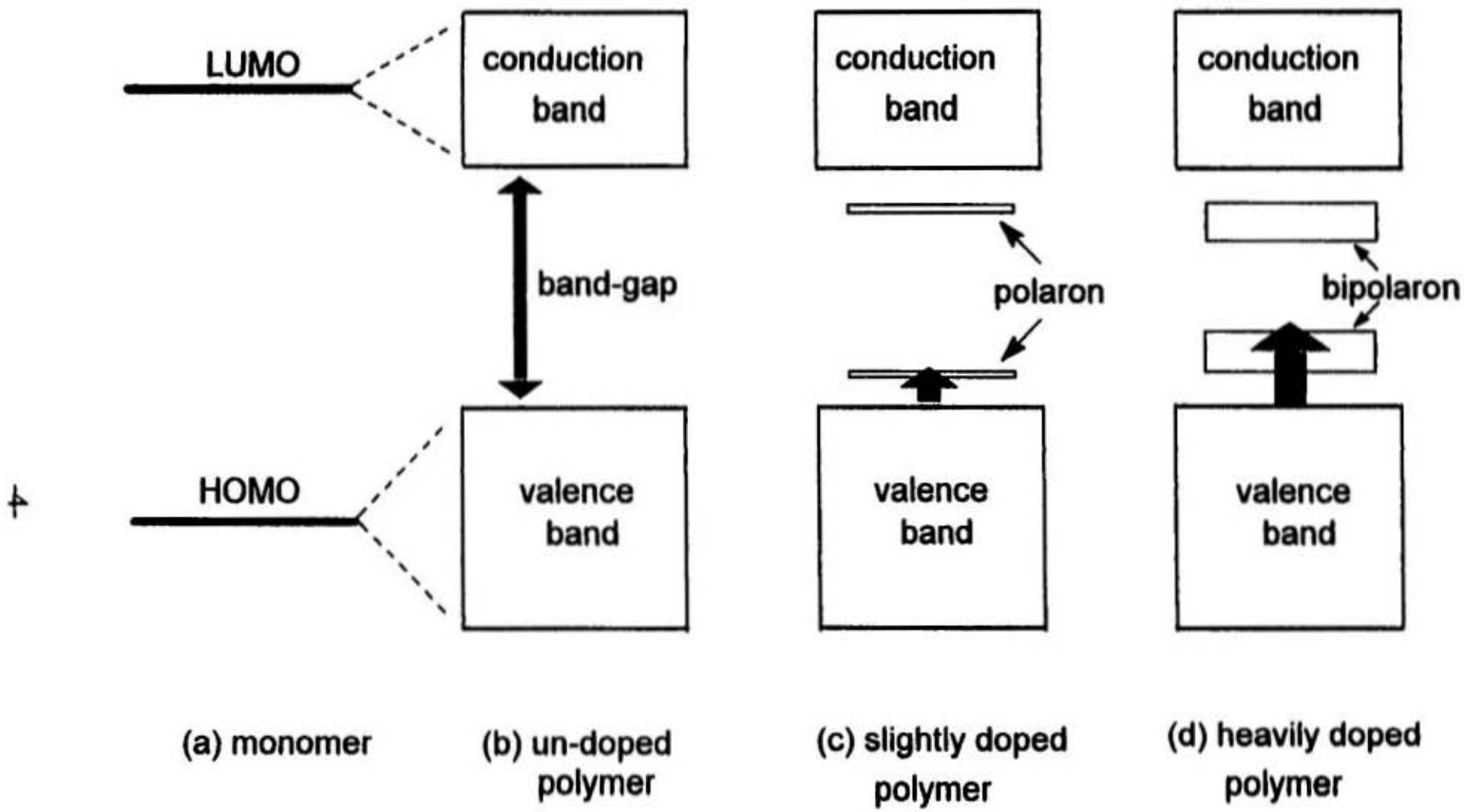

Fig 1.1 Schematic diagram of the evolution of the band structure of a conjugated polymer

Structure 1

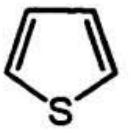

(a) thiophene

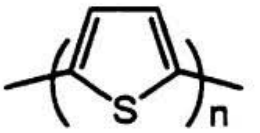

(b) polythiophene

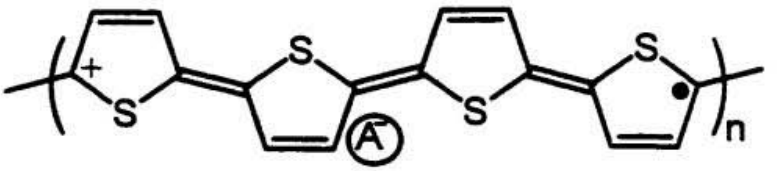

(c) polaron in polythiophene

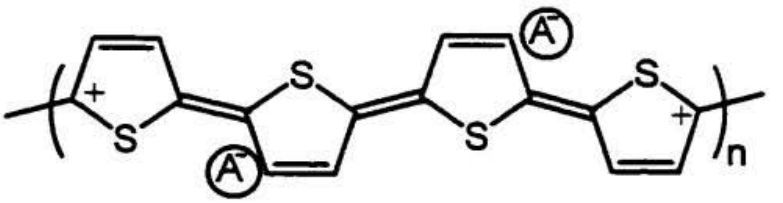

(d) bipolaron in polythiophene

Fig. 1.2 The structure of thiophene and polythiophene in neutral, partially-doped, and highly-doped states

Table 1.1 lists the band-gaps and the highest conductivities reported to date of some of the most studied conducting polymers. Typically, band-gaps are greater than 1.4 eV, which results in no significant intrinsic conductivity.

Table 1.1 Band-gaps and the maximum p-doping conductivities reported for some common conducting polymers

Polymer	Band-gap /eV	P-doping conductivity /S cm^{-1}
Trans-polyacetelyene	1.4 [40]	2×10^{5} [41]
Polypyrrole	3.2 [42]	2-3 $\times10^{3}$ [43, 44]
Polythiophene	2.1 [45]	2000 [46]
Polyaniline		760 [47]
Polyparaphenylene	3.4 [48]	500 [49]

When a conjugated polymer is oxidized (p-doped), electrons are removed from the valence band and vacancies, that is, radical cations in this case, are created. The radical cation is partially delocalized over several structural units and is called the polaron. Further oxidation of the polymer causes polarons in the same chain to combine to produce bipolarons. When a great many bipolarons are formed (highly p-doped), their energy states overlap at the edges, which creates narrow bipolaron bands in the gap. Similar states are formed when the polymer is reduced (n-doped), but the energy levels are below the conduction band [50]. Both polarons and bipolarons are mobile and can move along the polymer chain in an electric field, and thus conduct electrical current.

1.3 Polythiophene, Polybithiophene and Polyterthiophene

Studies of polythiophene (poly-Th) as a new generation of conducting polymers started in the early 1980s [51-53]. The emphasis of early work (before 1990) on this polymer was to achieve high electrical conductivity by extending the effective conjugation length [54-55] (that is, increasing α-α' linkage and reducing α-β' linkage defects), minimizing defects caused by overoxidation [56], and improving the morphology [57]. This objective was essentially pursued through the optimization of the electrochemical synthesis [58-60]. Effects of the electrolyte [61], the solvent [62-64], concentration of precursors [65], temperature [61], and the electrode materials [66, 67] have been taken into consideration. Various electrochemical synthesis techniques, such as constant potential [62, 68], constant current [69, 70], cyclic potential sweep [71] and current pulses [60, 72] have been employed to synthesize poly-Th. A systematic analysis in a review by Roncali [35] concluded that:

i. The electrolyte strongly affects the morphology and electrochemical properties of poly-Th films. PF_6^-, BF_4^-, ClO_4^-, and AsF_6^- are generally used to obtain smooth and compact polymers, while HSO_4^- and SO_4^{2-} lead to poorly conducting films [73].

ii. The solvent must have a high dielectric constant to ensure the ionic conductivity of the electrolytic medium. The presence of trace water in the solvent has deleterious consequences for the electropolymerization and hence for the conjugation length and conductivity of the polymer [74].

iii. Polymers prepared at lower temperature have a longer mean conjugation length than those prepared at higher temperature [61].

iv. Platinum, gold, tin oxide or indium-tin oxide (ITO) coated glass, titanium and iron have been used as the electrode materials to deposit poly-Ths [66, 67]. The most conductive polymers have been obtained on bulk platinum electrodes.

v. Decreasing the monomer concentration improves the conductivity of poly-Th [65]. However, at too low concentration (< 20 mM) [56], poly-Th films are difficult to deposit because the polymerization efficiency deceases significantly.

vi. The applied electrical conditions exert considerable effects on the morphology and properties of electrogenerated poly-Ths. The most homogeneous and conducting films are generally obtained under galvanostatic conditions [70, 75].

vii. Electrocatalytic polymerization of thiophene in the presence of bithiophene or terthiophene can reduce overoxidation, and hence increase the conductivity and conjugation length [76].

Under the optimum synthesis conditions, poly-Th films can be prepared with enhanced effective conjugation, with band-gaps reduced from 2.2 to 1.9 eV [73, 77] and conductivities reaching 2000 S cm^{-1} [75].

Besides the optimization of the electropolymerization conditions, thiophene oligomers, in particular, 2, 2'-bithiophene (BTh, structure **2**) and 2, 2': 5', 2"-terthiophene (TTh, structure **3**) [78-82], have been proposed as another approach to control the structure and properties of poly-Ths. Owing to their lower oxidation potentials [83, 84],

electropolymerization can be performed under milder conditions, eliminating overoxidation of the polymer [79] and furthermore, since the thiophene rings are exclusively α-α' linked in the starting molecule, one could expect the resulting polymer to contain less α-β' defects than the polymer prepared from the monomer [85].

Structure 2

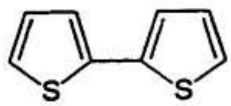

2, 2'-bithiophene

Structure 3

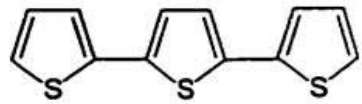

2, 2': 5', 2"-terthiophene

Despite the diversity of electrosynthesis conditions, consistent results have been obtained, showing that the resulting polymers differ markedly from that prepared with the monomer. As a matter of fact, poly-BTh and poly-TTh are generally obtained as powdery deposits with conductivities inferior by several orders of magnitude to that of poly-Th. Thus, the conductivity of poly-BTh reaches at best a few S cm^{-1}, while that of poly-TTh lies generally in the range of 10^{-2} S cm^{-1} [78, 80, 86, 87]. A comparative study of the electrochemical and spectroscopic properties of poly-Th, poly-BTh, and poly-TTh [78], has shown that increasing the length of the starting molecule leads to an increase of the oxidation potential and to blue shift of the absorption maximum of the resulting polymer. These results show that the lower conductivities of poly-BTh and poly-TTh are correlated to a decrease of the average length of the conjugated system in the polymer [88, 89]. This limited

conjugation can be explained by considering the changes in the reactivity of the substrate resulting from the delocalization of the π electrons over the entire molecule. On one hand, the overall reactivity of the substrate decreases or, in other words, the stability of the corresponding radical cation increases, which causes a decrease or even in some cases a complete loss of polymerizability. This conclusion is consistent with the limited electropolymerization of TTh [78], as shown by the fact that poly-TTh contains large amounts of unreacted TTh and of the compound resulting from a single coupling, e.g. sexithiophene [45, 78]. On the other hand and as already discussed, the conjugated structure of oligomers results in a decrease of the relative reactivity of the positions which has deleterious consequences for the stereoselectivity of the polymerization.

In summary, the electropolymerization of the monomer and oligomers does not lead to the same polymer. Contrary to what could be expected [85, 86], the use of a more conjugated precursor for electropolymerization yields finally a less conjugated and less conducting polymer. The thiophene monomer remains the most appropriate for efficient electrosynthesis of extensively conjugated and highly conducting poly-Ths.

1.4 Low band-gap conducting polymers

In order to achieve polymers with narrow band-gaps, we need to increase the energy level of the valence band, decrease the energy level of the conduction band, or both. Several

methods [34, 90-93] to realize this goal have been developed. They are summarized below as three approaches:

Approach **1**: increasing the quinoid character in the ground state of a conjugated polymer [90]

Approach **2**: building a polymeric chain with alternating donor (aromatic character) and acceptor (quinoid character) moieties [91, 92]

Approach **3**: introducing electron-withdrawing groups at a carbon bridging the β and β' positions of bithienyl precursors [93]

Following these ideas, a significant number of conducting polymers with band-gaps lower than 1.0 eV have been successfully synthesized [34]. The following will focus on the polymers obtained through these three approaches, which include structural modification of the thiophene unit and have proved effective to reduce the band-gap.

1.4.1 Low band-gap conducting polymers with increased quinoid character

a. Poly(isothianaphthene)

Among the low band-gap conducting polymers derived from approach **1** (as mentioned above), poly(benzo[*c*]thiophene) (also called poly(isothianaphthene) (poly-ITN), structure poly- **4**) [94] is the first example of a low band-gap conducting polymer. It has been viewed as the prototype of this approach, drawing extensive studies both from experimental and theoretical perspectives on its synthesis, properties and structure [95-97].

Structure 4

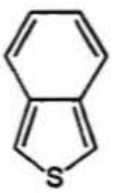

benzo[c]thiophene

Poly-ITN films were first successfully synthesized by Wudl and coworkers in 1984 [94]. Their choice of ITN was based on the idea that the limiting resonance form **d** (see **Fig. 1.3**) could be expected to be important and hence would contribute to stabilizing the quinoid form of the polymer. It was initially found that the electropolymerization of ITN was strongly electrolyte dependent. The use of non-nucleophilic anions, such as ClO_4^- or BF_4^-, commonly employed for the electrodeposition of poly-Ths, produced poly(dihydro-isothianaphthene) as a white precipitate [94]. While nucleophilic anions, e.g. Br^- and Cl^- led to formation of poly-INT [94, 98]. Later work has shown that satisfactory results can be obtained by the application of repetitive potential scans to solutions containing classical electrolytes such as Et_4NBF_4 or Bu_4NPF_6 in acetonitrile [99-101]. More recently, electropolymerization of bis(tri-butyldimethylsilyl)isothinanaphthene ((BTBDMS)ITN) instead of ITN was proposed [102]. This method has the advantage that (BTBDMS)ITN is a stable monomer under ambient conditions whereas ITN is unstable and must be prepared immediately prior to the polymerization.

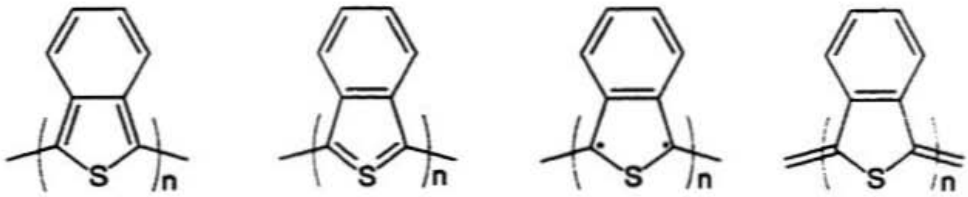

a b c d

Fig. 1.3 Four resonance structures of poly-ITN suggested by Wudl et al. [94]

Poly-ITN has also been prepared by means of chemical synthesis. Oxidation of the dihydro-derivative with atmospheric oxygen, $FeCl_3$ [103], sulfuric chloride [104], or N-chlorosuccinimide [105], leads directly to the doped conducting polymer. It has also been reported that poly-ITN could be directly obtained from phthalic anhydride or phthalide by reaction with P_4S_{10} [106].

Electrochemical studies of poly-ITN show the p-doping peak at ca. 0.5 V vs. SCE and n-doping peak at ca. -1.1 V giving an electrochemical band-gap of 1.0-1.2 V [100]. A conductivity of 50 S cm^{-1} has been reached for the iodine-doped polymer [107]. The UV-Vis-NIR absorption spectrum of the neutral poly-INT shows a peak at ca. 800 nm due to the interband excitation, and absorption onset at ca. 1200 nm, from which the band-gap is evaluated to be ca. 1.0 eV, consistent with the value of the electrochemical gap. This band-gap value is ca. 1.0 eV lower than poly-Th [108]. The undoped poly-INT film is blue in color, while the polymer in both the p-doping and n-doping states is colorless and transparent. Thus, application to electrochromic displays has been suggested.

Theoretical attention to poly-ITN has focused on band-gap structure calculations [109-112]. In the early stage, it was suggested that poly-ITN should have an aromatic structure (**Fig. 1.3 (a)**) in the electronic ground state for which a gap value of 0.54 eV [113] was calculated. Later work, however, concluded that a quinoid structure (**Fig. 1. 3 (d)**) is the ground state for the polymer with a calculated band-gap of 1.16 eV [109, 112]. This band-gap value is consistent with the experiment result [108]. From a comparative *in situ* Raman spectroscopic study of poly-ITN film in various oxidation states, it was concluded that the quinoid form was the ground state. This result is in agreement with NMR studies [113, 114].

b. Poly(isothianaphthene) derivatives

In order to achieve further reduction of the band-gap, a significant work has been devoted to the synthesis of substituted analogs of ITN.

Poly(5, 6-(methylenedioxy)isothianaphthene) (poly-DOMITN, structure poly-**5**) was one of the first derivatives of poly-ITN [115]. While the cyclic voltammogram of the monomer (DOMITN) revealed a significant decrease in the oxidation potential from ca. 1.4 V vs. Ag/Ag^+ for ITN to ca. 0.65 V, due to the electron-donating effect of the methylenedioxy substituent. This effect was not observed in cyclic voltammograms of the polymer which, in contrast, showed an oxidation potential slightly higher than poly-ITN. The band-gap of poly-DOMINT was comparable to that of poly-ITN, but the conductivity of both the chemically and electrochemically prepared polymers ($3\text{-}6\times10^{-2}$ S cm^{-1}) was considerably lower than that of poly-ITN (50 S cm^{-1}) [115].

Structure 5

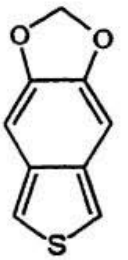

5,6-(methylenedioxy)isothianaphthene

Halogen substitution on the phenyl ring [116-119] causes positive shifts for the potentials of both p-doping and n-doping. The shift of p-doping potential is not as significant as that of the n-doping potential, e.g. the onset potential for n-doping shifted from -1.1 V vs. SCE for ITN to -0.35 V for the dichloro derivative, while the peak for p-doping, shifted from ca. 0.5 V for ITN to ca. 0.8 V for the dichloro derivative, respectively [116]. The dichloro derivative has an electrochemical gap of ca. 0.8 V [119]. Full substitution by fluorine produces a considerable increase of the band-gap from 1.10 to 2.10 eV, which has been attributed to both electronic and steric effects [118].

Several poly-INT derivatives with alkyl chains on the phenyl ring have been prepared [120]. Polymers of this class are soluble in common organic solvents. Poly(5-decylisothianaphthene) in solution showed a λ_{max} at 512 nm, while a solution-cast film exhibited an optical band-gap of 1.0-1.3 eV [121]. 5-methylisothianaphthene was reported to electropolymerize at a lower potential than unsubstituted ITN, however, the polymer oxidized at a higher potential than poly-ITN [116], similar to DOMINT mentioned above.

c. Poly(thieno[3,4-*b*]pyrazine)

Poly(thieno[3,4-*b*]pyrazine) (poly-TP, structure poly-**6**) is another representative conducting polymer of approach **1**. This polymer was designed on the basis of theoretical calculations predicting a band-gap smaller than that of poly-ITN (0.70 eV vs 0.80 eV) [122]. Furthermore, reduced steric interaction between adjacent monomer units was also expected. The monomer, 2,3-dihexylthieno[3,4-*b*]pyrazine, was chemically polymerized by $FeCl_3$. The undoped polymer was dissolved in chloroform. The electronic spectrum showed an absorption maximum at 915 nm for a solution cast film with a band-gap of 0.95 eV. Films cast after doping with $NOBF_4$ in solution exhibited a maximum four-probe conductivity of 3.6×10^{-2} S cm^{-1} [123]. More recently, other polymers derived from poly-TP with various alkyl chains have been investigated by Raman spectroscopy, and it was concluded that the polymer has a quinoid ground-state geometry in the neutral state and an aromatic one in the doped state [118].

Structure 6

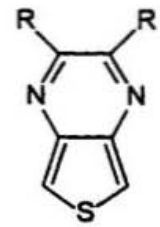

Thieno[3,4-*b*]pyrazine

1.4.2 Low band-gap conducting polymers with alternating donor or acceptor moieties along the chain

As soon as the idea that π-conjugated polymers with regular alternating aromatic-donors or quinoid-acceptors should present low band-gaps was proposed [91, 125, 126], several groups [127-129] almost simultaneously successfully synthesized poly(isothianaphthene-alt-bithiophene) (poly-INTBT, structure poly-7). In which the isothianaphthene unit behaves as the electron-acceptor and the two adjacent bithiophene units as the electron-donor.

Structure 7

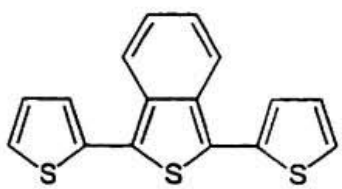

Structure 8

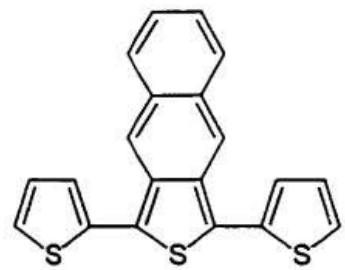

The oxidation potential of 7 occurred at 0.80 V vs. SCE [130], which was lower than that of terthiophene (1.05 V), due to the intrachain charge transfer between thiophene and isothianaphthene rings. The highest conductivity of the polymer measured by four-probe electrodes was about 10^{-2} S cm^{-1} [129], the same order of magnitude obtained for poly-TTh [72]. A UV-Vis-NIR study of the polymer in the neutral state showed the absorption onset

wavelength at ca. 730 nm, corresponding to a band-gap of 1.7 eV [127, 129], intermediate between those of poly-Th and poly-ITN. Although poly-**8** has a very similar structure to poly-7, a much lower band-gap of 0.65 eV was claimed [131]. This low value, however, was obtained at 0.0 V vs. SCE, a potential at which the polymer was still slightly doped judging from its CV.

Nonclassical thiophene units, such as thieno[3,4-*b*]pyrazine [132, 133] and thieno[3,4-*c*][1,2,5]thiadiazole [134, 135] have been used as the median rings in the trimmer instead of the isothianaphthene unit. One of the advantages of this substitution is that the steric interactions produced between the fused benzene ring and the adjacent thiophene rings in **8** are reduced [133]. When R=CH_3, compound **9** was irreversibly oxidized at 0.88 V vs. SCE, and reversibly reduced at -1.36 V [135]. Polymerization of compound **9** by repetitive potential scans led to a polymer with a band-gap of 1.40 eV. While electropolymerization of compound **10** produced a polymer with a band-gap of 0.90 eV. This small band-gap value was confirmed by its CV which showed oxidation and reduction peaks at 0.70 V and -1.10 V vs SCE with a 0.90 V difference between the threshold potentials for p-doping and n-doping [134, 135].

Structure 9

Structure 10

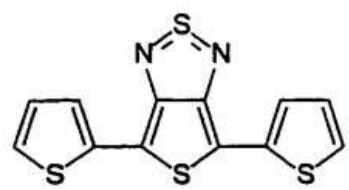

The median ring has been extended to tricyclic nonclassical thiophene systems [136, 137]. The electrogenerated polymer of compound **11** exhibited a very narrow electrochemical band-gap of ca. 0.30 V, estimated from the onset potentials for p-doping and n-doping. The absorption edge of the optical spectrum was below 0.50 eV [136]. More recently, the polymer electrosynthesized from compound **12**, which differs from **11** in the substitution of the two side thiophene rings with two pyrrole rings, produced a vanishingly small electrochemical band-gap between the p-doping and n-doping [137]. But there were no detailed studies on this ~zero band-gap polymer.

Structure 11

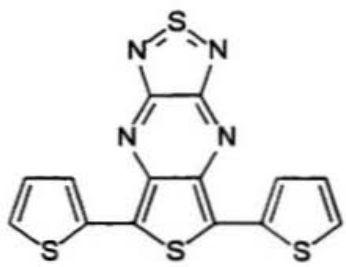

Structure 12

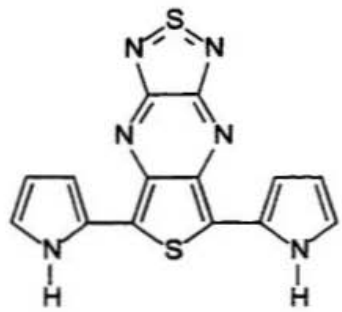

1.4.3 Low band-gap conducting polymers with electron-withdrawing groups bridging the β and β' positions

This approach was based on the idea that the effect of electron-withdrawing groups bridging the β and β' positions should decrease the aromaticity of the polymers, and hence

increase the quinoid character [34]. Following this approach, polymers electrosynthesized from cyclopenta[2, 1-*b*; 3, 4-*b*']dithiophene-4-one (CDT, structure **13**) [138, 139] and 4-dicyanomethylene-4*H*-cyclopenta[2, 1-*b*; 3, 4-*b*']dithiophene (CDM, structure **14**) [140, 141] are two representatives with band-gaps significantly reduced compared with poly-BTh. The oxidation potential of CDT was 1.26 V vs. SCE, very close to that of bithiophene [138], indicating that the carbonyl group has no significant effect on the energy level of the HOMO. The band-gap value determined by spectroelectrochemical experiments was 1.1-1.2 eV [138], in agreement with the electrochemical gap from its CV [139].

Structure 13

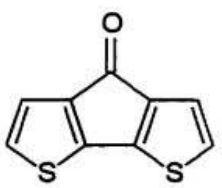

cyclopenta[2,1-*b*:3', 4'-*b*']-dithiophen-4-one

Structure 14

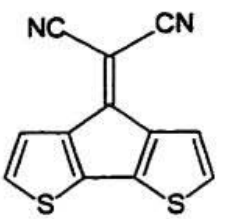

4-(dicyanomethylene)-4*H*-cyclopenta [2, 1-*b*:3, 4-*b*']dithiophene

Compared to CDT, the stronger electron-withdrawing effect of the dicyanoethene group in CDM lowers the LUMO level and leads to a decrease in band-gap confirmed by a 100 nm red shift of the longest absorption maximum [140]. This absorption band was assigned to a $\pi-\pi^*$ transition both by analogy with CDT and based on sovatochromic effects. The optical spectrum of poly-CDM is strongly reminiscent of that of poly-CDT with

the emergence of a new absorption band extending to the near IR and with a long wavelength edge at ca. 0.80 eV. The small difference observed between the onset potential for p- and n-doping was consistent with this low band-gap value [140].

With a (nonafluorobutyl)sulfonyl group substitution of one of cyano groups in CDM, similar to poly-**13** and poly-**14**, the electronic absorption spectrum of the neutral electrogenerated polymer exhibits a bathochromic extension toward the near IR region leading to an estimated band-gap of 0.67 eV [141].

1.5 *In situ* electronic conductivity measurements of conducting polymers

1.5.1 Techniques for *in situ* electronic conductivity measurement

The electronic conductivities of conducting polymers reported in the literature are mostly measured in the dry state by the two-probe or four-probe methods [142-145]. However, neither method can accurately reveal how the conductivity varies with the doping level. Thus, *in situ* conductivity measurement techniques, which can provide valuable insight into electron transport when the polymer is in the electrolyte solution wetted state under potential control, have been developed. The *in situ* techniques include two parallel band electrode voltammetry [146, 147], sandwiched dual-electrode voltammetry [148, 149], rotating disc voltammetry [150, 151] and AC impedance spectroscopy [152, 153]. They are

summarized in **Table 1.2** [39].

Table 1.2 Comparison of *in situ* conductivity measurement techniques

Technique	Conductivity measurement range/ S cm^{-1}
Two parallel band electrode voltammetry	$10^{-4} \sim 10^{2}$ [147]
Sandwiched dual-electrode voltammetry	$10^{-9} \sim 1$ [154]
Rotating disc voltammetry	$10^{-9} \sim 10^{-4}$ [150]
AC impedance spectroscopy	$10^{-7} \sim 10^{-2}$ [153]

Of these techniques, dual-electrode voltammetry can cover the largest conductivity range (from 10^{-9} to 1 S cm^{-1}). So it is perhaps the most suited technique for the measurement of conducting polymers at various states [154], that is, highly doped, lightly doped or even undoped (for low band-gap polymers). In this technique [157, 158], a small-amplitude potential difference is applied between a polymer-coated Pt electrode and a thin porous gold film deposited over the polymer film. The scanning potentials of the polymer and the gold film are controlled using a bipotentiostat. At any selected potential the polymer's electronic resistance can be obtained from the steady state current using Ohm's law. Thus the specific conductivity can be calculated if the thickness of the film is known.

The parallel band electrodes are constructed by placing an insulating spacer between two sheets of platinum foil [147]. The polymer is bridged between the two electrodes by deposition, or spin- or drop-coating. A bipotentiostat is used to control the scanning

potentials of the two electrodes with a fixed potential difference. The conductivity is calculated by comparing the resulting current with that of a standard polymethylthiophene film (= 60 S cm^{-1}) [155]. This method is well suited for the measurement of high conductivities (>10^{-4} S cm^{-1}). Conductivities obtained by this technique are, to some degree, dependent of the film thickness and the interband gap [147, 156].

Both rotating disc voltammetry and AC impedance spectroscopy have low practical conductivity measurement ranges, and thus are useful for investigating polymers having low conductivity or ones doped lightly. The main advantage of AC impedance is that it also can provide the *in situ* ionic conductivity against potential [152].

1.5.2 *In situ* conductivity of conducting polymers

The electronic conductivities of conducting polymers are known to be strongly dependent on their doping levels (oxidative (p-doping) or reductive (n-doping) states) [142, 159], and can vary over more than 10 orders of magnitude with changing potential [160, 161]. A typical *in situ* p-type conductivity against potential for a polymethylthiophene film is shown in **Fig. 1.4**, along with its cyclic voltammograms at different scan rates [162, 163].

The plot of resistance (or conductivity) against potential shows hysterisis between the anodic and cathodic scan, correlating with hysterisis in the cyclic voltammetry. In the neutral state (e.g. -0.4 V vs. Ag), the polymer is insulating with a resistance larger than 10^{10} Ω. Upon doping, the resistance decreases (or the conductivity increases) approximately

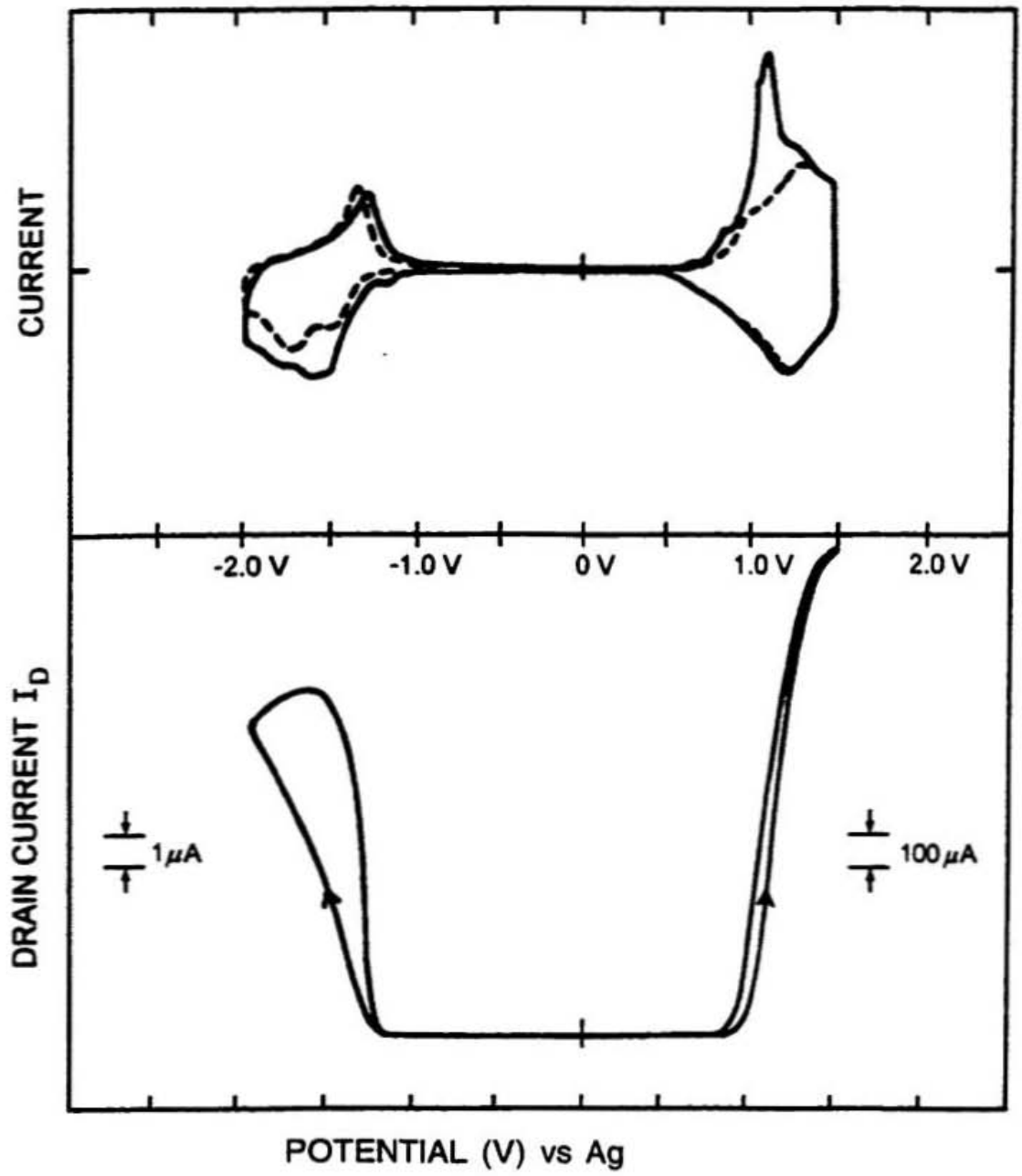

Fig. 1.4 *In situ* conductivity versus potential for a polymethylthiophene film[162]. The upper figure is the cyclic voltammograms of the film at different scan rates

exponentially with increasing potential. This is because in the lightly doped state, the electronic conductivity is proportional to the concentration of charge carriers (polarons), which increases exponentially with increasing potential. After ca. 0.2 V, the polymer reaches its maximum conductivity (resistance < 200 Ω), and exhibits a potential window with the highest conductivity from 0.2 V to 1.2 V. However, further oxidation of the polymer causes the conductivity to decline significantly (ca. 2×10^4 Ω at 1.8 V). At higher doping levels, bipolarons become the dominant charge carries [164-166]. The conduction of electrons is realized by electron hopping from bipolaron to polaron or unoxidized sites [163]. When the polymer is highly or close to fully oxidized, this type of "mixed valence" conductivity will decrease, making electron hopping difficult, and thus causing the reduction of the conductivity. Indeed, it has been shown that polyaniline has a maximum conductivity when it is oxidized to an extent of approximate 0.5 electron per aniline repeat unit, and becomes insulating when it is oxidized to about 1.0 electron per repeat unit [167].

There are reports on the electrochemical reduction (the n-doping) of poly-Ths [34], but the n-type conductivity has been studied much less than the p-type conductivity, because of the poor stability of most conducting polymers under n-doped condition, thus making the in situ conductivity measurement irreproducible. Until now, only n-doping conductivities of polymethylthiophene [168] and polydithienylvinylene [169] have been reported. The two polymers showed similar *in situ* conductivity behavior with potential. For the lightly doped polymers, the conductivity increases exponentially with potential scan cathodically. The n-doped type showed a much narrower window of high conductivity than the p-doped type,

and the maximum conductivity was about 100 times lower. These results suggest that the conduction band of the polymer (filled during n-doping) is narrower than its valence band (emptied during p-doping) [39], or the lower conductivity is attributed to the effect of the larger counterion inserted into the film [169]. For most low band-gap poly-Ths, the n-doping potential region shifts considerably anodically, making the n-doping state reasonably stable. Therefore, the measurement of n-type conductivities for the low band-gap polymers should be relatively easily carried out. However, there are lack of these data till now.

1.6 Scope of this thesis

Although a significant number of conducting polymers with band-gap lower than 1.0 eV are now known [34], there is lack of detailed characterization of these materials. Especially lacking is data on one of their most important properties, their conductivities, including their *in situ* conductivities and intrinsic conductivities. Therefore, the purpose of this work is to characterize known and novel low band-gap conducting polymers, and measure their *in situ* and intrinsic conductivities. It includes:

1. UV-visible spectroscopy and cyclic voltammetry of thiophene-based precursors, such as thiophene (Th), bithiophene(BTh), terthiophene(TTh), dicyano-methylene-cyclopenta-bithiophene (CDM), and ethylenedioxythiophene (EDOT). Correlation of experimental results with theoretical HOMO and LUMO energies.

2. Electrochemical polymerization of Th, BTh, TTh, CDM and EDOT. Characterization of their p- and n-doping properties by cyclic voltammetry, UV-Vis-NIR spectroelectrochemistry, and *in situ* conductivity measurements.

3. Copolymerization of EDOT with CDM. Characterization of p- and n-doping properties of the copolymer by cyclic voltammetry, impedance spectroscopy, UV-visible spectroelectrochemistry, and *in situ* conductivity measurements.

REFERENCES

[1] H. Shirakawa, E. J. Louis, A. G. MacDiarmid, C. K. Chiang, and A. J. Heeger, *J. Chem. Soc., Chem. Commun.*, 578 (1977)

[2] C. K. Chiang, Y. W. Park, A. J. Heeger, H. Shirakawa, E. J. Louis, and A. G. MacDiarmid, *J. Chem. Phys.*, **69**, 5098 (1978)

[3] H. Shirakawa and S. Ikeda, *Polym. J.*, **2**, 231 (1971)

[4] H. Shirakawa and S. Ikeda, *J. Polym. Sci. Chem.*, **12**, 929 (1974)

[5] A. F. Diaz, K. K. Kanazawa, and G. P. Gardini, *J. Chem. Soc., Chem. Commun.*, 635 (1979)

[6] S. Asavapiriyanout, G. K. Chandler, G. A. Gunawardena, and D. Pletcher, *J Electroanal. Chem.*, **177**, 229 (1984)

[7] R. E. Noffle and D. Pletcher, *J. Electroanal. Chem.*, **227**, 229 (1987)

[8] Z. Cai and C. R. Martin, *J. Am. Chem. Soc.*, ***111***, 4138 (1989)

[9] S. Kuwabata, S. Ito, and H. Yoneyama, *J. Electrochem. Soc.*, **135**, 1691 (1988)

[10] K. Uosaki, K. Okazaki, and Kita H., *J. Polym. Sci., Polym, Commun.*, **28**, 399 (1990)

[11] A. F. Diaz, *Chem. Scr.*, **17**, 142 (1981)

[12] G. Tourillon and F. J. Garnier, *J. Electroanal. Chem.*, **135**, 173 (1982)

[13] A. O. Patial, A. J. Heeger, and F. Wudl, *Chem. Rev.*, **88**, 183 (1988)

[14] A. F. Diaz and J. A. Logan, *J. Electroanal. Chem.*, **111**, 111 (1980)

[15] A. G. McDiarmid, J. C. Chiang, M. Halpern, H. S. Huang, S. L. Mu, N. L. D. Somasiri, W. Wu, and S. I. Yaniger, *Mol. Cryst. Liq. Cryst.*, **121**, 173 (1985)

[16] A. F. Diaz, J. F. Rubinson, and H. B. Mark Jr., *Adv. Polym. Soc.*, **84**, 113 (1988)

[17] M. Delamar, P. C. Lacaze, J. Y. Dumousseau, and J. E. Dubois, *Electrochim. Acta*, **27**, 61 (1982)

[18] J. Bargon, S. Mohamand, and R. J. Walman, *IBM J. Res. Develop.*, **27**, 330 (1983)

[19] M. Armand, J. Y. Sanchez, M. Gauthier, and Y. Choquette, *Polymeric Materials for Lithium Batteries*. In: *Electrochemistry of Novel Materials*. (Eds: J. Lipkowski and P. N. Ross) VCH, New York, 65 (1994)

[20] M. Kaneko and D. Wohrle, *Adv. Polym. Sci.*, **84**, 141 (1988)

[21] C. Arbizzani, M. Mastragostino, L. Meneghello, and R. Paraventi, *Adv. Mater.*, **8(4)**, 331 (1996)

[22] J. H. Burroughes, D. D. C. Bradey, A. R. Brown, R. N. Marks, K. Mackay, R. H. Friend, P. L. Burn, and A. B. Holmes, *Nature*, **347**,539 (1990)

[23] F. Corce, S. Panero, S. Passerini, and B. Scrosati, *Electrochim. Acta*, **39(2)**, 255 (1994)

[24] D. W. DeBerry, *J Electrochem. Soc.*, **132**, 1022 (1985)

[25] German Patent P 37 29 556.7, Zipperling Kessler & Co., 1987

[26] A. Deronzier and J. C. Moutet, *Acc. Chem. Res.*, **22**, 249 (1989)

[27] R. W. Murray, A. G. Ewing, and R. A. Durst, *Anal. Chem.*, **59**, 379A (1987)

[28] P. Vadgama and P. W. Crump, *Analyst*, **117(11)**, 1657 (1992)

[29] G. Zotti, *Synth. Met.*, **51(1-3)**, 373 (1992)

[30] K. Doblhofer and M. Vorotyntsev, *The membrane properties of electroactive polymer , films* In: *Electroactive polymer electrochemistry, Part 1: Fundamentals* (Ed: M. E. G. Lyons) Plenum Press, New York, 375 (1994)

[31] C. E. D. Chidsey and R. W. Murray, *Science*, **231**, 25 (1986)

[32] L. R. Dalton, L. S. Sapochak, and L. P. Yu, *J. Phys. Chem.*, **97(2)**, 2871 (1993)

[33] J. L. Bredas, *Science*, **263**, 487 (1994)

[34] J. Roncali, *Chem. Rev.*, **97**, 173 (1997)

[35] J. Roncali, *Chem. Rev.*, **92**, 711 (1992)

[36] J. H. Kaufman, N. Colameri, C. Scott, and G. B. Street, *Phys. Rev. Let.*, **53(10)**, 1005 (1984)

[37] R. L. Greene and G. B. Street, *Science*, **226**, 651 (1984)

[38] J. L. Bredas, *Electronic structure of highly conducting polymers*, in: *Handbook of conducting polymers*. Vol. 2. (Ed: T. A. Skotheim) Marcel Dekker, New York, 859(1986)

[39] P. G. Pickup, *Electrochemistry of Electronically Conducting Polymer Films*, in: *Modern Aspects of Electrochemistry* , 1998

[40] C. R. Fincher, D. L. Peebles, A. J. Heeger, M. A. Druy, Y. Matsumura, and A. G. McDiarmid , *Solid State Commun.*, **27**, 489 (1978)

[41] N. Basescu, Z. X. Liu, D. Moses, A. J. Heeger, H. Naarman, and J. Teophilou, *Nature*, **327**, 403 (1987)

[42] G. B. Street, T. C. Clark, M. Krounbi, K. Kanazawa, V. Lec, P. Pfluger, J. C. Scott, and S. Weiser, *Mol. Cryst. Li. Cryst.*, **83**, 253 (1982)

[43] Z. Cai and C. R. Martin, *J. Am. Chem. Soc.*, **111**, 4138 (1989)

[44] W. Cahalane and M. M. Labes, *Chem. Mater.*, **1**, 519 (1989)

[45] M. Kobayashi, N. Colaneri, M. Boysel, F. Wdul, and A. J. Heeger, *J. Chem. Phys.*, **82**, 5717 (1985)

[46] J. Roncali, A. Yassar, and F. Garnier, *J. Chem. Soc., Chem. Commun.*, 581 (1988)

[47] A. F. Diaz and J. A. Logan, *J. Electroanal. Chem., Interfacial Electrochem.* **111**, 111 (1980)

[48] D. M. Ivory, G. G. Miller, J. M. Sowa, L. W. Shacklette, R. R. Chance, and R. H. Baghman, *J. Chem. Phys.*, **71**, 1506 (1979)

[49] R. H. Baughmann, *Contemporary Topics in Polymer Science*, Vol. 5, Plenum, New York, 1984,

[50] J. L. Bredas, B. Themans, J. G. Fripiat, and R. R. Chance, *Phys. Rev.*, **B29** (1984)

[51] A. F. Diaz, J. Crowley, J. Bargon, G. P. Gardini, and J. B. Torrance, *J. Electroanal. Chem.* **121**, 355 (1981)

[52] G. Tourillon and F. Garnier, *J. Electroanal. Chem.* **135**, 173 (1982)

[53] K. Kaneto, K. Yoshina, and Y. Inuishi, *Jpn. J. Appl. Phys.*, **21**, L567 (1982)

[54] J.Roncali, M. Lemaire, R. Garreau, and F. Garnier, *Synth. Met.* **18**, 139 (1987)

[55] Y. Furukawa, M. Akimoto, and I. Harada, *Synth. Met.*, **18**, 189 (1987)

[56] D. Krische, M. Zagorska, Synth. Met., **28**, C263 (1989)

[57] B. Krische and M. Zagorska, *Synth. Met.*, **33**, 257 (1989)

[58] M. Sato, S. Tanaka, and K. Kaeriyama, *Synth. Met.*, **14**, 279 (1986)

[59] S. Hotta, *Synth. Met.*, **22**, 103 (1988)

[60] J. Roncali, A. Yassar, and F. Garnier., *J. Chem. Soc., Chem. Commun.*, 581 (1988)

[61] K. Imanishi, M. Satoh. Y. Yasuda, R. Tsushima, and S. Aoki, *J. Electroanal. Chem.* **260**, 469 (1989)

[62] R. J. Waltman, J. Bargon, and A. F. Diaz, *J. Phys. Chem.*, **87**, 1459 (1983)

[63] M. Sato, S. Tanaka, and K. Kaeriyama, *J. Chem. Soc., Chem. Commun*, 713 (1985)

[64] S. Horra, T. Hosaka, and W. Shimotsuma, *Synth. Met.*, **6**, 69 (1983)

[65] J. Roncali and F. Garnier, *New J. Chem.*, **4-5**, 237 (1986)

[66] Z. Deng, W. H. Shichiri, and H. S. White, *J. Electrochem. Soc.*, **136**, 2152 (1989)

[67] S. Aeiyach, A. Kone. M. Dieng, J. J. Aaron, and P. C. Lacaze. *J. Chem. Soc., Chem. Commun.*, 822 (1992)

[68] G. Tourillon and F. Garnier, *J. Phys. Chem.*, **87**, 2289, 1983

[69] S. Tanaka, M. Sato, and K. Kaeriyama, *Makromol. Chem.*, **185**, 1295 (1984)

[70] J. Roncali, A. Yassar, and F. Garnier, *Synth. Met.*, **28**, C275 (1989)

[71] G. Zotti, S. Cattarin, and N. Comisso, *J. Electroanal. Chem.*, **235**, 259 (1987)

[72] J. Roncali, A. Yassar, and F. Garnier, *J. Chim. Phys.*, **86**, 85 (1989)

[73] S. Hotta, T. Hosaka, and W. Shimotsuma, *Synth. Met.*, **6**, 69 (1983)

[74] A. J. Downard and D. Pletcher, *J. Electronanal. Chem.*, **206**, 147 (1986)

[75] J. Roncali, A. Yassar, and F. Garnier, *J. Chem. Soc., Chem. Commun.*, 581 (1988)

[76] Y. Wei, C-C. Chan, J. Tian, G-W. Jang, and K. F. Hsuch. *Chem. Mater.*, **3**, 888 (1991)

[77] A. Yassar, J. Roncali, and F. Garnier, *Macromolecules*, **22**, 804 (1989)

[78] J. Roncali, F. Garnier, M. Lemaire, and R. Garreau, *Synth. Met.*, **15**, 323 (1986)

[79] J. Heinze, J. Mortensen, and K. Hinkelmann, *Synth. Met.*, **21**, 209 (1987)

[80] E. E. Havinga and L. W. Van Horssen, *Makromol. Chem., Makromol. Symp.* **24**, 67 (1989)

[81] J. P. Ferraris and R. T. Hanlon, *Polymer*, **30**, 1319 (1989)

[82] R. M. Eales and A. R. Hillman, *J. Electroanal. Chem.*, **250**, 219 (1988)

[83] D. D. Cunningham, L. Laguren-Davidson, H. B. Mark, C. V. Pham, and H. Zimmer, *J. Chem. Soc., Chem. Commun.*, 1021 (1987)

[84] A. F. Diaz, J. Crowley, J. Bargon, G. P. Gardini, and J. B. Torrance, *J. Electroanal. Chem.*, **121**, 355 (1981)

[85] F. Martinez, R. Voelkel, D. Neegele, and H. Naarmann, *Mol. Cryst. Liq. Cryt.* **167**, 227 (1989)

[86] Y. Yumoto and S. Yoshimura, *Synth. Met.*, **13**, 185 (1985)

[87] O. Inganas, B. Liedberg, C. R. Wu, and H. Wynberg, *Synth. Met.*, **11**, 239 (1985)

[88] L. Laguren-Davidson, P. Chiem Van, H. Zimmer, and H. B. Mark Jr., *J. Electrochem. Soc.*, **135**, 1406 (1988)

[89] G. Zotti and G. Schiavon, *Synth. Met.*, **39**, 183 (1990)

[90] I. Hoogmartens, P. Adriaensens, D. Vanderzande, J. Gelan, C. Quattrochi, R. Lazzaroni, and J. L. Bredas, *Macromolecules*, **25**, 7347 (1192)

[91] E. E. Havinga, W. Ten Hoeve, and H. Wynberg, *Polym. Bull.*, **29**, 119 (1992)

[92] C. Kitamura, S. Tanaka, and Y. Yamashita, *J. Chem. Soc., Chem. Commun.*, 1585 (1994)

[93] T. M. Lambert and J. P. Ferraris, *J. Chem. Soc., Chem. Commun.*, 752 (1991)

[94] F. Wudl, M. Kobayashi, and A. J. Heeger, *J. Org. Chem.*, **49**, 3381 (1984)

[95] F. Wudl, M. Kobayashi, N. Colaneri, M. Boysel, and A. J. Heeger, *Mol. Cry. Liq. Cry.*, **118**, 195 (1985)

[96] M. Kobayashi, N. Colaneri, M. Boysel, F. Wudl, and A. J. Heeger, *J. Chem. Phys.*, **82**, 5717 (1985)

[97] N. Colaneri, M. Kobayashi, A. J. Heeger, and F. Wudl, *Synth. Met.*, **14**, 45 (1986)

[98] H.Yashima, M. Kobayashi, K.-B. Lee, T.C. Chung, A. J. Heeger, and F. Wudl, *J. Electrochem. Soc.*, **134**, 46 (1987)

[99] P. A. Christensen, J.C.H. Kerr, S. J. Higgins, and A. Hamnet, *J. Chem. Soc., Faraday Discuss.*, **88**, 261 (1989)

[100] S. M. Dale, A. Glide, and A. R. Hillman, *J. Mater. Chem.*, **2**, 99, (1992)

[101] M. Onoda, H. Nakayama, S. Morita, T. Kawai, and K. Yoshino, *Synth. Met.*, **69**, 605 (1995)

[102] M. Lapkowski, R. Kiebooms, J. Gelan, D. Vanderzande, A. Pron, T. P. Nguyen, G. Louarn and S. Lefrant, *J. Mater. Chem.*, **7**, 873 (1997)

[103] K.-Y. Jen and R. L. Elsenbaumer, *Synth. Met.*, **16**, 379 (1986)

[104] T. L. Rose and M. C. Liberto, *Synth. Met.*, **31**, 395 (1989)

[105] I. Hoogmartens, D. Vanderzande, H. Martens, and J. Gelan, *Synth. Met.*, **47**, 367 (1992)

[106] R. Van Asselt, I. Hoogmartens, D. Vanderzande, J. Gelan, P. E. Froehling, M. Aussems, O. Aagaard, and R. Schellekens, *Synth. Met.*, **74**, 65 (1995)

[107] K. Tanada, S. Yamashita, T. Koike, and T. Yamabe, *Synth. Met.*, **31**, 1 (1989)

[108] N. Colaneri, M. Kobayashi, A. J. Heeger, and F. Wudl, *Synth. Met.*, **14**, 45 (1986)

[109] Y. S. Lee and M. Kertesz, *J. Chem. Phys.*, **88**, 2609 (1988)

[110] J. L. Bredas, A. J. Heeger, and F. Wudl, *J. Chem. Phys.*, **85**, 4673 (1986)

[111] J. L. Bredas, B. Themans, J. M. Andre, A. J. Heeger, and F. Wudl, *Synth. Met.*, **11**, 343 (1986)

[112] Y. S. Lee and M. Kertesz, *Int. J. Quantum Chem. Symp.*, **21**, 163 (1987)

[113] G. Zerbi and M. C. Maganoni, *Adv. Mater.*, **7**, 1027 (1995)

[114] R. Kiebooms, I. Hoogmartens, P. Adriaensens, D. Vanderzande, and J. Gelan, *Macromolecules*, **28**, 4961, (1992)

[115] Y. Ikenoue, F. Wudl, and A. J. Heeger, *Synth. Met.*, **40**, 1 (1991)

[116] G. King and S. J. Higgins, *J. Chem. Soc., Chem. Commun.*, 825 (1994)

[117] G. M. Brooke and S. D. Mawson, *J. Chem. Soc., Perkin Trans.*, **1**, 1919 (1990)

[118] M. J. Swann, G. Brooke, and D. Bloor, *Synth. Met.*, **55-57**, 281 (1993)

[119] G. King and S. Higgins, *J. Mater. Chem.*, **5**, 447 (1995)

[120] E. Funatsu, Jpn Pat. 02 252 727, 11 Oct. 1990

[121] M. Pomerantz, B. Chaloner-Gill, L. O. Harding, J. J. Tseng, and W. J. Pomerantz, *Synth. Met.*, **55-57**, 960 (1993)

[122] K. Nayak and D. S. Marynick, *Macromolecules*, **23**, 2237 (1990)

[123] M. Pomerantz, B. Chaloner-Gill, L. O. Harding, J. J. Tseng, and W. J. Pomerantz, *J. Chem. Soc., Chem. Commun.*, 1672 (1992)

[124] J. Kastner, H. Kuzmany, D. Vegh, M. Landl, L. Cuff, M. Kertesz, *Macromolecules*, **28**, 2922 (1995)

[125] C. Kitamura, S. Tanaka, and Y. Yamashita, *J. Chem. Soc., Chem. Commun.*, 1585 (1994)

[126] E. E. Haviga, W. Ten Hoeve, and H. Wynberg, *Synth. Met.*, **55-57**, 299 (1993)

[127] D. Lorcy and M. P. Cava, *Adv. Mater.*, **5**, 1456 (1992)

[128] P. Bauerle, G. Gotz, P. Emerle, H. Port, *Adv. Mater.*, **4**, 564 (1992)

[129] S. Musmanni, J. P. Ferraris, *J. Chem. Soc., Chem. Commun.*, 172 (1993)

[130] I. Hoogmartens, P. Adriaensenes, R. Carleer, D. Vanderzande, H. Martens, and J. Gelan, *Synth. Met.*, **51**, 219 (1992)

[131] M. V. Lakshmikantham, D. Lorcy, C. Scordilis-Kelley, X-L. Wu, J. P. Parakka, R. M. Metzger, and M. P. Cava, *Adv. Mater.*, **5**, 723 (1993)

[132] C. Kitamura, S. Tanaka, and Y. Yamashita, *J. Chem. Soc., Chem. Commun.*, 1585 (1994)

[133] J. P. Ferraris, A. Bravo, W. Kim, and D. C. Hrncir, *J. Chem. Soc., Chem. Commun.*, 991 (1994)

[134] S. Tanaka and Y. Yamashita., *Synth. Met.*, **69**, 599 (1995)

[135] C. Kitamura, S. Tanaka, and Y. Yamashita, *Chem. Mater.*, **8**, 570 (1996)

[136] S. Tanaka and Y. Yamashita, *Synth. Met.*, **69**, 599 (1995)

[137] S. Tanaka and Y. Yamahsita, *Synth. Met.*, **84**, 229 (1997)

[138] T. M. Lambert and J. P. Ferraris, *J. Chem. Soc., Chem. Commun.*, 752 (1991)

[139] H. Brisset, C. Thobie-Gautier, A. Gorgures, M. Jubault, and J. Roncali, *J. Chem. Soc., Chem. Commun.*, 1305 (1994)

[140] J. P. Ferraris and T. M. Lambert, *J. Chem. Soc., Chem. Commun.*, 1268 (1991)

[141] J. P. Ferraris, C. Henderson, D. Torres, and D. Meeker, *Synth. Met.*, **72**, 147 (1995)

[142] A. F. Diaz, J. I. Castillo, J. A. Logan, and W. Y. Lee, *J. Electroanal. Chem.*, **129**, 115 (1981)

[143] G. Daoust and M. Leclerc, *Macromolecules*, **24**, 255 (1991)

[144] M. Sato, S. Tanaka, and K. Kaeriyama, *J. Chem. Soc., Chem. Commun.*, 873 (1986)

[145] E. M. Genies, P. Hany, M. Lapkowski, C. Santier, and L. Olmedo, *Synth. Met.*, **25**, 29 (1988)

[146] G. P. Kittlesen, H. S. White, and M. S. Wrighton, *J. Am. Chem. Soc.*, **106**, 7389 (1984)

[147] G. Schiavon, S. Sitran, and G. Zotti, *Synth. Met.*, **32**, 209 (1989)

[148] B. J. Feldman, P. Burgmayer, and R. W. Murray, *J. Am. Chem. Soc.*, **107**, 872 (1985)

[149] K. Wilbourn and R. W. Murray, *J. Phys. Chem.*, **92**, 3642 (1988)

[150] H. Mao and P. G. Pickup, *J. Am. Chem. Soc.*, **112**, 1776 (1990)

[151] J. Ochmanska and P. G. Pickup, *J. Electroanal. Chem.*, **297**, 211 (1991)

[152] P. G. Pickup, *J. Chem. Soc., Faraday Trans.*, **86**, 3631 (1990)

[153] X. Ren and P. G. Pickup, *J. Electroanal. Chem.*, **420**, 251 (1997)

[154] H. Huang and P. G. Pickup, *Acta Polymer.*, **48**, 455 (1997)

[155] G. Zotti, R. Salmaso, M. C. Gallazzi, and R. A. Marin, *Chem. Mater.*, **9**, 791 (1997)

[156] A. Yassar, J. Roncali, and F. Garnier, *Macromolecules,* **22**, 804 (1989)

[157] C. E. D. Chidsey and R. W. Murray, *Science*, **231**, 25 (1986)

[158] H. Mao and P. G. Pickup, *J. Electroanal. Chem.*, **265**, 127 (1989)

[159] A. F. Diaz and J. I. Castillo, *J. Chem. Soc., Chem. Commun.*, 297 (1980)

[160] G. Tourillon, *Handbook of Conducting Polymers*; T. A. Skotheim ED.; Marcel Dekker, New York, 1986; Vol. 1, Chapter 9

[161] G. K. Chandler and D. Pletcher, *Electrochemistry*, D. Pletcher Ed.; Royal Society of Chemistry: London, 1985; Vol. 10, Chapter 3

[162] D. Ofer and M. S. Wrighton, *J. Am. Chem. Soc.*, **110**, 4467 (1988)

[163] D. Ofer, R. M. Crooks, and M. S. Wrighton, *J. Am. Chem. Soc.*, **112**, 7869 (1990)

[164] G. Zotti, G. Schiavon, A. Berlin, and G. Pagani, *Adv. Mater.*, **5**, 551 (1993)

[165] S. N. Hoier and S. M. Park, *J. Phys. Chem.*, **96**, 5188 (1992)

[166] G. Zotti and G. Schiavon, *Chem. Mater.*, **3**, 62 (1991)

[167] E. W. Paul, A. J. Ricco, and M. S. Wrighton, *J. Phys. Chem.*, **89**, 1441 (1985)

[168] R. M. Crooks, O. M. R. Chyan, and M. S. Wrighton, *Chem. Mater.*, **1**, 2 (1989)

[169] G. Zotti and G. Schiavon, *Synth. Met.*, **63**, 53 (1994)

Chapter 2

Experimental Section

2.1 Chemicals and Reagents

Various thiophene precursors were used in our experiments. Thiophene (Th, Aldrich, 99%), bithiophene (BTh, Aldrich, 97%), and terthiophene (TTh, Aldrich, 99%) were used as received. 4-dicyanomethylene-4*H*-cyclopenta[2, 1-*b*; 3, 4-*b*'] dithiophene (CDM) and 3, 4-ethylenedioxythiophene (EDOT) were donated by Philips (The Netherlands) and Bayer Corp. (Pittsburgh), respectively.

Acetonitrile (CH_3CN, Fisher, HPLC grade, 99.97%) was used as received in our early experiments. In our later experiments, acetonitrile (LiChrosolv, for liquid chromatography, 99.7%) was first run through an alumina column and then distilled under Argon (Ar, Air Liquide, HP+) with calcium hydride powder (CaH_2, ~40 mesh, 90-95%) as the dessicant before use. In most cases acetonitrile was used as the solvent for cyclic voltammetry and electropolymerization of thiophene precursors, and electrochemical characterization of polymers. In the cases, where CDM was employed as the precursor for polymerization, nitrobenzene, in which CDM is soluble, was used. Nitrobenzene ($C_6H_5NO_2$, Fisher, Certified

A.C.S.) was purified by two distillations. It was first distilled following addition of diluted sulphuric acid (H_2SO_4, Fisher, Reagent A. C. S., 95.0-98.0%) to remove most of the impurities. The nitrobenzene distillate was then distilled after it was dried over calcium chloride granules ($CaCl_2$, Anachemia, anhydrous, 4-8 mesh).The middle part of the second distillate was collected and stored under Ar for later use.

The electrolyte tetrabutyl ammonium hexafluorophosphate (Bu_4NPF_6, Fluka, puriss, electrochemical grade, 99%) was used as purchased.

2.2 Experimental

a. Electrochemical synthesis and studies

A Pine Instruments RDE4 Potentiostat, a SE780 X-Y recorder (Goerz Metrawatt), and a conventional three-electrode cell were used for electrochemical experiments, which include electrochemical studies of thiophene precursors, electropolymerization, and electrochemical characterization of polymers. Polished or polymer-coated Pt discs (0.0052 cm^2) were used as working electrodes. A Pt wire was used as the counter electrode, and a SCE as the reference electrode. In all cases, the electrolyte concentration was 0.1 M. For the electrochemical studies, normally 100 mV/s was employed as the potential scan rate, except as specified in the text. Before each experiment, the solution was purged with Ar and the electrochemical studies were performed under Ar. O_2-Modified poly-CDM films were prepared using dry and pure O_2 (Air Liquide) to treat original poly-CDM films at a negative

potential (e.g. -0.6 V) for a certain time, then O_2 was purged from the solution by Ar before the measurements.

b. *In situ* conductivity measurement

As discussed in section **1.4.1**, among various *in situ* conductivity measurement techniques [1-5], dual-electrode voltammetry has the largest conductivity measurement range (from 10^{-9} to 1 S cm^{-1} [1]), and therefore it is suitable for the study of conducting polymers in either highly doped or lightly doped states, and was chosen in our experiments. **Fig. 2.1** shows the schematic structure of a dual-electrode for *in situ* conductivity measurement. The area of the Pt disc was 1.3×10^{-4} cm^2. One of the Pt discs was electrochemically coated with a polymer film. Following voltammetric characterization of the polymer, the dual-electrode was coated with a thin layer of gold by vacuum vapour deposition with resistive heating of a tungsten wire wrapped with a gold source. Electrical contact to the gold film was made by an adjacent Pt disk. A fixed potential difference ($\Delta E_{Pt\text{-}Au}$ = 20 mV) was maintained between the polymer coated Pt electrode and the gold film while the potential was slowly scanned. By scanning slowly (1 mV s^{-1}) the current due to the redox processes of the polymer film becomes negligible relative to the current driven across the film by the applied potential difference ($\Delta E_{Pt\text{-}Au}$). According to Ohm's law, the conductivity (σ) is calculated using the following equation

$$\sigma = \frac{I \times d}{\Delta E_{Pt-Au} \times A} \qquad \textbf{2-1}$$

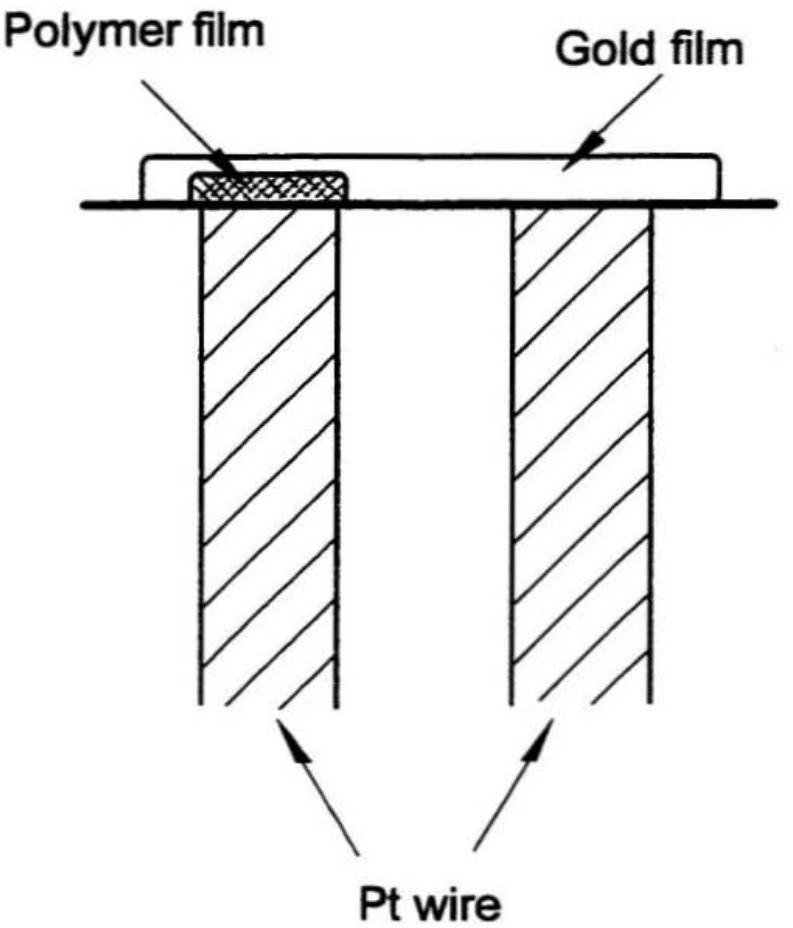

Fig. 2.1 Schematic dual-electrode used for the measurement of *in situ* conductivity against potential

where, I is the measured current, d is the thickness of the polymer film, and A is the electrode area.

c. UV-Vis-NIR spectroscopy

Spectroelectrochemical measurements were performed using an ITO electrode (0.8 cm^2, 10-20 Ohm/cm^2, Donnelly Corp.) coated with the polymer, a Cary 5E UV-VI-NIR spectrometer, and a thin-layer quartz cell containing an acetonitrile solution with 0.1 M Bu_4NPF_6 that can control the potential of the ITO electrode vs SCE.

d. Raman spectroscopy

Raman spectra of polymers were recorded using a Reneshaw Raman Imaging Microscope System 1000 using CCD31 as the detector and the Argon laser red line of 633 nm as the excitation source. Raman spectra for poly-CDM and poly-EDOT were measured in their neutral states. Poly-(CDM-co-EDOT), whose n- and p-doping processes overlap, was held at a potential corresponding to the current minimum in their voltammogram between n- and p-doping prior to Raman spectroscopy.

e. Scanning electron microscope

Scanning electron microscopy was performed with a Hitachi S-570 scanning electron microscope. Film thicknesses were estimated from the polymerization charge. A calibration relationship of 4.6 μm per 1 C cm^{-2} was obtained from scanning electron microscopy of poly-CDM films on Pt wire.

All experiments in this work were carried out at room temperature (21±2 °C)

Reference

[1] P. G. Pickup, *Electrochemistry of Electronically Conducting Polymer Films*, in: *Modern Aspects of Electrochemistry*, 1998

[2] G. P. Kittlesen, H. S. White, and M. S. Wrighton, *J. Am. Chem. Soc.*, **106**, 7389 (1984)

[3] G. Schiavon, S. Sitran, and G. Zotti, *Synth. Met.*, **32**, 209 (1989)

[4] B. J. Feldman, P. Burgmayer, and R. W. Murray, *J. Am. Chem. Soc.*, **107**, 872 (1985)

[5] P. G. Pickup, *J. Chem. Soc., Faraday Trans.*, **86**, 3631 (1990)

Chapter 3

Band-Gaps and Redox Potentials of Thiophene Oligomers and Their Polymers

3.1 Introduction

Among various kinds of conducting polymers, polythiophene (poly-Th) has become the subject of considerable interest, since it not only has high conductivity comparable to other conducting polymers [1-3], but also has good environmental stability in both its p-doped and undoped states [1, 4]. In addition, its structural versatility [5] makes possible the development of numerous poly-Th polymers with different desired properties, such as high stability [6, 7], superior conductivity [8, 9], good processability [10, 11], good solubility [12-14] and low band-gap [15-18]. In order to achieve poly-Th of good quality, in addition to the careful optimization of electrosynthesis conditions via thiophene (Th) monomer [19-20], oligomers, particularly 2, 2'-bithiophene (BTh) and 2, 2': 5', 2"-terthiophene (TTh) have been employed as precursors for polymerization [21-25]. Owing to their lower oxidation potentials and exclusive α-α' linkage in their precursor structures, polybithiophene (poly-BTh) and polyterthiophene (poly-TTh) are expected to possess better

quality than the polymer from Th monomer [26, 27]. Substantial work on comparative studies of the electrical, electrochemical and spectroscopic properties of polymers synthesized from Th, BTh, and TTh has been reported [5, 28-30]. One of the most puzzling results is the observation that, contrary to the former prediction [31], the polymer derived from Th monomer, which has the shortest conjugation length,among thiophene oligomers, exhibits the highest conductivity and it is also claimed to have the best electrochemical cyclability [5, 28] (i.e. charging (doping) and discharging (de-doping) cycles).

To better understand the properties of different poly-Th polymers associated with their starting molecules, this chapter has re-investigated redox potentials and band-gaps of thiophene oligomers and their resulting polymers. Comparative studies of the n-doping of poly-Ths originating from different oligomers, which is lacking in the literature, are also present in this chapter.

3.2 Band-gaps and redox potentials of thiophene oligomers

3.2.1 Electrochemistry of thiophene and its oligomers

a. Oxidation of thiophene oligomers

Fig. 3.1 shows cyclic voltammograms of the oxidation of thiophene oligomers including Th (15 mM), BTh (5 mM) and TTh (5 mM) at Pt electrodes in acetonitrile containing 0.1 M Bu_4NPF_6.

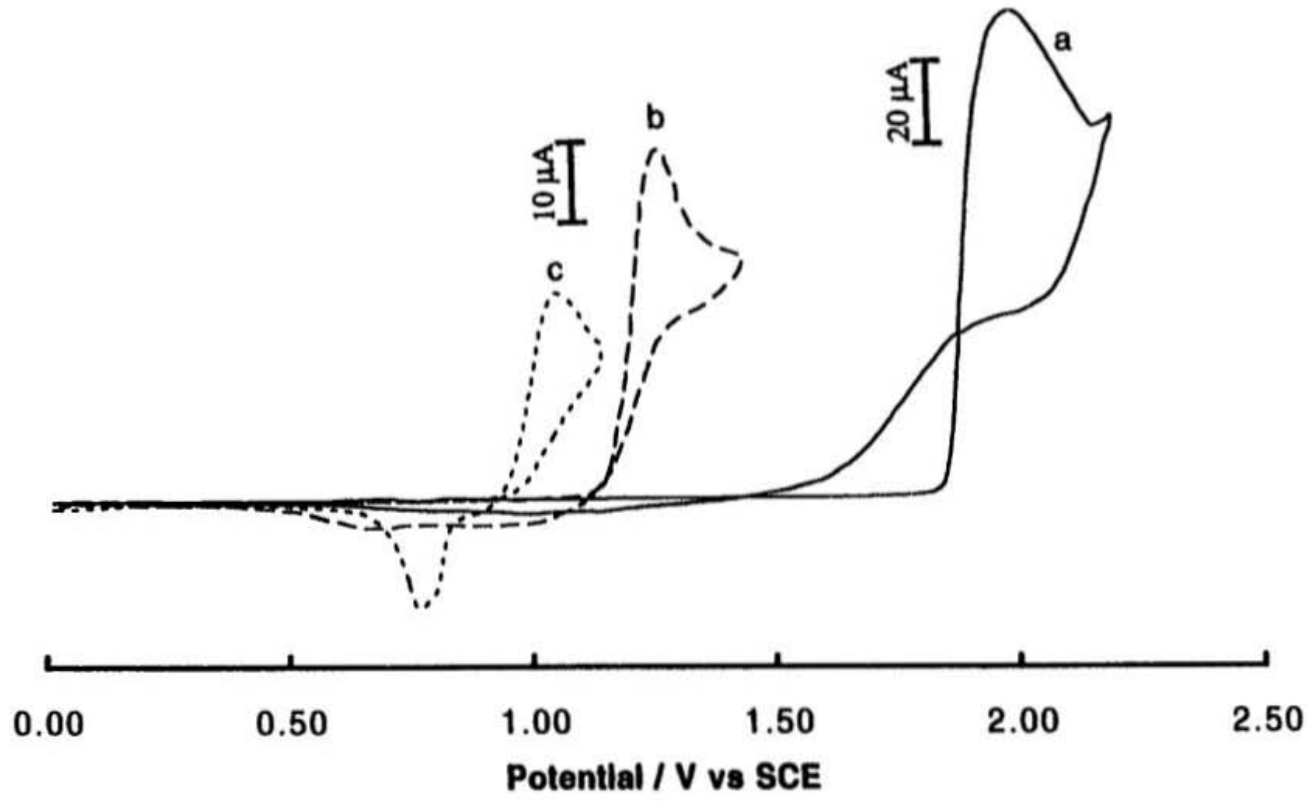

Fig. 3.1 Cyclic voltammograms of oxidation of oligothiophenes in acetonitrile containing 0.1 M Bu_4NPF_6 on Pt electrodes (0.0052 cm^2). Potential scan rate: 100 mV/s.
(a) Thiophene: 15 mM; Potential range: 0.00 - 2.20 V
(b) Bithiophene: 5 mM; Potential range: 0.00 - 1.45 V
(c) Terthiophene: 5 mM; Potential range: 0.00 - 1.15 V

Curve (a) illustrates the oxidation behavior of Th monomer in the potential range from 0.00 to 2.20 V, which exhibits a 'nucleation loop' commonly observed for the electrodeposition of metals proceeding via a nucleation and phase growth mechanism [32]. When the potential was scanned forward, the oxidation of Th commenced at 1.86 V and the oxidation current rose sharply to the peak at 2.01 V. When the potential was scanned backward, a corresponding reduction peak to the oxidation was not observed, indicating that the oxidation of Th is an irreversible process. However a small reduction current over a broad potential range was produced due to the de-doping of the polymer formed during the oxidation. If the potential scanning was continued to higher positive potentials (>2.2 V), another oxidation peak appeared at ca.2.3 V. Under this condition no reduction current was observed in the reverse scan, thus suggesting the activity of the polymer was destroyed during the second oxidation process, which is termed the overoxidation [33].

Curve (b) in **Fig. 3.1** is for the oxidation of BTh in the potential range from 0.00 to 1.45 V. The oxidation of BTh started at 1.19 V, and reached a peak current when the potential was 1.32 V. The reduction current of the de-doping of poly-BTh was clearly visible in the reverse scan, showing a peak at ca. 0.75 V.

The oxidation of TTh from 0.00 to 1.15 V is shown as curve (c) in **Fig. 3.1**. At 0.95 V, TTh already began to oxidize, and at 1.05 V showed an oxidation peak. When the potential was scanned back, a reduction current peak was seen at 0.76 V with a shoulder at 0.81 V. This peak was relatively narrow but high compared with those of Th and BTh.

Cyclic voltammograms for Th, BTh and TTh all show irreversible oxidation waves, due to the formation of polymers by coupling of the starting molecules and the simultaneous doping of ions into the resulting polymers. The reduction current during the reverse scan is due to the de-doping of the polymers, the reverse process of doping. Compared with its oxidation current, significantly smaller de-doping currents are generated for poly-Th than those for poly-BTh and poly-TTh, since more charge is needed for coupling of Th units and less charge is used for doping of the formed polymer. Furthermore, poly-Th is polymerized at such high potential that the overoxidation of the polymer can not be avoided [33, 34], thus decreasing the activity of the polymer.

From **Fig. 3.1**, as expected, both the onset oxidation potential and peak oxidation potential reduce significantly with increasing the number of Th units in the precursor, thus reflecting the higher HOMO energy level with longer conjugation length of the Th oligomers.

b. Reduction of thiophene oligomers

Cyclic voltammograms of the reduction behaviors of BTh and TTh are illustrated in **Fig. 3.2** as curve (**a**) and curve (**b**) respectively. For BTh, its reduction began at -2.28 V and peaked at -2.59 V, while for TTh, as expected, the onset reduction potential shifted anodically to -1.92 V, and the peak potential to -2.20 V. Reduction processes of both oligomers were irreversible. The reduction of Th monomer took place at very negative potentials, where decomposition of the electrolyte occurred. The onset reduction potential

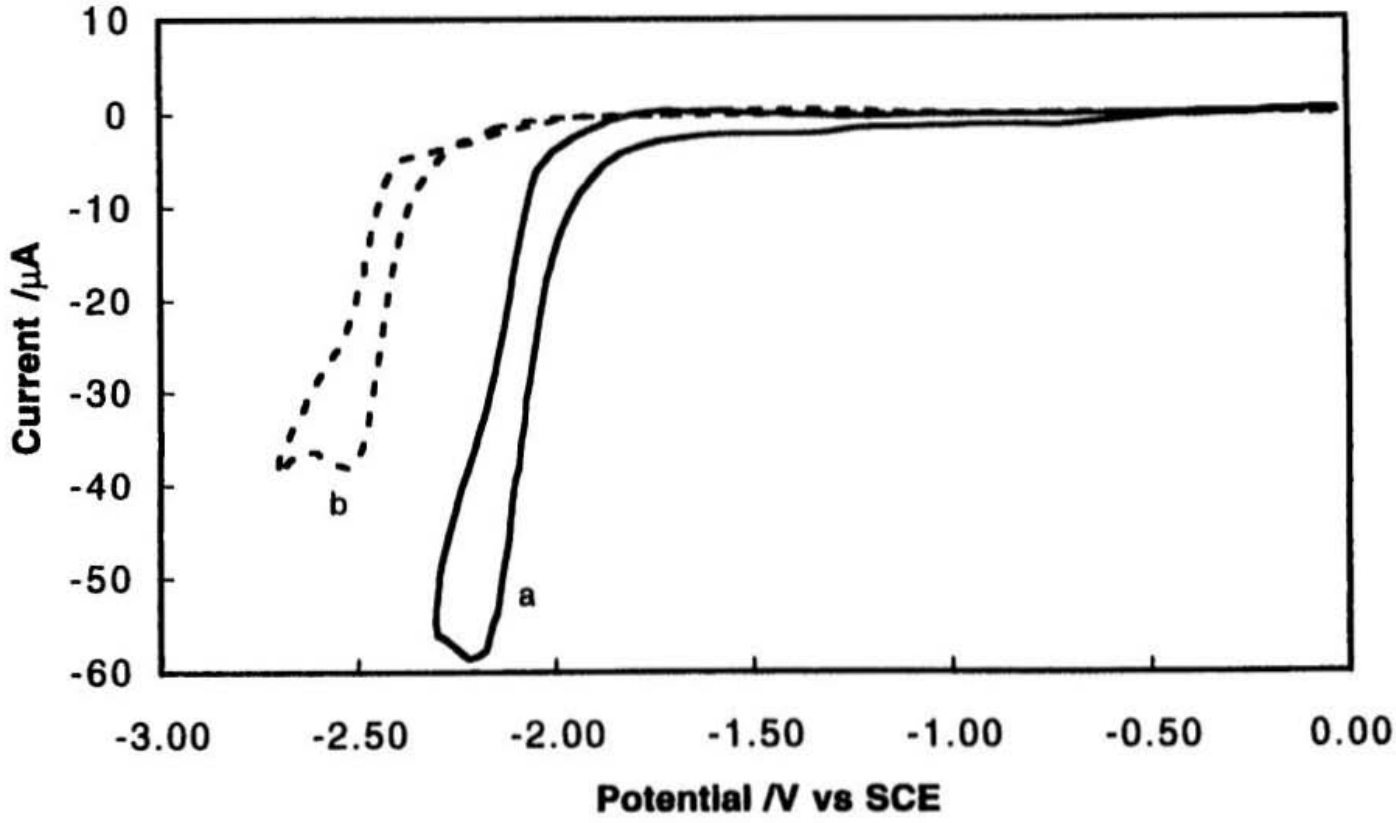

Fig 3.2 Cyclic voltammograms of reduction of oligothiophenes in acetonitrile containing 0.1 M Bu_4NPF_6 on Pt electrodes (0.0052 cm^2). Potential scan rate: 100 mV/s
(**a**) Bithiophene: 5 mM; Potential range: 0.00 - -2.70 V
(**b**) Terthiophene: 5 mM; Potential range: 0.00 - -2.30 V

for Th was estimated to be -3.1 V. The above results indicate that as the conjugation length increases in the starting material, the LUMO energy level decreases.

From the onsets of oxidation and reduction potentials of BTh and TTh, the electrochemical band-gaps for BTh and TTh were estimated to be 3.47 V and 2.87 V respectively. And the electrochemical gap for Th monomer was estimated as 4.96 V.

3.2.2 UV-Visible spectroscopic results of Th, BTh and TTh

Fig. 3.3, curves **(a)**, **(b)**, and **(c)** illustrate the UV-Visible spectra of Th, BTh and TTh, respectively in acetonitrile solutions. The optical absorption maximum of Th occurs at 231 nm, which is the result of a $\pi-\pi^*$ absorption transition. In accordance with expectation, the longer conjugation lengths in BTh and TTh make the absorption peaks move bathochromically to 302 and 352 nm respectively. Following the same trend, the absorption onset wavelength increases as the number of Th units in the starting material increases. From their clear absorption edges, onset wavelengths for Th, BTh, and TTh are obtained as 246, 344, and 407 nm, corresponding to optical band-gaps of 5.02, 3.60, and 3.04 eV, respectively.

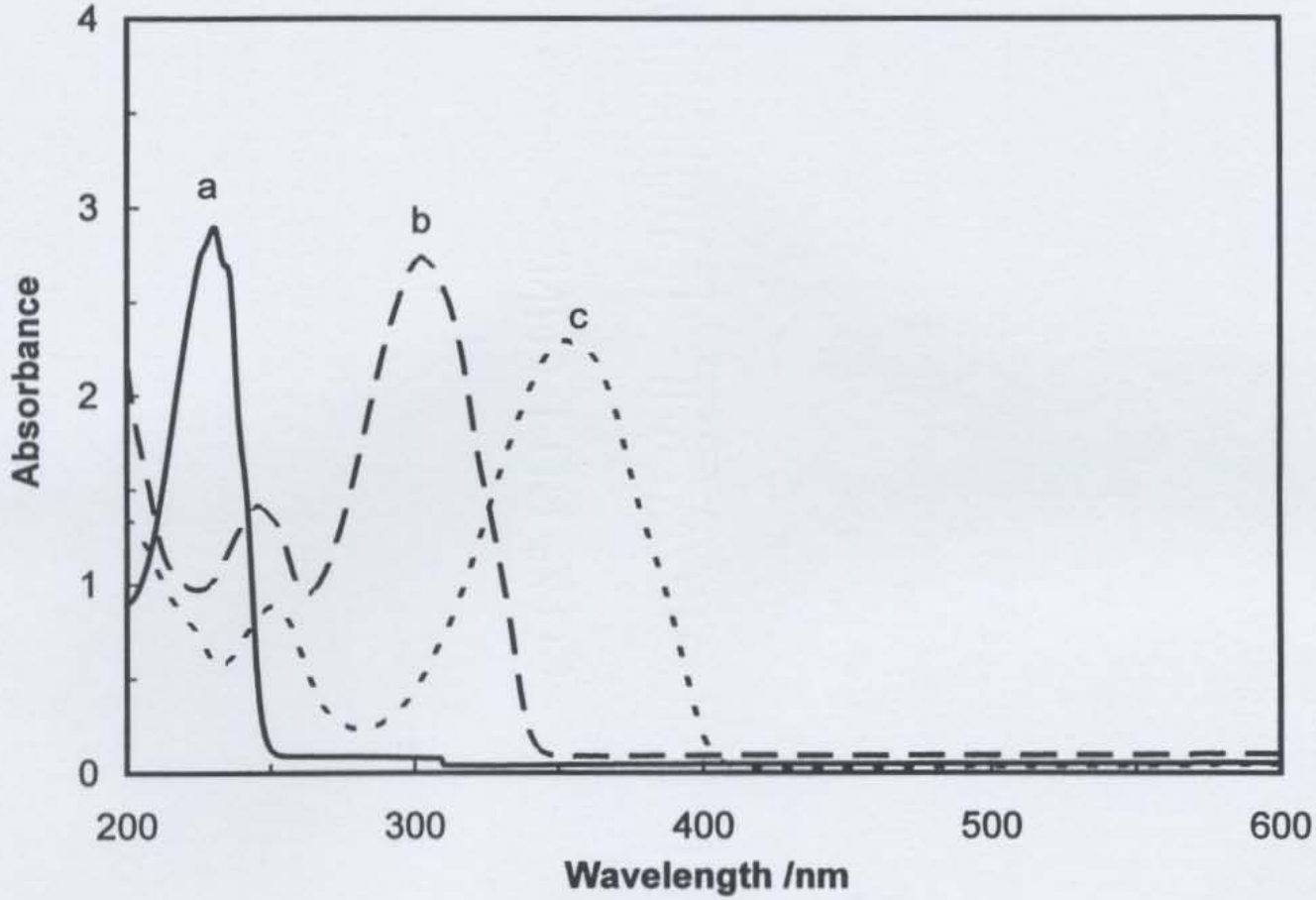

Fig. 3.3 UV-Visible absorption spectra for thiophene oligomers in acetonitrile
a: thiophene, b: bithiophene, c: terthiophene

3.3 Electrochemical studies of poly-Th, poly-BTh and poly-TTh

3.3.1 P-doping and n-doping of poly-Th

Poly-Th films were electrochemically grown on Pt electrodes from 0.1 M Th in CH_3CN, in the presence of 0.1 M Bu_4NPF_6, using galvanostatic methods. With a current density of 1 mA/cm^2 for 240 s, poly-Th films with thickness of about 1 μm were produced [35].

Fig. 3.4 shows cyclic voltammograms of p-doping (from 0.00 to 0.90 V) and n-doping (from -0.90 to -2.00 V) of a 1 μm poly-Th film at different potential scan rates in 0.1 M Bu_4NPF_6/CH_3CN. The results are listed in **Table 3.1**.

Table 3.1 Electrochemical data of the p- and n-doping of a 1 μm poly-Th film

	p-doping				n-doping			
scan rate /mV/s	$E_{p(ox)}$ /V	$i_{p(ox)}$ /μA	$E_{p(red)}$ /V	$i_{p(red)}$ /μA	$E_{n(red)}$ /V	$i_{n(red)}$ /μA	$E_{n(ox)}$ /V	$i_{n(ox)}$ /μA
20	0.69	7.0	0.81	-7.0	-1.82	-3.8	-1.69	4.3
40	0.70	14	0.82	-14.5	-1.85	-7.4	-1.69	8.2
60	0.74	22	0.82	-19.5	-1.88	-10.4	-1.68	11.6
80	0.77	30	0.83	-25.0	-1.91	-13.0	-1.68	14.4
100	0.80	39	0.84	-30.5	-1.93	-15.1	-1.68	16.7

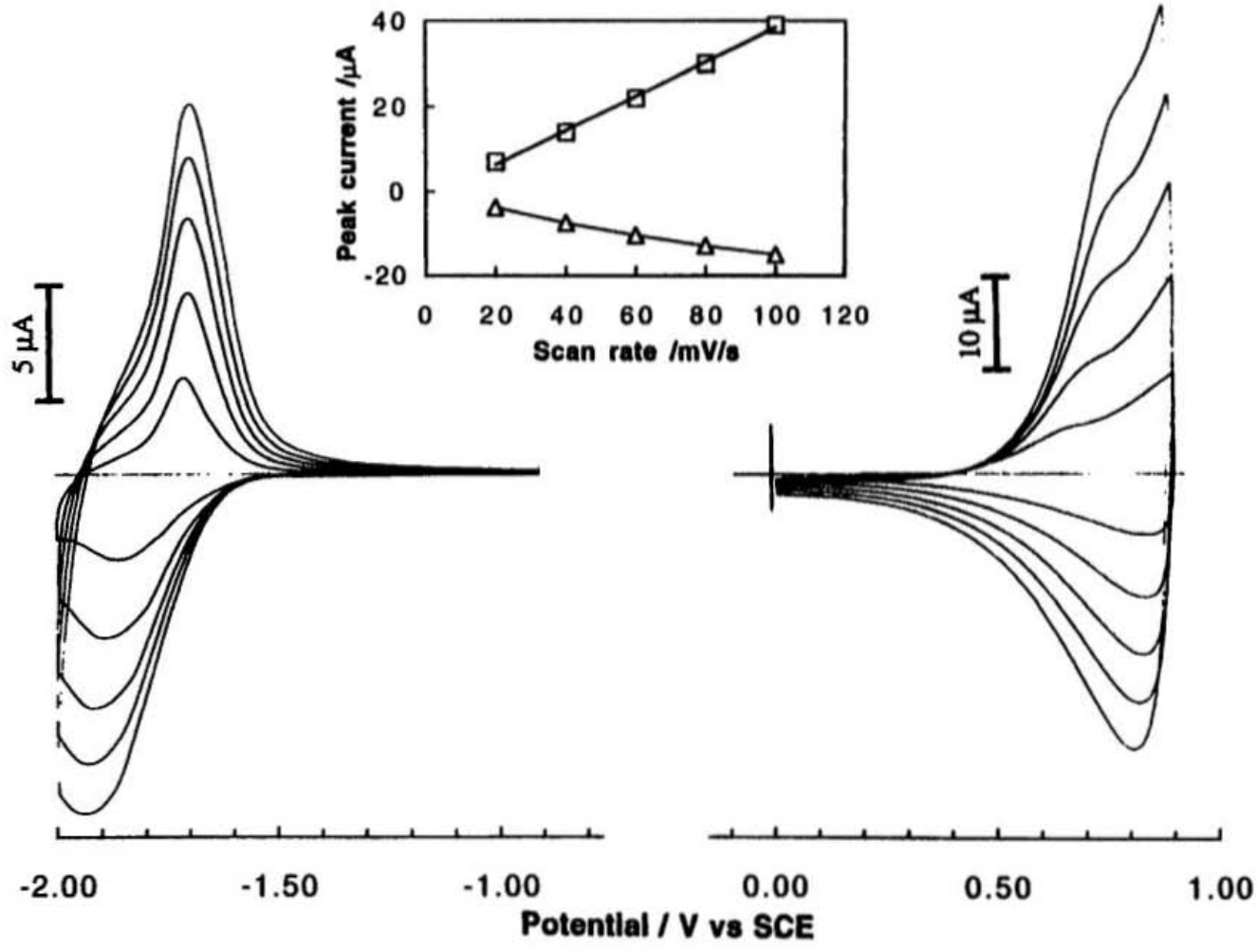

Fig. 3.4 Cyclic voltammograms of the p-doping (0.00 - 0.90 V) and n-doping (-0.90 - -2.00 V) of polythiophene in acetonitrile containing 0.1 M Bu_4NPF_6
Insert: the plot of the peak current ($i_{p(ox)}$ and $i_{p(red)}$) against the scan rate

In the case of the p-doping of poly-Th, redox waves with good reversibility, typically observed for conducting polymers were obtained; the de-doping charge was approximately equal to the doping charge, and the doping peak current was proportional to the scan rate (see insert plot). As the scan rate increased from 20 to 100 mV/s, the p-doping peak potential shifted positively from 0.69 to 0.81 V, whereas the de-doping peak potential remained almost at the same position for all the scan rates studied. The charge for p-doping of poly-Th was 22.2 mC/cm^2. Using equation [4]

$$Dopinglevel \approx \frac{n}{3} \times \frac{Q_{doping}}{Q_T - Q_{doping}} \qquad \textbf{3-1}$$

where Q_T is the total charge consumed for synthesis and doping of a polymer, Q_{doping} is the charge used for doping, and n is 6 for poly-Th, the doping level was estimated to be 20.4%. A stability test of the p-doping showed that, after multiple cycles, there was little change of the CV of the polymer.

For n-doping of poly-Th, the CV showed clear and well-shaped peaks for both doping and de-doping processes, and the latter gave a sharp peak. Like its p-doping behavior, the position of n-doping potential also varied with potential scan rate; as the scan rate was increased from 20 to 100 mV/s, it shifted negatively from -1.82 to -1.93 V. Taking the CV at 20 mV/s for consideration, which involved 10.6 mC/cm^2 doping charge, the n-doping level was calculated to be 9.2% from equation **3-1**. The de-doping efficiency, which is defined as the ratio of the charges for de-doping and doping, was less than 90%,

indicating that a significant part of doped charges were trapped in the polymer matrix [36, 37] and/or were lost by self-discharge [38]. The relationship between the peak current and the potential scan rate deviated from linearity (see insert plot) due to ionic transport difficulty in the polymer [39]. The average potential separation between n-doping and its de-doping was 190 mV. The stability of n-doping was not as good as for p-doping. In fact, after 20 cycles, the current was reduced by ca. 30%.

From the CVs of poly-Th, the onset potential for p-doping is ca. 0.50 V and for n-doping it is ca. -1.60 V, and hence electrochemical band-gap is ca. 2.1 V.

3.3.2 P-doping and n-doping of poly-BTh

Under similar electropolymerization conditions to those used for poly-Th, poly-BTh films of ca. 1 μm thickness were synthesized at 1 mA/cm^2 in 5 mM BTh acetonitrile solution for 120 s. Cyclic voltammograms of the p-doping (from 0.00 to 1.20 V) and n-doping (from -0.90 to -2.10 V) of a resulting poly-BTh film at different potential scan rates are shown in **Fig. 3.5**, along with a plot of the doping current (both p- and n-doping) against the scan rate. Data derived from the CVs are given in **Table 3.2**.

The p-doping behavior of the poly-BTh film differed strikingly from that of the poly-Th film, having a sharp and narrow p-doping peak and a broad de-doping range with two distinct peaks. The plot of the peak current against the scan rate was a good straight line. Positions of these peak potentials were practically independent of the potential scan

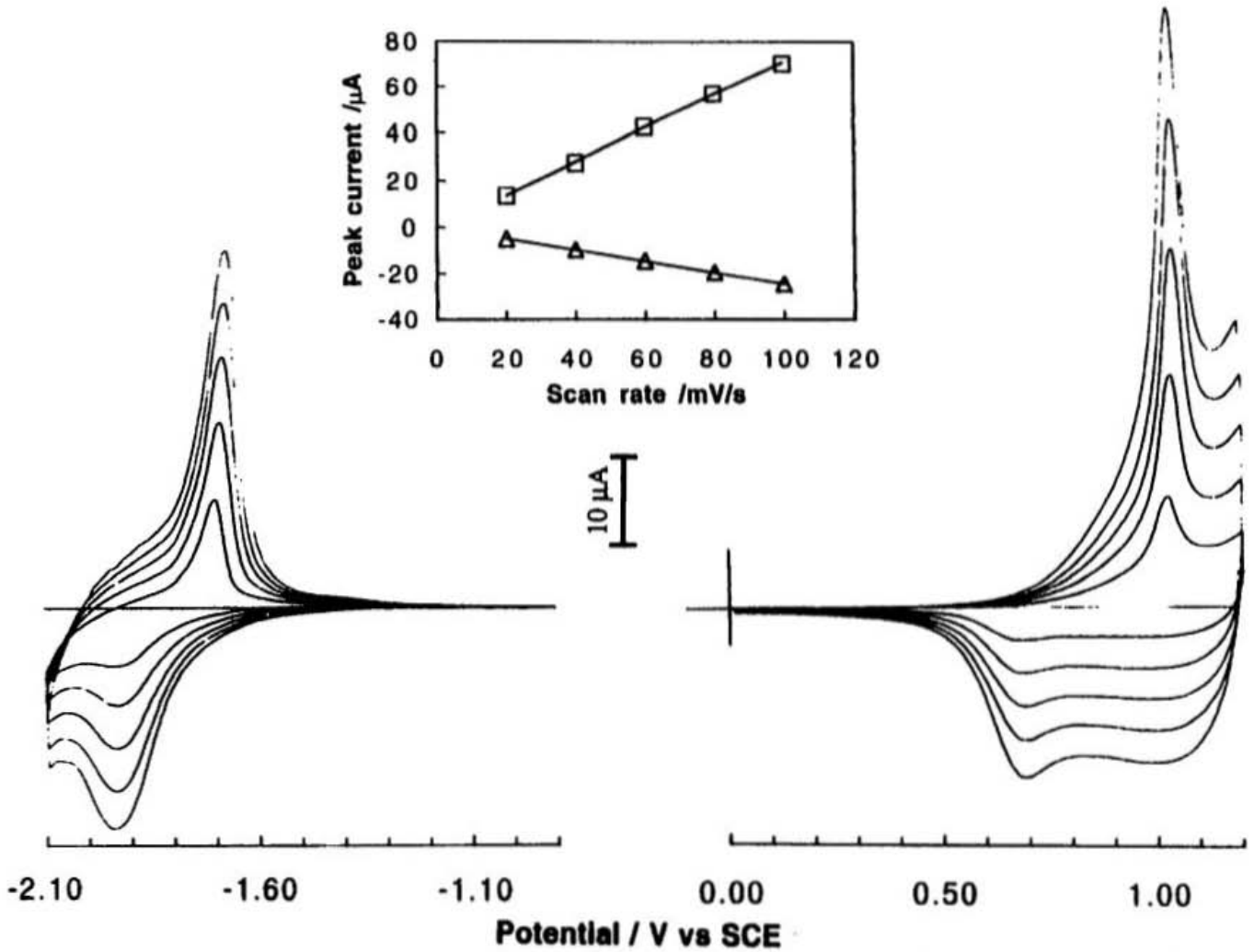

Fig. 3.5 Cyclic voltammograms of the p-doping (0.00 - 1.20 V) and n-doping (-0.90 - -2.10 V) of polybithiophene in acetonitrile containing 0.1 M Bu_4NPF_6
Insert: the plot of the peak current ($i_{p(ox)}$ and $i_{n(red)}$) against the scan rate

rate. The p-doping charge was 21.7 mC/cm^2. Using equation **3-1**, where n equals 3 for poly-BTh, the doping level was calculated to be 22%. P-doping was sufficiently stable; after multiple cycles, there was a little change of the peak current.

Table 3.2 Electrochemical data of p- and n-doping of a 1 μm poly-BTh film

	p-doping						n-doping			
Scan rate /mV s^{-1}	$E_{p(ox)}$ /V	$i_{p(ox)}$ /μA	$E_{p(re1)}$ /V	$i_{p(re1)}$ /μA	$E_{p(re2)}$ /V	$i_{p(re2)}$ /μA	$E_{n(re)}$ /V	$i_{n(re)}$ /μA	$E_{n(ox)}$ /V	$i_{n(ox)}$ /μA
20	1.03	13.5	1.02	-3.6	0.68	-3.9	-1.91	-4.9	-1.69	12.3
40	1.03	27.5	1.03	-7.4	0.69	-7.8	-1.91	-9.8	-1.68	20.9
60	1.04	42.5	1.03	-11.0	0.69	-11.9	-1.92	-14.5	-1.67	28.4
80	1.04	57.0	1.03	-14.6	0.70	-15.6	-1.93	-19.5	-1.67	34.4
100	1.04	70.5	1.03	-18.3	0.70	-20.0	-1.93	-24.6	-1.67	40.6

The n-doping feature of poly-BTh was similar to that of poly-Th with a comparatively broad n-doping wave and a sharp de-doping wave. However, the n-doping peak potential positions of poly-BTh did not shift with scan rate and are a little more negative than those of poly-Th. The average peak potential difference between n-doping and its de-doping was 240 mV, larger than the value for poly-Th. A linear dependence of the n-doping current with the scan rate was observed(see insert plot). The n-doping level reached 13.9% (the n-doping charge was 14.6 mC/cm^2).

From **Fig. 3.5**, the difference between the onsets of p-doping (0.60 V) and n-doping (-1.63 V) of poly-BTh was measured to be 2.23 V, a value higher than that for poly-Th,

which is evidence that the conjugation length of the poly-BTh was shorter than that of the poly-Th.

3.3.3 P-doping and n-doping of poly-TTh

Poly-TTh films of 1μm thickness were synthesized at 1 mA/cm^2 from 5 mM TTh acetonitrile solution for 80 s under similar conditions as for the synthesis of poly-Th and poly-BTh films. **Fig. 3. 6** presents cyclic voltammograms of the p-doping (from 0.00 to 1.20 V) and n-doping (from -0.90 to -2.10 V) of the synthesized poly-TTh film, and **Table 3.3** is the collection of the electrochemical data.

Table 3.3 Electrochemical data of p- and n-doping of a 1 μm poly-TTh film

	p-doping				n-doping			
scan rate /mV/s	$E_{p(ox)}$ /V	$i_{p(ox)}$ /μA	$E_{p(re)}$ /V	$i_{p(re)}$ /μA	$E_{n(re)}$ /V	$i_{n(re)}$ /μA	$E_{n(ox)}$ /V	$i_{n(ox)}$ /μA
20	1.09	17.0	0.63	-6.1	-1.95	-6.0	-1.66	15.9
40	1.09	34.5	0.63	-12.3	-1.95	-11.9	-1.65	18.8
60	1.10	50.0	0.64	-18.9	-1.96	-17.9	-1.65	27.5
80	1.10	64.0	0.64	-25.0	-1.97	-23.5	-1.64	34.3
100	1.10	78.0	0.64	-31.5	-1.97	-29.8	-1.64	40.5

The p-doping wave of poly-TTh is similar to that of poly-BTh showing a sharp and narrow doping peak, the position of which did not vary with the scan speed. It is located

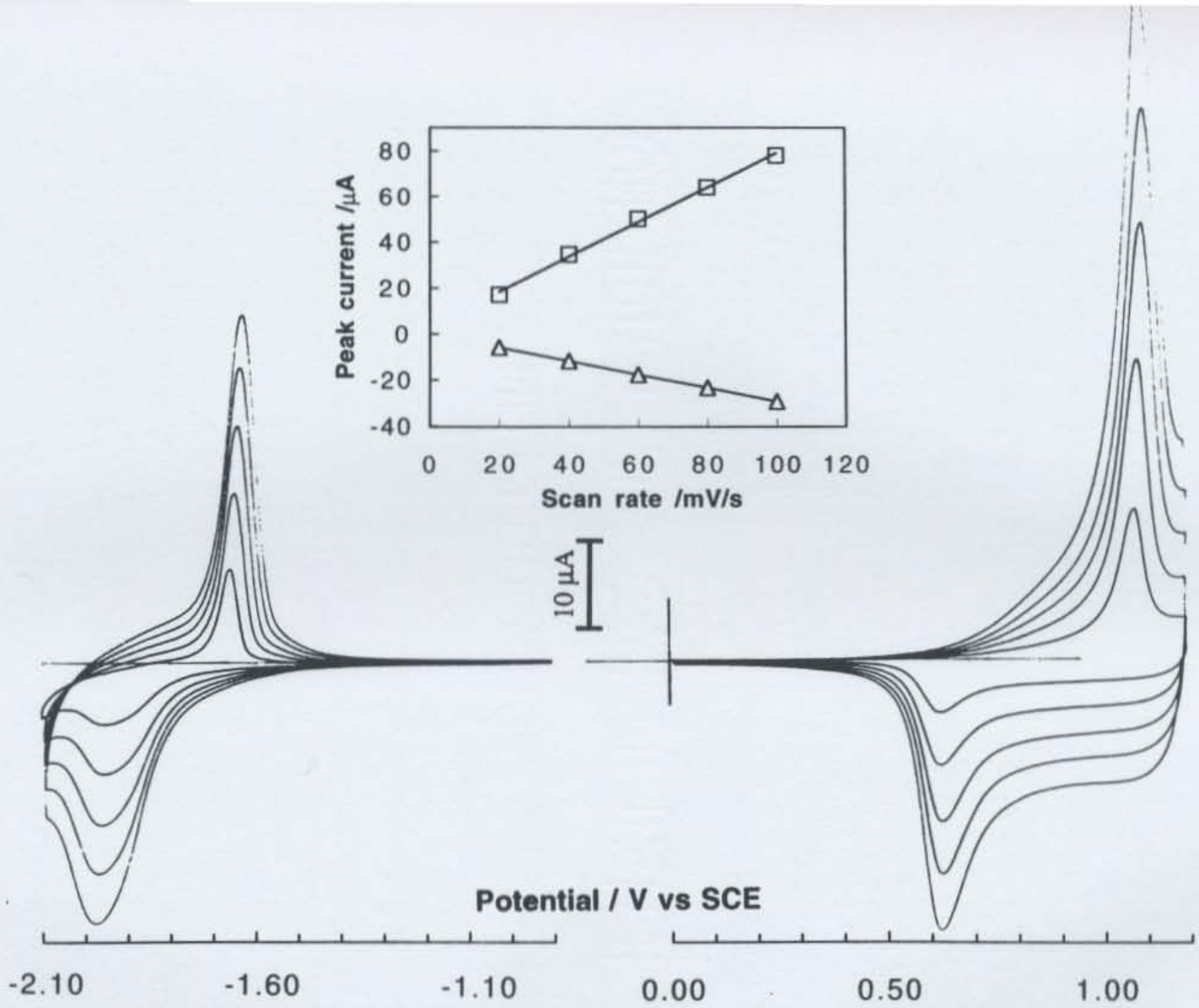

Fig. 3.6 Cyclic voltammograms of the p-doping (0.00 - 1.20 V) and n-doping (-0.90 - - 2.10 V) of polyterthiophene in acetonitrile containing 0.1 M Bu_4NPF_6
Insert: the plot of the peak current ($i_{p(ox)}$ and $i_{n(red)}$) against the scan rate

at the highest positive potential among the polymers derived from the monomer, dimer and trimer of Th. The doping current was linear with the scan speed (see insert plot). The de-doping process had a well-defined peak at 0.64 V with a broad shoulder. The doping charge of the poly-TTh film was 23.1 mC/cm^2, resulting in a doping level of 27.1% (using equation **3-1**, where n is 2 for poly-TTh). The p-doping stability of poly-TTh was comparable to that of poly-Th and poly-BTh.

The features of the n-doping of poly-TTh are close to both poly-Th and poly-TTh, but the doping potential lied at a more negative potential. The potential difference between n-doping and its de-doping increased to 310 mV. The relationship between the doping current and the scan rate was linear (see insert plot). A n-doping level of 15.3% was achieved by doping 14.9 mC/cm^2 cations into the polymer. The n-doping stability of poly-TTh is the best among these three poly-Ths, since after multiple cycles, there was no significant reduction of the peak current. The electrochemical band-gap measured from the potential difference between the onsets of p-doping (0.63 V) and n-doping (-1.65 V) is 2.28 V for poly-TTh.

3.4 Discussion

Electrochemical and UV-Visible absorption spectroscopic results of Th oligomers and polymers are summarized in **Table 3.4** for comparison. Data of tetrathiophene, hexathiophene, and octathiophene are cited from the literature [40-42].

Table 3.4 Summary of electrochemical and spectroscopic properties of thiophene oligomers

	E_{pa} /V	$E_{ox(onset)}$ /V	$E_{rc}^{0'}$ /V	$E_{rc(onset)}$ /V	$E_{g(electrochem)}$ /V	λ_{max} /nm	λ_{onset} /nm	$E_{g(optical)}$ /eV
thiophene	2.01	1.86		-3.10[a]	4.96	231	246	5.04
bithiophene	1.31	1.19	-2.59[b]	-2.28	3.47	302	344	3.60
terthiophene	1.05	0.95	-2.20[b]	-1.92	2.87	352	407	3.04
tetrathiophene	0.95[c]					385		
hexathiophene	0.88[c]	0.74-0.79[c]						
octathiophene	0.84[c]	0.60[c]	-2.0[c]	-1.70	2.30	380[e]	575	2.16
polythiophene	0.80	0.50	-1.93	-1.60	2.10			
polybithiophene	1.04	0.60	-1.93	-1.63	2.23			
polyterthiophene	1.10	0.63	-1.97	-1.65	2.28			

a estimated
b the peak potential, chemically irreversible
c from reference 40
d from reference 41
e from reference 42

From the electrochemical data for the Th oligomer series, it can be seen that, as the number of monomer units in oligomers increases, the p-doping potential (both the peak potential and the onset potential) shifts negatively, while the n-doping potential (both the peak and the onset) moves positively, thus resulting in the reduction of the electrochemical band-gap. The same tendency has been reported for other types of oligomer, such as the pyrrole and benzene oligomer series [40]. These changes are reasonable. According to Molecular Orbital Theory, extension of the π-π conjugation in the molecule will increase the HOMO energy level and decrease the LUMO energy level. The effects on the electrochemical characteristics are that the reduction (n-doping) potential shifts positively following the lower LUMO energy level and the oxidation (p-doping) potential becomes lower because of the higher HOMO energy level [43, 44]. Actually, a linear dependence of the p- and n-doping peak potentials of oligomer series (such as thiophene, pyrrole, benzene oligomers) on the inverse chain length has been claimed [40, 45].

From the optical absorption data, including the absorption peak and the absorption onset, of oligothiophenes, the optical band-gap shows the same trend as the electrochemical band-gap. That is, as the number of thiophene units increases in the oligomer, the optical band-gap shifts bathochromically, reflecting the narrowing energy gap between the LUMO and HOMO level.

Electrochemical gaps and optical gaps of oligothiophenes are plotted against their reciprocal conjugation length in **Fig. 3.7**, giving two lines with close to linear relationships, which can be described by the following two equations,

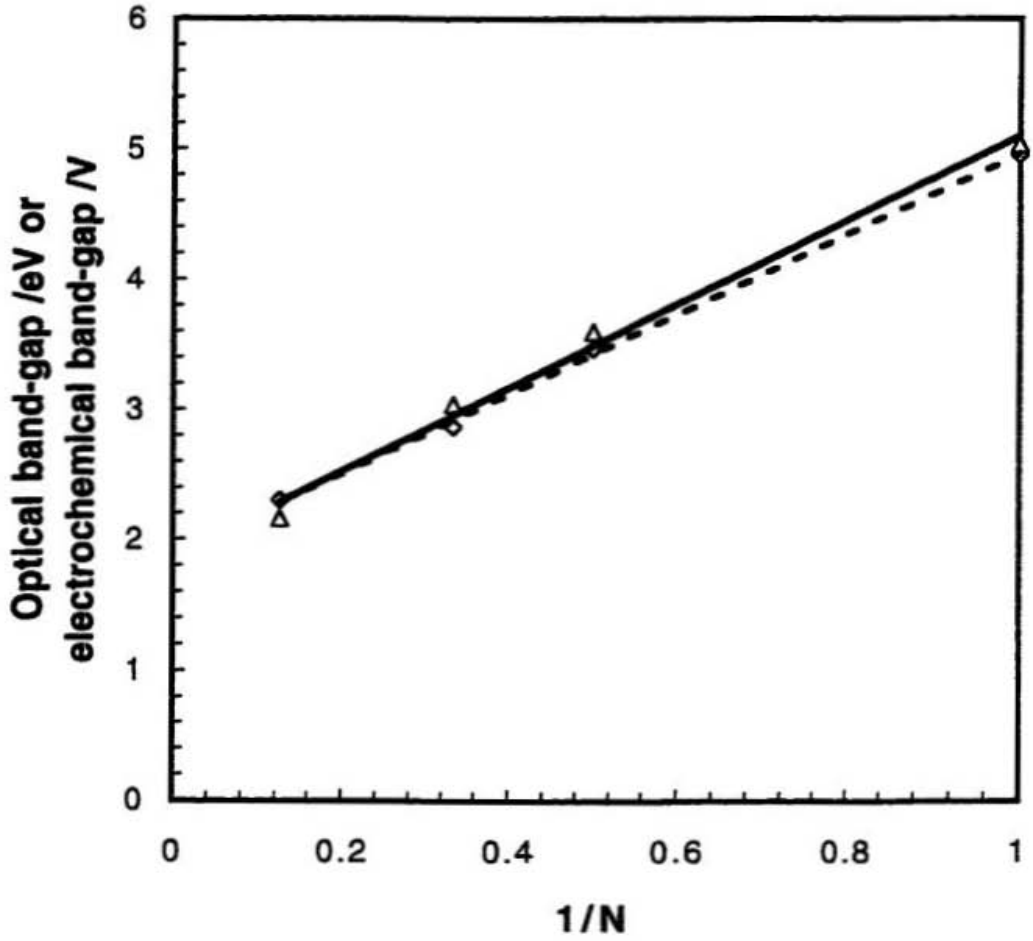

Fig. 3.7 Plot of the optical (solid line) and electrochemical (dashed line) band-gaps against 1/N. N is the conjugation length of thiophene oligomers

$$E_g(electrochem.)=\frac{3.06}{N}+1.90 \qquad \textbf{3-2}$$

and

$$E_g(optical)=\frac{3.22}{N}+1.88 \qquad \textbf{3-3}$$

where N is the number of thiophene units in the oligomer. The electrochemical and optical band-gap of an ideal polymer with infinite chain length can be deduced by extrapolation to the E_g axis following the relationship given by above equations. They are 1.90 V and 1.88 eV respectively, and are expectedly consistent. However, for poly-Th consisting of pure thiophene units, normally band-gaps of ca. 2.1 eV are reported [28]. This practical value is slightly higher than our prediction, because of the α-β' linkage defects, distortion of polymer backbone upon doping, and limited chain length of the real polymer [24, 46-48].

Poly-Ths synthesized from Th, BTh, and TTh have been reported extensively. The most contradictory result among previous work was the claim that poly-Ths derived from longer conjugated oligomers had longer chain lengths and higher conductivities [26, 27], while others had reported the opposite result [28]. Through careful studies and comparison of their electrochemical behavoirs, several pieces of evidence clearly support the claim that longer chain length oligothiophenes lead to shorter chain length polymers.

i) As already discussed for oligothiophenes, peak potential can be related to the extent of conjugation. The increase of the p-doping potential from poly-Th to poly-TTh

reflects a short range of conjugated chain lengths in poly-BTh and poly-TTh. The same result is obtained for the n-doping potential, which shifts negatively from poly-Th to poly-TTh.

ii) Separation of peak potential of the n-doping and its de-doping is also related to the conjugation length of the polymer. For the longer chain polymer, basically doping and the de-doping should be more reversible, that is, the peak separation is narrower than for a shorter polymer. For poly-Th, poly-BTh and poly-TTh, their n-doping peak separation are 190, 240, 310 mV respectively, suggesting that the reversibility becomes worse, and hence conjugation length becomes shorter from poly-Th to poly-TTh.

iii) In our experiments, electrochemical band-gaps for poly-Th, poly-BTh, and poly-TTh are obtained as 2.10, 2.23 and 2.28 V from their CVs respectively. According to equation **3-2**, the corresponding effective average conjugation lengths are about 16, 9 and 8 for poly-Th, poly-BTh and poly-TTh respectively. The value for poly-Th is in agreement with the result obtained from IR spectra of poly-Ths selectively labeled with deuterium at the α and/or β positions [49]. Considering effects of α-β' linkage defects and distortion of the polymer backbone upon doping, the real polymer chains should be longer than these conjugation lengths. However, thy do, to some degree, quantitatively illustrate that more conjugated oligomers produce shorter chain length polymers.

This result can be explained by considering the changes in the reactivity of the substrate resulting from the delocaliztion of the π electrons over the entire molecule [24]. On one hand, the overall reactivity of the substrate decreases or, in other words, the

stability of the corresponding radical cation increases, which causes a decrease or even in some cases a complete loss of polymerizability. This conclusion is consistent with the limited electropolymerization of TTh, as shown by the fact that poly-TTh contains large amounts of unreacted TTh and of the compound resulting from an unique coupling [28, 50], e.g. sexithiophene. On the other hand, the conjugated structure of oligomers results in a decrease of the relative reactivity of α positions which has deleterious consequences for the stereoselectivity of the polymerization [51, 52].

From the different features of CVs of poly-Th, poly-BTh and poly-TTh, another result that can be deduced is that poly-Th films are more compact than poly-BTh and poly-TTh films. As the scan rate is increased, p-doping peak potentials of poly-Th shifted positively, while n-doping potentials shifted negatively, which is not the case for poly-BTh and poly-TTh, peak potentials (both p- and n-doping) of which were practically the same. The observation indicates that ion transport (both cations and anions) is difficult because of the compact morphology of the polymer film [53]. Other evidence is that the n-doping current of poly-Th is not linear with scan rate, which is contrary to the normal characteristics of conducting polymers, and arises from the difficulty of the transport of the cation Bu_4N^+, which has a large size (0.5 nm in diameter) [54]. In fact, n-doping of poly-Th was so difficult that a film synthesized by cyclic voltammetry could not be n-doped in our experiment, while poly-BTh and poly-TTh, which had a more porous morphology, could easily be n-doped.

3.5 Conclusion

As expected, electrochemical and optical results for Th oligomers including the monomer, dimer and trimer, indicate that increasing of thiophene units in the oligomer decreases the electrochemical and optical band-gaps. Similar linear relationships were obtained from plots of electrochemical band-gap and optical band-gap against the inverse of the number of Th units in the oligomer, from which a band-gap (both electrochemical and optical) of ca. 1.89 eV was predicted for an ideal polymer with infinite chain length.

Poly-Ths were electrosynthesized under similar conditions from the thiophene monomer, dimer and trimer. Comparative study of these resulting polymers show that the conjugation length of the polymers decrease steadily with increasing chain length of the starting oligomer. In our experiments, the average conjugated length involved in poly-Th, Poly-BTh and poly-TTh are determined to be 16, 9 and 8 respectively. Poly-Th is compact, while poly-BTh and poly-TTh are porous. Extensive conjugation and compact structure of poly-Th result in superior properties to poly-BTh and poly-TTh, such as substantially higher conductivity, which is consistent with the published results.

References

[1] G. Tourillon and F. Garnier, *J. Electroanal. Chem.*, **135**, 173 (1982)

[2] K. Kaneto, Y. Kohno, K. Yoshino, and Y. Inuishi, *J. Chem. Soc., Chem. Commun.*, 382 (1983)

[3] J. Roncali, A. Yassar, and F. Garnier, *J. Chim. Phys.*, **86**, 85 (1989)

[4] B. Rasch and W. Vielstich, *J. Electroanal. Chem.*, **370**, 109 (1994)

[5] J. Roncali, *Chem. Rev.*, **92**, 711 (1992)

[6] G. Tourillon and F. Garnier, *J. Electrochem. Soc.*, **130**, 2042 (1983)

[7] M. Dietrich, J. Heinze, G. Heywang, and F. Jonas, *J. Electroanal. Chem.*, **369**, 87 (1994)

[8] J. Roncali, A. Yassar, and F. Garnier, *J. Chem. Soc., Chem. Commun.*, 581 (1989)

[9] A. Yassar, J. Roncali, and F. Garnier, *Macromolecules*, **22**, 804 (1989)

[10] H. Wang, L. Toppare, and J. E. Fermandez, *Macromolecules*, **23**, 1053 (1990)

[11] J. C. Dubois, O. Sagnes, and F. Henry, *Synth. Met.*, **28**, C871(1989)

[12] M. Sato, S. Tanaka, and K. Kaeriyama, *J. Chem. Soc., Chem. Commun.*, 873 (1986)

[13] S. Hotta, S. D. D. V. Rughooputh, A. J. Heeger, and F. Wudl, *Macromolecules*, **20**, 212 (1986)

[14] M. Feldhues, G. Kampf,H. Litterer, J. Mecklenbarg, and P. Wegener, *Synth. Met.*, **28**, C487 (1989)

[15] F. Wudl, M. Kobayashi, and A. J. Heeger, *J. Org. Chem.*, **49**, 3382 (1984)

[16] J. P. Ferraris and T. M. Lambert, *J. Chem. Soc., Chem. Commun.*, 1268 (1991)

[17] M. Karikomi, C. Kitamura, S. Tanaka, and Y. Yamashita, *J. Am. Chem. Soc.*, **117**, 6791 (1995)

[18] J. Roncali, *Chem. Rev.*, **97**, 173 (1997)

[19] J. Roncali and F. Garnier, *New J. Chem.*, **4-5**, 237 (1986)

[20] S. Hotta, *Synth. Met.*, **22**, 103 (1988)

[21] A. Gald, E. T. Lwais. O. Y. Ataman, H. Zimmer, and H. B. Mark Jr., *J. Polym. Sci.*, **27**, 1891 (1989)

[22] J. Heinze, J. Mortensen, and K. Hinkelmann, *Synth. Met.*, **21**, 209 (1987)

[23] R. M. Eales and A. R. Hillman, *J. Electroanal. Chem.*, **250**, 219 (1988)

[24] G. Zotti and C. Schiavon, *Synth. Met.*, **39**, 183 (1990)

[25] J. P. Ferraris and R. T. Hanlon, *Polymer*, **30**, 1319 (1989)

[26] Y. Yumoto and S. Yoshimura, *Synth. Met.*, **13**, 185 (1985)

[27] F. Martinez, R. Voelkel, D. Naegele, and H. Naarmann, *Mol. Cryst. Liq. Cryst.*, **167**, 227 (1989)

[28] J. Roncali, F. Garnier. M. Lemaire, and R. Garrean, *Synth. Met.*, **15**, 323 (1986)

[29] B. Krische and M. Zagorska, *Synth. Met.*, **33**, 257 (1989)

[30] L. Funt and S. V. Lowen, *Synth. Met.*, **11**, 129 (1985)

[31] R. J. Waltman, J. Bargon and A. F. Diaz, *J. Phys. Chem.*, **87**, 1459 (1983)

[32] A. J. Downard and D. Pletcher, *J. Electroanal. Chem.*, **206**, 147 (1986)

[33] U. Barsch and F. Beck. *Electrochim. Acta*, **41**, 1761 (1996)

[34] B. Krische and M. Zagorska, *Synth. Met.*, **28**, C263 (1989)

[35] G. Zotti, S. Cattarin, and N. Comisso, *J. Electroanal. Chem.*, **235**, 259 (1987)

[36] R. M. Crooks, O. M. Chyan, and M. S. Wrighton, *Chem. Mater.*, **1**, 2 (1989)

[37] G. Zotti, G. Schiavon, and S. Zecchin, *Synth. Met.*, **72**, 275 (1995)

[38] P. Buttol, M. Mastragostino, S. Panero, and B. Scrosati, *Electrochim. Acta*, **31**, 783 (1986)

[39] A. R. Hillman, D. C. Loveday, M. J. Swann, R. M. Eales, A. Hamminett, S. J. Higgins, S. Bruckenstein, and C. P. Wilde, *Fara. Discus. Chem. Soc.*, **88**, 151 (1989)

[40] K. Meerholz and J. Heinze, *Electrochim. Acta*, **41**, 11 (1996)

[41] R. A. Friedel and M. Orchin, *Ultraviolet Spectra of Aromatic Compounds*, Wiley, New York, 1951

[42] R. Hajlaoui, D. Fichou, G. Horowitz, B. Nessokh, M. Constant, and F. Garniar, *Adv. Mater.*, **9**, 557 (1997)

[43] R. O. Loutfy, *J. Chem. Phys.*, **66**, 4781 (1977)

[44] L. E. Lyons, *Aust. J. Chem.*, **33**, 1717 (1980)

[45] A. F. Diaz, J. Crowley, J. Baugon, G. P. Gardini, and J. B. Torrance, *J. Electroanal. Chem.*, **121**, 355 (1981)

[46] G. Tourillon and F. Garnier, *J. Phys. Chem.*, **87**, 2287 (1983)

[47] L. Laguren-Davidson, Chiem Van Pham, H. Zimmer, and H. B. Mark Jr., *J. Elctrochem. Soc.*, **135**, 1406 (1988)

[48] J. L. Sauvajol, D. Chenouni, J. P. Pere-Oorte, C. Chorro, B. Moukala, and J. Petrissans, *Synth. Met.*, **38**, 1 (1990)

[49] D. Delabouglise, R. Garreau, M. Lemaire, and J. Roncali, *New. J. Chem.*, **12**, 155 (1988)

[50] R. M. Eales and A. R. Hillman, *J. Mater. Sci.*, **25**, 3806 (1990)

[51] R. J. Waltman and J. Bargon, *Tetrahedron*, **40**, 3963 (1984)

[52] R. J. Waltman and J. Bargon, *J. Can. Chem.*, **64**, 76 (1986)

[53] M. Lemaire, W. Buchner, R. Garreau, A. J. Huynh, A. Guy, and J. Roncali, *J. Electroanal. Chem.*, **281**, 293 (1990)

[54] P. Marque, J. Roncali, and F. Garnier, *J. Electroanal. Chem.*, **218**, 107 (1987)

Chapter 4

Electrochemical, Spectroscopic, and *In Situ* Conductivity Studies of Poly-CDM

4.1 Introduction

Conducting polymers prepared from bithiophene (BTh) precursors with electron withdrawing groups at an sp^2-carbon bridging the β and β' positions form an important and interesting branch of conducting polymers with reduced band-gaps (E_g < 1.5 eV) [1, 2]. The first example in this branch was the polymer electrosynthesized from cyclopenta[2,1-*b*:3,4-*b*']-dithiophen-4-one (CDT; structure **1**) [3]. Poly-CDT has a band-gap of 1.10 ~ 1.20 eV determined by spectroelectrochemical experiments [3] and later confirmed by the cyclic voltammograms [4]. Compared with the band-gap of its parent, polybithiophene (poly-BTh) (ca. 2.23 eV, see section **3. 3. 2**), the band-gap of poly-CDT is significantly lowered. This is ascribed to the electron withdrawing effects of the ketone group which decreases the aromatic character and increases the quinoid character along the conjugated backbone [1-3]. Following this clue, stronger electron withdrawing groups

replacing the ketone group at the bridging carbon are expected to reduce the band-gap further. Hence, the monomer, 4-dicyanomethylene-4*H*-cyclopenta[2,1-*b*;3,4-*b'*]dithiophene (CDM; structure **2**), which has dicyanoethene, a stronger electron withdrawing group than the ketone group, was successfully synthesized [5]. The electronic absorption spectrum of an electrogenerated poly-CDM film in the neutral state exhibits a bathochromic extension toward the near IR region leading to a band-gap of ca. 0.8 eV, one of the lowest band-gap values reported to date [1, 6-8]. The electrochemical band-gap judged from its cyclic voltammetry is consistent with this optical result [5]. The band-gap value for poly-CDM is 0.3 ~ 0.4 eV lower than that for poly-CDT, strongly supporting the success of this methodology. More evidence is that the substitution of one of cyano groups in CDM with a (nonafluorobutyl)sulfonyl group has been reported to further reduce the band-gap for this type of conducting polymers to 0.67 eV [9].

Structure 1

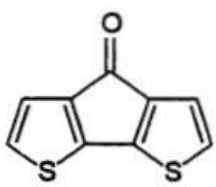

cyclopenta[2,1-*b*:3', 4'-*b'*]-dithiophen-4-one

Structure 2

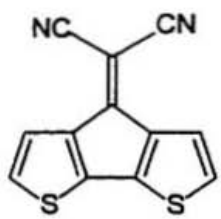

4-(dicyanomethylene)-4*H*-cyclopenta [2, 1-*b*:3, 4-*b'*]dithiophene

Among the conducting polymers in this family, poly-CDM is of particular interest, because it has one of the highest known formal potentials for n-doping (-0.78 V vs. SCE) [1, 5]. It is therefore reasonably stable when n-doped, and attractive for use in polymer p-n junction devices. However, there are a lack of further studies on this polymer. We investigated this polymer in detail (including the synthesis, and electrochemistry, spectroelectrochemistry, and *in situ* conductivity for both p-doping and n-doping of the polymer), and report the results in this chapter.

4.2 Redox potentials and band-gap of CDM

4.2.1 Redox potentials of CDM

The monomer, CDM, was not very soluble in acetonitrile (solubility < 2 mM), but more soluble in nitrobenzene and benzonitrile (solubility $\sim$ 10 mM). In our experiments, nitrobenzene, which was carefully purified, was used as the solvent. **Fig. 4.1** shows cyclic voltammograms of the oxidation (first two cycles) and reduction of CDM monomer (5 mM) at a Pt electrode in nitrobenzene in presence of 0.1 M Bu_4NPF_6.

Oxidation of CDM monomer was investigated in the potential range from 0.00 to +1.50 V at a scan rate of 100 mV/s. It shows electrochemically irreversible behavior.

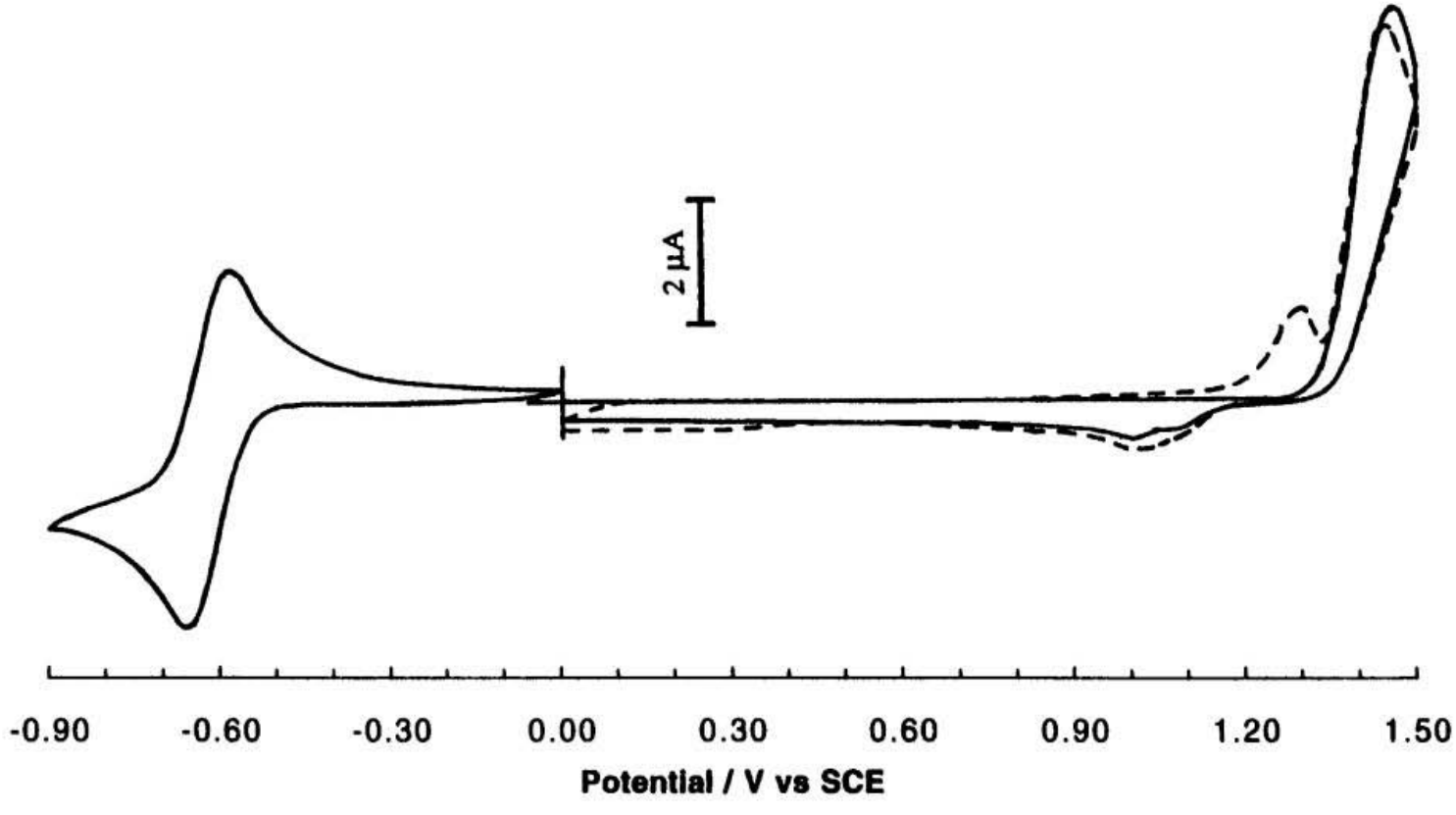

Fig. 4.1 Cyclic voltammograms of the oxidation (the first two cycles; 0.00 - 1.50 V) and the reduction (0.00 - -0.90 V) of CDM (5 mM) in nitrobenzene containing 0.1 M Bu_4NPF_6. Scan rate: 100mV/s

During the first cycle (solid line), as the potential is scanned forward, CDM begins to oxidize at ca. +1.31 V, and then the oxidation current increases quickly to reach a maximum at +1.45 V. In the reverse scan, there is a reduction wave with a main current peak at +1.02 V and a small shoulder at +1.10 V, both of which are due to the de-doping (reduction) of the polymer deposited on the electrode during the forward scan. In the second cycle (dashed line), apart from the main oxidation current at +1.44 V as in the first scan, another well defined oxidation current peak is observed at lower potential (ca. +1.31 V). This peak was absent in the first cycle, and so clearly results from the p-doping of the polymer. The reduction current has increased compared to the first cycle.

Reduction of CDM was studied in the potential range from 0.00 to -0.90 V. In contrast to the normal reduction behavior of other Th precursors [4], which is irreversible in most cases, CDM shows a wave form typical of a one-electron reversible reaction. The peak potential separation ($\Delta E = E_{pa} - E_{pc}$) is close to 60 mV, the reduction peak current (i_{pc}) equals the oxidation peak current (i_{pa}), and the peak currents (both i_{pc} and i_{pa}) are proportional to the square root of the scan rate. The formal potential for this reduction is determined as -0.63 V (average of E_{pa} and E_{pc}). From the onset potentials for the oxidation and reduction of CDM, the electrochemical band-gap of the CDM monomer is found to be ca. 1.8 V.

E_{pa} for the oxidation of CDM is +1.45 V, compared to +1.32 V for BTh [4, 10]. Thus, the bridging dicyanoethene group does not appear to decrease greatly the energy level of the HOMO in CDM compared to BTh. This is consistent with the antisymmetry

of that orbital which places a node at the bridging group [5]. However, E_{pc} for the reduction of CDM is -0.68 V, which is much less negative than that for BTh (-2.58 V, see section **3.2.1**), indicating that the LUMO energy level of CDM has been reduced greatly [5]. This effect is obviously due to the strong electron withdrawing group -- dicyanoethene. This substantial shift of the LUMO to low energy level makes CDM one of Th oligomers (Ths, BThs, and TThs) with the lowest band-gap [1].

4.2.2 Optical study of CDM

Acetonitrile was adopted instead of nitrobenzene as the solvent to carry out UV-Vis absorption spectroscopy of CDM, since nitrobenzene has a strong absorption at 450 nm. **Fig. 4.2** shows the resulting UV-Vis spectrum of CDM in acetonitrile. CDM has an optical absorption maximum at 570 nm, associated with the π-π^* electronic transition. Owing to the strong electron-withdrawing effect of the dicyanoethene group, the absorption maximum is shifted ca. 270 nm bathochromically, compared to its parent, BTh. The absorption edges at 730 nm for CDM, correspond to an optical band-gap of ca. 1.7 eV, which is about 2 eV lower than for BTh, and even lower than that of poly-Th (2.1 eV) [11]. The optical band-gap of CDM is in agreement with the electrochemical band-gap (1.8 V).

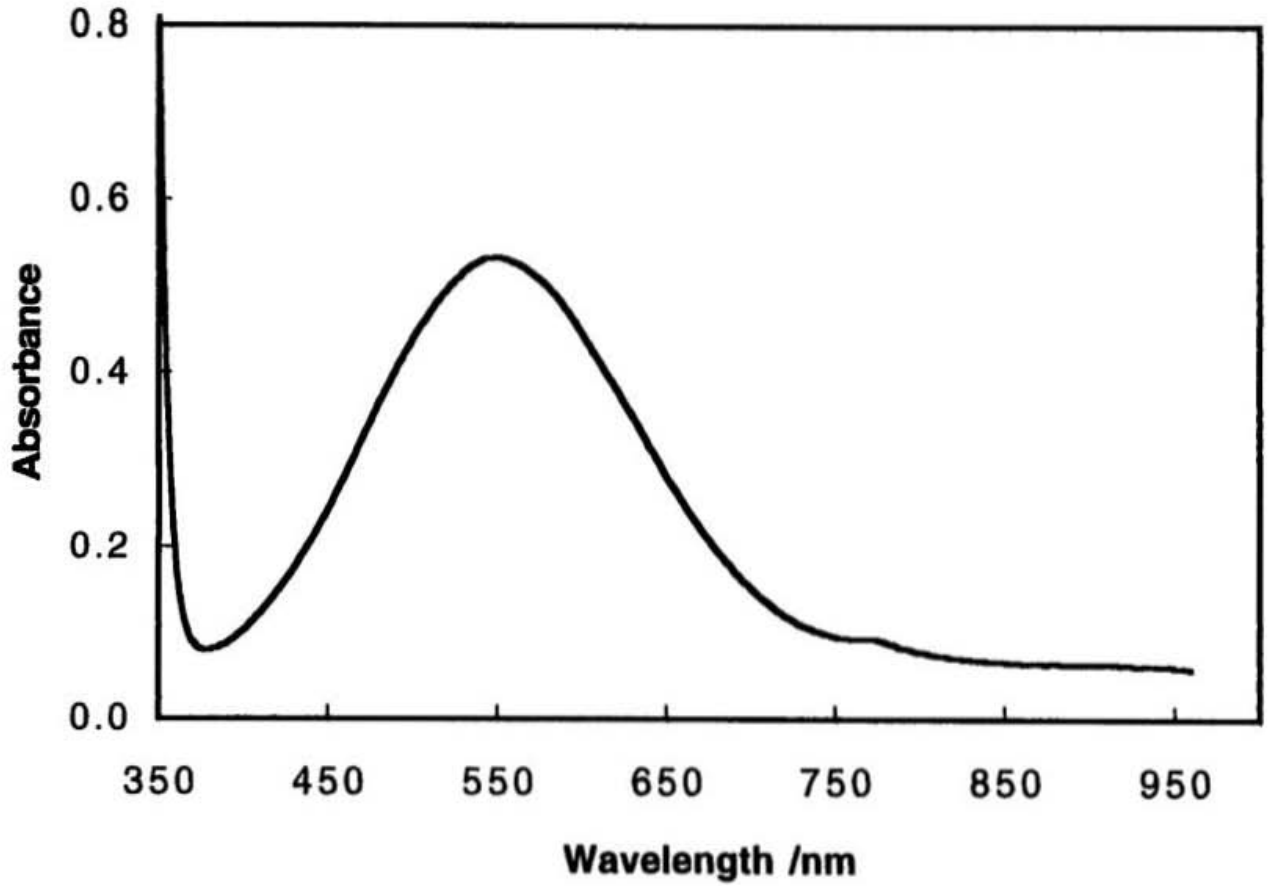

Fig. 4.2 UV-Visible absorption spectrum of CDM in acetonitrile

4.3 Electropolymerization of poly-CDM

Several electrochemical synthesis techniques, such as repetitive potential sweep, constant current, and potential step, were employed in our experiments to synthesize poly-CDM films.

4.3.1 Repetitive potential sweep

Fig 4.3 shows the typical cyclic voltammograms for the electrogeneration of a poly-CDM film on a Pt electrode in 5 mM CDM solution in nitrobenzene containing 0.1 M Bu_4NPF_6. Continuous potential scanning between 0.00 and 1.50 V results in the current responses at peak A, B and C, and the later two peaks become progressively higher and higher. Peak A is the oxidation of the monomer to the radical cation. Its position is independent of cyclic numbers, that is, there is no difference between depositing the polymer on the polymer coated electrode and on the bare Pt electrode, supporting a radical-radical coupling (RRC) rather than a radical-substrate coupling (RSC) electropolymerization mechanism [12] for the growth of the poly-CDM film. Peak B is the oxidation (p-doping) of the polymer deposit, and peak C is its reduction (de-doping) in the reverse scan. A red or red-brown poly-CDM film is visible on the electrode after multiple

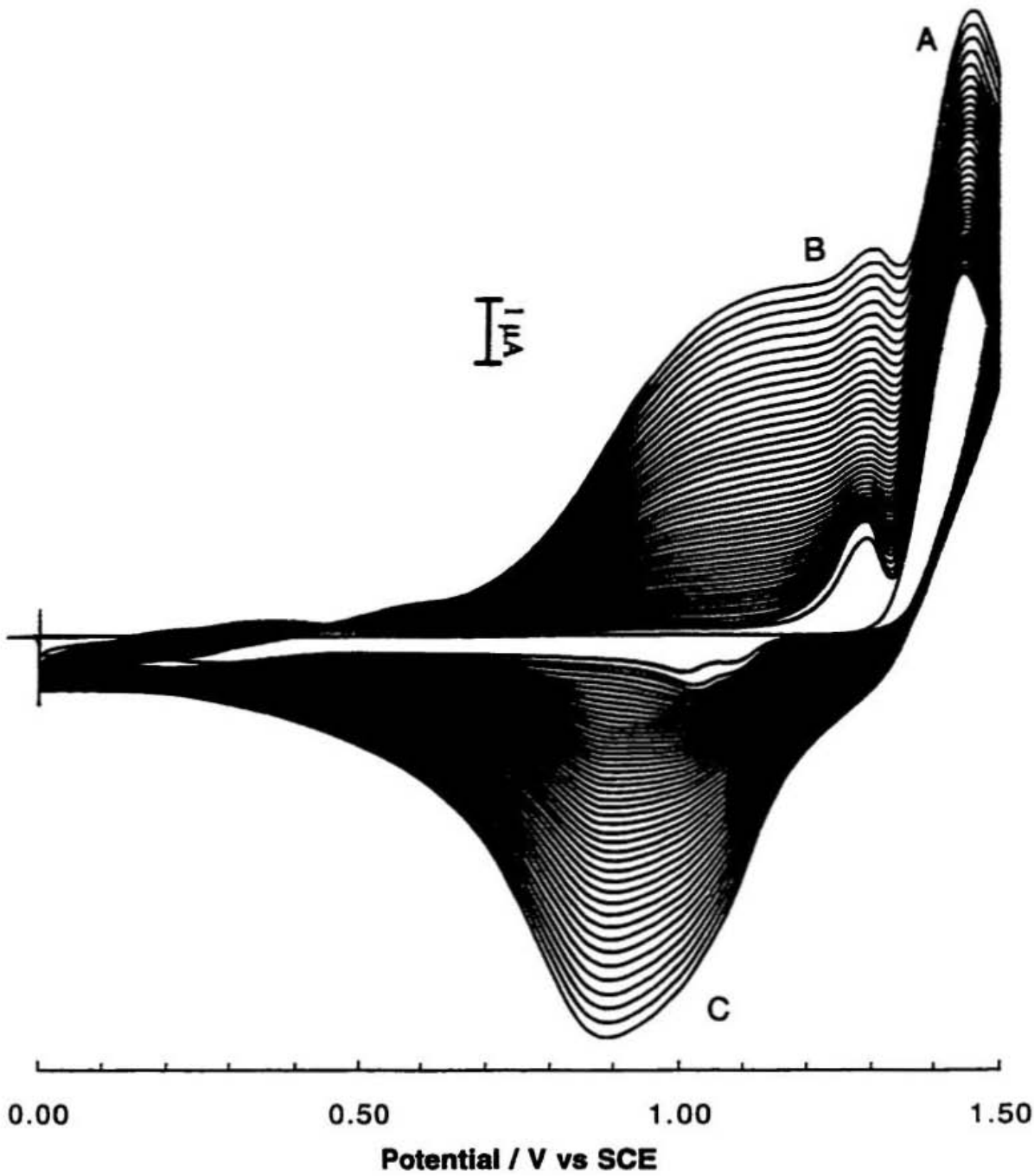

Fig. 4.3 Repetitive potential sweep polymerization of CDM (5 mM) on a Pt electrode in nitrobenzene containing 0.1 M Bu_4NPF_6
Potential range: 0.00 - 1.5 V; Scan rate: 100 mV/s

cycles. Poly-CDM films adhere to the Pt electrode tightly, unlike poly-BTh films, which are powdery and easily wiped off [13], suggesting the poly-CDM films are compact.

4.3.2 Constant current

Fig. 4.4 shows potential-time (E-t) curves for the electropolymerization of CDM in the same solution as specified in section **4.3.1** under galvanostatic synthesis conditions. Current densities employed in the experiment were 0.05, 0.1, 0.2, 0.3, and 0.4 mA/cm^2.

At a low current densities, e.g. 0.05 mA/cm^2, the E-t curve (curve (**a**)) shows two different stages. The potential exhibits an increasing slope in the early stage, where progressive nucleation takes place, and then becomes constant at 1.37 V as the polymer film becomes thicker in the second stage. For current densities of 0.1 and 0.2 mA/cm^2, a different curve form (curve (**b**) and (**c**)) is obtained. When the current is applied, the potential rises rapidly to a constant value of ca. +1.4 V. When electropolymerization is carried out at higher current densities (e.g. 0.3 mA/cm^2), the curve (curve (**d**)) differs again from the previous cases and is characterized by a plateau at ca. +1.45 V for 32 s, corresponding to the potential for electropolymerization of poly-CDM, followed by a second plateau at ca. +1.71 V, where the simultaneous overoxidation of the polymer is probably occurring. This phenomena has also been observed when polymerizing Th at constant current [14-16]. By comparison of the resulting CV of poly-CDM synthesized at 0.3 mA/cm^2 with that at 0.1 mA/cm^2, the effect of overoxidation is clearly seen, since the

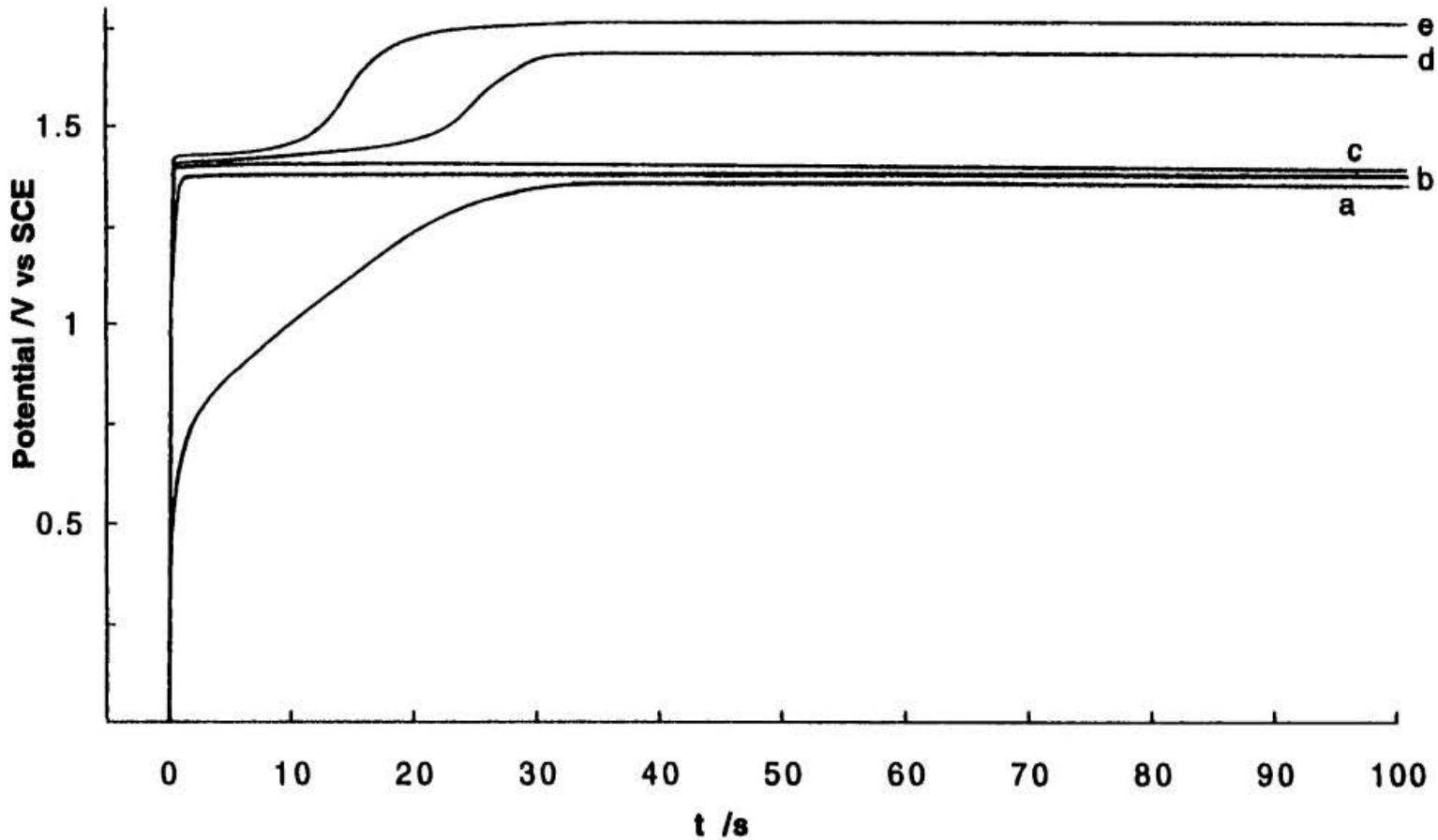

Fig. 4.4 Galvanostatic polymerization of CDM (5 mM) in nitrobenzene containing 0.1 M Bu_4NPF_6 at currents of (a) 0.05, (b) 0.1, (c) 0.2, (d) 0.3, (e) 0.4 mA/cm^2

former polymer shows lower doping (p- and n-type) currents and the doping/undoping waves are much less symmetrical. Therefore, to prepare poly-CDM films of good quality, low current (less than 0.2 mA/cm^2) should be used (This value is very low compared to a reported current of 750 mA/cm^2 [5]). When the current density is increased to 0.4 mA/cm^2 (curve (e)), the second plateau occurs after only 18 s polymerization, in agreement with the Sand equation [17]

$$i\tau^{1/2} = \frac{nFAD^{1/2}\pi^{1/2}}{2} = constant \qquad \textbf{4-1}$$

from which the diffusion coefficient of 2.52×10^{-6} cm^2 s^{-1} is obtained, by using n=2.5 (i.e., 2e/molecule for polymerization, and 0.5 for doping of the polymer).

In these experiments, we found that fairly low doping charges were obtained for poly-CDM films due to the low polymerization efficiency. To obtain the synthesis efficiency, a comparison experiment between poly-CDM and poly-BTh was carried out. Under the same polymerization conditions (0.1 mA/cm^2 for 400 s), a 2.85 mC/cm^2 doping charge was obtained for the resulting poly-CDM film, while 7.08 mC/cm^2 was obtained for poly-BTh. Assuming that the doping level of both polymers are equal and the synthesis efficiency for poly-BTh was 100%, the synthesis efficiency for poly-CDM is calculated to be ca. 40%.

Film thickness can be estimated from the polymerization charge. A calibration relationship of 4.6 μm per 1 C cm^{-2} was obtained from scanning electron microscopy of

films on Pt wire. This relationship is close to that obtained for polymethylthiophene (poly-MTh; ca. 5 μm per 1 C cm^{-2}) [19]. But CDM contains two thiophene units in its structure, therefore, the synthesis efficiency should be slightly lower than 50%, in agreement with our result of ca. 40%.

4.3.3 Potential step

Electropolymerization of CDM by potential step experiments was carried out in the same solution as in Section **4.3.1**. **Fig. 4.5** shows current-time (I-t) transients from a series of experiments in which the potential was stepped from +0.00 V to a value in the range from +1.40 V to +1.46 V. At all potentials studied, the chronoamperometric responses exhibited a huge current spike upon application of the potential step, followed by a monotonic current decay to an approximately constant small value. This behavior is similar to that seen for BTh [20], but different from that for Ths containing only one Th unit [21-25]. For the later Th monomers, the electrodeposition of polymers by potential step techniques generally presents a well defined I-t curve with a characteristic rising I-t transient in the initial stages, then in most cases a decay of the current to a constant value. Hillman [21] analyzed these curves and concluded that, for these polymers, a monolayer of polymer is initially formed, on which instantaneous nucleation and three-dimensional growth then occurs. The large number of overlapping nuclei formed during the early stages of deposition led to subsequent one-dimensional growth perpendicular to the

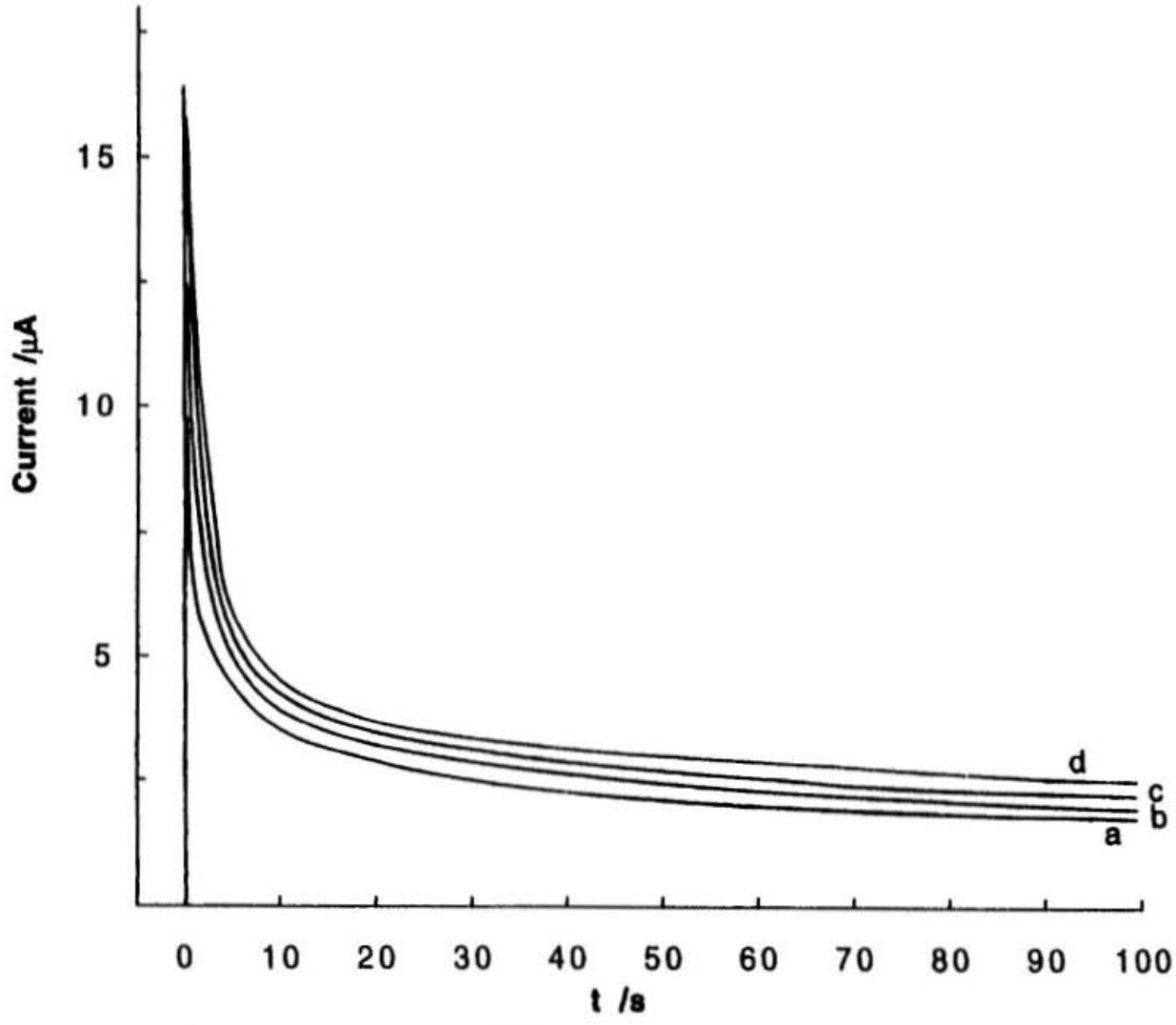

Fig. 4.5 Electropolymerization of CDM (5 mM) in nitrobenzene containing 0.1 M Bu_4NPF_6 by potential step. (a) 1.40 V, (b) 1.42 V, (c) 1.44 V, (d) 1.46 V

electrode surface with a linear increase in thickness with time. The difference may arise from the fact that the growth of poly-CDM is controlled by diffusion of the electroactive monomer, due to the low concentration of CDM and the high viscosity of the nitrobenzene solution.

The time dependence of the current under such circumstances is described by the Cottrell equation [17]

$$i=nFA(\frac{D}{\pi t})^{1/2}C \qquad \textbf{4-2}$$

A linear $i \sim t^{-1/2}$ plot is diagnostic for diffusion controlled behavior. **Fig. 4.6** shows the predicted linearity for the i-t curve at 1.44 V. From the slope, a value of the diffusion constant for CDM (5mM, in nitrobenzene containing 0.1 M Bu_4NPF_6) is obtained to be 2.15×10^{-6} cm^2/s, with n=2.5. This value is in accordance with that obtained by the Sand equation, and is slightly lower than that for Th in acetonitrile.

4.4 Electrochemistry of poly-CDM

The cyclic voltammetry, as a function of the sweep rate, of a poly-CDM coated Pt electrode in acetonitrile containing 0.1 M Bu_4NPF_6 is shown in **Fig. 4.7**. The polymer was

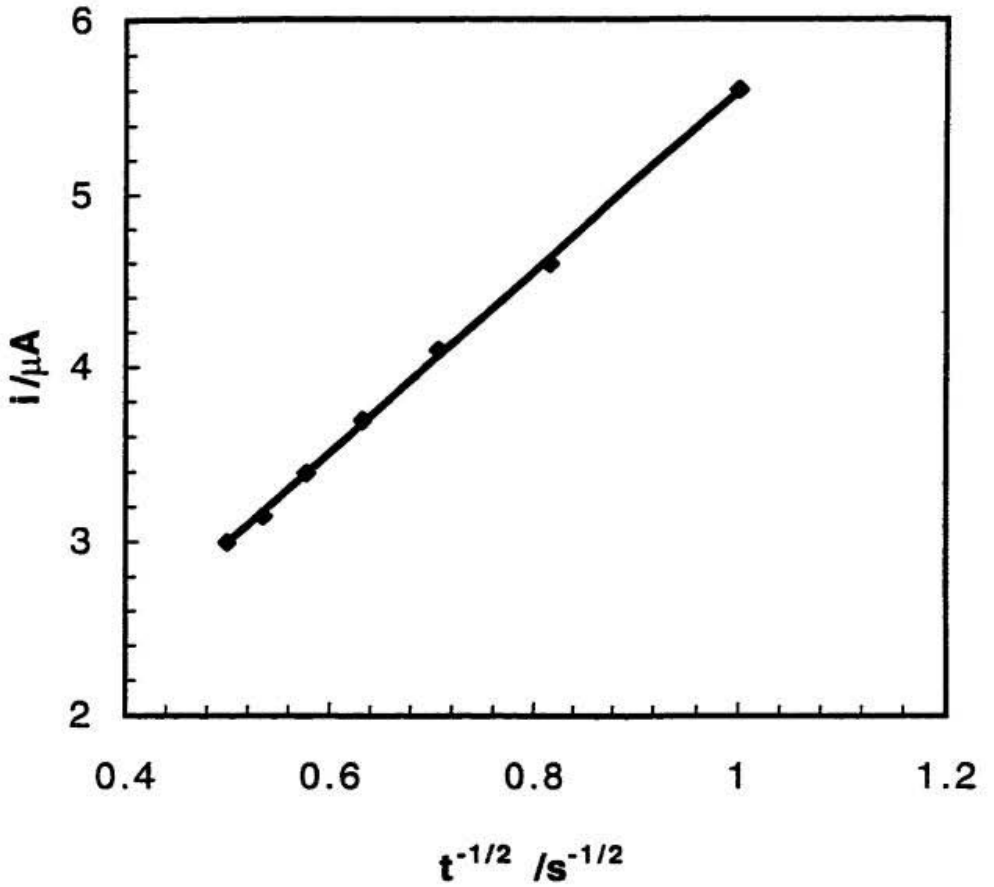

Fig. 4.6 Plot of i vs. $t^{-1/2}$ derived from a potential step synthesis curve at 1.44 V

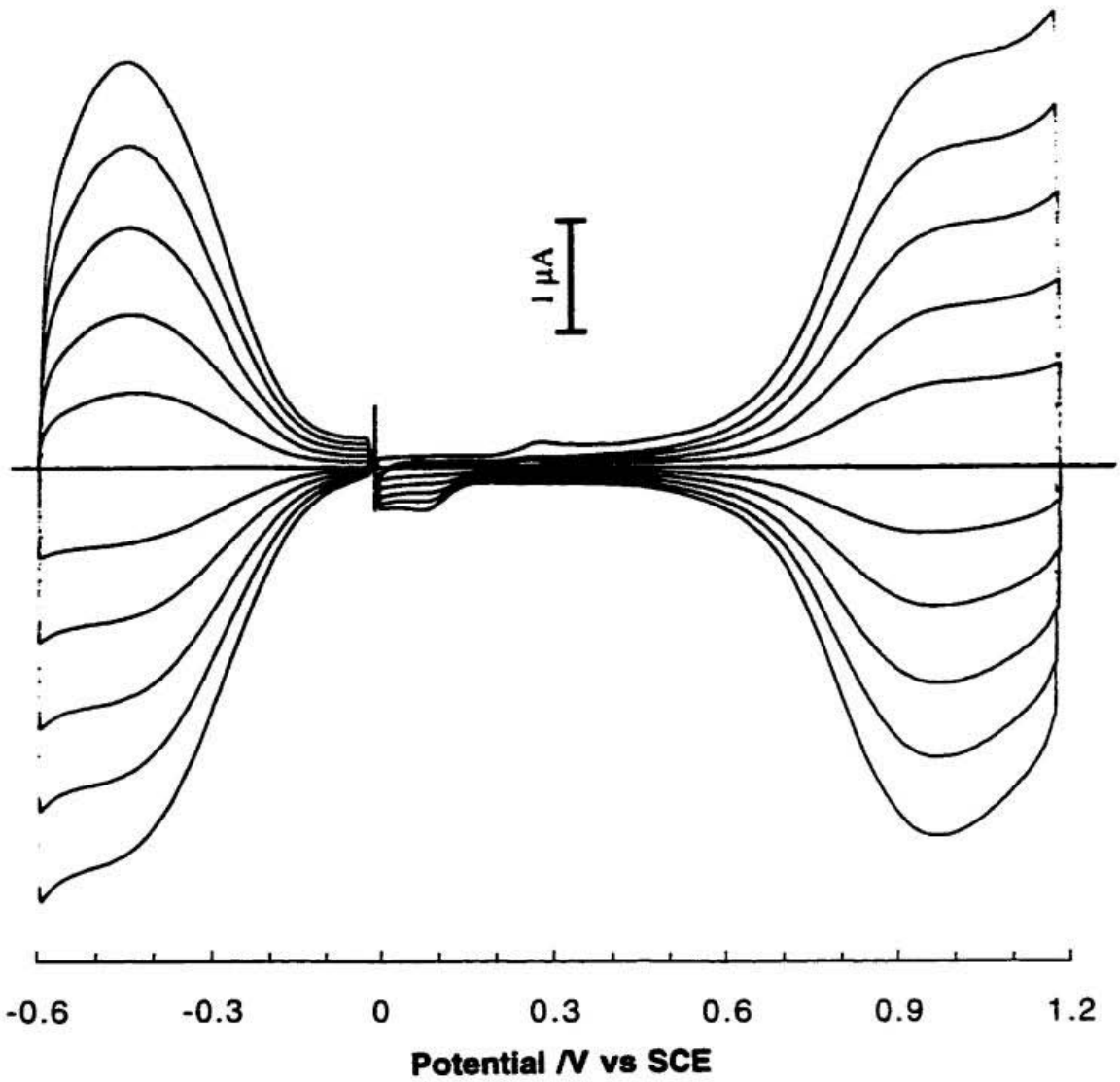

Fig. 4.7 Cyclic voltammograms of p-doping (0.00 - 1.20 V) and n-doping (0.00 - -0.60 V) of poly-CDM in acetonitrile containing 0.1 M Bu_4NPF_6 at different scan rates (100, 80, 60, 40, 20 mV/s)

synthesized at 0.1 mA/cm^2 for 400 s on a Pt electrode. From the figure, the electrochemical data of poly-CDM are summarized in Table **4. 1**.

Table 4.1 Electrochemical data for the p-doping and n-doping of poly-CDM

Scan rate /mV/s	$E_{p(ox)}$ /V	$i_{p(ox)}$ /μA	$E_{p(re)}$ /V	$i_{p(re)}$ /μA	$E_{n(re)}$ /V	$i_{n(re)}$ /μA	$E_{n(ox)}$ /V	$i_{n(ox)}$ /μA
20	0.99	0.74	0.95	-0.59	-0.48	-0.70	-0.44	0.69
40	1.01	1.45	0.96	-1.25	-0.48	-1.40	-0.44	1.39
60	1.02	2.20	0.97	-1.85	-0.49	-2.15	-0.44	2.14
80	1.02	2.91	0.97	-2.65	-0.50	-2.90	-0.44	2.92
100	1.03	3.72	0.97	-3.36	-0.50	-3.65	-0.44	3.68

P-doping (between 0.00 and 1.20 V) exhibits a symmetric reversible (in the context of conducting polymers) redox wave form with the doping peak at 1.03 V and the dedoping peak at 0.97 V (100 mV/s). Peak currents (both p-doping and p-dedoping) are linearly dependent on the potential sweep rate. The p-dedoping charge is equal to the doping charge. These curves are very similar in shape to those obtained for poly-Ths derived from monomers with one Th unit (e.g. Th, MTh) [26, 27], but not for the polymers synthesized from BTh and TTh precursors [4, 26, 28, 29], which generally produce sharp and narrow oxidation peaks. This fact suggests that poly-CDM is produced with a long conjugated chains. Other evidence supporting this result is that the p-doping potential of poly-CDM is comparable to or even lower than the value for poly-BTh. If poly-CDM has the same chain length as poly-BTh, it should have a higher p-doping

potential (although this difference should not be large), because of the strong electron withdrawing effect of the dicyanoethene group. Therefore, the reduced p-doping peak potential compared to BTh means that longer conjugated chain lengths have probably been achieved for poly-CDM.

The very high formal potential for reduction of CDM potential ($E^{0'}$ =-0.63 V) extends to its polymer. N-doping of the resulting polymer was performed between 0.00 to -0.60 V. The polymer has a n-doping formal potential of -0.47 V (average of the n-doping and de-doping peak potentials), about 1.5 V higher than that of poly-BTh [4], reflecting a substantial reduction of the LUMO energy. In fact, this formal potential is one of the highest potentials for n-doping of known polymers [1]. The voltammetric features for n-doping are similar to those observed for p-doping. Linear relationships between peak currents and scan rates are obtained for both the n-doping and n-dedoping processes. The ratio of the n-dedoping charge to the n-doping charge is approximately equal to unity. The peak potential separation is less than 60 mV for all scan rates studied. The above facts indicate that n-doping of poly-CDM is very reversible. These characteristics differ from those observed for other poly-Ths [30-35], which have a relatively broad n-doping wave, and a sharp n-dedoping peak in the reverse scan. The electrochemical band-gap for poly-CDM is ca. 0.8 V.

Fig. 4.8 (**a**) and (**b**) illustrates the CVs of p-doping and n-doping respectively of a poly-CDM film over different potential ranges. When potential was scanned between 0.00 and 1.20 V, and 0.00 and 1.40 V, doping levels of 22% and 33% were calculated

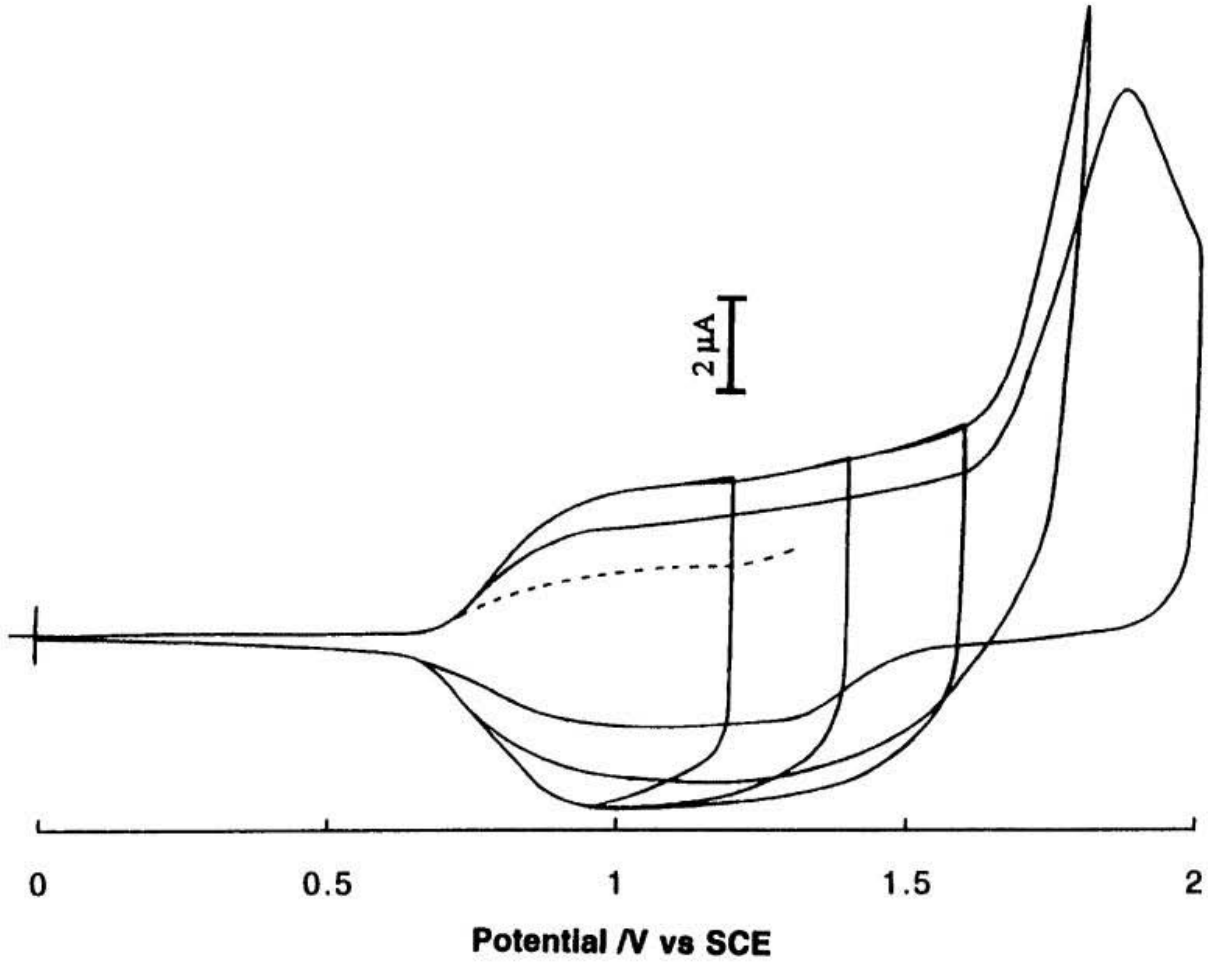

Fig. 4.8 (a) Oxidation of poly-CDM over different potential ranges in acetonitrile containing 0.1 M Bu_4NPF_6. The higher switch potentials from left to right are +1.20, +1.40, +1.60, +1.80, and +2.00 V respectively. Scan rate: 100 mV/s

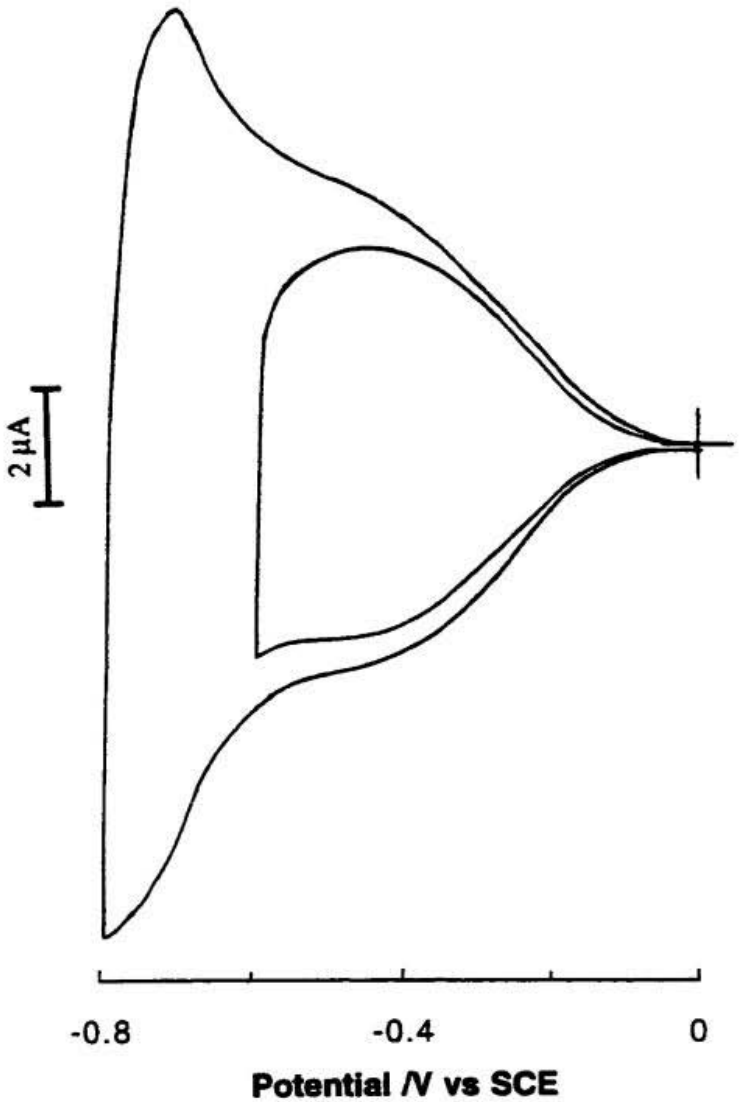

Fig. 4.8 (b) Reduction of poly-CDM over different potential ranges in acetonitrile containing 0.1 M Bu_4NPF_6 . Scan rate: 100 mV/s The lower switch potentials from right to left are -0.60 and -0.80 V

respectively, by using the synthesis efficiency of 40% (section **4.3.2**) and equation **3-1**. Over these potential ranges, poly-CDM has good stability. The current shows a slight decrease during the first several cycles, and then becomes unchanged in the following cycles. When the upper potential is increased to +1.6 V, a doping level of 45% is achieved in the first cycle. However, during following cycles the current decreases gradually. After 25 cycles, 93% of the original activity remains. For the potential range of 0.00 to 1.80 V, the current rises quickly after 1.65 V as rapid overoxidation of the polymer begins. De-doping in the reverse scan shows a significant loss of the charge. When the potential is switched at 2.0 V, an overoxidation peak is observed at 1.86 V.

For n-doping of poly-CDM, multiple cycles do not result in a significant reduction of the current, when the potential is cycled between 0.00 and -0.60 V. A doping level of 19% is obtained. But for the potential range from 0.00 to -0.80 V, a 13% decrease in current is observed after 15 cycles.

4.5 Spectroelectrochemical studies of poly-CDM

A thin film of poly-CDM was galvanostatically deposited on an ITO electrode ($10\Omega/cm^2$, 0.8 cm^2, Donnelly Corp.) for spectroelectrochemical measurements. **Fig. 4.9 (a)** and **(b)** shows the UV-Vi-NIR absorption spectra of the polymer under p-doping (from 0.20 to 1.20 V) and n-doping (from 0.00 to -0.80 V) conditions, respectively.

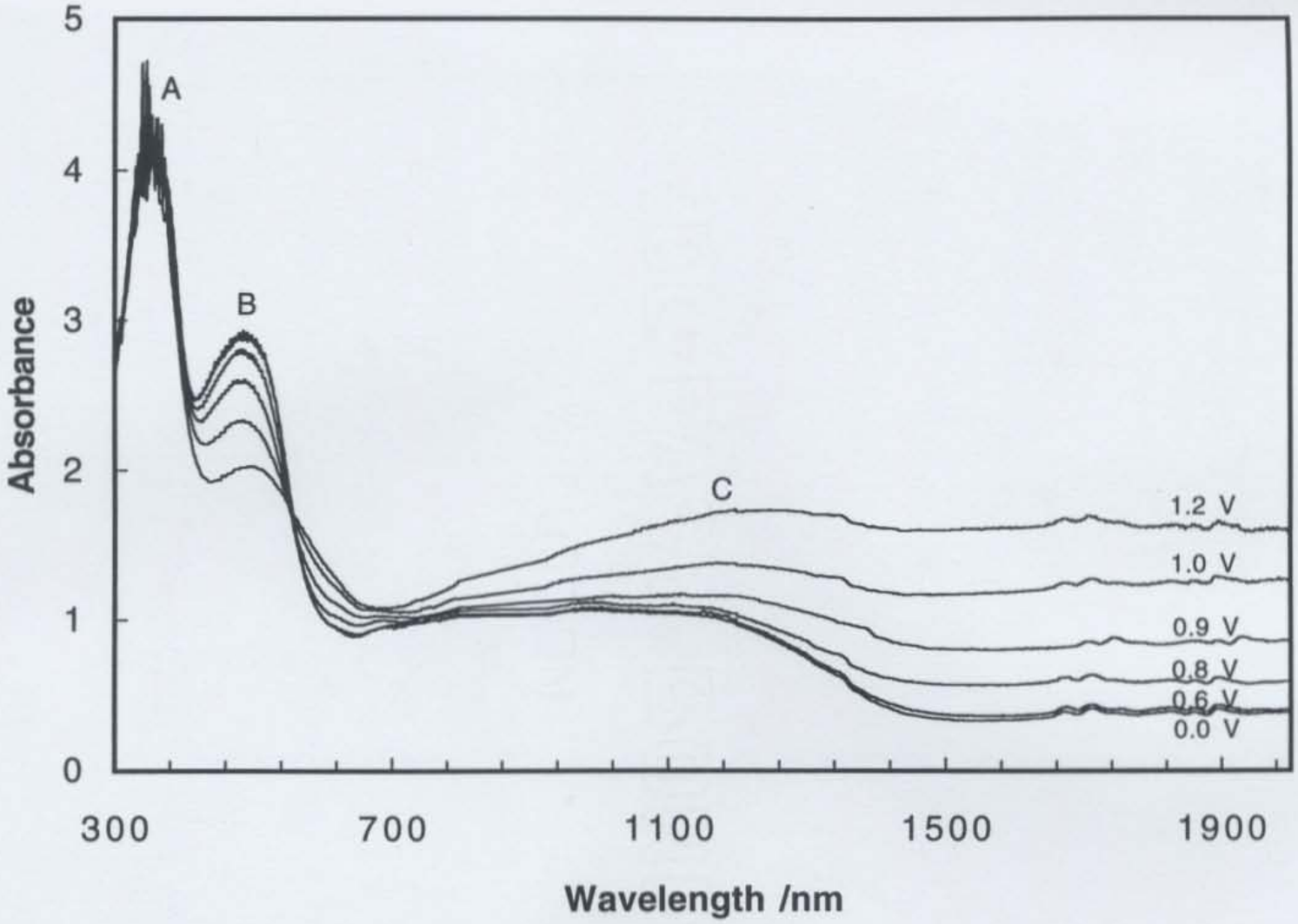

Fig. 4.9 (a) Spectroelectrochemical studies of p-doped poly-CDM

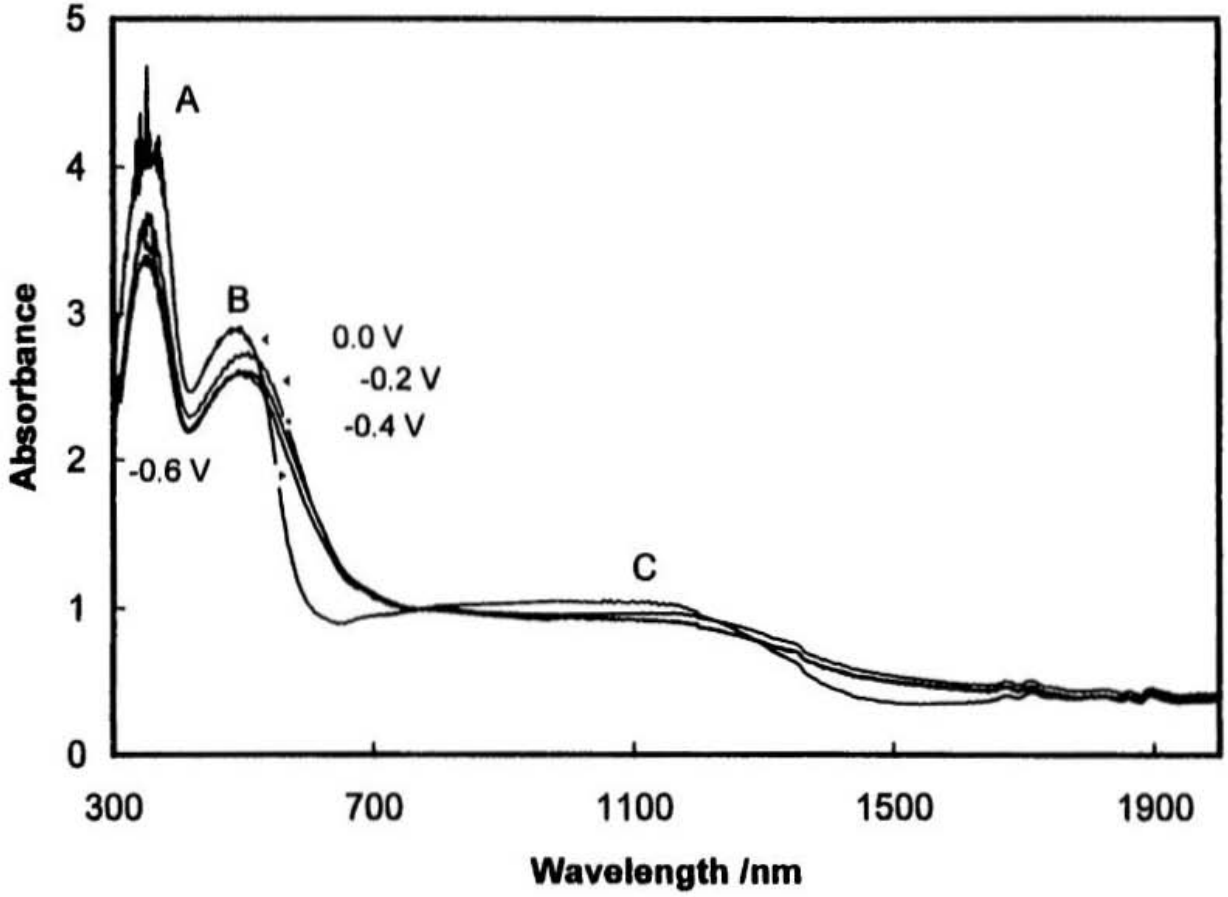

Fig. 4.9 (b) Spectroelectrochemical studies of n-doped poly-CDM

In **Fig. 4. 9 (a)**, at 0.0 V the polymer is undoped and in the neutral state. The optical spectrum exhibits two wavelength absorption peaks, and a broad π-π^* band with a maximum at ca. 1000 nm. For convenience, these three absorptions are named as absorptions A, B, and C as the wavelength increases. From the onset (ca. 1490 nm) of absorption C, a band-gap of 0.83 eV is obtained, in excellent agreement with the band-gap derived from CV. This band-gap is much lower than that of poly-BTh (2.23 eV), making poly-CDM one of the lowest band-gap conducting polymers known.

With increasing potential, poly-CDM is oxidized to the p-doped state. The intensity of B decreases while A increases only slightly. In the NIR region, a new absorption (1500-2000 nm) grows. It should be noted that when the potential is increased to 0.60 V, the intensity of C decreases slightly compared to its value at 0.0 V, but when higher potentials are applied, it increases. This change is ascribed to a coincidental overlap of a peak that decreases in intensity upon doping with one that increases in intensity [5]. These optical results for p-doping are in accordance with features in the CV. When the potential increases from 0.20 to 0.60 V, the polymer is only very lightly doped, indicating little change the absorption curve. In the potential range from 0.80 to 1.00 V, dramatic changes in absorption intensity are observed, corresponding to a rapid increase of the doping level as seen in CV.

Upon n-doping (**Fig. 4.9 (b)**), however, the absorption spectra are quite different from those for p-doping. Absorption A decreases, and absorption B decreases and shifts slightly to the red. Absorption C decreases only slightly, and there is a small absorption

increase at around 1500 nm. For potentials of -0.40 and -0.60, no significant difference in the absorption spectra are observed. When the potential is decreased from 0.00 to -0.20 V, a relatively large change in the spectrum is observed. The electronic absorption changes upon n-doping indicate that the n-doping is located on the substituent and not extensively delocalized along the thiophene backbone.

4.6 *In situ* conductivity measurements

The *in situ* electronic conductivities of poly-CDM films against potential were measured in acetonitrile containing 0.1 M Bu_4NPF_6 by using the dual-electrode sandwich technique [36]. **Fig. 4.10** displays a log(conductivity) vs. potential plot for a 0.23 μm poly-CDM film and the corresponding CV of this film. The p-type conductivity of the polymer rises to a maximum of 0.59 S/cm (average of four films) at 1.2 V and is very stable. The n-type conductivity is ca. 100 times smaller, peaking at an average (four films) of 5.4 mS cm^{-1} at ca. -0.5 V. This maximum is reproducible over multiple scans. The ratio of the n- to p-type conductivity for poly-CDM is similar to that observed for poly(3-methylthiophene) [37]. As the polymer is doped (n- and p-) its conductivity increases approximately exponentially with potential (with decreasing E for n-doping), as observed in previous studies of polythiophene [19] and polypyrroles [38]. This reflects the exponentially increasing concentration of charge carriers [38]. The p-type conductivity

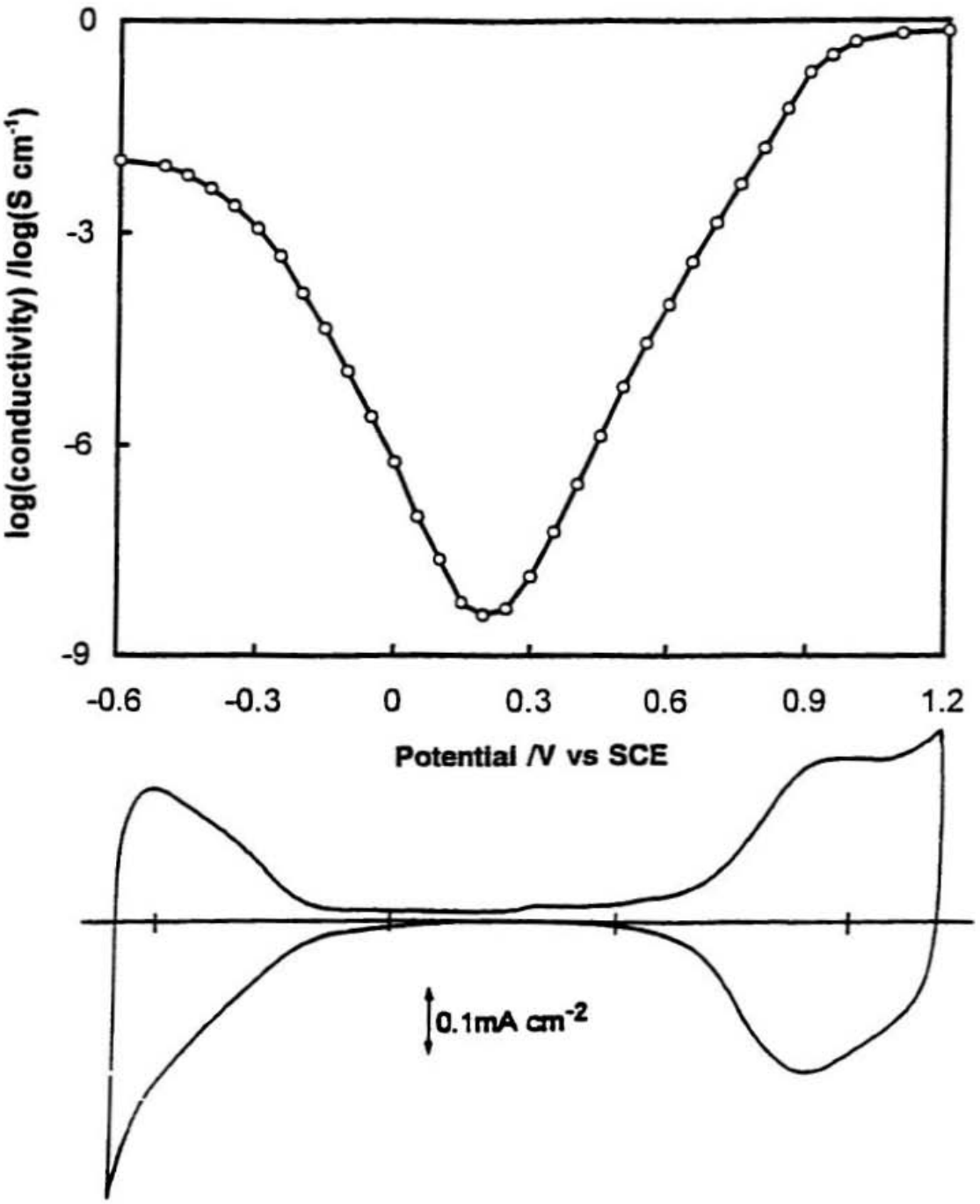

Fig. 4.10 Plot of log(conductivity) vs. potential for a 0.23 μm poly-CDM film and the corresponding cyclic voltammogram of this film

levels off at high potentials when the valence band is approximately half empty [39]. The peak in the n-type conductivity corresponds to a half-full conduction band, with further reduction resulting in a reversible decrease in conduction as the density of states begins to decrease [37]. This indicates that the conduction band is significantly narrower than the valence band, as in poly(3-methylthiophene) [37], and in agreement with computational results [40].

The low n-type conductivity relative to the p-type conductivity is due in part to the lower doping level that can be achieved. The doping level at a particular potential can be calculated from the charge under the voltammogram from un-doping. If we assume that the conductivity is limited by electron hopping between chain segments, and that there are no interactions between charge carriers, then it will be given by the following equation [41]

$$\sigma = FC_n\mu_n + FC_p\mu_p \qquad \textbf{4-3}$$

where C_n and C_p are the effective concentrations of the n- and p-type carriers, respectively, and μ_n and μ_p are their mobilities. C_n and C_p depend on the doping level and the concentration of undoped sites to which that charge carriers can hop. They are given by

$$C_n, C_p = \frac{C_{ox}C_{red}}{C_{ox}+C_{red}} \qquad \textbf{4-4}$$

where, for p-doping, C_{ox} is the concentration of p-doped sites and C_{red} is the concentration of undoped sites. For n-doping, C_{red} is the concentration of n-doped sites and C_{ox} is the concentration of undoped sites.

The conductivity will reach a maximum when $C_{ox} = C_{red}$, and $C_{n\text{ or }p,max} = C_{ox}/2$ or $C_{red}/2$. In **Fig. 4. 10**, the n-type conductivity peaks at ca. -0.5 V, when the n-doping charge(which is proportional to C_{red}) is 0.045 μC. For p-doping, the intrinsic maximum conductivity was not reached in our experiments. However, we can estimate from the charge under the voltammogram at 1.2 V that the p-doping charge (which is proportional to C_{ox}) is $>$ 0.12 μC at $C_{p,max}$. Thus, based on the carrier concentrations alone, the p-type conductivity should be $\sim$ 2.6 times higher than the n-type conductivity. The experimental difference is ca. 40 times larger than this, indicating that the mobility of the n-type charge carriers is ca. 40 times lower than for the p-type carriers (i.e. $\mu_p/\mu_n \sim 40$).

Fig. 4.11 shows the variation of conductivity with potential at its minimum. In this potential range, the polymer switches from being lightly n-doped to lightly p-doped as the potential is increased. The conductivity in this potential range will be due to both n- and p-type carriers, and should follow equation **4-3**. Since $\mu_p/\mu_n \sim 40$, the intrinsic conductivity of the polymer (when $C_n = C_p$) will be dominated by p-type carriers, and will be the conductivity at a potential (at $E_{intrinsic}$) ca. 60 mV positive of the minimum conductivity (at E_{min}) in **Fig.4. 11** (since from the slopes of the linear regions of **Fig. 4. 10**, $\log\sigma_n/\sigma_p = 26.1(E_{min}-E)$, and $\sigma_p/\sigma_n \sim 40$ at $E_{intrinsic}$). From the data in **Fig. 4.11**, the intrinsic conductivity can therefore be estimated to be 1.0×10^{-8} S cm^{-1}.

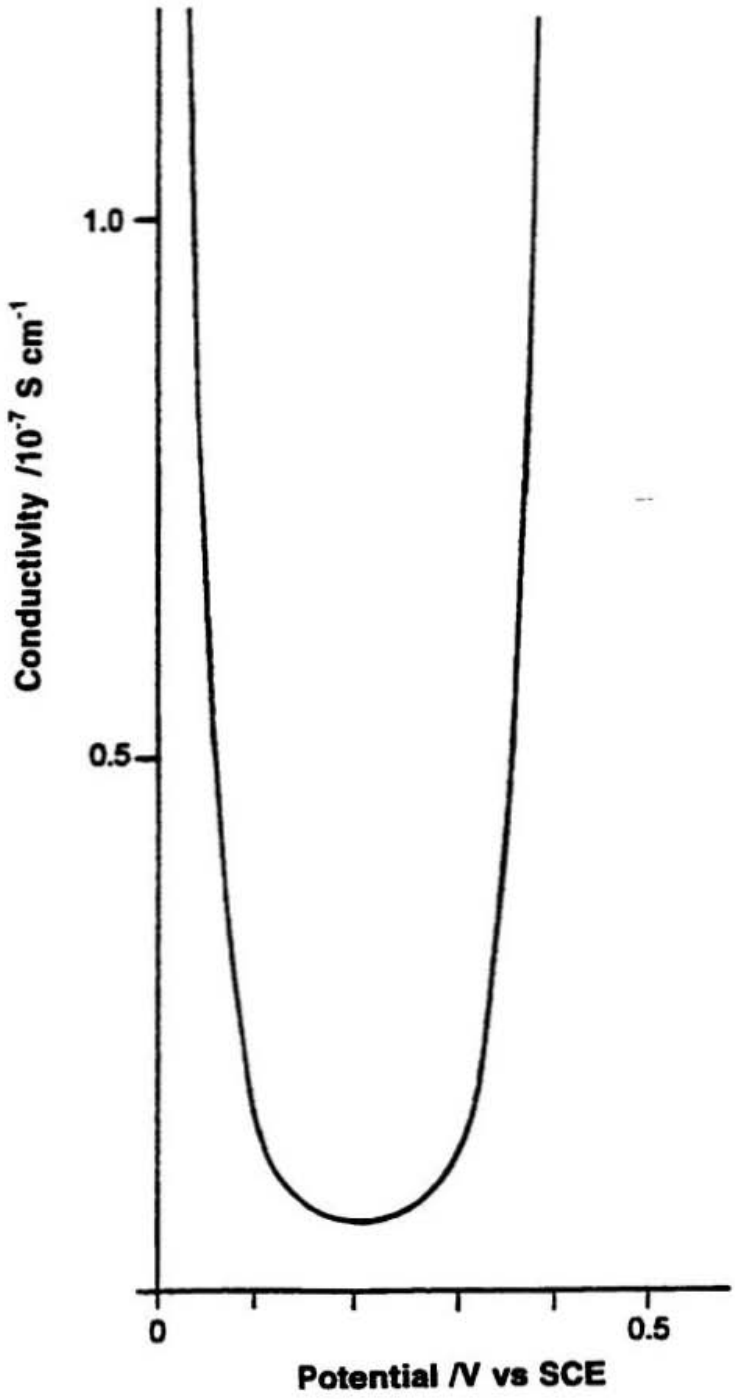

Fig. 4.11 Plot of conductivity against potential at the minimum

By comparing the intrinsic conductivity with the maximum p-type conductivity, we obtain a relative charge carrier concentration ($C_{p,\,intrinsic}/C_{p,max}$) of 1.7×10^{-8} mol/cm^3, From the charge under the voltammogram for p-doping (**Fig. 4. 10**), $C_{p,max}$ is ca. 8.5×10^{-4} mol/cm^3, and so $C_{p,intrinsic}$ is 1.4×10^{-11} mol/cm^3. From the usual equation for the thermal excitation of a semiconductor, $C_{p,intrinsic}$ [42]

$$C_{p,intrinsic}=4.2\times10^{-5}\exp\frac{-E_g}{2kT} \qquad \textbf{4-5}$$

the band-gap (E_g) can be estimated to be 0.75 eV. This is in remarkably good agreement with the optical gap of 0.83 eV.

4.7 Conclusion

The CDM monomer exhibits a substantial anodic shift of its formal potential for reduction, and a slightly anodic shift of its formal potential for oxidation compared to BTh, indicating that the strong electron-withdrawing group, dicyanoethene, decreases the LUMO energy level significantly, but has little effect on the HOMO. These characteristics of the monomer are extended to its polymer, giving the polymer one of the lowest band-gaps known.

Both electrochemical and optical studies yield the band-gap value of ca. 0.8 eV for poly-CDM. P-doping and n-doping show good stability after multiple cycles over different potential ranges. The much smaller change of the electronic absorption for n-doping compared with those for p-doping suggest that n-doping is located on the substituent in the branch and does not delocalize well along the thiophene backbone.

In situ conductivity measurements of the polymer provide both p- and n-doping conductivities as a function of the potential. The maximum p- and n-doping conductivities were found to be 0.59 and 5.4×10^{-3} S cm^{-1} respectively. A conductivity minimum at 0.2 V yields the intrinsic conductivity of 1.0×10^{-8} S cm^{-1}, consistent with the band-gap of ca. 0.8 eV.

References

[1] J. Roncali, *Chem. Rev.*, **97**, 173 (1997)

[2] G. Zotti, G. Schiavon, A. Berlin, G. Fontana, and G. Pagani, *Macromolecules*, **27**, 1938 (1994)

[3] T. M. Lambert and J. P. Ferraris, *J. Chem. Soc., Chem. Commun.*, 752 (1991)

[4] H. Brissert, C. Thobie-Gautier, A. Gorgues, M. Jubault, and J. Roncali, *J. Chem. Soc., Chem. Commun.*, 1305 (1991)

[5] T. M. Lambert and J. P. Ferraris, *J. Chem. Soc., Chem. Commun.*,1268 (1991)

[6] F. Wudl, M. Kobayashi, and A. J. Heeger, *J. Org. Chem.*, **49** 3381 (1984)

[7] I. Hoogmartens, D. Vanderzande, H. Martens, and J. Gelan, *Synth. Met.*, **47**, 367(1992)

[8] C. Kitamura, S. Tanaka, and Y. Yamashita, *Chem. Mater.*, **8**, 570 (1996)

[9] J. P. Ferraris, C. Henderson, D. Torres, and D. Meeker, *Synth. Met.*, **72**, 147 (1995)

[10] J. Roncali, F. Garnier, M. Lemaire, and R. Garreau, *Synth. Met.*, **15**, 323 (1986)

[11] M. Kobayashi, N. Colaneri, M. Boysel, F. Wdul, and A. J. Heeger, *J. Chem. Phys.*, **82**, 5717 (1985)

[12] J. Heinze, *Topics in Current Chemistry*, Vol. 152, Springer, Berlin, 1990, pp.1-47

[13] J. Roncali, *Chem. Rev.*, **92**, 711 (1992)

[14] B. Krische and M. Zagorska, *Synth. Met.*, **33**, 257 (1989)

[15] B. Krische and M. Zagorska, *Synth. Met.*, **28**, c263 (1989)

[16] E. A. Bazzaoni, S. Aeiyach, and P. C. Lacaze, *J. Electroanal. Chem.*, **364**, 63 (1994)

[17] D. T. Sawyer and Jr. J. L. Roberts, *Experimental Electrochemistry for Chemists*; John Wiley & Sons, Inc., New York, 1974

[18] J. Zerbino, W. J. Plieth, and G. Kossmehl, *J. Elctroanal. Chem.*, **260**, 361 (1989)

[19] J. Ochmanska and P. G. Pickup, *J. Elctroanal. Chem.*, **297**, 211 (1991)

[20] B. L. Funt and S. V. Lowen, *Synth. Met.*, **11**, 129 (1985)

[21] A. R. Hillman and E. F. Mallen, *J. Electroanal. Chem.*, **220**, 351 (1987)

[22] A. J. Downard and D. Pletcher, *J. Electroanal. Chem.*, **206**, 147 (1986)

[23] Z. S. Zhao and P. G. Pickup, *J. Chem. Soc., Faraday Trans.*, **90**, 3097 (1994)

[24] L. Zhou and G. Xue, *Synth. Met.*, **87**, 193 (1997)

[25] Y. Ikenoue, F. Wudl, and A. J. Heeger, *Synth. Met.*, **40**, 1 (1991)

[26] L. Laguren-Davidson, C. V. Pham, J. Zimmer, and Jr., H. B. Mark, *J. Electrochem. Soc.*, **135**, 1406 (1988)

[27] F. Garnier, G. Tourillon, M. Gazard , and J. C. Dubois, *J. Electroanal. Chem.* **148**, 299 (1983)

[28] M. Lapkowski, M Zagorska, I. Kulszewicz-Bajer, K. Koaie, and A. Pron, *J. Electroanal. Chem.*, **310**, 57 (1990)

[29] J. Roncali, M. Lemaire, R. Garreau, and F. Garnier, *Synth. Met.*, **18**, 139 (1987)

30] M. Onoda, J. Nakayama, S. Morita, T. Kawai, and K. Yoshino, *Synth. Met.*, **69**, 605 (1995)

[31] C. Kitamura, S. Tanaka, and Y. Yamashita, *Chem. Mater.*, **8**, 570 (1996)

[32] S. Tanaka and Y. Yamashita, *Synth. Met.*, **55-57**, 1251 (1993)

[33] G. King and S. J. Higgins, *J. Chem. Soc., Chem. Commun.*, 825 (1994)

[34] A. Berlin, E. Brenna, G. A. Pagani, and F. Sannicolo, *Synth. Met.*, **51**, 287 (1992)

[35] H. Sarker, Y. Gofer, J. G. Killian, T. O. Poehler, and P. C. Searson, *Synth. Met.*, **88**, 179 (1997)

[36] H. Mao and P. G. Pickup, *J. Electroanal. Chem.*, **265**, 127 (1989)

[37] R. M. Crooks, O. M. R. Chyan, and M. S. Wrighton, *Chem. Mater.*, **1**, 2 (1989)

[38] H. Mao and P. G. Pickup, *J. Am. Chem. Soc.*, **112**, 1776 (1990)

[39] D. Ofer, R. M. Crooks, and M. S. Wrighton, *J. Am. Chem. Soc.*, **112**, 7869 (1990)

[40] J. M. Toussaint and J. L. Bredas, *Synth. Met.*, **61**, 103 (1993)

[41] C. E. D. Chidsey and R. W. Murray, *J. Phys. Chem.*, **90**, 1479 (1986)

[42] A. J. Bard and L. R. Faulkner, *Electrochemical Methods: Fundamentals and Applications*, Wiley, New York, 1980

Chapter 5

Poly-CDM Modified by O_2: A Tunable and Extremely Low Band-Gap Polymer

5.1 Introduction

π-Conjugated electroactive polymers have attracted considerable attention in the last two decades. In this field, the search for low band-gap conducting polymers has become one of the central goals in recent years [1], since band-gap governs the intrinsic electronic and optical properties of conjugated polymers [1, 2]. Low band-gap polymers have high intrinsic electrical conductivities, and possibly even intrinsic metallic conductivities [3]. Also they are stable when doped, due to the lower p-doping potential or less negative n-doping potential associated with their narrow gaps [4, 5]. In addition, in contrast to highly doped polymers, they maintain the processibility, which is attractive for commercialization.

Several approaches to the design and synthesis of low band-gap polymers have been developed. Increasing the weight of the quinoid structure in the ground state of the conjugated polymer [6-8], constructing regular alternating donor and acceptor moieties along the polymeric chain [9-11], and the introducing electron-withdrawing groups at the carbon

bridging the β and β' positions of bithienyl precursors [12, 13] have proved effective methods. Following these ideas, a significant number of conducting polymers with band-gap less than 1 eV have now been successfully synthesized [1]. More recently, an electroactive polymer exhibiting a vanishingly small electrochemical band-gap has been reported [14].

Among low band-gap conducting polymers, poly-4-dicyanomethylene-4*H*-cyclopenta [2,1-*b*; 3,4-*b* ']dithiophene (poly-CDM) has one of the lowest band-gaps reported to date [1, 15-17]. When we investigated the p- and n-type *in situ* conductivities of poly-CDM films vs. potential [18], we found that when O_2 was present in the solution and the polymer-coated electrode was maintained at a negative potential (e.g. -0.60 V) rather than a positive potential, a new electroactive polymer with a variable and extremely low band-gap was produced. The electrochemical, optical, and electrical properties, and the structural modification of this O_2-modified polymer are reported in this chapter.

5.2 Electrochemistry of O_2-modified poly-CDM

Poly-CDM films were synthesized galvanostatically on Pt electrodes at 0.1 mA/cm^2 for 800 s in 5 mM CDM nitrobenzene solution in the presence of 0.1 M Bu_4NPF_6. According to the calibration relationship between the synthesis charge and the film thickness (4.6 μm per C cm^{-2} (Section **4.3.2**) obtained by SEM, these films were 0.37 μm thick. Cyclic voltammetric studies of the original and modified polymer were performed in acetonitrile containing 0.1 M Bu_4NPF_6 in the potential range from -0.60 to +1.20 V at 100 mV/s.

Fig. 5.1 (a) shows a cyclic voltammogram (dotted line) of an original poly-CDM film. The p-doping peak potential is +0.99 V, similar to the potential value of most polythiophenes [19-23]. While the n-doping peak occurs at -0.50 V. The formal potential ($E^{o'}$; average of the doping and de-doping peak potential) for the n-doping is -0.47 V, which is much higher than that of other polythiophenes [19, 22-26]. This substantial anodic shift of the n-doping region causes poly-CDM to be reasonably stable when n-doped as discussed in Chapter **4**. The electrochemical band-gap between the onsets of p-doping and n-doping is ca. 0.8 V.

When the poly-CDM film was maintained at -0.60 V in an O_2-saturated solution first for 2 min, then for 6 min, the cyclic voltammograms shown in **Fig. 5.1 (b)** and **(c)** as the dashed line and the solid line, respectively were obtained. In comparison with the original polymer, both the n- and p-doping peak currents of the modified film decrease, and the n-doping peak shifts slightly to more negative potentials. A new doping current appears and grows within the band-gap between the original onsets of n-doping and p-doping potential (-0.1 V to +0.7 V) of the unmodified poly-CDM. This change gives the modified polymer a narrower band-gap than the original polymer.

Comparing **Fig. 5.1 (b)** and **(c)**, increasing the reaction time with O_2 decreases further the n-doping and p-doping peak currents, but increases the new current in the potential range from -0.1 to +0.7 V, resulting in a flat and broad p-doping region, and therefore a lower electrochemical band-gap. As the time is increased, the position of the current minimum between n– and p- doping also shifts cathodically from -0.1 to -0.2 V. Because of the overlap of n-doping and p-doping in this potential region, it is difficult to measure the

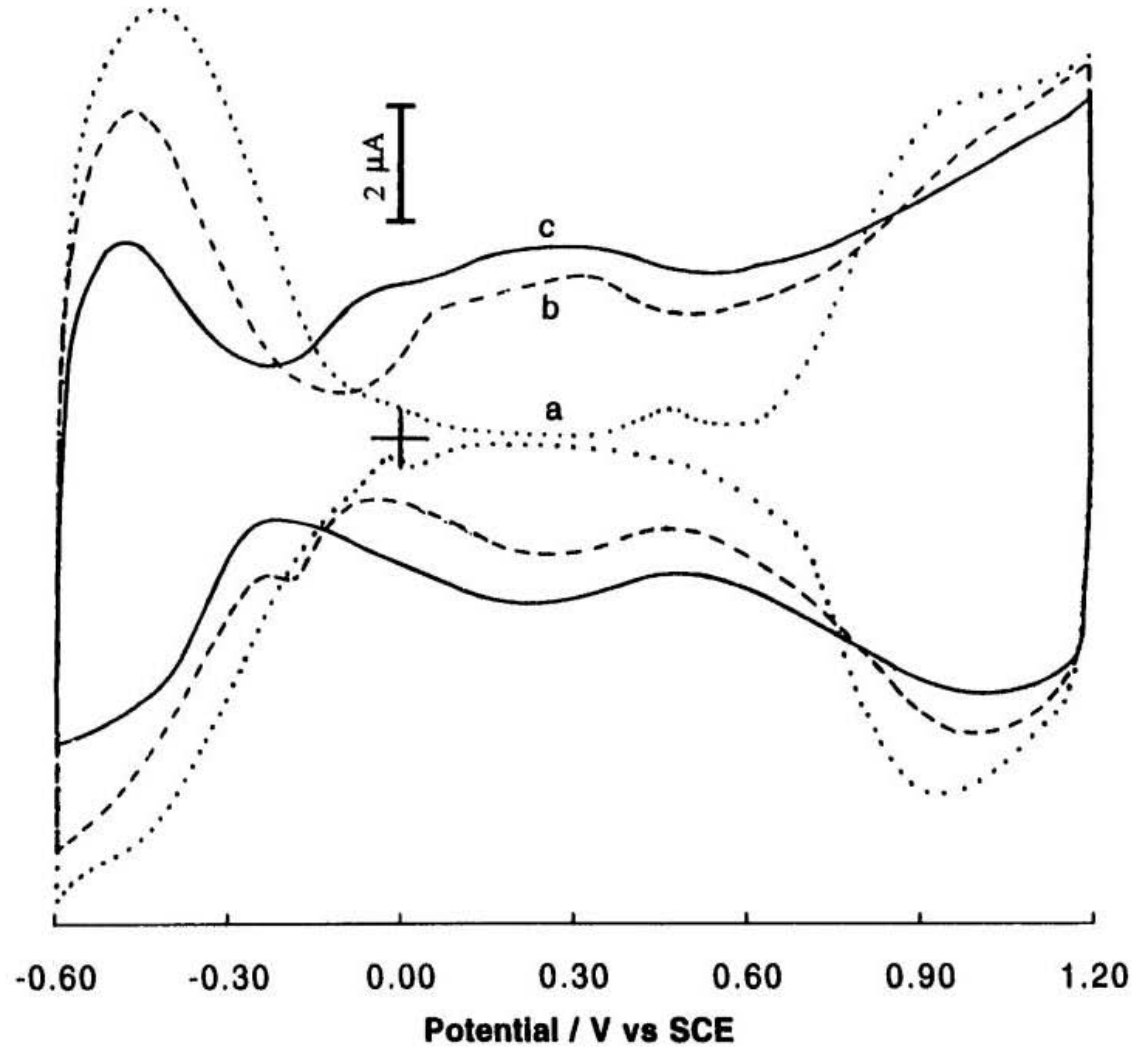

Fig. 5.1 Cyclic voltammograms (n- and p-doping) of (a) the original poly-CDM, (b) poly-CDM modified with O_2 for 2 min, and (c) poly-CDM modified with O_2 for 6 min. Potential range: -0.60 - 1.20 V. Scan rate: 100 mV/s

electrochemical band-gaps of the modified polymers. However, it is clear that by controlling the reaction time, polymers with various band-gaps can be achieved.

Doping levels (n- and p-doping) measured from the cyclic voltammograms (**Fig. 5.1**) versus potential are plotted in **Fig. 5.2** as curve **(a)**, **(b)** and **(c)** for the original film and the two O_2-modified films, respectively. In the potential range studied the highest p-doping level reaches 22.0% at +1.20 V for the original poly-CDM film, and the highest n-doping level is 21.2 % at -0.60 V. The maximum n-doping level is approximately the same (~96%) as that for the p-doping, indicating that a relatively high n-doping level can be achieved for poly-CDM, in contrast to most other polythiophenes [25, 27, 28], which normally have significantly lower doping levels for the n-doping. After the polymer has been reacted with O_2 for 2 or 6 min, the p-doping level increases to 31.2% and 35.5%, while the n-doping level decreases to 16.9% and 13.3%, respectively. The gain in the p-doping level occurs in the potential range between -0.1 and +0.7 V, in which the original polymer is undoped. As the reaction time is increased, this current growth becomes higher and the potential for the minimum doping level shifts from ca. -0.1 to ca. -0.2 V.

Cyclic voltammogram against scan rate for an O_2-modified polymer are shown in **Fig. 5.3**. The electrochemical results are listed in **Table 5.1**. In the figure, all peak potentials are practically unchanged with the scan rate. The formal potentials for the p-doping are +0.32 V ($E^{0'}_{p1}$) and +1.02 V ($E^{0'}_{p2}$). For n-doping, the formal potential ($E^{0'}_{n}$) is -0.51 V, which is slightly negative compared to the original film ($E^{0'}$ = -0.47 V). All peak currents, including the doping and de-doping processes for both n- and p-type doping, are linear with the scan rate as indicated in **Fig. 5.4**. Both the n-doping and p-doping processes of the modified poly-

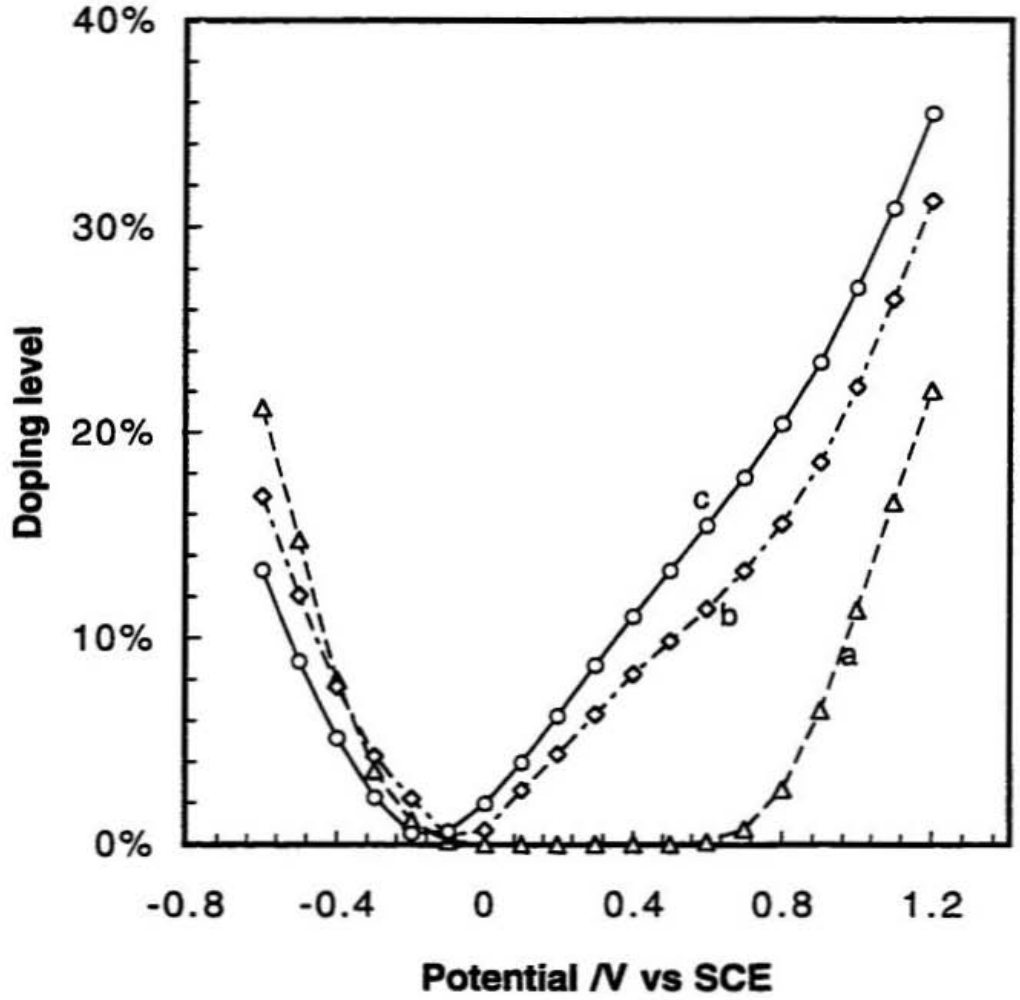

Fig. 5.2 Doping level (n- and p- doping) versus potential for
(a) the original poly-CDM;
(b) poly-CDM modified with O_2 for 2 min;
(c) poly-CDM modified with O_2 for 6 min

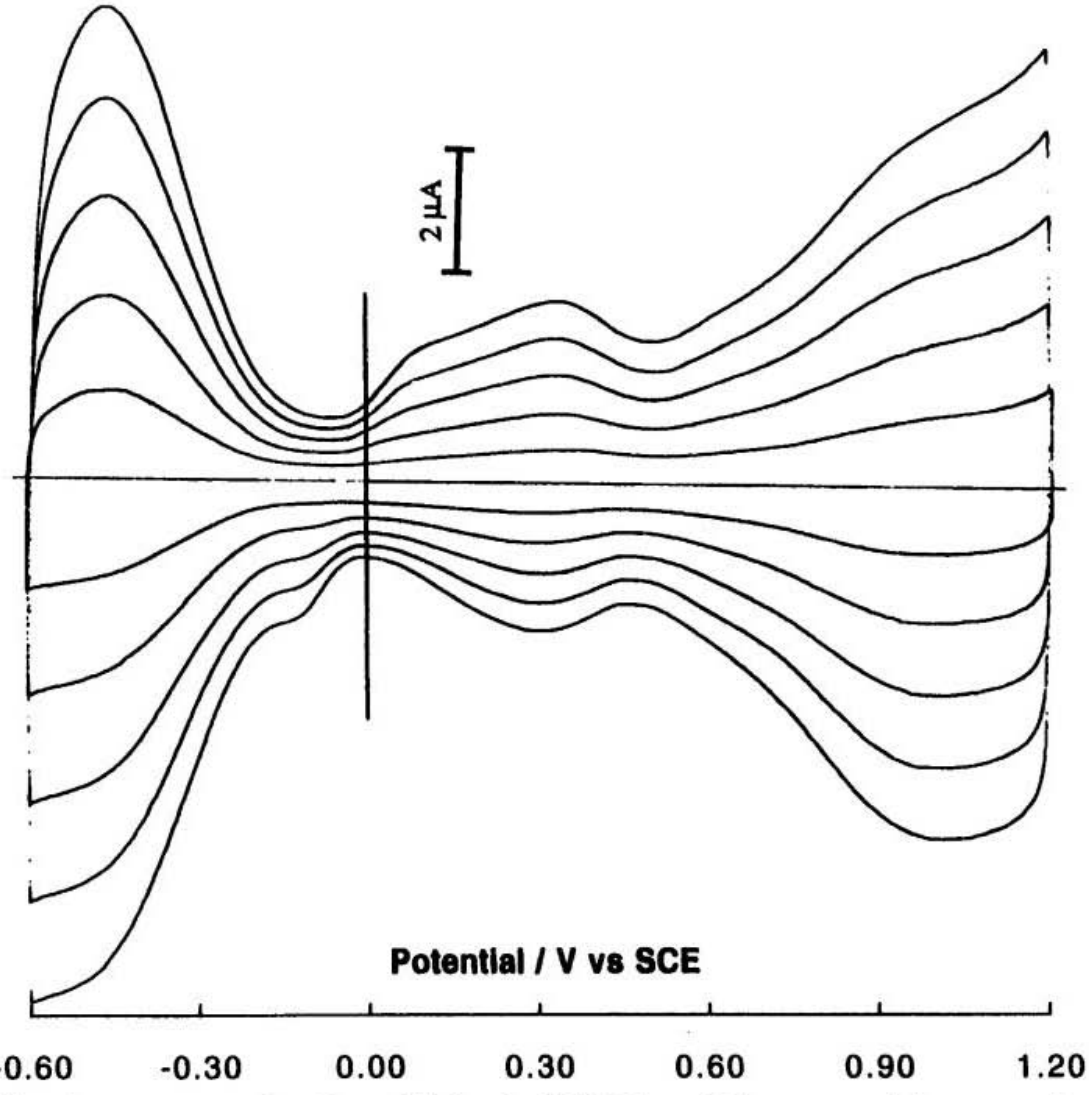

Fig. 5.3 Cyclic voltammograms of an O_2-modified poly-CDM film at different potential scan rates in acetonitrile containing 0.1 M Bu_4NPF_6. Potential range: -0.60 - 1.20 V. Scan rate: 100, 80, 60, 40, 20 mV/s

Table 5.1 Voltammetric data for an O_2-modifed poly-CDM film

	p-doping								n-doping			
v /mV/s	$E_{p(ox1)}$ /V	$i_{p(ox1)}$ /μA	$E_{p(red1)}$ /V	$i_{p(red1)}$ /μA	$E_{p(ox2)}$ /V	$i_{p(ox2)}$ /μA	$E_{p(red2)}$ /V	$i_{p(red2)}$ /V	$E_{n(re)}$ /V	$i_{n(re)}$ /μA	$E_{n(ox)}$ /V	$i_{n(ox)}$ /μA
20	0.34	0.61	0.30	-0.51	1.03	1.29	1.00	-1.17	-0.53	-1.80	-0.48	1.59
40	0.34	1.21	0.30	-1.03	0.34	2.66	1.00	-2.32	-1.91	-3.60	-0.48	3.21
60	0.34	1.90	0.30	-1.57	0.34	3.93	1.00	-3.57	-1.92	-5.39	-0.48	4.92
80	0.34	2.53	0.30	-2.08	0.34	5.22	1.00	-4.76	-1.93	-7.18	-0.48	6.57
100	0.34	3.19	0.30	-2.54	0.34	6.50	1.00	-5.96	-1.93	-8.88	-0.48	8.20

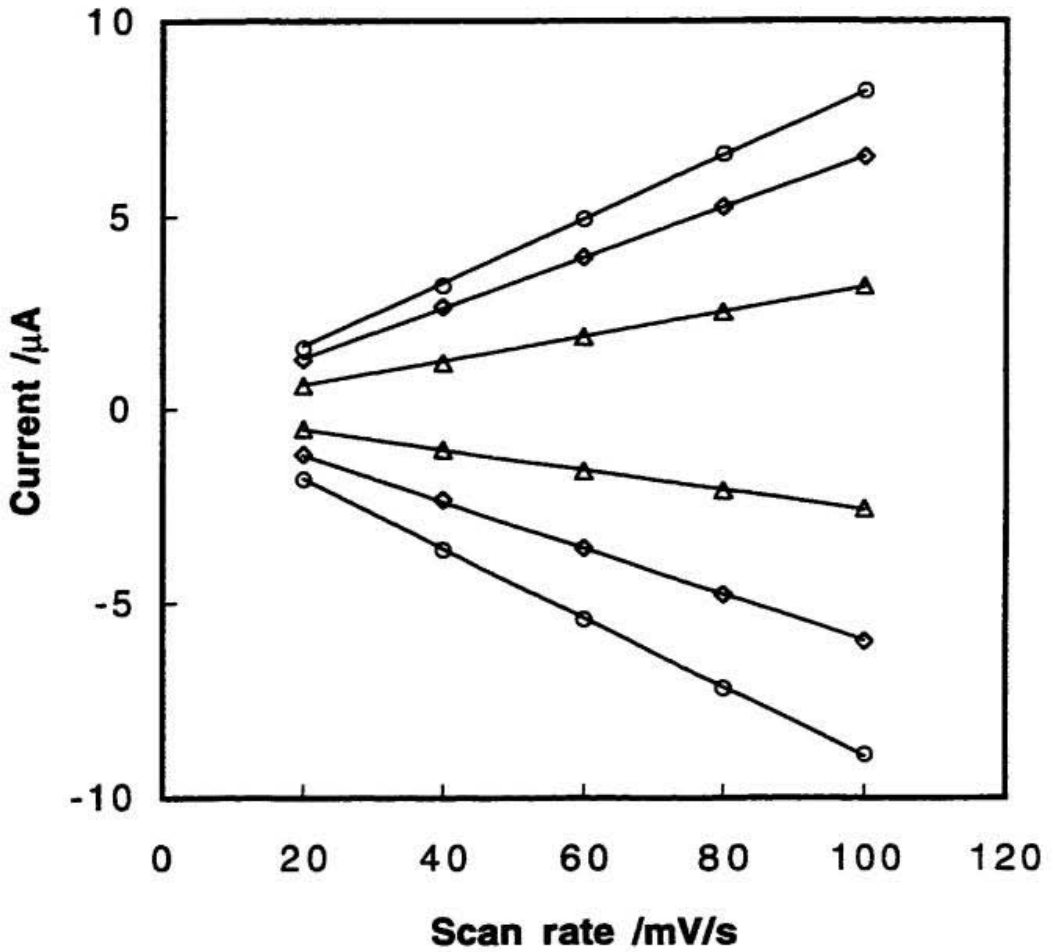

Fig. 5.4 Peak currents versus scan rates for a 0.37 μm poly-CDM film modified with O_2 for 2 min in acetonitrile containing 0.1 M Bu_4NPF_6

CDM exhibit good stability during multiple scans under Argon.

In contrast to the results described above, maintaining a poly-CDM coated Pt electrode at an anodic oxidation potential (e.g. +1.40 V) in the presence of O_2 does not lead to a low band-gap polymer. It produces two obvious pre-peaks, which grow and separate as longer time is used. We have not fully investigated the reasons why the polymer exhibits different behaviors when maintained at negative and positive potentials, but we assume that it is the result of attack by different species, i.e. electrophilic attack of the reduced polymer by O_2 vs nuleophilic attack of the oxidized polymer by trace H_2O (overoxidation) [3].

5.3 Electronic absorption spectra of O_2-modified poly-CDM

ITO electrodes (0.8 cm^2, 10~20 Ω, Donnelly) coated galvanostatically (0.1 mA/cm^2) with a thin layer poly-CDM were used for electronic absorption spectroscopies. The measurements were carried out in acetonitrile containing 0.1 M Bu_4NPF_6 with control of the potential of the poly-CDM coated ITO electrode. For the original poly-CDM film, the potential was set at +0.20 V, where the polymer is in the neutral state. While for the O_2 modified films, the potential was kept at -0.10 V, where the polymer is at its minimum doping level. The Vis-NIR absorption spectra of the original polymer, and after reaction with O_2 for 2 and 6 min are shown in **Fig. 5.5** as curves **(a)**, **(b)** and **(c)**, respectively. The optical absorption onset for the original polymer is 1520 nm, corresponding to a band-gap of ca. 0.8

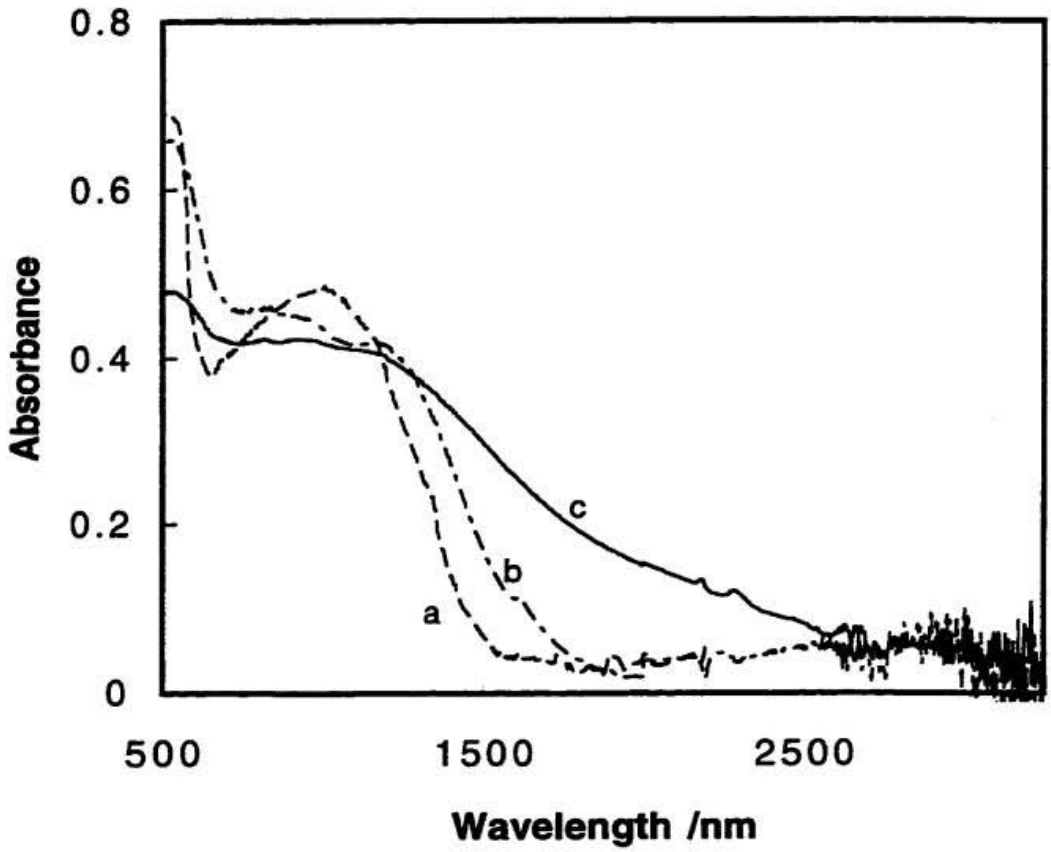

Fig. 5.5 Electronic absorption spectra for (a) the original poly-CDM, (b) poly-CDM modified with O_2 for 2 min, and (c) poly-CDM modified with O_2 for 6 min on an ITO electrode in 0.1 M Bu_4NPF_6 acetonitrile solution

eV. Following reaction with O_2 for 2 and 6 min, it shifts to ca. 1850 (0.67 eV) and ca. 2600 nm (0.48 eV), respectively, showing a significant reduction of the band-gap, in good agreement with the new features of the CVs (see **Fig. 5.1**). With controlled O_2 treatment, the band-gap can be tuned down to values that are too low to measure by our UV-Vis-NIR spectrometer cell.

5.4 *In situ* conductivity measurement

In situ conductivity data on a log scale against potential are plotted in **Fig. 5.6**. Curves **(a)**, **(b)** and **(c)** are for an original poly-CDM film (0.37 μm), and the modified polymer following reaction with O_2 at -0.6 V for 20 min and 30 min, respectively. Longer times were needed to modify the polymer, because of the covering of a thin layer of porous gold film needed for the conductivity measurements. **Table 5.2** lists the results of the conductivity measurements, including maximum conductivities for n-doping ($\sigma_{max,n}$) and p-doping ($\sigma_{max,p}$), the minimum conductivity (σ_{min}) and its corresponding potential (E_{min}), and calculated results of the intrinsic conductivities ($\sigma_{intrinsic}$) and band-gaps [18, 29].

In curve **(a)**, the p-type conductivity of the original poly-CDM rises to a maximum of 1.1 S cm^{-1} at +1.2 V. The n-type conductivity is ca. 90 times smaller, peaking at 0.012 mS cm^{-1} at -0.5 V. Further n-doping to more negative potentials decreases the conductivity. The low n-type conductivity relative to the p-type conductivity is due mainly to the lower mobility or the n-type carriers [30] and in part to the lower doping level when conduction

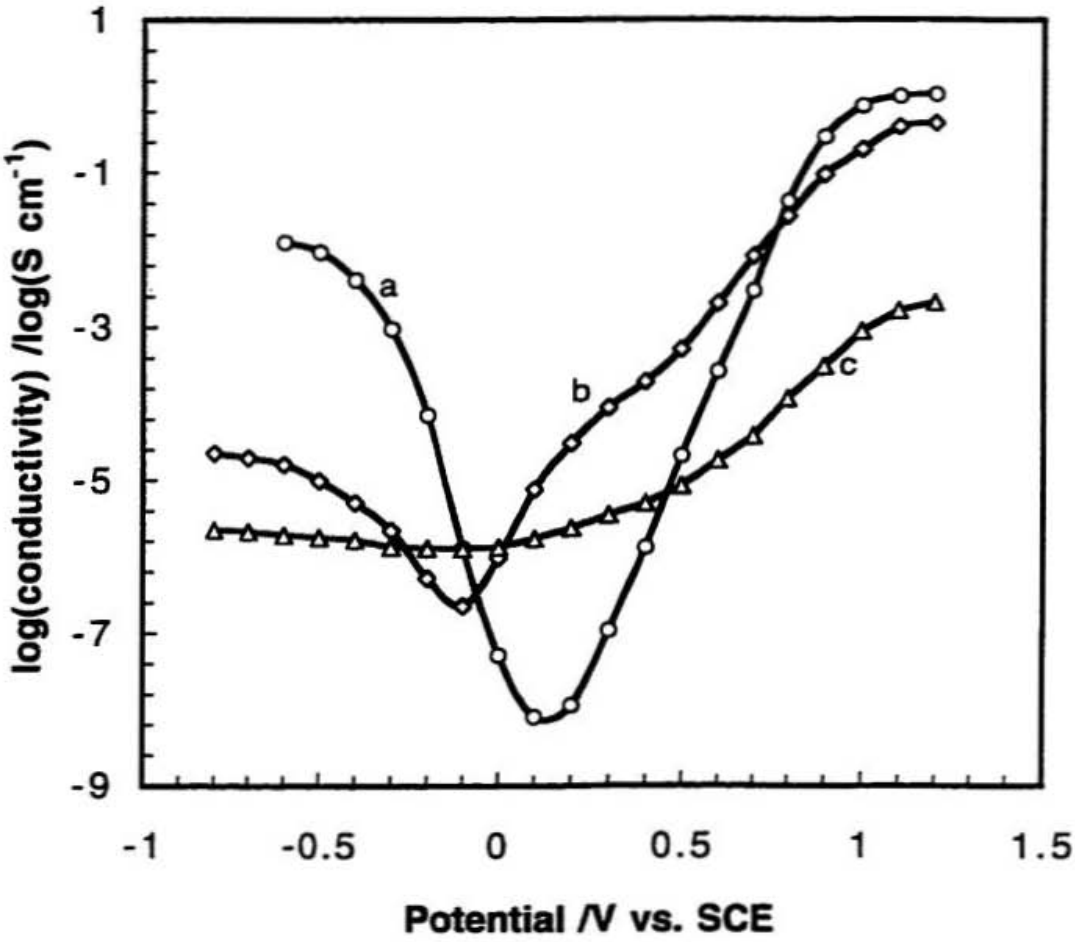

Fig. 5.6 Influence of reaction with O_2 on the conductivity of poly-CDM
(a) the original poly-CDM;
(b) poly-CDM reacted with O_2 for 20 min;
(c) poly-CDM reacted with O_2 for 30 min

band is half filled during n-doping [18]. The intrinsic conductivity and band-gap are calculated as 1.0×10^{-8} S cm^{-1} and 0.78 eV, respectively.

Table 5.2 Electrical properties of original and O_2-modified poly-CDM films

Curve	$\sigma_{max,p}$ /S cm^{-1}	$\sigma_{max,n}$ /S cm^{-1}	σ_{min} /S cm^{-1}	E_{min} /V	$\sigma_{intrinsic}$ /S cm^{-1}	E_g /eV
a	1.1	1.2×10^{-3}	7.9×10^{-9}	0.18	1.0×10^{-8}	0.78
b	0.44	2.3×10^{-5}	2.2×10^{-7}	-0.05	8.0×10^{-7}	0.52
c	2.0×10^{-3}	2.2×10^{-6}	1.2×10^{-6}	-0.20	1.3×10^{-6}	0.22

note: a: the fresh-made poly-CDM;
b: poly-DM modified with O_2 for 20 min;
c: poly-CDM modified with O_2 for 30 min

In curve (b), when O_2 is used to modify the poly-CDM, maximum conductivities for both n- and p-doping of the resulting polymer decrease to 0.44 and 2.3×10^{-5} S cm^{-1} respectively, and the potential of maximum n-type conductivity moves negatively. However, the minimum conductivity at -0.1 V has improved by a factor of ca. 30, to 2.2×10^{-7} S cm^{-1}. Further reaction with O_2 (curve (c)) reduces the maximum n-type and p-type conductivities further to 2.2×10^{-6} and 2.0×10^{-3} S cm^{-1} respectively, and increases the minimum conductivity to 1.2×10^{-6} S cm^{-1}, which is ca. 150 times higher than that of the original polymer. Calculations as described in section **4.7** show that the intrinsic conductivities was increased to 8.0×10^{-7} S cm^{-1} by the 20 min treatment and to 1.3×10^{-6} S cm^{-1} by the 30 min treatment, and the band-gap was reduced to 0.52 and 0.22 eV, respectively.

5.5 Raman spectra of O_2-modified poly-CDM

A structural change that would explain the effect of O_2 on poly-CDM at negative potentials is proposed in **Scheme 1** [31]. That is, -OH groups are forming at β positions when O_2 attacks reduced poly-CDM. Support for this scheme was obtained from Raman spectrocopy.

Fig. 5.7 (a) and **(b)** shows Raman spectra of an original poly-CDM film on Pt electrode and the same film after reaction with O_2 at -0.65 V for 8 min. Assignments of Raman shifts of both films are listed in **Table 5.3** [7, 32-35].

Vibrational frequencies of bonds, which are not involved in the backbone of the chain including C≡N, C-CN, C=C(CN)$_2$ and C_β-C, are almost unchanged. The inner C_α=C_β bonds and the inter-ring $C_{\alpha'}$-C_α bonds are in the backbone but remote from the proposed modified positions. Their vibrational frequencies shift slightly. A new mode at 2759 cm^{-1} is characteristic of a -OH group. The significant impact of modification occurs on the C_β-$C_{\beta'}$ single bond, and the outer C_α=C_β bonds, which are in the backbone and adjacent to the proposed -OH group. The C_β-$C_{\beta'}$ stretch position shifts positively to 1381cm^{-1} from 1345 cm^{-1}, while the outer C_α=C_β stretch moves negatively from 1434 cm^{-1} and split into 1417 and 1396 cm^{-1}.

The result of the modification proposed in **Scheme 1** is that the HOMO energy level increases significantly, but the LUMO energy level increases only slightly, and hence the band-gap is decreased. However, a ⟩C=O tautomeric structure will exist in equilibrium with the C-OH structure. The existence of the ⟩C=O structure is shown by the new peak

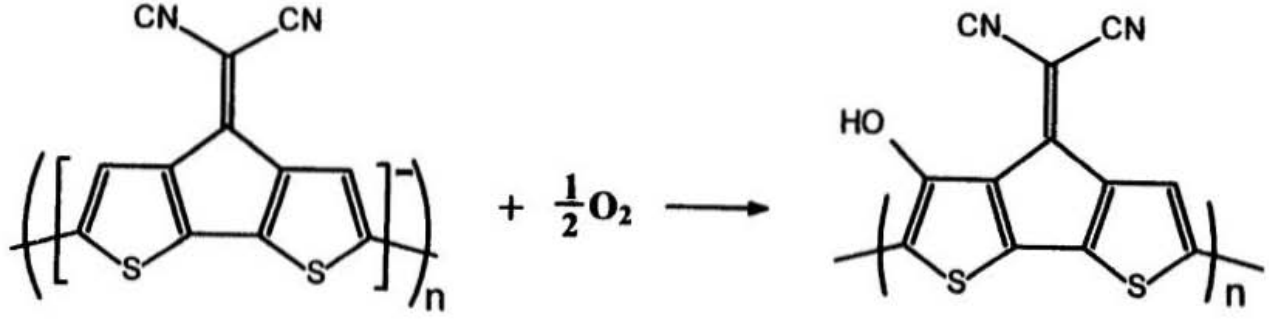

Scheme 1

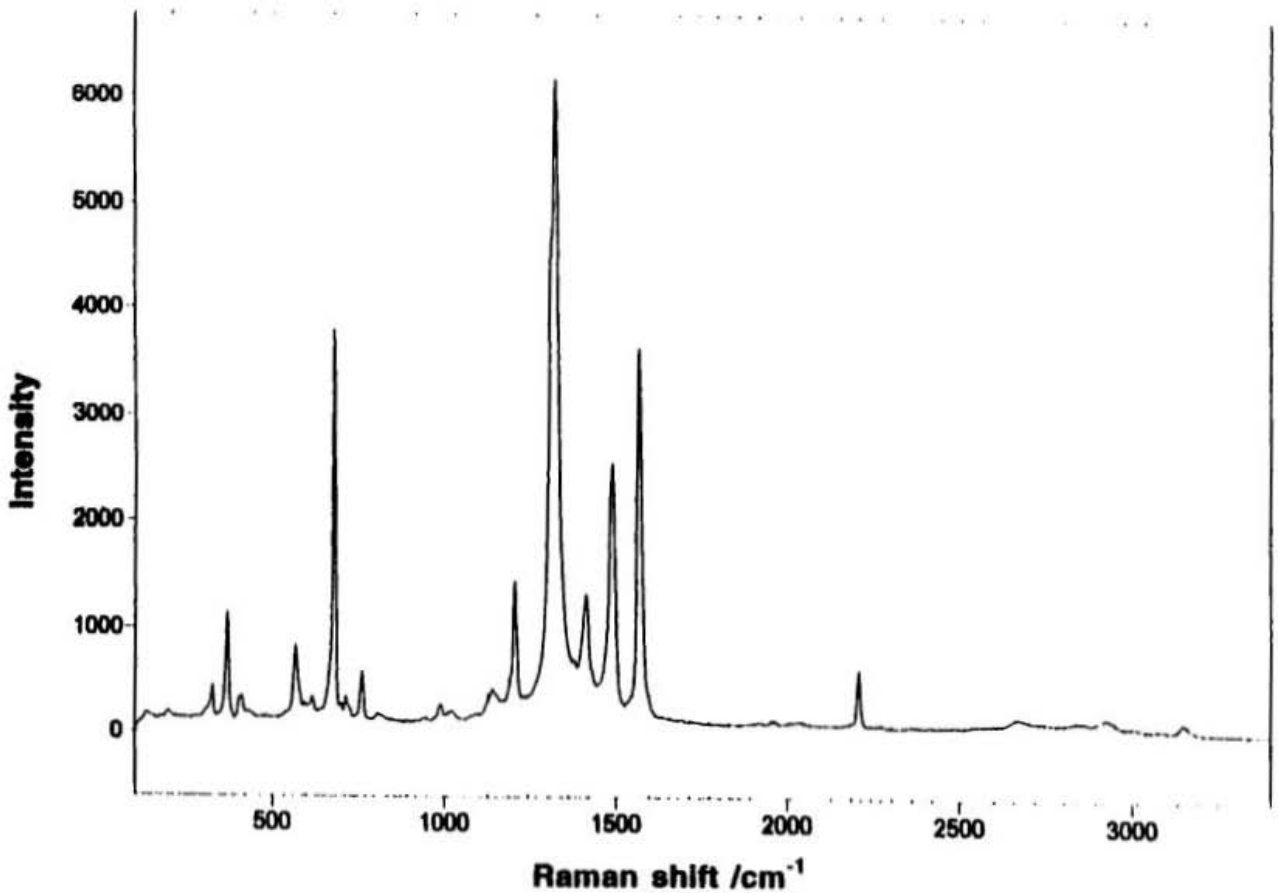

Fig. 5.7 (a) Raman spectrum of an original poly-CDM film

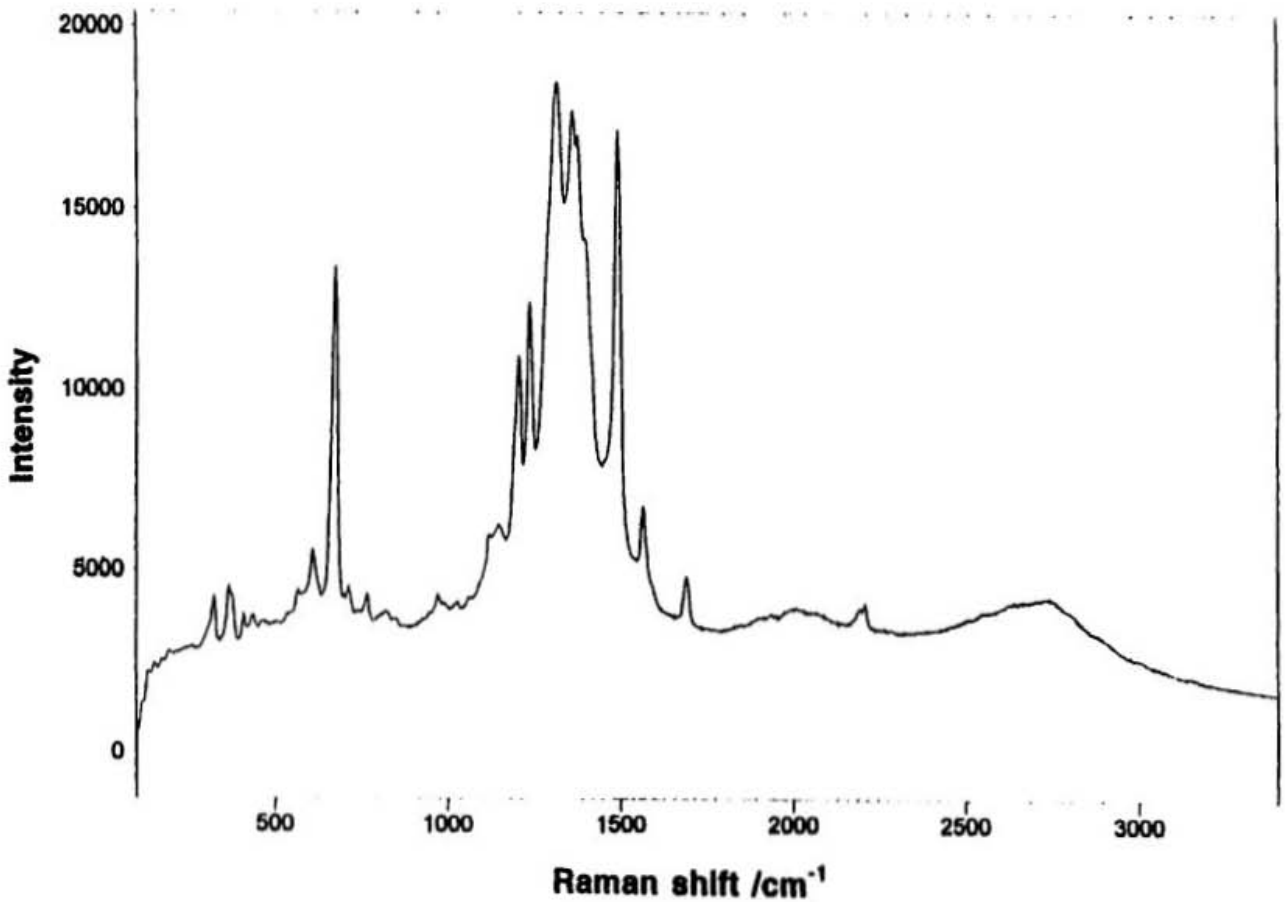

Fig. 5.7 (b) Raman spectrum of an O_2-modified poly-CDM film after the polymer was maintained at E_{min}

Table 5.3 Assignment of Raman spectra of an original poly-CDM film and an O_2-modified poly-CDM film

Poly-CDM		O_2-modified poly-CDM	
Bond	Wave number /cm^{-1}	Bond	Wave number / cm^{-1}
C_β-H	3171	O-H	2759
C≡N	2230	C≡N	2230
		C_β=O	1712
C=C(CN)$_2$	1589	C=C(CN)$_2$	1587
C_α=C_β	1511, 1434	C_α=C_β	1511, 1417, 1396
C_β-$C_{\beta'}$	1345	C_β-$C_{\beta'}$	1381
=C-CN	1334	=C-CN	1335
		C_β-OH	1256
$C_{\beta'}$-C=	1225	$C_{\beta'}$-C=	1225
inter ring C_α-$C_{\alpha'}$	1161	inter ring C_α-$C_{\alpha'}$	1168
C-S-C	702, 782	C-S-C	695

at 1712 cm^{-1}. This structure destroys the conjugation along the backbone and reduce the maximum conductivities for both p- and n-doping.

5.6 Conclusion

A tunable and extremely low band-gap polymer has been successfully achieved by modifying poly-CDM in the reduced state (e.g. at -0.6 V) with O_2. Cyclic voltammograms of the O_2-modified polymer show a new p-doping wave appearing within the band-gap between the onsets of n- and p-doping (-0.1 V to 0.7 V) of the original polymer. This results in a lower band-gap, as confirmed by optical studies. The band-gap of the original poly-CDM is 0.83 eV. Upon reaction with O_2 for 2 or 6 min, it reduces to 0.67 or 0.48 eV, respectively. With controlled O_2 treatment, the band-gap can be tuned down to values that are too low to measure by UV-Vis-NIR spectroscopy. *In situ* conductivity measurement show that both the maximum p- and n-type conductivities decrease when the polymer is modified with O_2, but the minimum conductivity increases remarkably by up to several orders of magnitude. An intrinsic conductivity of 1.3×10^{-6} S/cm measured for one O_2-modified polymer corresponds to a band-gap as low as 0.22 eV. Raman spectroscopy suggests that substitution of the polymer in the β positions with hydroxyl groups is responsible for the lowered band-gap.

References

[1] J. Roncali, *Chem. Rev.*, **97**, 173 (1997)

[2] R. L. Greene and G. B. Street, *Science*, **226**, 651 (1984)

[3] J. L. Bredas, A. J. Heeger, and F. Wudl, *J. Chem. Phys.* **85**, 4673 (1986)

[4] C. Arbizzani, M. Catellani, M. Mastragostino, and C. Mingazzini, *Electrochim. Acta*, **40**, 1871 (1995)

[5] C. Arbizzani and M. Mastragostino, *Adv. Mater.*, **8**, 331 (1996)

[6] F. Wudl, M. Kobayashi and A. J. Heeger, *J. Org. Chem.*, **49**, 3382 (1984)

[7] C. Kitamura, S. Tanaka, and Y. Yamashita, *Chem. Mater.*, **8**, 570 (1996)

[8] Y. Ikenoue, F. Wudl, and A. J. Heeger, *Synth. Met.*, **40**, 1 (1991)

[9] E. E. Havinga, W. ten Hoeve, and H. Wynberg, *Synth. Met.*, **55-57**, 299 (1993)

[10] J. M. Toussaint and J. L. Bredas, *Synth. Met.*, **61**, 103 (1993)

[11] Q. T. Zhang and J. M. Tour, *J. Am. Chem. Soc.*, **119**, 5065 (1997)

[12] T. Lambert and J. P. Ferraris, *J. Chem. Soc., Chem. Commun.*, 752 (1991)

[13] H. Brisset, C. Thobie-Gautier, A. Gorgues, M. Jubault, and J. Roncali, *J. Chem. Soc., Chem. Commun.*, 1305 (1994)

[14] S. Tanaka and Y. Yamashita, *Synth. Met.*, **84**, 229 (1997)

[15] J. P. Ferraris and T. L. Lambert, *Chem. Commun.*, 1268 (1991)

[16] S. R. Gunatunga, G. W. Jones, M. Kalaji, P. J. Murphy, D. M. Taylor and G. O. Williams, *Synth. Met.*, **84-86**, 973 (1997)

[17] R. Beyer, M. Kalaji, G. Kingscote-Burton, P. J. Murphy, V. M. S. C. Pereira, D.

M. Taylor, and G. O. Williams, *Synth. Met.*, **92**, 25 (1998)

[18] H. Huang and P. G. Pickup, *Polymer. Acta*, , **48**, 455 (1997)

[19] J. Roncali, *Chem. Rev.*, **92,** 711 (1992)

[20] J. Roncali, F. Garnier, M. Lemaire, and R.Garreau, *Synth. Met.*, **15,** 323 (1986)

[21] P. Margue, J. Roncali, and F. Garnier, *J. electroanal. Chem.*, **218,** 107 (1987)

[22] J. P. Farraris and M. D. Newton, *Polymer*, **33**, 391 (1992)

[23] B. Ballaria, R. Seeber, D. Tonelli, F. Audreani, P. Costa Bizzarri, C. Della Casa, and E. Salatelli, *Synth. Met.*, **88**, 7 (1997)

[24] S. M. Dale, A. Glide, and A. R. Hillman, *J. Mater. Chem.*, **2**, 99 (1992)

[25] Y. Fu, H. Cheng, and R. L. Elsenbaumer, *Chem. Mater.*, **9**, 1720 (1997)

[26] M. Onoda, H. Nakayama, S. Morita, and K. Yoshino, *J. Electrochem. Soc.*, **141**, 338 (1994)

[27] D. J. Guerrero, X. Ren, and J. P. Ferraris, *Chem. Mater.*, **6**, 1437 (1994)

[28] H. Sarker, Y. Gofer, J. G. Killian, T. O. Poehler, and P. C. Searson, *Synth. Met.*, **88**, 179 (1997)

[29] C. E. D. Chidsey and R. W. Murray, *J. Phys. Chem.*, **90**, 1479 (1986)

[30] D. J. Guerrero, X. M. Ren, and J. P. Ferraris, *Chem. Mater.*, **6**, 1437 (1994)

[31] A. A. Pud, *Synth. Met.*, **66**,1 (1994)

[32] E. Faulques, W. Wallnofer, and H. Kuzmany, *J. Chem. Phys.*, **90**, 7585 (1989)

[33] G. Louarn, J. Y. Mevellec, J. P. Buisson, and S. Lefrant, *Synthetic Met.*, **55-57**, 587 (1993)

[34] G. Louarn, J. P. Buisson, S. Lefrant, and D. Fichou, *J. Phys. Chem.*, **99**, 11401 (1995)

[35] L. Cuff and M. Kertesz, *J. Chem. Phys.*, **106,** 5541 (1997)

Chapter 6

Electrochemical and Spectroscopic Characterization, and *In Situ* Conductivity Measurement of Poly(3, 4-ethylenedioxythiophene)

6.1 Introduction

Modification of the structure of the thiophene (Th) ring by substitution at the 3- or 3- and 4-positions has enabled the synthesis of a large number of Th derivatives, resulting in numerous polymers with diverse of properties, such as stability, conductivity, solubility, and band-gap [1]. Introduction of a functional group, particularly an electron donating group such as an alkyl [2], alkoxy [3], or aryl [4] group (monomers with an electron withdrawing group, such as -F, -Cl, -Br [5,6], -CN [7], and -NO_2 [7] have been found to be difficult to electropolymerize due to the high oxidation potential) at the 3 position, can lead to not only a decrease in the oxidation potential, but also to a decrease in the number of the coupling defects (α-β' linkage). Thus polymers with high conductivities and lower band-gaps can be formed [5,8]. However, pronounced reduction of band-gaps has not been realized by using this method. For instance, electropolymerization of 3-methylthiophene

produced a polymer having a conductivity of 2000 S cm^{-1} [9], the highest value among poly-Ths reported to date, and a band-gap of 1.9 eV [10], which is slightly lower than that of poly-Th (2.1 eV) [11, 12], and close to the value expected for a perfect poly-Th chain [13].

As a further step in this direction, disubstitution at the 3- and 4- positions has appeared as an interesting method to synthesize perfectly stereoregular polymers by eliminating any possibility of α-β' linkage. However, poly(3,4-dialky-thiophenes) normally have higher oxidation potentials, higher optical band-gaps and lower electrical conductivities than mono-subsitituted polymers [14-16]. This can be explained the severe steric hindrance between substituents grafted on consecutive structural units which distorts the conjugated π system, providing a considerable loss of effective conjugation.

However, this steric interaction between neighboring monomer units is significantly reduced by a cyclo-substituent fused at the 3- and 4- positions [17-19]. Two representatives of this type polymer are poly(benzo[c]thiophene) (poly-BCT or poly-INT) [20] and poly(3,4-ethylenedioxythiophene) (poly-EDOT) [19]. The former is viewed as the first effectively reduced band-gap polymer [21], drawing considerable interests [22-26] in both theoretical and experimental studies. However, the INT monomer is not stable, and needs to be prepared immediately prior to the polymerization. Poly-EDOT is one of the most promising poly-Th derivatives [27-30], because it shows not only higher conductivity and a much lower band-gap, but also better environmental stability and a higher doping level than its parent poly-Th.

In this chapter, the electrochemical and optical properties of the EDOT monomer and its electrochemically synthesized polymer are described. A study of the *in-situ* electronic conductivity of the polymer is also present.

6.2 Redox potential and band-gap of EDOT

Fig. 6. 1 shows the first two cycles for the oxidation (from -0.80 to +1.50 V) of 5 mM EDOT (structure 1) in acetonitrile containing 0.1 M Bu_4NPF_6. The first cycle (the solid line) gives an electrochemically irreversible wave and shows the hysterisis typically observed in the first cycle during the synthesis of a conducting polymer [31, 32]. In the forward scan, the oxidation of EDOT monomer begins at +1.35 V and peaks at +1.45 V. In the reverse scan, the reduction behavior shows a broad wave (from +1.18 to -0.68 V) with two peaks identified at +0.18 and -0.46 V. This reduction current is attributed to the de-doping of the polymer formed when EDOT is oxidized.

Structure 1

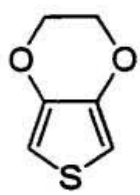

3. 4-ethylenedioxythiophene

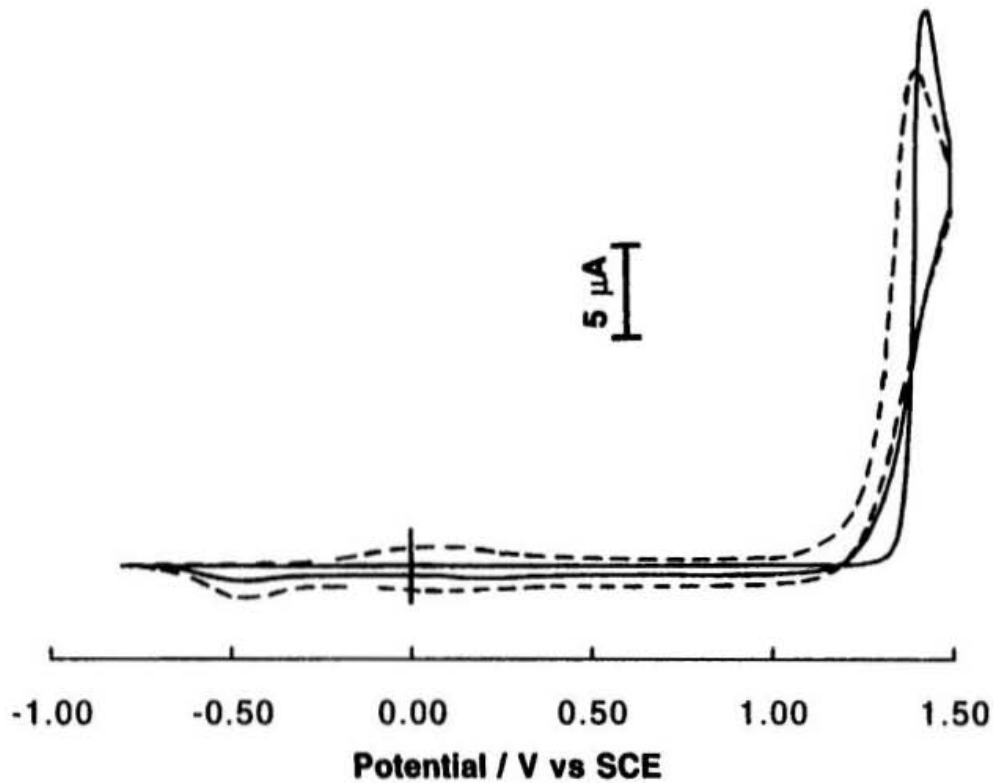

Fig. 6.1 Cyclic voltammograms of EDOT (5 mM) on a Pt electrode (0.0052 cm^2) in acetonitrile containing 0.1 M Bu_4NPF_6. Potential range: -0.80 - 1.50 V. Scan rate: 100 mV/s
The first cycle: the solid line; The second cycle: the dashed line

In the second cycle (the dashed line), a current appears at +0.04 V, which was absent during the first cycle, resulting from the oxidation (p-doping) of the polymer. Compared with the first cycle, both the oxidation onset potential for the monomer and the peak potential of the second cycle shift cathodically to +1.24 and +1.40 V respectively. These cathodic shifts have also been observed for Th monomers containing one Th unit in their structures [32-34], but not in the cases of those containing two or more Th units [35-38], implying that oxidation of the monomer is easier on the polymer coated electrode than on the bare electrode, and nucleation from one Th unit precursors is more difficult than that from two or more Th unit precursors. Based on this hypothesis, catalysis of the polymerization of Th by bithiophene (BTh) and terthiophene (TTh) has been suggested [39].

It should be noted that the oxidation of EDOT occurs at potentials much less than those required for oxidation of Th (E_{pa} = +2.07 V) [12, 40] and close to the range for BTh (E_{pa} = +1.35 V) [12, 40]. This means that the electropolymerization of EDOT can be carried out at relatively low potentials, where overoxidation [41, 42], which seriously degrades the properties of electrochemically prepared poly-Th, is completely eliminated. This low electrosynthesis potential is attributed to the strong electron donating effect of ethylenedioxy fused at 3- and 4- positions, which raises the HOMO energy level of the Th ring significantly.

This strong electron donating group also raises the LUMO energy of EDOT, causing the reduction of EDOT to be even more difficult than that of Th, but this effect

is not so great as that on the HOMO energy. The onset of the reduction of EDOT was estimated as ca. -3.2 V from CV, thus giving the electrochemical band-gap of ca. 4.5 V.

An optical absorption spectrum of the EDOT monomer in acetonitrile is shown in **Fig. 6.2**. The absorption peak due to the $\pi \rightarrow \pi^*$ transition appears at 258 nm and the absorption edge occurs at 277 nm. Both are shifted bathochromically compared with the Th monomer (231 and 250 nm for the absorption peak and edge of Th, respectively (see section **3.2.2**)), indicating that a lower optical band-gap has been achieved with EDOT. This optical band-gap is 4.47 eV, in agreement with the electrochemical band-gap (ca. 4.5 V).

6.3 Redox potential and band-gap of poly-EDOT

6.3.1 Synthesis of poly-EDOT films

In our experiments, repetitive potential sweep and constant current techniques were employed to synthesize poly-EDOT films. **Fig 6.3** shows a typical sequence of voltammograms for the electrochemical generation of a poly-EDOT film on a Pt electrode from EDOT (5 mM) in acetonitrile containing 0.1 M Bu_4NPF_6. The broad cathodic processes and anodic processes at lower potentials, which increases progressively in intensity with the number of cycles, result from the de-doping and doping of the polymer

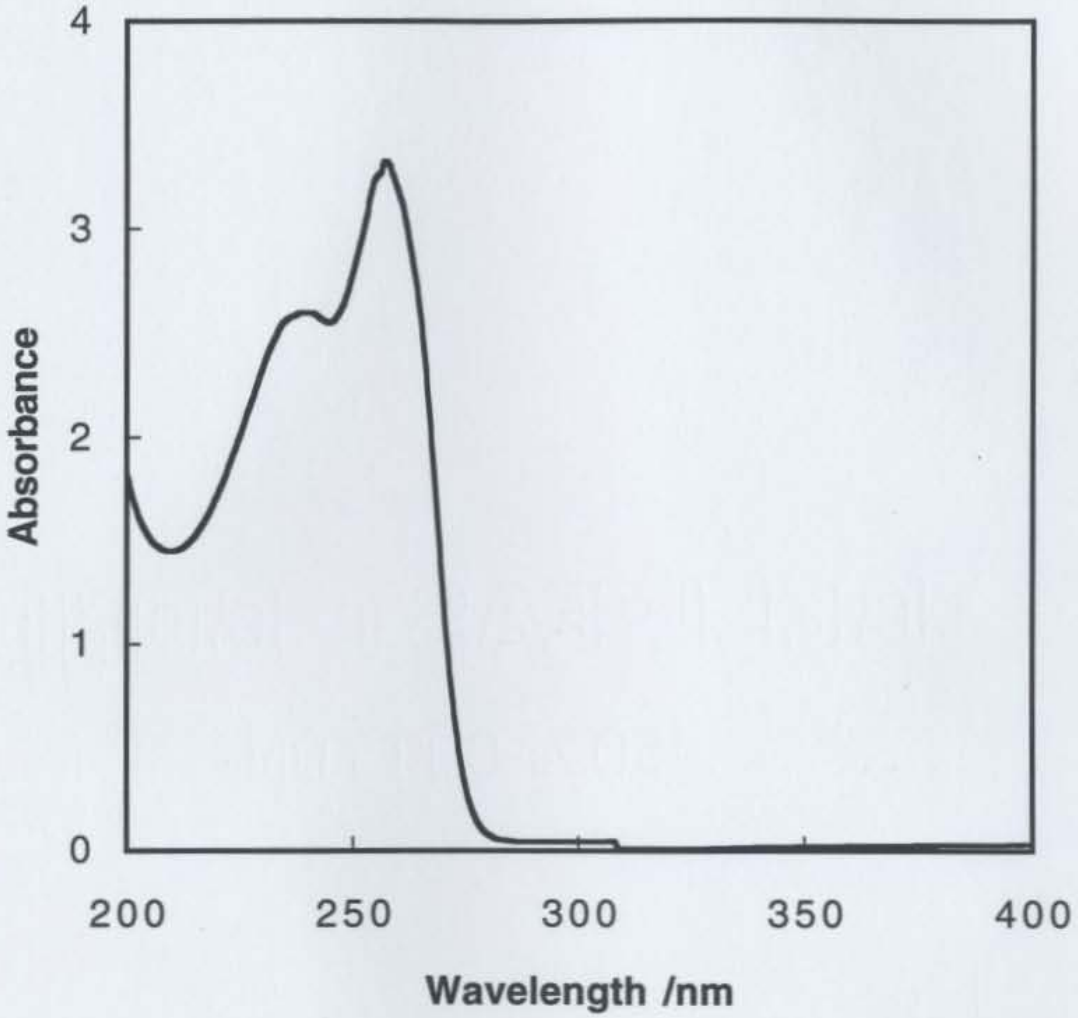

Fig. 6.2 UV-Visible absorption spectrum of 3,4-ethylenedioxythiophene (EDOT) in acetronitrile solution

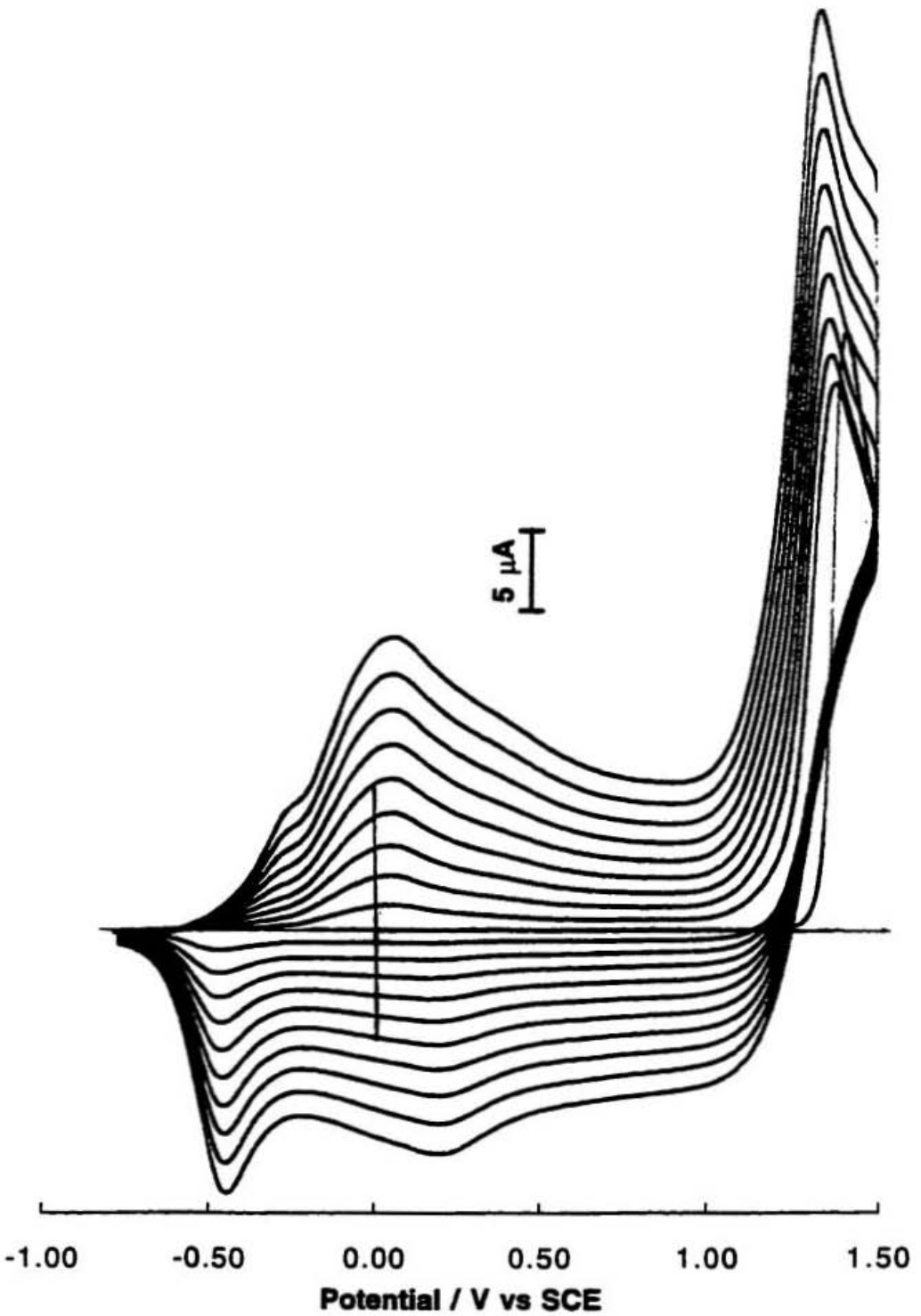

Fig. 6.3 Multisweep voltammograms of EDOT (5 mM) on a Pt electrode (0.0052 cm^2) in acetonitrile containing 0.1 M Bu_4NPF_6
Potential range: -0.80 - 1.50 V. Scan rate: 100 mV/s

grown during the anodic process at higher potentials. A dark blue film was observed on the electrode after the final electrochemical reduction.

It has been found that electrochemical growth of poly-EDOT is much easier than for its parent, poly-Th. This has been explained by the stress caused by the ethylenedioxy ring fused at 3- and 4- positions which prevents an optimal conjugation between the lone pairs of the two oxygen atoms and the Th moiety and increases the relative reactivity of the α-carbons for coupling [43-45].

6.3.2 Electrochemistry of poly-EDOT

A poly-EDOT film of ca. 0.3 μm was synthesized on Pt electrode (0.0052 cm^2) by using a constant current density of 0.5 mA/cm^2 for 80 s. Cyclic voltammograms for p-doping and n-doping of the film in acetonitrile + 0.1 M Bu_4NPF_6 at different potential scan rates are shown in **Fig. 6.4** (**a**) and (**b**) respectively. Electrochemical data for the p-doping are given in **Table 6.1**.

Table 6.1 Electrochemical data of p-doping for poly-EDOT

Scan speed /mV/s	$E_{p(ox)}$ /V	$i_{p(ox)}$ /μA	$E_{p(re1)}$ /V	$i_{p(re1)}$ /μA	$E_{p(re2)}$ /V	$i_{p(re2)}$ /μA
20	0.04	0.79	0.20	-0.38	-0.48	0.56
40	0.04	1.60	0.20	-0.76	-0.48	1.15
60	0.05	2.45	0.20	-1.18	-0.48	1.74
80	0.05	3.20	0.21	-1.55	-0.48	2.30
100	0.05	4.01	0.21	-1.91	-0.48	2.87

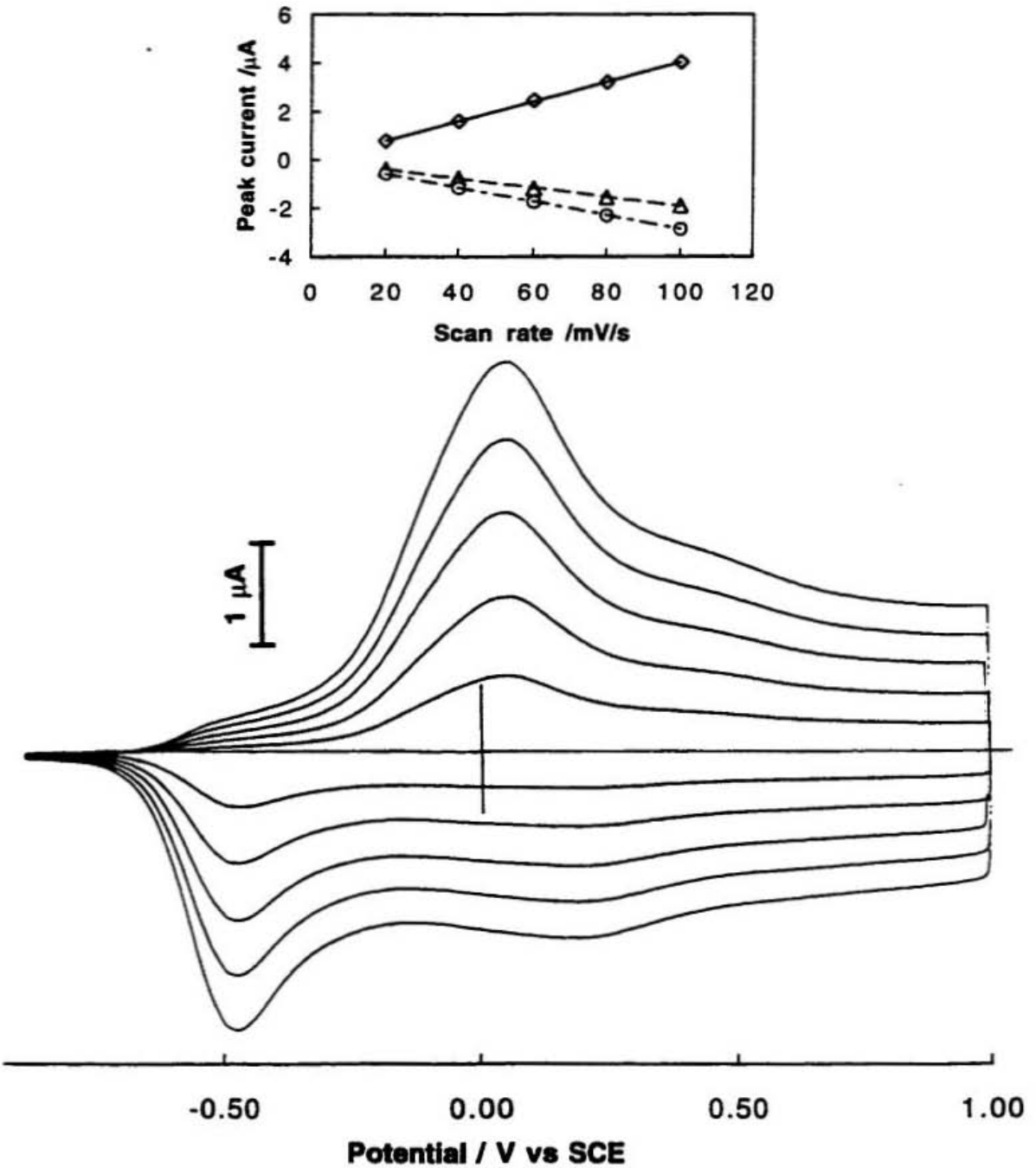

Fig. 6.4a Cyclic voltammograms for the p-doping (-0.90 - 1.00 V) of poly-EDOT in acetonitrile containing 0.1 M Bu_4NPF_6 at different scan rates (100, 80, 60, 40, 20 mV/s) Insert: the plot of peak currents versus scan rates

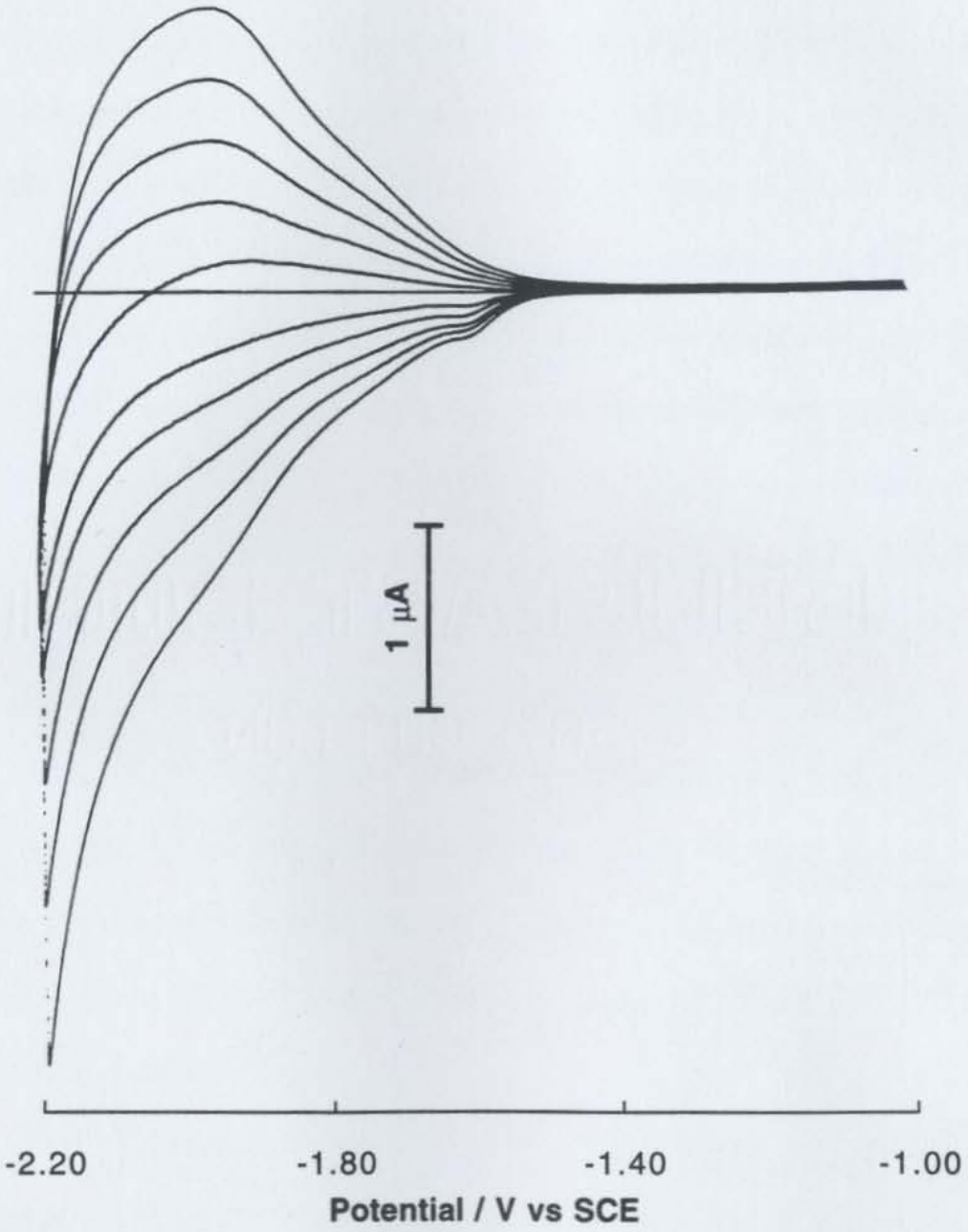

Fig. 6.4b Cyclic voltammograms for the n-doping (-1.00 - -2.20 V) of poly-EDOT in acetonitrile containing 0.1 M Bu_4NPF_6 at different scan rates (100, 80, 60, 40, 20 mV/s)

The p-doping of poly-EDOT was carried out in the potential range between -0.90 and +1.50 V. The CVs show an oxidation wave with a peak at +0.05 V, followed by a broad flat plateau and, in the reverse sweep, a flat reduction wave at +0.21 and a main reduction peak at -0.48 V. These peak positions are practically independent of the scan rate. The plot inserted in **Fig. 6.4 (a)** displays the peak currents for the doping and de-doping processes against the scan rate. The currents increase linearly with increasing scan rate. The CV behavior and the ratio between the de-doping charges and doping charges, which is unity, show that p-doping of poly-EDOT is a very reversible process.

The stability of poly-EDOT films was tested by continuous cycling over different potential ranges. Over the potential ranges of -1.00 to +1.00 V and -1.00 to +1.20 V, the polymer is very stable (100 cycles). Even when the upper switch potential limit was increased to +1.40 V, no significant decrease in the current was detected after 100 cycles. However, when the positive limited potential was set to +1.60 V, a rapid decay of the current was observed during the first several cycles, followed by a gradual decrease. It has been claimed that poly-EDOT is even stable in aqueous media [19, 47] and at high temperatures (e.g. 110^{0}C) [48].

It is worth noting that poly-EDOT has one of the lowest onset potential for p-doping among the poly-Th family [1] and has an extremely wide potential range for p-doping. Based on the CVs, the relationship between the doping level and potential is plotted in **Fig. 6.5**. The doping level is calculated according to equation **3-1**, where n

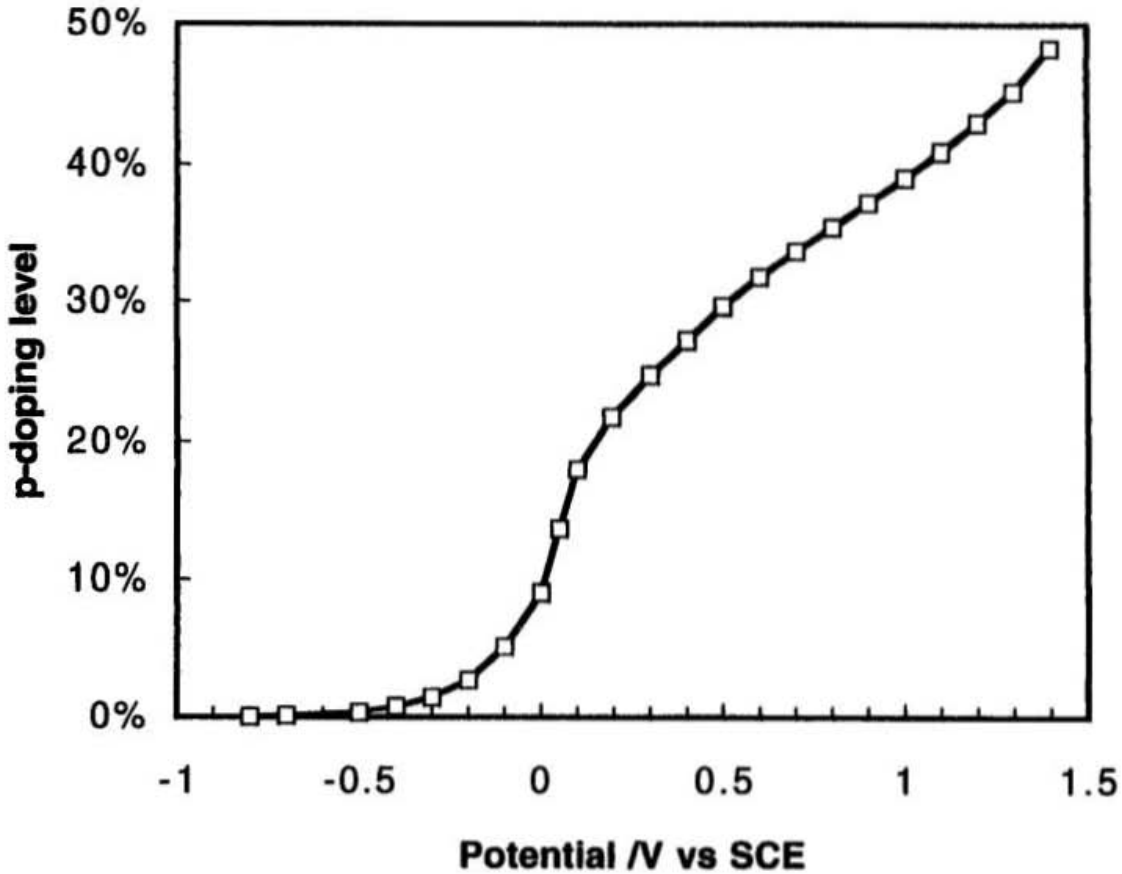

Fig. 6.5 P-doping levels of poly-EDOT against potentials

equals 6, and the charge used for doping of the polymer during its synthesis is 6.67 mC/cm^2. The p-doping level becomes appreciable at -0.2 V, and accelerates quickly in the potential range from -0.1 to +0.3 V, after which it increases steadily. At +1.40 V, a doping level of 48.2% was reached. This value is much higher than for most poly-Ths (typically 15%-30% [49-53]). At +1.60 V, a doping level of ca. 60% has been achieved, making it one of the most heavily doped polymer known. Because of its excellent stability and large doping capacity, poly-EDOT is a promising electrode material for batteries [19] and supercapacitors [54].

N-doping of poly-EDOT was studied in the potential range from -0.90 to -2.20 V. The voltammetric waves are not so regular and reversible as for p-doping. The ratio between the de-doping charge and the doping charge was substantially less than unity (<75%), indicating that a large amount of charge is trapped or lost and can not be recovered [55]. Charge trapping is proven by a huge pre-peak that appears when the potential is scanned into the p-doping range. The n-doping of poly-EDOT is also unstable; after 20 cycles, the current decreases to about 66% of its initial value. The formal potential for n-doping, $E^{0'}$, is -2.09 V (average of the doping peak potential and the de-doping peak potential), less than that of poly-Th (-1.83 V, see section **3.3.1**).

The electrochemical band-gap for poly-EDOT is ca. 1.4 V (the onset potentials for p-and n-doping are -0.25 V and -1.65 V respectively). This value is in accordance with a published result [30], but lower than the value given by optical studies (1.6 eV). This difference may be due to the effects of solvation [56-58].

6.3.3 Spectroelectrochemical characterization of poly-EDOT

A thin poly-EDOT film was deposited on an ITO electrode (10Ω/cm^2, 0.8 cm^2, Donnelly Corp.) at 0.5 mA/cm^2 for 800 s. **Fig. 6.6** shows UV-Vi-NIR absorption spectra of the polymer under different controlled potentials.

At -0.80 V, poly-EDOT is undoped and in the neutral state. The optical spectrum shows a strong and narrow absorption band with a maximum at 598 nm, corresponding to the conjugated $\pi-\pi^*$ transition, and giving the film in a dark-blue color. Compared with its parent polymer, poly-Th (480 nm), this absorption maximum is shifted ca. 120 nm bathochromically. From the onset (ca. 770 nm) of the absorption, a band-gap of 1.61 eV is obtained. This band-gap is 0.5 eV lower than that of poly-Th (2.1 eV), indicating that poly-EDOT is one of the lowest band-gap conducting polymers.

When the potential is increased to -0.40 V, a weak absorption appears in the high wavelength region. At 0.00 V (a doping level of 9.1%), the absorption due to the $\pi-\pi^*$ transition (598 nm) decreases, and two new absorption bands appear at longer wavelengths. One at λ_{max} = 950 nm (1.3 eV), corresponds to absorption by polarons, and the other which is above 1300 nm (<0.9 eV) is due to bipolarons. It is clearly evident that at this doping level (9.1%), undoped units ($\pi-\pi^*$ transition), polarons (low doping level), and bipolaron (high doping level) coexisted along the polymer chain. At +0.40 V (a doping level of 27%), the $\pi-\pi^*$ transition disappears, turning the color of the polymer to light blue (almost colourless), and the absorption bands associated with polarons and

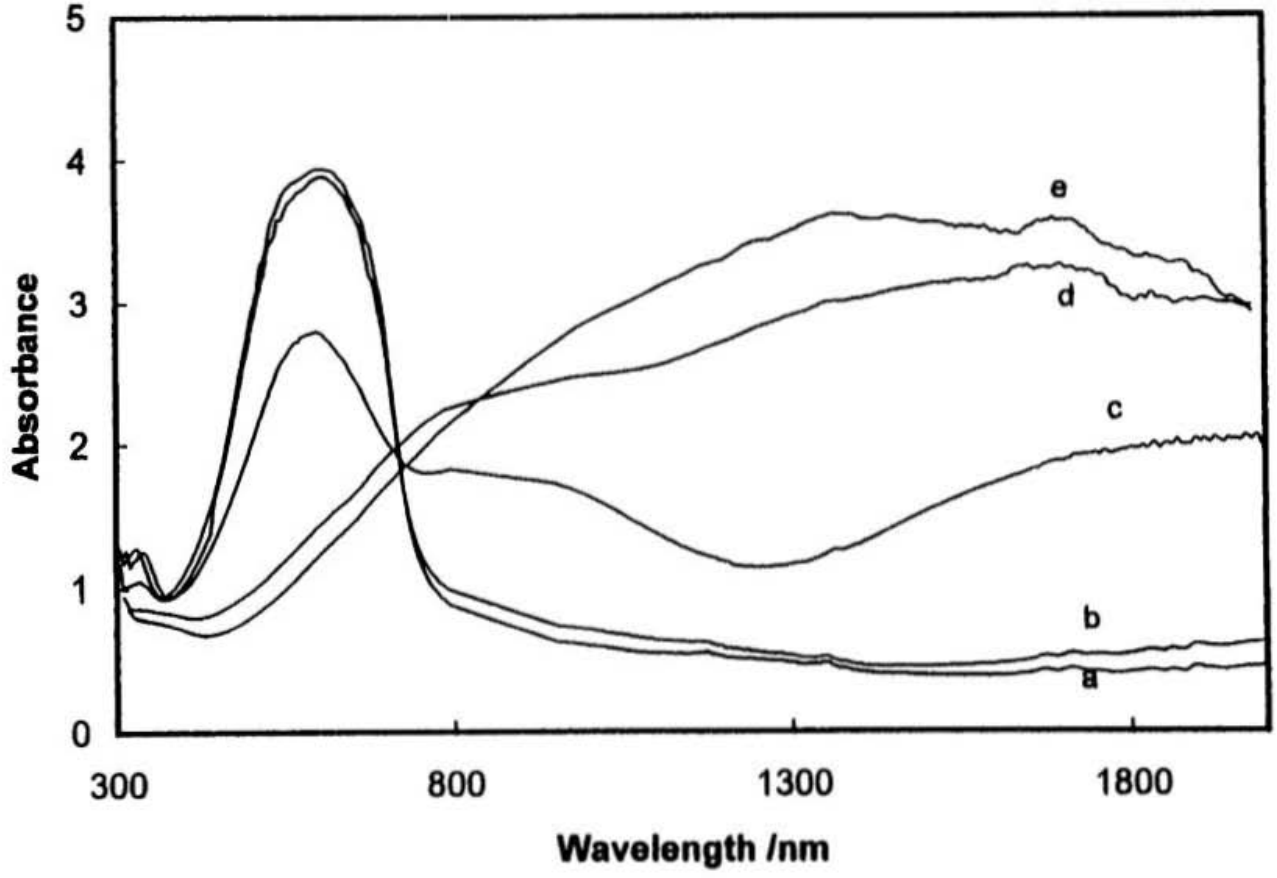

Fig. 6.6 Spectroelectrochemical studies of a poly-EDOT film on ITO electrode in acetonitrile containing 0.1 M Bu_4NPF_6 at **(a)** -0.8, **(b)** -0.4, **(c)** 0, **(d)** 0.4, and **(e)** 0.8 V

bipolarons becomes stronger. At higher potentials, e.g. +0.80 V (doping level of 35%), the polarons and bipolarons merge, producing a broad absorption with a peak at ca. 1400 nm (0.85 eV).

6.4 *In situ* conductivity measurements on a poly-EDOT film

In situ p- and n-type conductivities of poly-EDOT were measured as a function of potential by using the dual-electrode sandwich technique [59, 60]. A poly-EDOT film of ca. 0.3 μm thickness was synthesized at 0.5 mA/cm^2 for 80 s, and the potential scan rate of 1 mV/s was used for the measurement of conductivity. The results are plotted in log format in **Fig. 6.7**.

For low levels of p-doping (i.e. < 5.2%, in the potential range from -0.50 to -0.10 V), the conductivity increases exponentially with increasing potential, reflecting the exponential increase of the concentration of charge carriers. Even at a doping level as low as 1% (at -0.35 V), a fairly high conductivity of ca. 10^{-4} S cm^{-1} was observed. When the potential reaches +0.20 V (doping level > 22%), the conductivity becomes constant at 0.60 S cm^{-1}. The same conductivity profile was reproducible over multiple cycles indicating that the polymer is very stable when p-doped.

The n-type conductivity of poly-EDOT also shows the exponential increase of conductivity as the doping level increases (decreasing potential). At -2.2 V, it reaches a

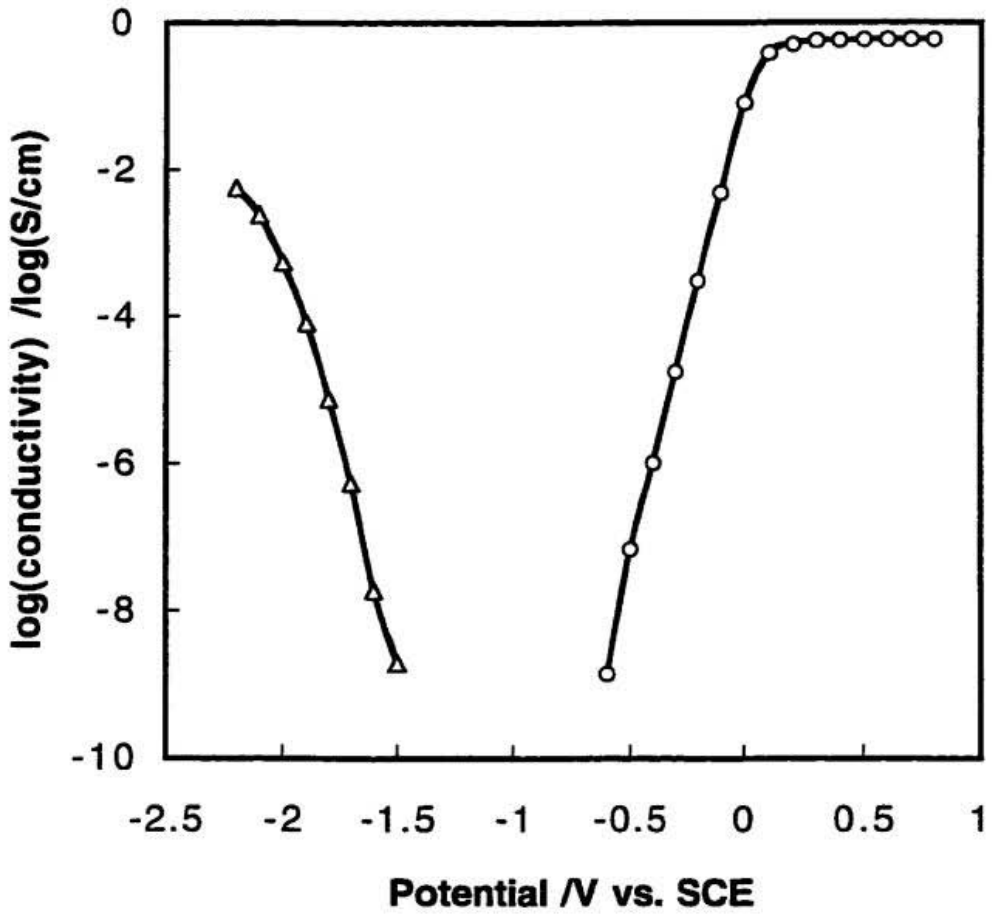

Fig. 6.7 Plot of log(conductivity) versus potential for a poly-EDOT film
Open circle: p-type conductivity; Open triangle: n-type conductivity

maximum of 5.7×10^{-3} S cm^{-1}, about 100 times smaller than the maximum p-type conductivity. However, lower conductivities (max. 3.5×10^{-3} S cm^{-1}) are measured for the second cycle suggesting the n-doped state is not stable.

6.5 Conclusion

Electrochemical studies of the EDOT monomer have revealed that due to the strong electron-donating effect of dioxyethylene group fused at the 3 and 4 positions, EDOT has a significantly higher HOMO energy level compared to Th. This results in a reduced band-gap for the monomer, as seen from the UV-Vis absorption spectrum.

Upon polymerization, the resulting poly-EDOT maintains the characteristics of the monomer, that is, the polymer has a reduced band-gap and much low oxidation potential (p-doping) compared to poly-Th. Two other remarkable properties of poly-EDOT are that it can be heavily p-doped (doping levels of 48% and 60% at 1.4 V and 1.6 V, respectively) and it exhibits excellent cycling stability for the p-doping. Measurement of the *in situ* conductivity against potential of the polymer shows a wide potential range (>0.1 V) for highest p-type conductivity, in agreement with cyclic voltammetry. Maximum p- and n-type conductivities were found to be 0.60 and 5.7×10^{-3} S cm^{-1}, respectively.

References

[1] J. Roncali, *Chem. Rev.*, **92**, 711 (1992)

[2] M. Sato, S. Tanaka, and K. Kaeriyama, *J. Chem. Soc., Chem. Commun.*, 873 (1986)

[3] M. R. Brye, A. Chissel, P. Kathirgamanathan, D. Parker, and N. M. R. Smith, *J. Chem. Soc., Chem. Commun.*, 466 (1987)

[4] M.Lemaire, R. Garreau, F. Garnier, and J. Roncali, *New J. Chem.*, **11**, 703 (1987)

[5] R. J. Waltman, J. Bargon, and A. F. Diaz, *J. Phys. Chem.*, **87**, 1459 (1983)

[6] H. S. Li, J. Roncali, and F. Garnier, *J. Electroanal. Chem.*, **263**, 155 (1989)

[7] R. J. Walman and J. Bargon, *Can. J. Chem.*, **64**, 76 (1986)

[8] G. Tourillon and F. Garnier, *J. Phys. Chem.*, **87**, 2289 (1983)

[9] J. Roncali, A. Yassar, and F. Garnier, *J. Chem. Soc., Chem. Commun.*, 581 (1988)

[10] A. Yassar, J. Roncali, and F. Garnier, *Macromolecules*, **22**, 804, 1989

[11] J. Roncali, M. Lemaire, R. Garreau, and F. Garnier, *Synth. Met.*, **18**, 139 (1987)

[12] T. C. Chung, J. H. Kaufman, A. J. Heeger, and F. Wudl, *Phys. Rev., B*, **30**, 702 (1984)

[13] K. Meerholz and J. Heinze, *Electrochim. Acta*, **41**, 1839 (1996)

[14] G. Tourillon and F. Garnier, *J. Electroanal. Chem.*, **161**, 51 (1984)

[15] M. Feldhues, G. Kampf, J. Litterer, T. Mecklenburg, and P. Wegener, *Synth. Met.*, **28**, C487 (1989)

[16] G. Daoust and M. Leclerc, *Macromolecules*, **24**, 455 (1991)

[17] F. Jonas and L. Schrader, *Synth. Met.*, **41-43**, 831 (1991)

[18] J. Roncali, F. Garnier, R. Garreau, and M. Lemaire, *J. Chem. Soc., Chem. Commun.*, 1500 (1987)

[19] M. Dietrich, J. Heinze, G. Heywang, and F. Jonas, *J. Electroanal. Chem.*, **369**, 87 (1994)

[20] F. Wudl, M.Kobayashi, and A. J.Heeger, *J. Org. Chem.*, **49**, 3382 (1984)

[21] J. Roncali, *Chem. Rev.*, **97**, 173 (1997)

[22] I. Hoogmartens, P.Adriaensens, D. Vanderzande, J. Gelan, C. Quattrochi, R. Lazzaroni, and J. L. Bredas, *Macromolecules*, **25**, 7347 (1992)

[23] J. L. Bredas, A. J. Heeger, and F. Wudl, *J. Chem. Phys.*, **85**, 4673 (1986)

[24] Y. S. Lee and M. Kertesz, *Int. J. Quantum Chem. Symp.*, **21**, 163 (1987)

[25] P. A. Christensen, J. C. H. Kerr, S.J. Higgins, and A. Hamnet, *Faraday Discuss., J. Chem. Soc.*, **88**, 261 (1989)

[26] S. M. Dale, A. Glide, and A. R. Hillman, *J. Mater. Chem.*, **2**, 99 (1992)

[27] G. Heywang and F. Joans, *Adv. Mater.*, **4**, 116 (1992)

[28] Q. Pei, G. Zuccarello, M. Ahlskog, and O.Inganas, *Polymer*, **35**, 1347 (1994)

[29] G. A. Sotaing and J. R. Reynolds, *Chem. Mater.*, **8**, 882 (1996)

[30] Y. Fu, J. Cheng, and R. L. Elsenbaumer, *Chem. Mater.*, **9**, 1720 (1997)

[31] A. J. Dowanard and D. Pletcher, *J. Electroanal. Chem.*, **206**, 139 (1986)

[32] A. J. Dowanard and D. Pletcher, *J. Electroanal. Chem.*, **206**, 147 (1986)

[33] B. Ballarin, R. Seeber, D. Tonelli, F. Andreani, P. Costa Bizzarri, C. Della Casa, and E. Salatelli, *Synth. Met.*, **88**, 7 (1997)

[34] S. J. Higgins, C. Jones, G. King, K. H. D. Slack, and S. Petidy, 78, 155 (1996)

[35] J. P. Ferraris and M. D. Newton, *Polymer*, **33**, 391 (1992)

[36] G. Zotti, M. C. Callazzi, G. Zerbi, and S. V. Meille, *Synth. Met.*, **73**, 217 (1995)

[37] B. Krische and M. Zagorska, *Synth. Met.*, **33**, 257 (1989)

[38] M. Hasik, J. E. Laska, A. Pron, I. Kulszewica-Bajer, K. Koziel, and M. Laplowski, *J. of Poly. Sci., Part A: Poly. Chem.*, 30, 1741 (1992)

[39] Y. Wei, C-C, Chan, J. Tian, G-W Jang, and K. F. Hsuech, *Chem. Mater.*, **3**, 888 (1991)

[40] A. F. Diaz, J. Crowcay, J. Bargon, G. P. Gardini, and J. B. Torrance, *J. Electroanal. Chem.*, **12**, 355 (1981)

[41] B. Krishe and M. Zagorska, *Synth. Met.*, **28**, C263 (1989)

[42] M. Barsch and F. Beck, *Eletrochim. Acta*, **41**, 1761 (1996)

[43] M. Lemaire, W. Buchner, A. H. Huynh, A. Guy, and J. Roncali, *J. Electroanal. Chem.*, **281**, 293 (1990)

[44] A. Berlin, G. A. Pagani, and F. Sannicolo, *J. Chem. Soc., Chem. Commun.*, 1663 (1986)

[45] J. Roncali, A. Guy, M. Lemaire, R. Garreau, and A. H. Huynh, *J. Elcetroanal. Chem.*, **312**, 277 (1991)

[46] G. Zotti, S. Cattarin, and N. Comisso, *J. Electroanal. Chem.*, **235**, 259 (1987)

[47] A. G. Bayer, *European patent*, 03339340 (1989)

[48] Q. Pei, G. Zuccarello, M. Ahlskog, and O. Inganas, *Polymer*, **35**, 1347 (1994)

[49] B. Rasch and W. Vielstich, *J. of Electroanal. Chem.*, **370**, 109 (1994)

[50] A. F. Diaz and J. C. Lacroix, *New J. Chem.*, **12**, 171 (1988)

[51] A. O. Patil, A. J. Heeger, and F. Wudl, *Chem. Rev.*, **88**, 183 (1988)

[52] K. Kaneto, Y. Kohno, K. Yoshino, and Y. Inuishi, *J. Chem. Soc., Chem. Commun.*, 382 (1983)

[53] K. Kaneto, K. Yoshno, and Y. Inuishi, *Jpn. J. Appl. Phys.*, **21**, L567 (1982)

[54] J. C. Carlberg and O. Inganas, *J. Electrochem. Soc.*, **144**, L61 (1997)

[55] G. Zotti, G. Schiavon, and S. Zecchin, *Synth. Met.*, **72**, 275 (1995)

[56] V. D. Parker, *J. Am. Chem. Soc.*, **98**, 98 (1976)

[57] L. E. Lyons, *Aust. J. Chem.*, **33**, 1717 (1980)

[58] R. O. Loutfy and Y. C. Cheng, *J. Chem. Phys.*, **73**, 2902 (1980)

[59] C. E. D. Chidsey and R. W. Murry, *Science*, **231**, 25 (1986)

[60] H. Huang and P. G. Pickup, *Acta Polymer.*, **48**, 455 (1997)

Chapter 7

Poly-(CDM-co-EDOT): A Very Low Band-Gap Conducting Polymer with High Intrinsic Conductivity

7.1 Introduction

According to band theory [1, 2], conjugated polymers with narrow band-gaps can be achieved either by increasing the energy level of the valence band, or by lowering the energy level of conduction band, or by both. Several approaches [3-6] have been developed to realize this goal. One of them is to build a polymeric chain with alternating donor and acceptor moieties [7, 8]. There are now a significant number of examples in the literature which appear to prove that this approach is effective [9-14].

Here we present a new copolymer with a very small band-gap (<0.2 eV) and high intrinsic conductivity (ca. 0.7 mS cm^{-1}). This copolymer has been prepared by copolymerization of a monomer having a high HOMO energy (the electron donor sub-unit) with another monomer having a low LUMO energy (the electron acceptor sub-unit). 4-dicyanomethylene-4*H*-cyclopenta[2,1-*b*; 3,4-*b* ']dithiophene (CDM, structure **1**) and 3,4-ethylenedioxy-thiophene (EDOT, structure **2**) have been chosen as for this purpose.

Structure 1

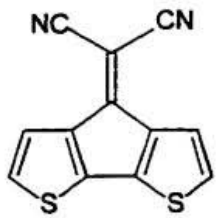

4-(dicyanomethylene)-4*H*-cyclopenta [2, 1-*b*:3, 4-*b*']dithiophene

Structure 2

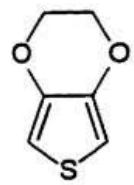

3. 4-ethylenedioxythiophene

CDM and its polymer were first studied by Ferraris and Lambert in 1991 [15]. As discussed in Chapter **4**, an electrochemical study of CDM, in comparison with bithiophene, showed that CDM has an oxidative peak potential (E_{pa}) at +1.44 V (vs. SCE), which is a little higher than the E_{pa} of bithiophene (1.31 V, see section **3. 2. 1**), however its formal potential for reduction ($E_{rc}^{0'}$) is -0.63 V, much higher than that of bithiophene (-2.2 V, see section **3.2.1**). This indicates that the dicyanoethene group bridging at the β and β' positions has little effect on the HOMO but a large effect on the LUMO [15], making CDM one of the monomers that have the lowest LUMO energy level.

EDOT has been discussed in Chapter **6**. It has an ethylenedioxy substituent fused in the 3 - and 4- positions [16, 17]. Due to the strong electron donation of the ethylenedioxy group, EDOT has an E_{pa} of +1.43 V [16] much lower than that of thiophene (+2.07 V, see section **3.2.1**) and close to that of bithiophene, indicating that EDOT has a high HOMO energy level.

In addition, the oxidation potentials for CDM and EDOT are very close (oxidation

potential peaks are at +1.44 and +1.43 V, respectively) allowing their copolymerization to be carried out readily by electrochemical methods.

7.2 Synthesis of poly-(CDM-co-EDOT) copolymer

Cyclic voltammograms of the two monomers (CDM (5 mM) and EDOT (5 mM)) separately in nitrobenzene containing 0.1 M Bu_4NPF_6 show that, in the first cycle, both have very similar potentials for the oxidation peak and onset (E_{pa} and E_{onset} for CDM are +1.44 and +1.32 V, and for EDOT are +1.43 and +1.32 V, respectively). However, EDOT gives much higher peak currents (~ 4 times higher than CDM), and in the second cycle, the oxidation onset for EDOT shifts cathodically to +1.18 V, while that for CDM shifts only slightly to +1.30 V. These observations indicate that poly-EDOT is more easily deposited than poly-CDM. Therefore, in order to achieve effective copolymerization, a relative low concentration of EDOT (2 mM) to CDM (8 mM) was chosen. Repetitive potential sweep and potential step techniques were employed to prepare poly-(CDM-co-EDOT) films in our experiments.

7.2.1 Repetitive potential sweep

Fig. 7.1 shows typical multisweep cyclic voltammograms of a mixture of CDM (8

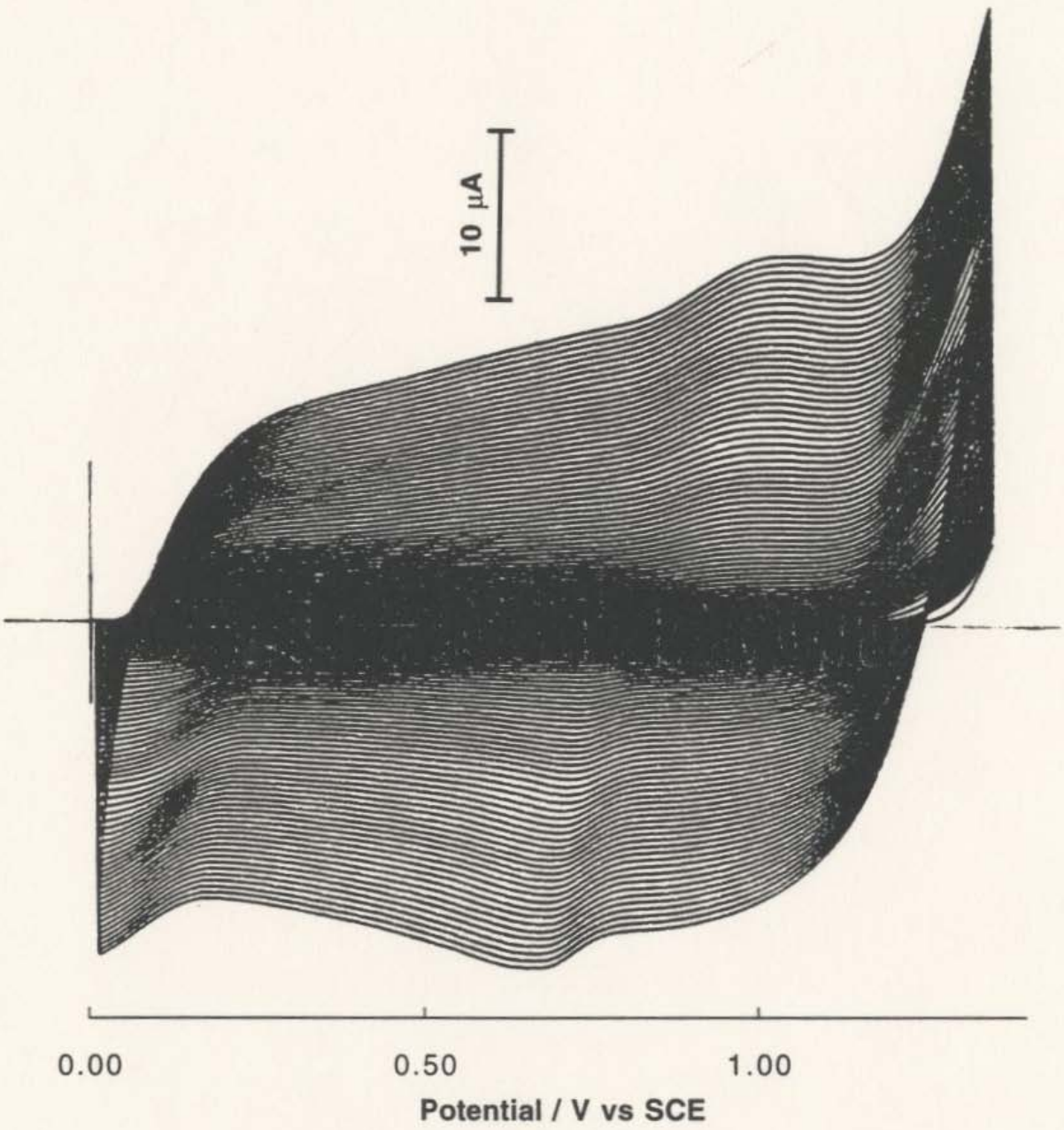

Fig. 7.1 Multisweep voltammograms of a mixture of CDM (8 mM) and EDOT (2 mM) in nitrobenzene containing 0.1 M Bu_4NPF_6 on a Pt electrode (0.0052 cm^2) Potential range: 0.00 - 1.35 V. Scan rate: 100 mV/s

mM) and EDOT (2 mM) in nitrobenzene containing 0.1 M Bu_4NPF_6 in the potential range between 0.00 and +1.35 V. The first cycle exhibits a "nucleation loop" commonly observed when a conducting phase is deposited [18-21]. The rising current at higher potentials (> +1.25 V) is the oxidation of the monomers to radical cations [22]. Polymer is subsequently formed either by radical-radical coupling or by a radical-substrate reaction [23]. The broad cathodic processes and anodic processes at lower potential, which increase in intensity with the number of cycles, result from the growth of the polymer. It is interesting that these multisweep CVs of a mixture of CDM and EDOT are different from a simple combination of those of CDM (see **Fig. 4. 3**) and EDOT (see **Fig. 6. 3**). The characteristic oxidation peaks at ca. +1.3 V for CDM and ca. +0.05 V for EDOT, and the reduction peaks at ca. +0.9 V for CDM and +0.21 V for EDOT are absent in **Fig. 7. 1**. Instead, a new oxidation peak at ca. +1.0 V and a new reduction peak at ca. +0.65 V, which are characteristic of a copolymer are seen. These differences strongly support our contention that a true copolymer is produced and not blends of two homopolymers.

7.2.2 Potential step

Copolymerization of CDM and EDOT by potential step techniques was carried out in the same solution as was used in repetitive cyclic voltommetric synthesis. The potentials employed were 1.26, 1.28, 1.30, 1.32, and 1.34 V, and the corresponding current-time (i vs.t) curves are shown in **Fig. 7. 2**.

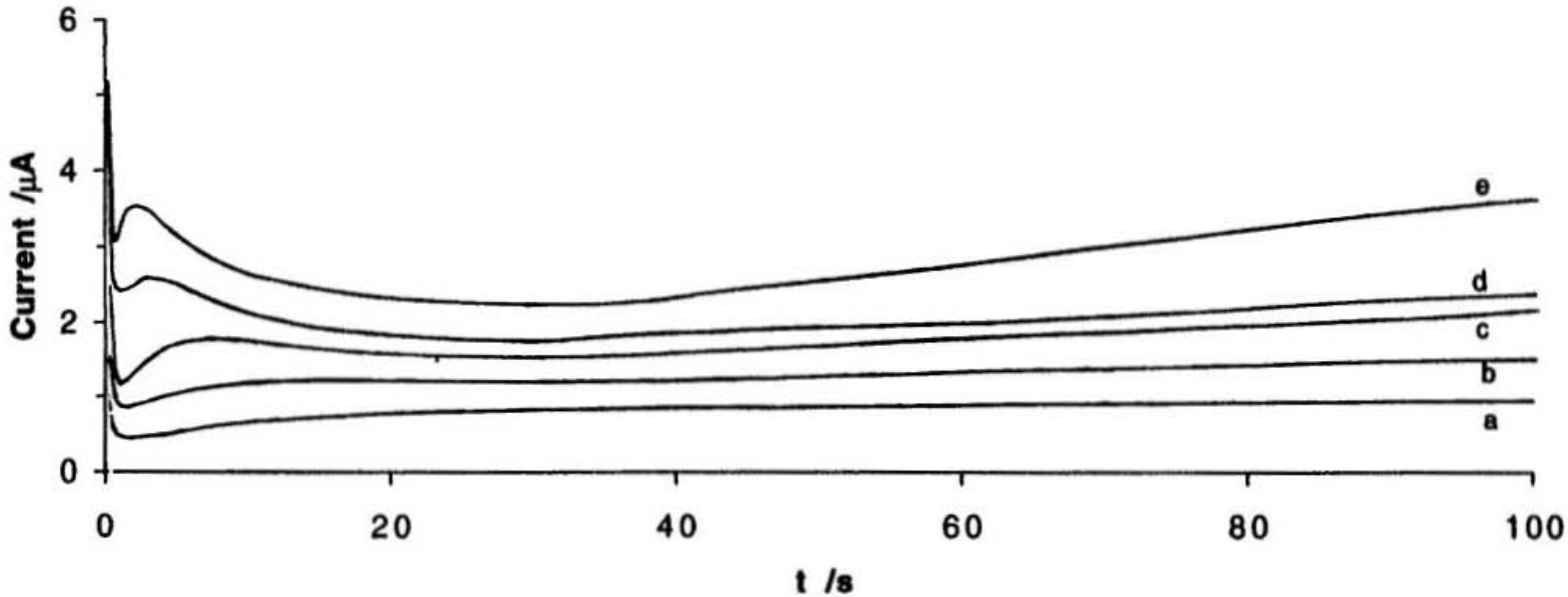

Fig. 7.2 Electrochemical polymerization of CDM (8 mM) and EDOT (2 mM) in nitrobenzene containing 0.1 M Bu_4NPF_6 on Pt electrodes (0.0052 cm^2)by potential step
Potentials are (a) 1.26 V, (b) 1.28 V, (c) 1.30 V, (d) 1.32 V, and (e) 1.34 V

In all cases the chronoamperometric response exhibits a huge current spike upon application of the oxidizing potential. A decreasing i-t transient follows in the early stages of the polymerization. This transient is shorter when a higher potential is applied. After this decrease, the current begins to increase in most cases, and for higher potentials, this increase is more pronounced. At 1.26 V. when a longer total time was used, this current increase is also very evident.

According to Hillman's analysis of the mechanism for the nucleation and growth of polythiophene [24], a monolayer of polymer is rapidly formed initially on the electrode surface. Instantaneous nucleation and three-dimensional growth of the polymer take place subsequently, causing a characteristic rising i-t transient. When the nuclei overlap, continued growth is only possible perpendicular to the substrate (one-dimensional growth), and is characterized by an approximately constant current.

In our experiments, the current continues to increase during 1-D growth. This may be due to an increasing surface area for growth as more polymer is deposited. This enlargement should be quicker as higher potential is applied. The i~t behavior for the mixture of CDM and EDOT is different from that for poly-CDM alone (Section **4. 3. 2**). In the later case, we have confirmed that the electropolymerization of CDM is controlled by monomer diffusion.

The resulting copolymers prepared at different potentials exhibit different colors. Copolymers synthesized at 1.26 and 1.28 V are blue in color, suggesting that EDOT is dominant in the structure, while at 1.34 V, the film is reddish, suggesting that CDM is dominant. Copolymers synthesized at 1.30 and 1.32 V are purple.

7.3 Electrochemistry of poly(CDM-co-EDOT)

Fig. 7.3 makes a comparison of the cyclic voltammograms of the two homopolymers: poly-CDM (dashed line; curve (**a**)) and poly-EDOT (dotted line; curve (**b**)), and the poly-(CDM-co-EDOT) (solid line; curve (**c**)) synthesized at +1.30 V. Curve (**a**) shows both the p-doping and n-doping of poly-CDM in the potential range from -0.60 to +1.20 V, corresponding to an electrochemical band-gap of ca. 0.8 V (section **4. 4**). Curve (**b**) only shows the p-doping of poly-EDOT, because its n-doping, which takes place below -2.0 V (section **6.3.2**), is not observed in the potential range of the experiment. The p-doping process of poly-EDOT occurs over a very broad potential region from -0.4 V to more than +1.2 V for the anodic scan. It is clearly seen that the electrochemical band-gap (from -0.1 to +0.7 V) of poly-CDM is covered by the range for the p-doping of poly-EDOT. Therefore, copolymerization of the two monomers would be expected to produce very low band-gap conducting polymers.

Curve (**c**) in **Fig. 7.3** shows that the copolymer does have a significantly reduced band-gap. The p-doping current, which obviously originates from the EDOT subunit, appears within the electrochemical band-gap of poly-CDM, resulting in a much lower band-gap. E_{pc} of the copolymer occurs at -0.78 V, more negative than that of poly-CDM (-0.45 V). This can be explained by the fact that EDOT is an electron-donating unit causing the LUMO energy level of the attached CDM units to increase. The cathodic shift of E_{pc} is further

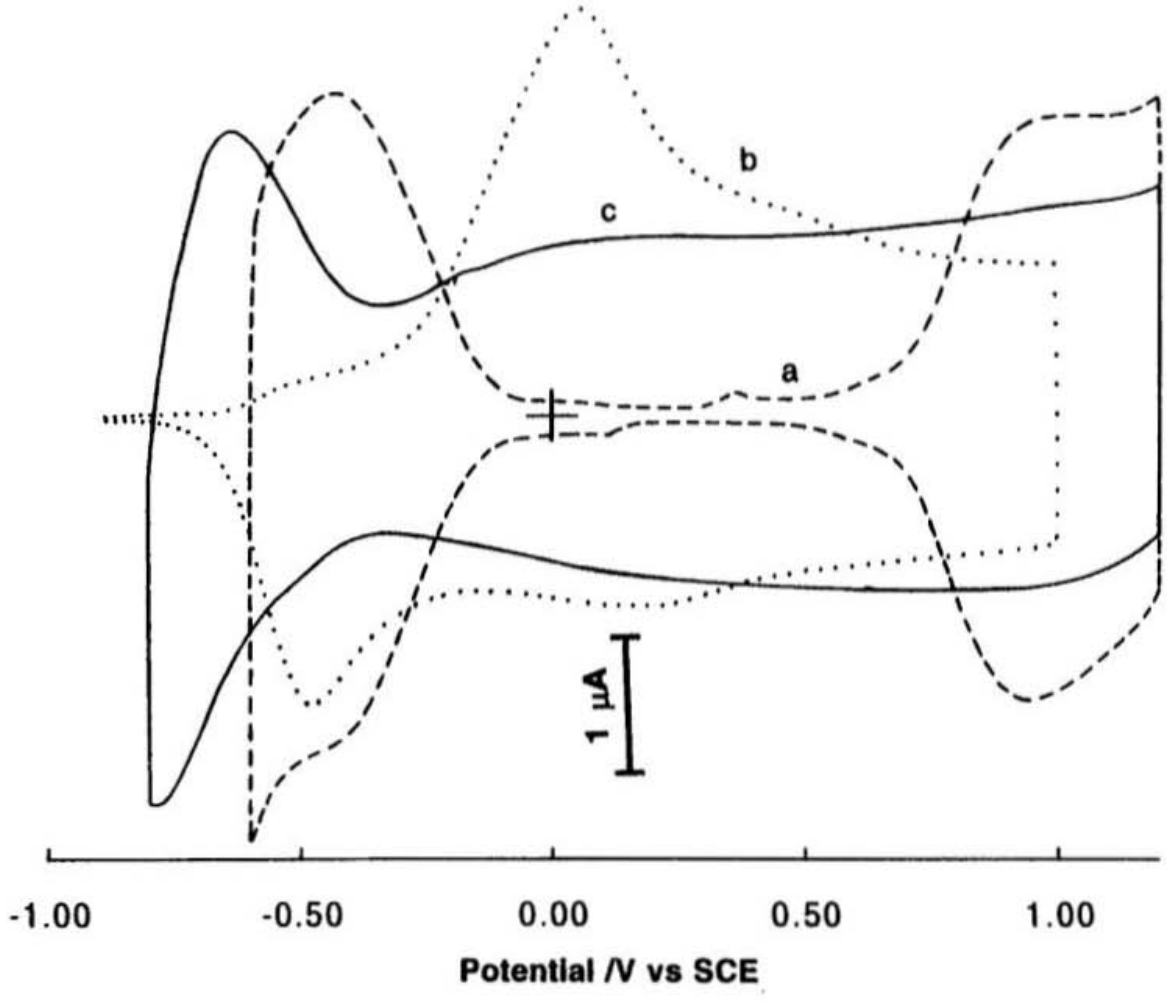

Fig. 7.3 Comparison of cyclic voltammograms of (a) poly-CDM, (b) poly-EDOT, and (c) poly-(CDM-co-EDOT) in acetonitrile containing 0.1 M Bu_4NPF_6 Scan rate: 100 mV/s

evidence that this polymer is a true copolymer, not a mixture of poly-CDM and poly-EDOT.

Fig. 7.4 shows the cyclic voltammograms at different scan rates of a poly-(CDM-co-EDOT) film synthesized at 1.30 V for 100 s, and **Table 7.1** gives the electrochemical data.

Table **7.1** electrochemical data for a poly-(CDM-co-EDOT)

	p-doping						n-doping			
scan rate /mV/s	$E_{p(ox1)}$ /V	$i_{p(ox1)}$ /μA	$E_{p(ox2)}$ /V	$i_{p(ox2)}$ /μA	$E_{p(re2)}$ V	$i_{p(re2)}$ /μA	$E_{n(re)}$ /V	$i_{n(re)}$ /μA	$E_{n(ox)}$ /V	$i_{n(ox)}$ /μA
20	0.21	0.284	1.10	0.320	0.73	-0.284	-0.78	-0.604	-0.62	0.372
40	0.21	0.564	1.10	0.656	0.73	-0.560	-0.78	-1.19	-0.63	0.726
60	0.21	0.840	1.10	0.956	0.73	-0.840	-0.78	-1.80	-0.63	1.21
80	0.21	1.12	1.10	1.28	0.73	-1.12	-0.78	-2.38	-0.64	1.68
100	0.21	1.40	1.10	1.58	0.73	-1.40	-0.78	-3.04	-0.64	2.15

In the potential range from -0.25 V to +1.20 V is the very broad p-doping region, peaking at ca. +0.2 and +1.0 V, which represents the oxidation of EDOT and CDM units in the copolymer respectively. These processes are reversible and very stable over multiple cycles (no significant change after 30 cycles). The n-doping process starts at -0.3 V and ends at -0.8 V with a sharp reduction peak at -0.78 V. The formal potential ($E^{0'}$) for the n-doping is -0.72 V. This process is also stable over multiple cycles (no significant change after 20 cycles). Both the p-doping and n-doping peak currents are linear with the scan rate (see the insert plot of **Fig. 7. 4**). The overlap of the p-doping and n-doping regions suggests that the electrochemical band-gap of the copolymer has vanished.

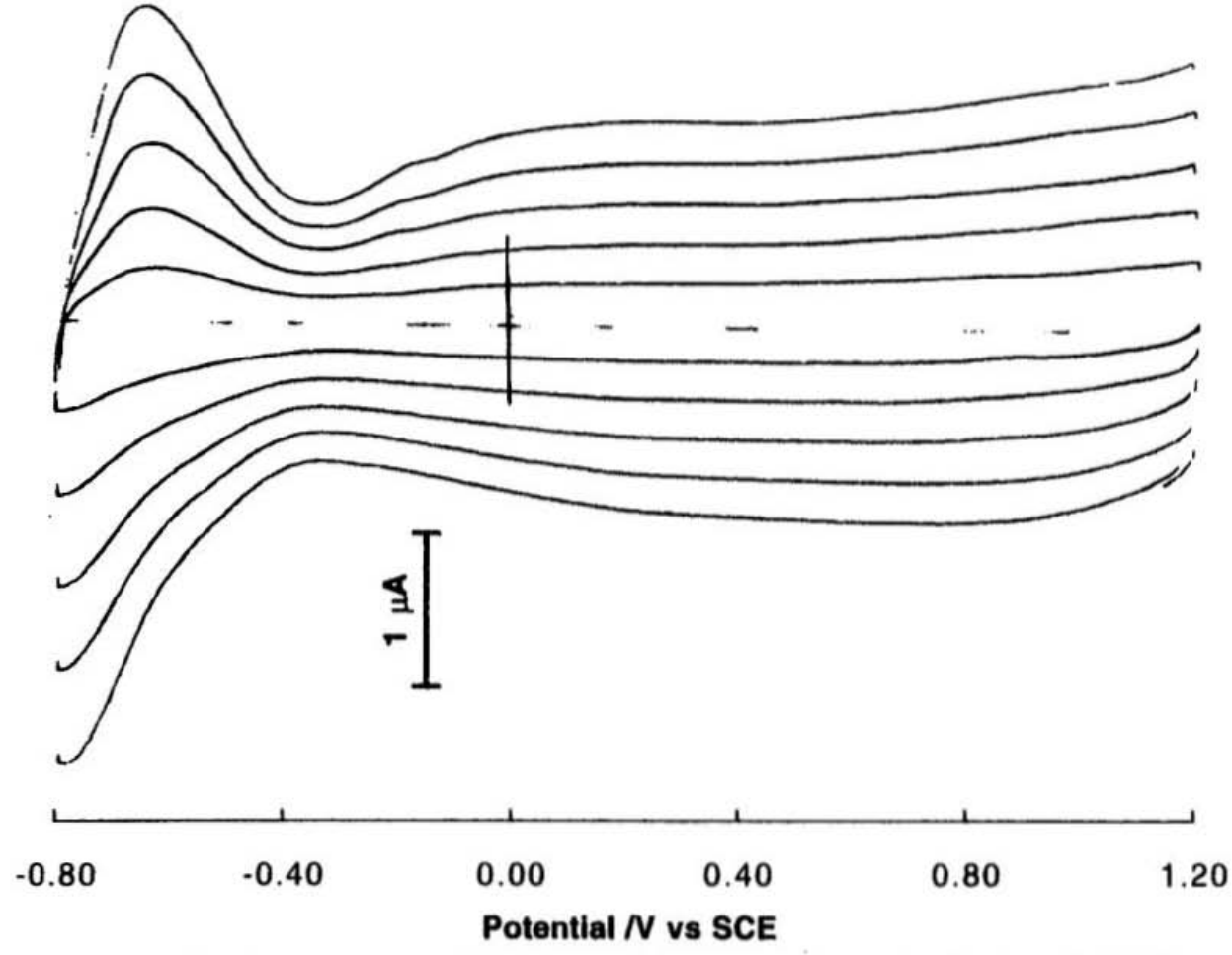

Fig. 7.4 Cyclic voltammograms at different potential scan rates for a poly-(CDM-co-EDOT) film in acetonitrile containing 0.1 M Bu_4NPF_6. Scan rates: 100, 80, 60, 40, 20 mV/s

Fig. 7. 5 shows cyclic voltammograms of various poly-(CDM-co-EDOT) films prepared at different potentials. As the polymerization potential increases, the peaks at ca. -0.75 V due to the n-doping of polymer segments rich in CDM increase relative to the p-doping region. This reflects the increasing CDM:EDOT ratio in the structure. Interestingly, the potential of these peaks does not shift significantly with changing composition (although they do appear to split into two separate waves), indicating that the n-type charge carriers formed by CDM are not extensively delocalized. This conclusion is supported by the fact that the reduction wave of the CDM monomer ($E^{0'}_{re}$ = -0.63 V) is shifted very little compared with its polymer ($E^{0'}_{re}$ = -0.45 V).

Only the films with the highest CDM:EDOT ratio show a significant feature at ca. +0.90 V that could be attributed to the p-doping of poly-CDM. This provides further strong evidence that we are dealing with true copolymers, rather than polymer blends. Based on the size of the -0.78 V peaks in **Fig. 7. 5** and the similar heights of the p- and n- doping waves of poly-CDM (**Fig. 7.3**), all of the copolymer films would have shown significant peaks at ca. +0.90 V if they were mixtures of poly-CDM and poly-EDOT.

7.4 Raman spectra of poly-(CDM-co-EDOT)

Poly-(CDM-co-EDOT) films were synthesized at 1.34, 1.32, 1.30, and 1.28 V in nitrobenzene containing 2 mM EDOT and 8 mM CDM in the presence of 0.1 M Bu_4NPF_6. **Fig. 7. 6** shows the Raman spectra of these copolymer films (**b, c, d, e**), together with the

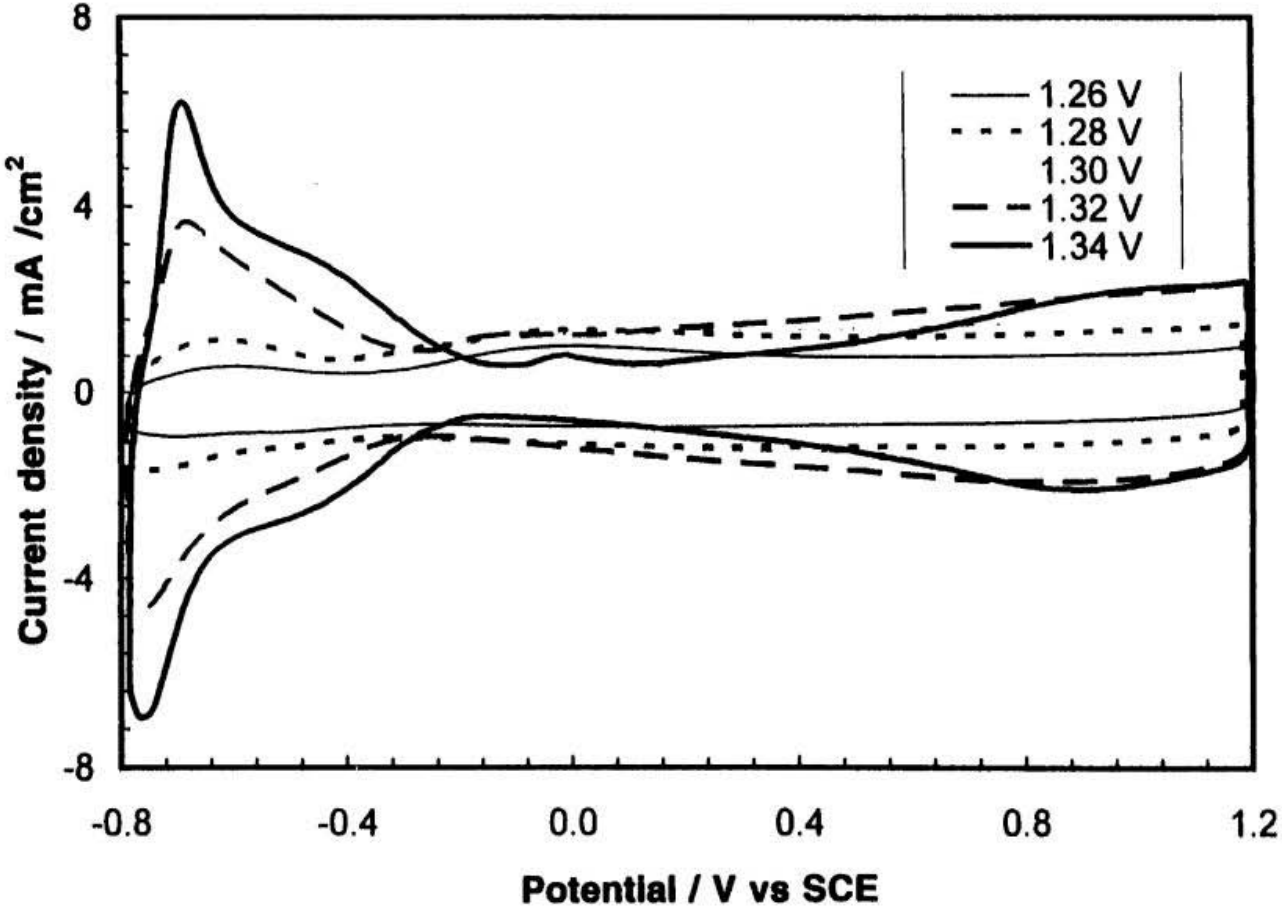

Fig. 7.5 Cyclic voltammograms in acetonitrile containing 0.1 M Bu_4NPF_6 of poly-(CDM-co-EDOT) films prepared at 1.26, 1.28, 1.30, 1.32, 1.34 V

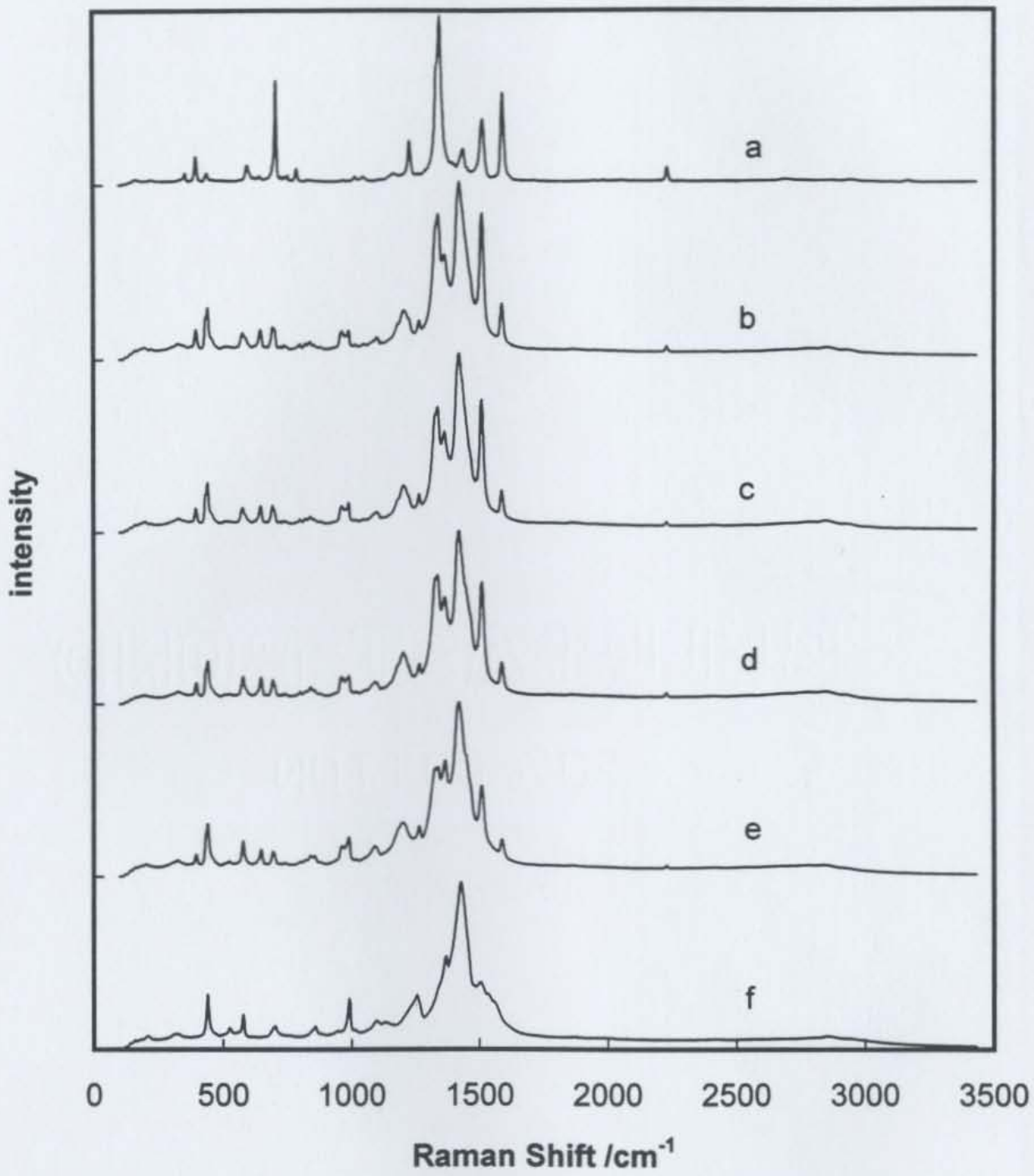

Fig. 7.6 Raman spectra of poly-CDM, poly-EDOT, and poly-(CDM-o-EDOT) films. (**a**): poly-CDM; (**b**), (**c**), (**d**), (**e**): copolymers synthesized at 1.30, 1.32, 1.33, 1.34 V, respectively; (**f**): poly-EDOT

Table 7.2 Assignments of some main modes in Raman spectra of poly-CDM, poly-EDOT and copoly-(CDM-co-EDOT)

Poly-CDM		Poly-EDOT		Copoly-(CDM-co-EDOT)	
Bond	Wave number /cm^{-1}	Bond	Wave number /cm^{-1}	Bond	Wave number /cm^{-1}
C-H	3171	ethyl C-H	2849	ethyl C-H	2848
C≡N	2230			C≡ N	2230
C=C(CN)$_2$	1589			C=C(CN)$_2$	1590
C_α=C_β	1438, 1514	C_α=C_β	1504, 1429	C_α=C_β (CDM)	1512
C_β-$C_{\beta'}$	1348	C_β-$C_{\beta'}$	1370	C_α=C_β (EDOT)	1423
				C_β-C_β (EDOT)	1369
				C_β-C_β (CDM)	1341
		C-O-C	~1257, 859	C-O-C	1267, 858
inter ring C_α-$C_{\alpha'}$	1161	inter ring C_α-$C_{\alpha'}$	~1257	inter ring $C_{\alpha'}$-$C_{\alpha'}$	1203
C-S-C	782	C-S-C	702	C-S-C	695, 701

two homopolymers: poly-CDM (**a**) and poly-EDOT (**f**) respectively. Assignments of some main modes are given in **Table 7.2.** [25-27]

It is clear from the **Fig. 7. 6** that the spectra of the copolymers are not the simple overlap of the spectra of the individual components. The C-H, C-C and C-O-C bonds in the ethylenedioxy group, and C≡N and $C=C(CN)_2$ bonds in dicyanoethene group are not involved in the backbone of the polymer chain and remote from the inter-ring connection site. Their vibrational modes are not or only slightly affected by the copolymerization. The stretch of the outer $C_\alpha=C_\beta$ bonds which are adjacent to the inter-ring connection site, moves from 1429 to 1422 cm^{-1}, due to the electron-withdrawing effect of the CDM unit. The C_α-C_α inter-ring stretches of poly-CDM and poly-EDOT are 1166 and 1257 cm^{-1} respectively. Both modes disappear in the spectra of the copolymer and instead, a new mode which is associated with the interring C_α-C_α coupling between CDM and EDOT units occurs at 1203 cm^{-1}.

The new band at 964 cm^{-1} in the copolymer spectra is probably due to the C_β-H band of monomer CDM units that are adjacent to monomer EDOT units. This band occurs at 990 cm^{-1} in the homopolymer. The new band at 648 cm^{-1} can probably be assigned to a C-S-C ring deformation, which would be expected to be significantly shifted in a copolymer. The corresponding bands in the homopolymer are presumably those at 596 cm^{-1} in poly-CDM and 578 cm^{-1} in poly-EDOT. The 578 cm^{-1} band and a shoulder at ~590 cm^{-1} are still seen in the copolymer spectra.

As potential increases, the features of poly-CDM in the Raman spectra increases indicating the trend that the higher potential used the more CDM component in the copolymer, in agreement with the result obtained from the electrochemical studies. The

above spectroscopic evidences strongly support the contention that the polymer is a true copolymer.

7.5 Measurements of the in situ conductivity and estimation of the band-gap

Fig. 7.7 shows *in situ* conductivities against potential for poly-(CDM-co-EDOT) films synthesized at 1.31 (curve (**b**)), 1.32 (curve (**c**)), 1.33 (curve (**d**)), and 1.34 V (curve (**e**)), together with that of poly-EDOT (curve (**a**)) and that of poly-CDM (curve (**f**)) for comparison. Despite the low potential scan rate (1 mV/s) used during collection of these data there was hysteresis between conductivities obtained from cathodic and anodic scans, particularly for poly-EDOT and the copolymer prepared at 1.31 V. The data shown in **Fig. 7. 7** are for the cathodic scans. Similar trends with changing composition were observed in data from anodic scans.

There is only p-type conductivity in this potential range (between -0.80 and +1.20 V) for poly-EDOT. For this polymer, conductivity reaches the highest value (ca. 0.60 S cm^{-1}) and remains unchanged when the potential is scanned positively higher than +0.2 V. As the potential is scanned negatively to less than -0.1 V, however, its conductivity drops dramatically and it becomes insulating after -0.6 V (conductivity < 10^{-8} S cm^{-1}).

A study of the *in situ* conductivity against potential of poly-CDM has been discussed

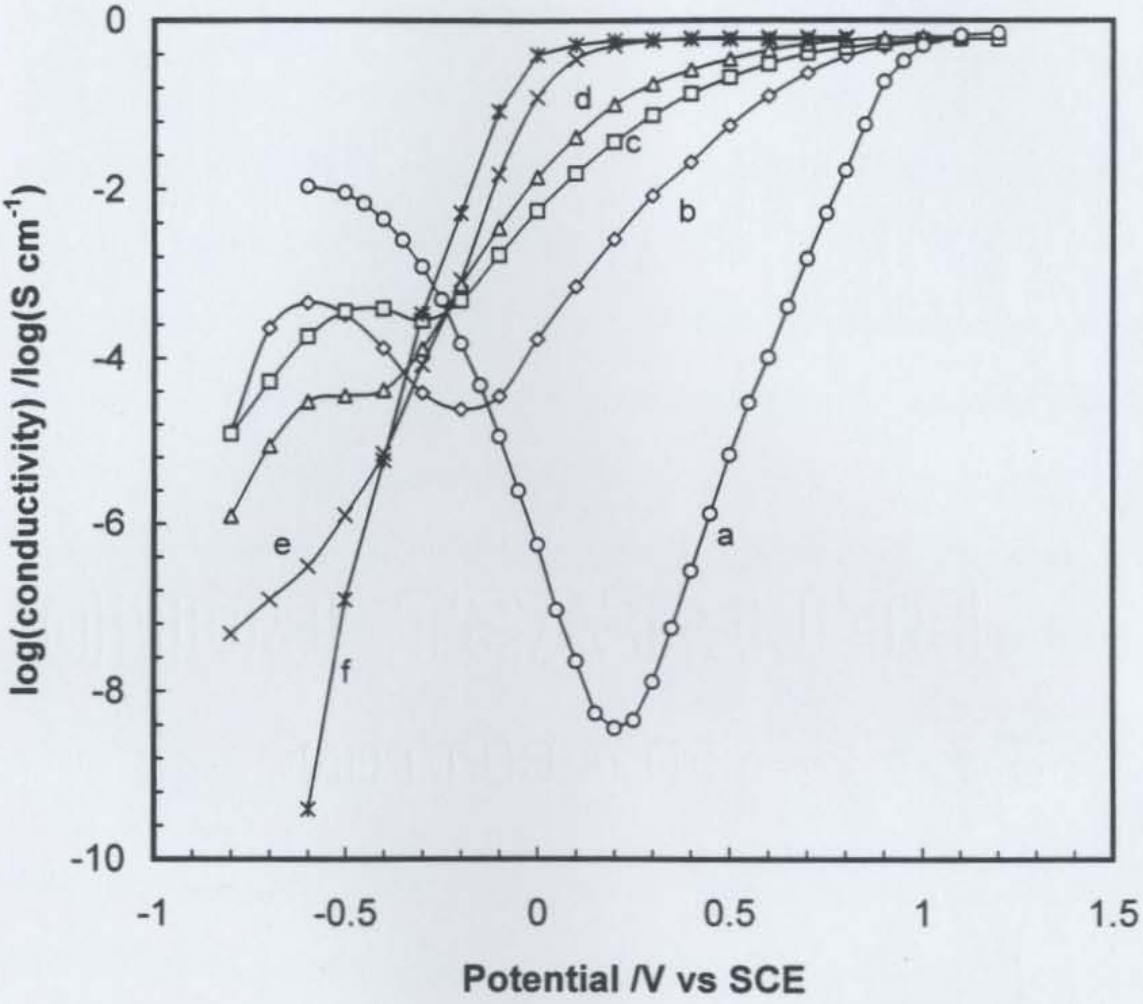

Fig. 7.7 In situ conductivity against potential of poly-CDM, poly-EDOT, and poly-(CDM-co-EDOT) films.
(**a**): poly-CDM; (**b**), (**c**), (**d**), and (**e**): copolymers synthesized at 1.31, 1.32, 1.33, and 1.34 V, respectively; (**f**): poly-EDOT

in Chapter 4. Poly-CDM film has maximum n- and p-doping conductivities of 0.59 and 0.54×10^{-3} S cm^{-1} respectively. The intrinsic conductivity was found to be 1.0×10^{-8} S cm^{-1}, in agreement with a band-gap of 0.8 eV [28].

When EDOT is copolymerized with CDM, the conductivity rises in the potential region from -0.3 to -0.8 V , owing to the n-doping of the CDM subunit. As the synthesis potential is increased, the n-doping conductivity increases.

As discussed in section 4. 6, the intrinsic conductivity is somewhat higher than the minimum conductivity in a conductivity vs. potential plot because the p-type charge carriers are more mobile than the n-type carriers. Since $\mu_p >> \mu_n$ (μ is the mobility), the intrinsic conductivity of the polymer (when $C_n = C_p$; C = concentration of charge carriers) is dominated by p-type carriers. The potential at which $C_n = C_p$ ($E_{intrinsic}$) can be estimated from:

$$E_{intrinsic} = E_{min} - 0.038 log \frac{\mu_n}{\mu_p} \qquad 7\text{-}1$$

where E_{min} is the potential of the conductivity minimum. The band-gap can be estimated from the intrinsic conductivity by using equation 4-5. Data for these calculations, and estimated band gaps are shown in Table 7.3 for the copolymers which exhibited a conductivity minimum between the n- and p- doping regions. From these data, it can be seen that the band gap decreases with increasing content of EDOT. This is to be expected since the onset of p-doping shifts to lower potentials as the content of EDOT is increased. By extrapolation, the copolymers prepared at potentials below 1.32 V would be expected to have band-gaps below the minimum value of 0.19 eV reported in Table 7.3.

Table 7.3 Conductivity data and band-gaps for selected copolymers

$E_{polymerization}$ /V	$\sigma_{p,max}$ /mS cm^{-1}	$\sigma_{n,max}$ mS cm^{-1}	$C_{n,max}/C_{p,max}$	μ_n/μ_p	$E_{intrinsic}$ /V	$\sigma_{intrinsic}$ /mS cm^{-1}	Band-gap /eV
1.32	0.60	0.22	0.2	0.0018	-0.34	0.69	0.19
1.33	0.74	0.48	0.3	0.0022	-0.19	0.68	0.21
1.34	0.62	0.44	0.4	0.0018	-0.11	0.052	0.33

The conductivity profile for the film prepared at 1.31 V is consistent with this hypothesis in that it exhibits significantly higher conductivities than poly-EDOT in the expected n-doping region (ca. -0.3 to -0.8 V) but no conductivity minimum. Unfortunately, the absence of a conductivity minimum makes it difficult to estimate the band-gap for this film. However, if we assume that $E_{intrinsic}$ = -0.34 V, as for the film prepared at 1.32 V, then we obtain an estimated band-gap of zero for data from a cathodic scan and 0.16 eV for data from an anodic scan (note that the hysteresis in the conductivity profile was largest for this copolymer). Since we have almost certainly assumed an $E_{intrinsic}$ that is too anodic, we can conclude that the band-gap of the film prepared at 1.31 V was significantly lower than 0.16 eV, and probably close to zero. The absence of a significant band-gap is consistent with the voltammetric results.

The mobility ratios for the copolymers ($\mu_n/\mu_p \sim 0.002$ (Table 7.3) are significantly less than for poly-CDM ($\mu_n/\mu_p \sim 0.025$). This is presumably because the n-doped sites are diluted and therefore less mobile.

7.6 Conclusion

Copolymerization of CDM and EDOT appears to have little influence on the potential at which the dicyanoethene bridged bithiophene moiety is reduced. This presumably arises because the n-type charge carriers thus generated are not significantly delocalized beyond the bithiophene unit. This leads to facile n-doping of all of the copolymers.

In contrast, p-type charge carriers are more delocalized so that the potential at which they begin to form is strongly dependent on the composition of the copolymer. As the ratio of the electron rich 3, 4-ethylenedioxythiophene moiety to the electron deficient dicyanoethene bridged bithiophene moiety is increased, p-doping becomes easier and the band-gap of the polymer decreases. The mobility of the p-type carriers remains high because they are delocalized.

As a consequence of these effects, copolymers with vanishingly small band-gaps and high intrinsic conductivities can be produced. The low mobility of the n-type carriers in such materials is of little consequence since their intrinsic conductivities are dominated by the more mobile p-type carriers.

References

[1] R. L. Greene and G. B. Street, *Science*, **226**, 651 (1984)

[2] J. L. Bredas, *Electronic structure of highly conducting polymers*, in: *Handbook of conducting polymers*. Vol. 2. (Ed: T. A. Skotheim) Marcel Dekker, New York, 859(1986)

[3] F. Wudl, M. Kobayashi, and A. J. Heeger, *J. Org. Chem.*, **49**, 3382 (1984)

[4] H.Yashima, M. Kobayashi, K.-B. Lee, T.C. Chung, A. J. Heeger, and F. Wudl, *J. Electrochem. Soc.*, **134**, 46 (1987)

[5] C. Kitamura, S. Tanaka, and Y. Yamashita, *J. Chem. Soc., Chem. Commun.*, 1585 (1994)

[6] T. M. Lambert and J. P. Ferraris, *J. Chem. Soc., Chem. Commun.*, 752 (1991)

[7] E. E. Havinga, W. Ten Hoeve, and H. Wynberg, *Polym. Bull.*, **29**, 119 (1992)

[8] C. Kitamura, S. Tanaka, and Y. Yamashita, *J. Chem. Soc., Chem. Commun.*, 1585 (1994)

[9] E. E. Haviga, W. Ten Hoeve, and H. Wynberg, *Synth. Met.*, **55-57**, 299 (1993)

[10] D. Lorcy and M. P. Cava, *Adv. Mater.*, **5**, 1456 (1992)

[11] P. Bauerle, G. Gotz, P. Emerle, and H. Port, *Adv. Mater.*, **4**, 564 (1992)

[12] S. Musmanni and J. P. Ferraris, *J. Chem. Soc., Chem. Commun.*, 172 (1993)

[13] G. Gagani, A. Berlin, A. Canavesi, G. Schiavon, S. Zecchin, and G. Zotti, *Adv. Mater.*, **8**, 819 (1996)

[14] F. Demanze, A. Yassar, and F. Garnier, *Adv. Mater.*, **7**, 907 (1995)

[15] J. P. Ferraris and T. L. Lambert, *J. Chem. Soc., Chem. Commun.*, 1268 (1991)

[16] M. Dietrich, J. Heinze. G. Heywang, and F. Joans, *J. Electroanal. Chem.*, **369**, 87 (1994)

[17] G. A. Soating and J. R. Reynolds, *Chem. Mater.*, **8**, 882 (1996)

[18] A. J. Downard and D. Pletcher, *J. Electroanal. Chem.*, **206**, 139 (1986)

[19] A. J. Downard and D. Pletcher, *J. Electroanal. Chem.*, **206**, 147 (1986)

[20] S. Aeiyach, A. Kone. M. Dieng, J-J Aaron, and P-C Lacaze, *J. Chem. Soc., Chem. Commun.*, 822, 1991

[21] Z. S. Zhao and P. G. Pickup, *J. Electroanal. Chem.*, **404**, 55 (1996)

[22] B. Ballarin, R. Seeber. D. Tonelli, F. Andreani, P. Costa Bizzarri, C. Della Casa, and E. Salatell, *Synth. Met.*, **88**, 7 (1997)

[23] J. Heinze, *Topics in Current Chemistry*, vol.152, Springer, Berlin, 1990, pp.1-47

[24] A. R. Hillman and E. F. Mallen, *J. Electroanal. Chem.*, **220**, 351 (1987)

[25] G. Louarn, J. Y. Mevellec, J. P. Buisson, and S. Lefrant, *Synth. Met.*, **55-57**, 587 (1993)

[26] G. Louarn, J. P. Buisson, S. Lefrant, and D. Fichou, *J. Phys. Chem.*, **99**, 11401 (1995)

[27] L. Cuff and M. Kertesz, *J. Chem. Phys.*, **106**, 5541 (1997)

[28] H. Huang and P. G. Pickup, *Polymerica Acta*, **48**, 455 (1997)

Chapter 8

Conducting Polymer-Based Supercapacitors

8.1 Introduction

Significant advances have been made in the application of battery technology for portable electrical equipment (e.g. laptop computers, cellular phones) during the past decade. However, existing batteries can not fully satisfy the requirement of the equipment, because batteries have high internal resistance (typically $> 0.15\ \Omega$) and the required loads are not constant but rather span a range of power levels [1-3]. For example, digital communication, which allows several users to conduct conversations simultaneously on the same transmission frequency, requires higher instantaneous power (e. g., discharge current of 4 A for 15 ms) than the conventional analog systems [4]. As the current is increased, the internal impedance of the battery produces a large voltage drop, and sometimes the drop is so significant that the output voltage is brought below the operating cut-off voltage of an electronic device, effectively disabling the device. Supercapacitors, which have high power densities and long cycling lives relative to batteries, and high energy densities relative to conventional capacitors, are designed to operate in parallel with

a battery as a secondary power source. They can provide the peak power output, minimizing the drop of source voltage and stabilizing the output during the pulse [5, 6]. Another promising application for supercapacitors is in the hybrid electric vehicles to ensure high power output during acceleration and hill climbing [7, 8]. The combination of battery and supercapacitor often yields a better system, which can offer less volume and mass, better performance and longer battery life.

Currently, there are two types of supercapacitor under investigation, namely double layer and redox capacitors. In the double layer supercapacitors, carbon materials (e.g., various active carbon [9-14], carbon fibers [15, 16], modified glassy carbons [17, 18]) are the most studied electrode material. Since the electrostatic charge is stored at the carbon/electrolyte double layer interface, carbon with high specific surface areas is needed, for example carbons with 2400 and 3000 m^2/g show capacitances up to 120 [19] and 145 F/g [20] respectively. However, electronic conductivity decreases with higher surface area and voltage limitations are observed. These restrict the power capability and increase the time constant (RC) of the capacitor. Recently, carbon nanofibers [21] and carbon nanotubes [22] have been introduced as electrode materials for supercapacitors. One of the main advantages of these materials is that they have high capacitance responses at very high frequencies. For example, for a carbon nanotube supercapacitor [22], most of its stored energy is accessible at a frequency of 100 Hz and the capacitance is 49 F/g, and even at a frequency of 1000 Hz, a rather high capacitance (13 F/g) is available. This good response to high frequency makes them very suitable for pulse applications.

Redox supercapacitors fall into two classes according to *pseudo*-capacitive material: metal compounds [23-31] (mainly including metal oxides, metal hydrous oxides, and metal nitrides) and conducting polymers [32-34].

It has been shown that ruthenium(IV) oxide hydrate as an active material in a supercapacitor, provides a specific capacitance of up to 50 F/g [30]. The electrochemical properties of ruthenium(IV) oxide depend dramatically upon the method of preparation and upon the chemical composition. For a material prepared by a sol-gel process [31] at low temperatures, an amorphous form is obtained which shows a specific capacitance of about 720 F/g [31]. The problem with this material is its high cost. Molybdenum nitride seems to be an interesting and cheaper alternative to ruthenium(IV) oxide. The measured values for its capacitance are about 40 F/g [25, 26].

The application of electronic conducting polymers in supercapacitors is associated with their reversible and fast ion doping/dedoping processes, and their high charge densities. The versatility of conducting polymers enables different redox supercapacitor configurations. Three distinct schemes referred to as type I, II, III have been developed [35]. In type I, both electrodes are formed from the same p-dopable conducting polymer, such as polyaniline [36-38], polythiophene [39], or polypyrrole [34, 40, 41]. Type II uses two different p-dopable conducting polymers, e.g. polypyrrole/polymethyl-thiophene [42]. And type III adopts both a p-dopable and an n-dopable conducting polymer as the electrode active materials [35, 43-45]. Compared with other classes of conducting polymers,

polythiophenes are structurally versatile and can readily to be p- and n-doped, and hence they are the focus of most studies of type III capacitors.

In terms of energy density, type III is the most favorable alternative among these three types of supercapacitor. since it provides the highest cell voltage and the highest capacitance. According to the equation $E=1/2CV^2$, to achieve higher energy density one must increase the cell voltage or improve the capacitance. In addition, when a type III capacitor is charged, both electrodes have a high electronic conductivity, while for types I and II, one of the electrode is in undoped state, resulting in a high electronic resistance. However, these advantages of type III supercapacitors are offset by the lower stability of the n-doped state relative to the p-doped state, due to the very negative potentials ($<$-2.0 V vs. Ag/Ag^+) that are normally required for n-doping. Use of a low band-gap conducting polymer, which can be n-doped at less negative potentials, has been proposed to achieve better n-doping stability.

Previous studies at Los Alamos National Laboratory [35, 43, 46] on various poly(phenyl)thiophenes have identified poly[3-(p-fluorophenyl)thiophene] (poly-PFPT, structure poly-**1**) as a promising candidate for a type III supercapacitor. However the n-type stability does not meet the requirement for a supercapacitor. For a poly-PFPT film deposited on a Pt electrode, the n-type charge for the 100th cycle was reduced to 40% of that for the initial cycle [46]. This work aims to improve and test the n-type stability of poly-PFPT grown on carbon paper electrodes and measure its conductivity (electronic and ionic) and capacitance.

Structrue 1

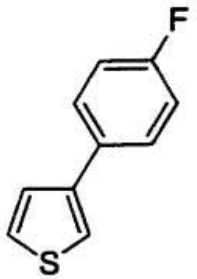

3-(p-fluorophenyl)thiophene

8.2 Experimental

Chemicals

Acetonitrile (Aldrich. 99.8%, anhydrous, H_2O < 50 ppm) and Carbon paper (Spectrocarb, 8 μm fibers, 17 mil thickness, 0.28 g/cm^3) were used as received.

Various electrolytes were used. $Et_4NCF_3SO_3$ (Fluka, puriss) and Bu_4NPF_6 (Fluka, puriss) were used as received. Et_4NBF_4 (Fluka, Chemika, >99%) was purified through four recrystallizations from methanol (Fisher, HPLC Grade), and then dried under vacuum at 250 °C for 24 hrs. Et_4NPF_6 (Fluka, Chemika, >98%) was recrystallized four times from methanol (95%)/H_2O (5%), and dried under vacuum at 150 °C for 36 hrs. $Me_4NCF_3SO_3$ (prepared in this lab previously) was purified by dissolving first in hot

acetone and recrystallization by addition of hexane. After recrystallization in this way three times, it was dried at 75 °C under vacuum for 32 hrs.

3-(p-fluorophenyl)-thiophene (PFPT) was received from the Chemistry Department of University of Texas, Dallas. The synthesis method of this monomer was described previously in the literature [46, 47].

Stability test

Cycling stability tests on poly-PFPT were carried out in an H-cell with a large area carbon paper as the counter electrode and Ag/Ag^+ (silver wire in 0.2 mM $AgNO_3$ + 0.3 M Et_4NBF_4/acetonitrile) as the reference electrode, using an EG&G Model 273A Potentiostat and Model 270 software. For n-doping, the electrode potential was cycled between -1.00 and -2.15 V at 20 mV/s. For p-doping, the potential was scanned between 0.00 and 0.90 V at 20 mV/s. The electrode was tested for 1000 cycles and every 10th cycle was recorded. The dedoping charge (for both n- and p- doping) was integrated and used to represent the activity of the polymer.

AC impedance spectroscopy

For impedance measurements, the 273 A potentiostat was connected to a Solarton Instruments 1260 Impedance/Gain Phase Analyzer. Zplot for windows (Version 1.1, Scriber Assit. Inc.) was used to control the experiments and acquire data. The measured impedance response is different for the doping process and the de-doping process because

of hysterisis. In a capacitor, discharge is associated with the de-doping process and so in our experiments impedance was measured from high doping levels to low doping levels (e.g. for p-doping, from high potentials to low potentials, while for n-doping, from low potentials to high potentials).

The impedance response of a conducting polymer deposited on porous carbon paper electrode can be modeled using the equivalent circuit shown in **Fig. 8.1** [48-51], where R_E and R_I are the distributed polymer electronic and ionic resistances respectively, R_S is the uncompensated solution resistance, and C_F represents the polymer film's Faradaic capacitance. A typical Nyquist plot shape is characterized by a 45^0 Warburg-type line followed by a straight line response vertical to the real impedance axis, from which, R_E and R_I can be calculated out using the following two equations

$$\frac{1}{R_{\sim}} = \frac{1}{R_E} + \frac{1}{R_I} \qquad \textbf{8-1}$$

$$R_{\Sigma} = R_E + R_I \qquad \textbf{8-2}$$

where $R_{\sim}$ is given by the subtraction of R_S from the intercept at high frequency in the Nyquist plot (e.g. $R_{\sim} = R_{high} - R_S$) , and R_{Σ} is obtained by extrapolation of the linear portion at low frequency of the Nyquist plot to the real axis (e.g., $R_{\Sigma} = 3(R_{low} - R_S)$). The capacitance ($C_F$) of the polymer film is given by

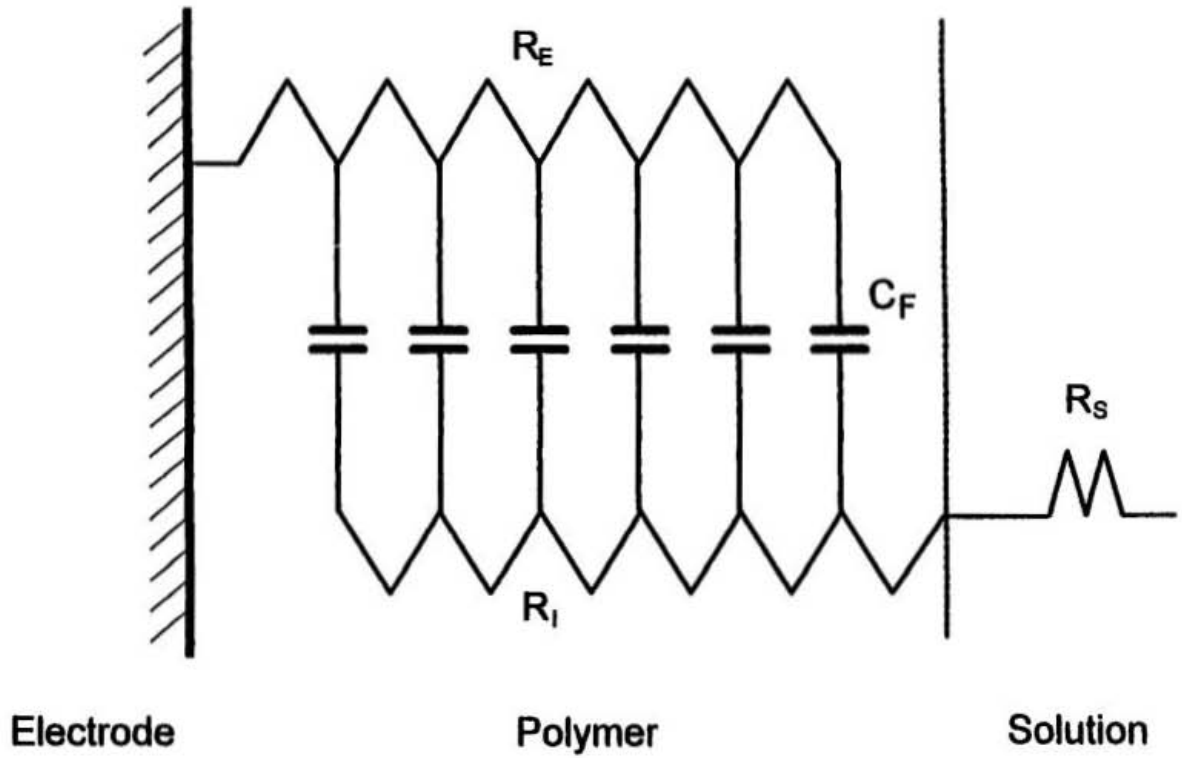

Fig. 8.1 Equivalent circuit for a conducting polymer-coated porous carbon paper electrode

$$C_F = -\frac{1}{2\pi f Z''} \qquad \text{8-3}$$

where f is the frequency and Z'' is the imaginary impedance.

8.3 Part I. Poly-PFPT grown using constant current

8.3.1 Stability tests on poly-PFPT

a. P-doping stability

Et_4NBF_4, $Et_4NCF_3SO_3$, and Et_4NPF_6 which have the same cation but three different anions, were chosen as the electrolyte for the cycling solution to test the effect of anions on the p-doping stability of poly-PFPT. The polymer was grown galvanostatically on 0.5 cm^2 carbon paper at 10 mA/cm^2 for 500 s in 0.05 M FPT acetonitrile solution containing 1 M Et_4NPF_6. The potential-time (E-t) curves that were obtained for PFPT were typical of those commonly observed when other thiophene monomers were polymerized at constant current. When the current was applied, there was a sharp jump of potential, followed by a characteristic decay of the potential to a constant value. The constant potential value was ca. 1.07 V, corresponding to the synthesis current of 10 mA/cm^2.

Cyclic voltammograms (the second cycle) of poly-PFPT electrodes in 1 M Et_4NBF_4, 1 M $Et_4NCF_3SO_3$, and 1 M Et_4NPF_6 solutions are shown in **Fig. 8.2** as curve (**a**), (**b**) and (**c**) respectively. The potential was scanned between 0.00 and 1.00 V at a sweep rate of 20 mV/s. **Table 8.1** lists data derived from the figure.

Table 8.1 Effect of anions (BF_4^-, $CF_3SO_3^-$, and PF_6^-) on the cyclic voltammogram (the second cycle) of poly-PFPT

P-doped ions	$E_{p\text{-doping}}$ /V	$E_{p\text{-dedoping}}$ /V	ΔE /V	$Q_{p\text{-doping}}$ /mC	$Q_{p\text{-dedoping}}$ /mC	η^*
BF_4^-	0.845	0.586	0.259	274.4	272.8	99.4%
$CF_3SO_3^-$	0.865	0.568	0.297	273.4	270.0	98.8%
PF_6^-	0.870	0.555	0.315	263.5	262.3	99.5%

* η is the discharge efficiency, which is the ratio of $Q_{de\text{-}doping}$ and Q_{doping}.

For these three electrolytes, the discharge efficiencies in all cases are close to the unity, indicating a good charge balance between the p-doping and p-dedoping processes for poly-PFPT. The polymer doped with BF_4^-, which is the smallest anion, shows the narrowest separation (0.259 V) between the doping and dedoping peaks, and has the highest dedoping charge (272.8 mC), while the polymer doped with PF_6^-, the largest anion, has the largest peak separation (0.315 mV) and the lowest charge (262.3 mC).

Fig. 8.3 shows the p-type stability test results for poly-PFPT carbon paper electrodes in these three electrolyte solutions. For these electrolytes, all curves of stability vs cyclic number show two stages. The first stage is a pronounced decrease of activity (the

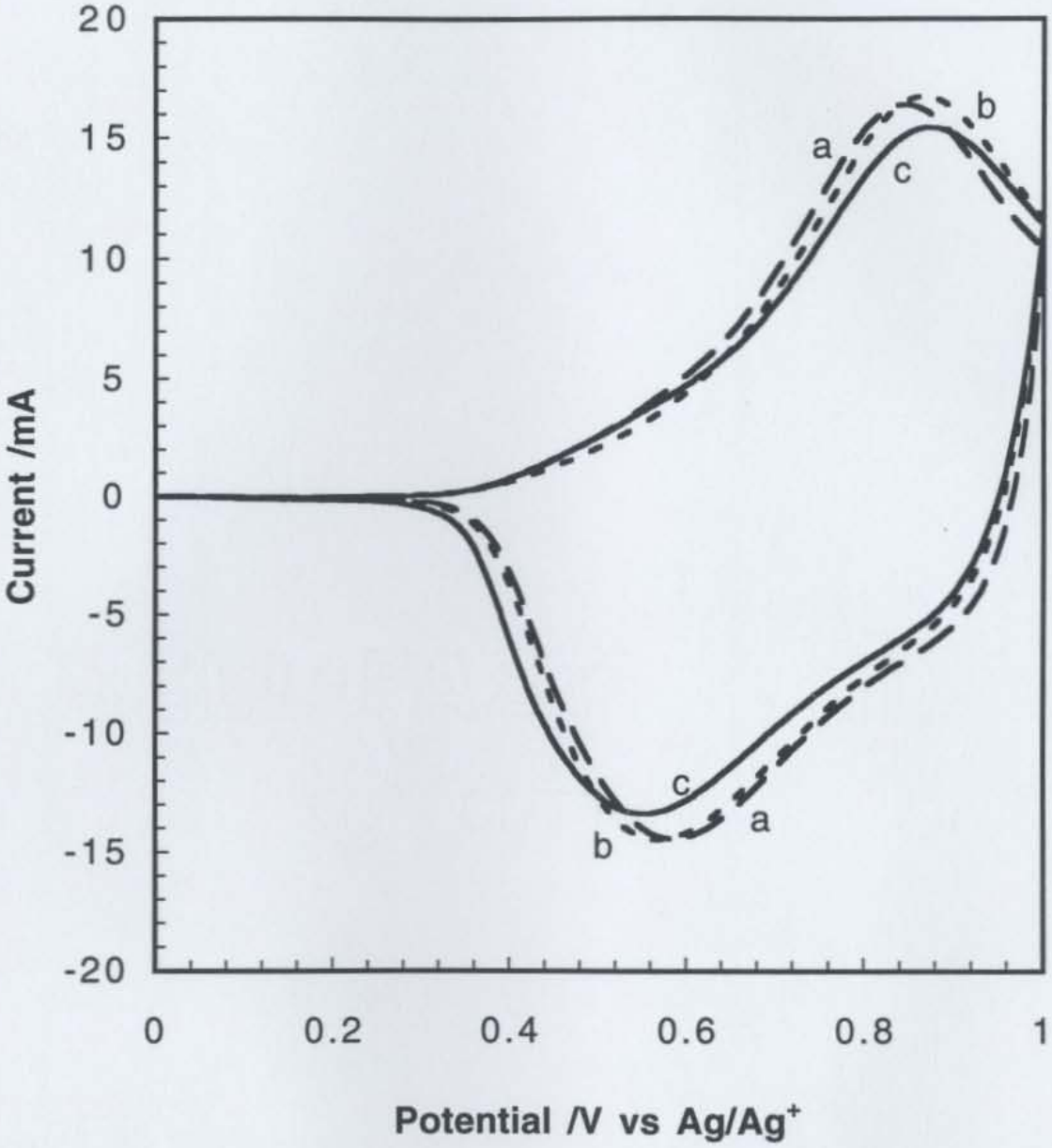

Fig. 8.2 Effect of electrolyte on the cyclic voltammogram (the second cycle) of poly-PFPT. a) 1M Et_4NBF_4, b) 1M $Et_4NCF_3SO_3$, and c) 1M Et_4NPF_6. Poly-PFPT was synthesized in 0.1 M PFPT acetonitrile solution containing 1 M Et_4NPF_6

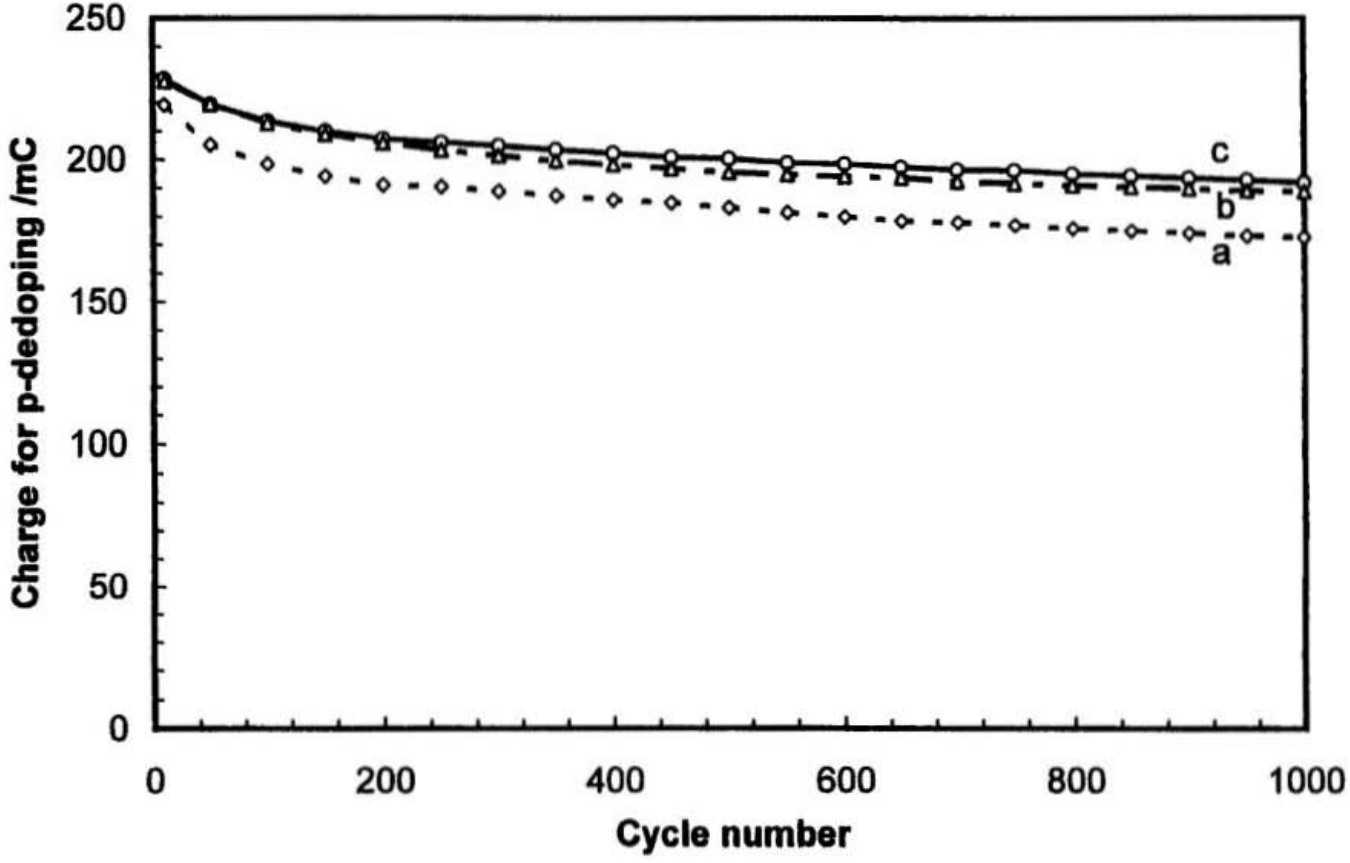

Fig. 8. 3 Effect of electrolyte on the p-doping stability of poly-PFPT. a) 1M Et_4NBF_4, b) 1M $Et_4NCF_3SO_3$, and c) 1M Et_4NPF_6. Poly-PFPT was synthesized in 0.1 M PFPT acetonitrile solution containing 1M Et_4NPF_6 at 10 mA/cm^2 for 500 s.

dedoping charge) with cyclic number for about 100 cycles. The decreases of activity in the first stage for BF_4^-, $CF_3SO_3^-$, and PF_6^- are 6.5%, 6.4%, and 9.4% respectively. After the first stage, the slope of the curve becomes almost constant, reflecting a decrease of the polymer activity at a constant rate. The slope for BF_4^- is 1.96 mC/100 cycles, for $CF_3SO_3^-$ is 1.99 mC/100 cycles, and for PF_6^- is 2.23 mC/100 cycles. After 1000 deep charge/discharge cycles, 79% of the initial charge has been maintained for PF_6^-, 83% for $CF_3SO_3^-$, and 84% for BF_4^-. Among these three p-doped polymers, the polymer doped with BF_4^- has the slightly highest activity and stability.

b. Effect of cations on the n-type stability

Poly-PFPT was deposited on carbon paper using the identical synthesis conditions as above. Commonly used tetraalkyl ammonium cations, such as Bu_4N^+, Et_4N^+, and Me_4N^+ were chosen to test their effects on the n-doping stability of poly-PFPT. Although cations are predominately involved when a polymer is n-doped, anion and electrolyte transport into the polymer can accompany the cation. To eliminate the effect of the anion, it is better to chose electrolytes with the same anion. However, most tetramethyl ammonium salts are poorly soluble in acetonitrile (the solubilities of Me_4NBF_4 and Me_4NPF_6 in acetonitrile are less than 0.1 M) except for $Me_4NCF_3SO_3$, which is very soluble (the solubility is about 1.4 M at room temperature). Therefore, $Me_4NCF_3SO_3$ was used in our experiments.

The initial cyclic voltammograms of poly-PFPT coated carbon paper electrodes immersed in 1 M Bu_4NPF_6, 1 M Et_4NPF_6, and 1 M $Me_4NCF_3SO_3$ are shown in **Fig. 8.4** as curve (**a**), (**b**) and (**c**) respectively. The potential range is from -1.00 to -2.15 V and the sweep rate is 20 mV/s. The initial charge for the polymer doped with different cations varies significantly. The initial n-dedoping charge for the polymer doped with Me_4N^+ was 182.1 mC, the highest charge among these three cations, indicating the high penetration and transport ability for Me_4N^+ in the polymer. These abilities are associated with its small ion size. The polymer doped with Bu_4N^+, the largest cation, shows much lower activity with an initial charge of 57.03 mC. For the polymer doped with Et_4N^+, the initial charge was 163.9 mC, close to the value for the polymer doped with Me_4N^+. Compared with the initial charge for p-doping, the initial charge for n-doping is much lower. For example, charge obtained by n-doping with Et_4N^+ was about 60～70% of the charge for p-doping.

N-type stability test results for poly-PFPT electrodes are illustrated in **Fig. 8.5**. In the figure, curve (**a**), (**b**) and (**c**) are for the polymers doped with Bu_4N^+, Et_4N^+, and Me_4N^+ respectively. In the initial stage of cycling when the polymer is n-doped, the activity of the polymer increases. This increase is more pronounced for the polymer doped with Bu_4N^+, for which the charge increased from an initial value of 57.03 mC to a maximum of 102.8 mC after 50 cycles. For films doped with Me_4N^+ and Et_4N^+, the maximum charges (214 mC for Me_4N^+ and 194 mC for Et_4N^+) are reached after several cycles. The initial increase of activity is not seen when the polymer is p-doped. After the

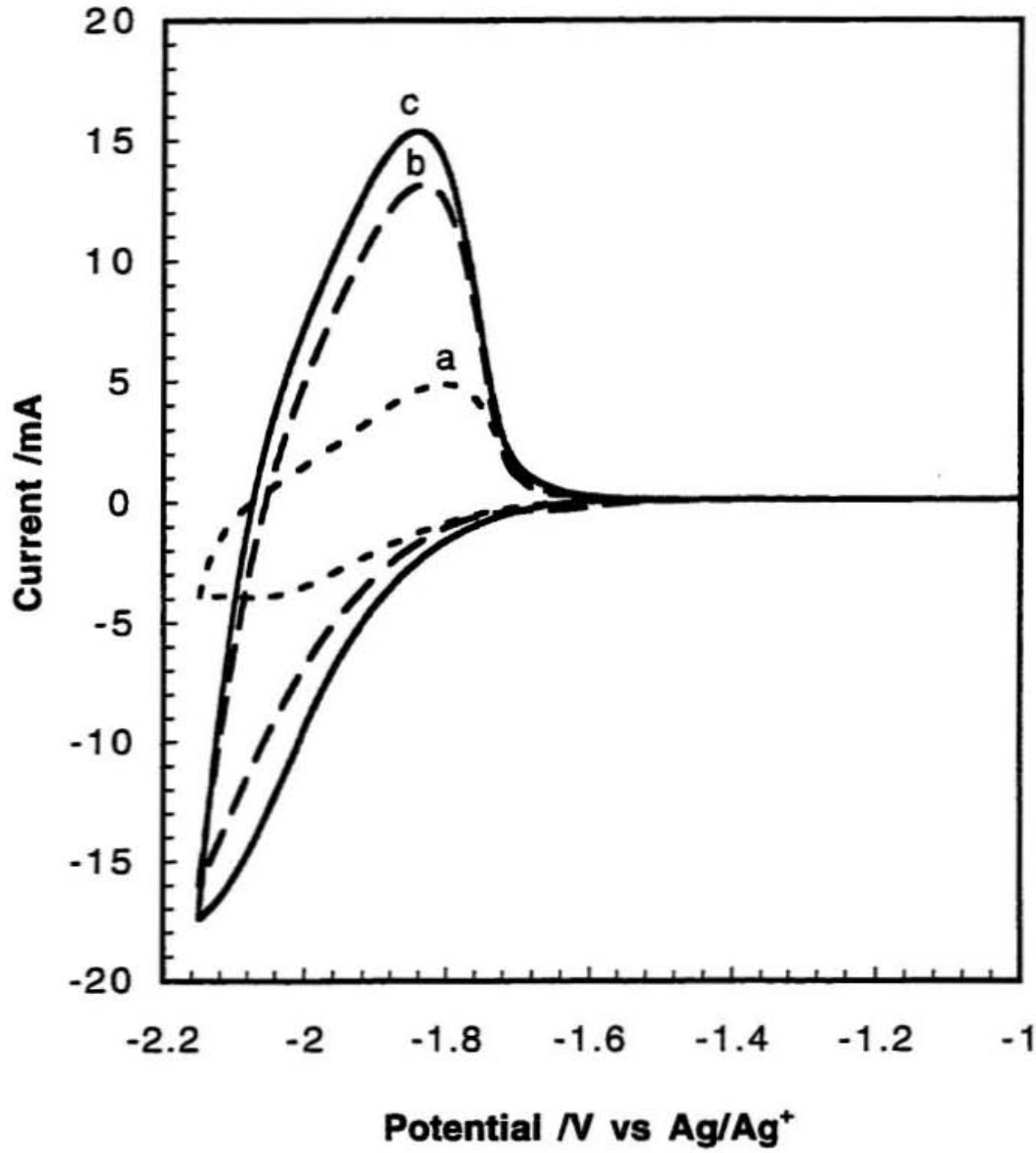

Fig. 8.4 Effects of electrolyte on the initial cyclic voltammogram of poly-PFPT. a) Bu_4NPF_6, b) Et_4NPF_6, and c) $Me_4NCF_3SO_3$

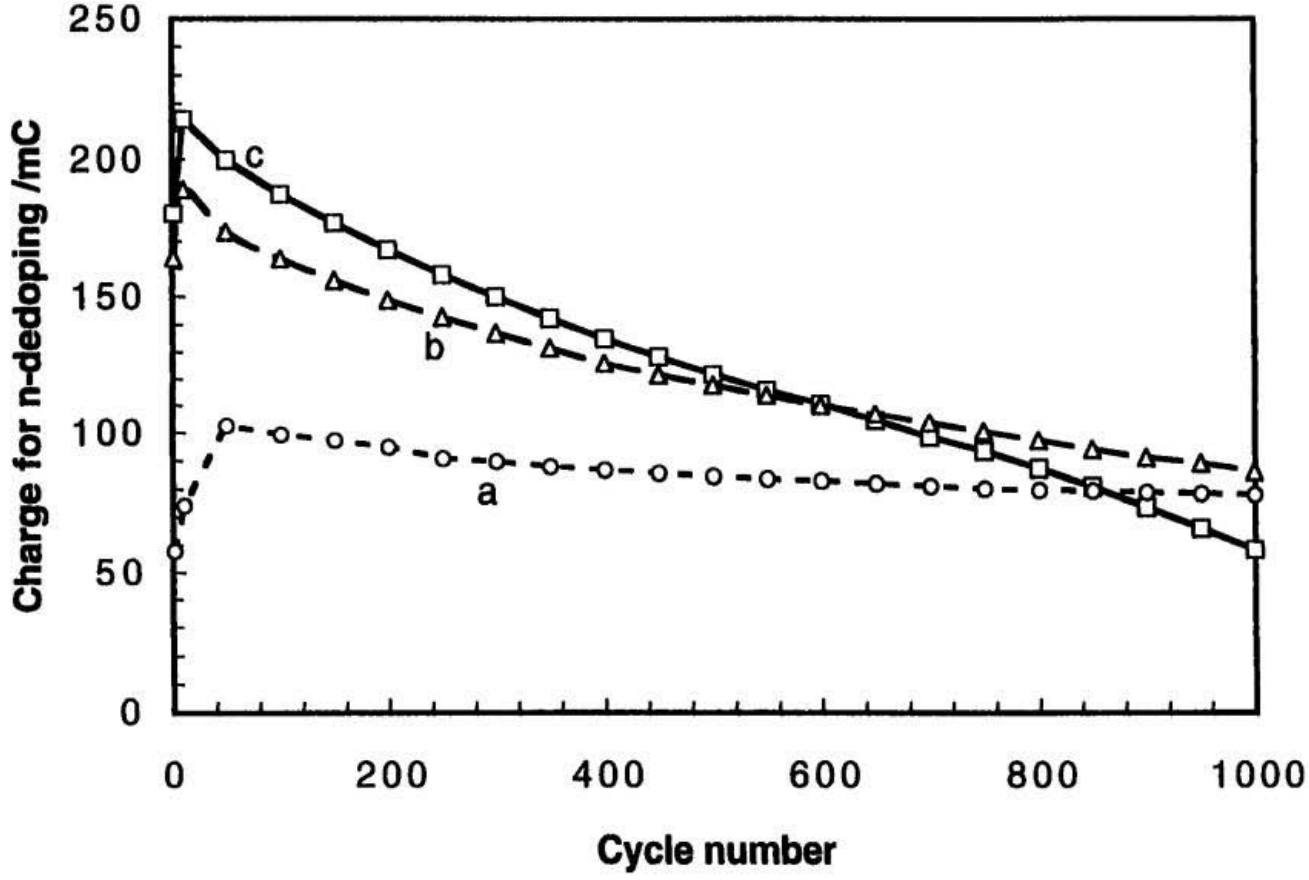

Fig. 8.5 Effect of electrolyte on n-type stability of poly-PFPT
a) Bu_4NPF_6, b) Et_4NPF_6, and c) $Me_4NCF_3SO_3$

initial increase, the activity decreases. The rate of decrease of the activity can be defined as the slope of the curve when the rate of decrease becomes almost constant. The rate of decrease of activity for films doped with Bu_4N^+, Et_4N^+, and Me_4N^+ are 2.08, 7.86, and 13.6 mC/100 cycles respectively. After 1000 cycles, the percentages of maximum charge that are maintained are 76%, 47%, and 27% for Bu_4N^+, Et_4N^+, and Me_4N^+ respectively. The polymer doped with Bu_4N^- shows superior stability over films doped with Me_4N^+ and Et_4N^+. However, the charge involved for Bu_4N^+ is much lower, especially in the first 500 cycles.

c. Effect of electrolyte used for polymer growth on the n-doping

Since p-doping of the polymer with anions accompanies the polymerization of the monomer to form polymer, anions play an important role in polymer growth. To evaluate the effect of the anion on the properties of poly-PFPT, Et_4NPF_6 (1 M), Et_4NBF_4 (1 M), and $Et_4NCF_3SO_3$ (1 M), which have the same cation but different anions, were used as electrolyte solutions for synthesis of the polymer. Other conditions for the synthesis are the same as above. Three poly-PFPT coated carbon paper electrodes were prepared and tested in 1 M Et_4NBF_4 electrolyte solutions.

Fig. 8. 6 (a), (b) and (c) are the initial cyclic voltammograms for the n-doping of the polymers synthesized with BF_4^-, $CF_3SO_3^-$, and PF_6^- anions respectively. The charges obtained for n-doping and n-dedoping are significantly different. The polymer synthesized with BF_4^- has the lowest initial charge (56.09 mC), while the polymer synthesized with

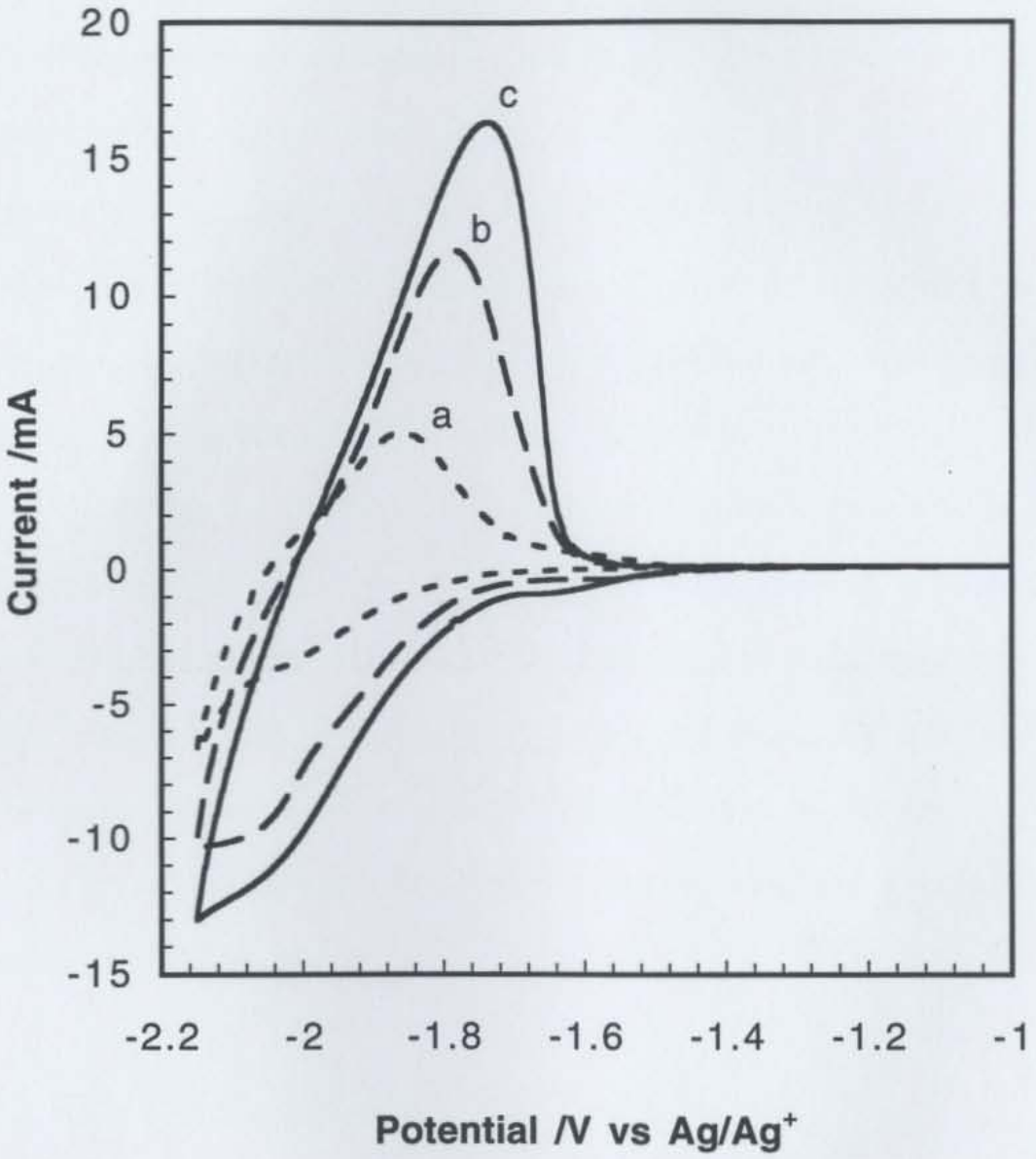

Fig. 8.6 Initial cyclic voltammograms of n-doping for poly-PFPT synthesized in a)1M Et_4NBF_4, b) 1M $Et_4NCF_3SO_3$ and c) 1M Et_4NPF_6

PF_6^- has the highest initial charge (180.2 mC), suggesting that the later polymer has a more open structure and that it is easier for cations to migrate to the doping sites.

Plots of charge for n-dedoping vs. cycle number are shown in **Fig. 8.7** (**a**), (**b**) and (**c**) for the three polymer electrodes synthesized with BF_4^-, $CF_3SO_3^-$, and PF6-, respectively. Similar trends for activity vs. cyclic number were obtained for the three polymer electrodes. The activity increases with cyclic number over the initial cycles, and decays after this initial increase. For the polymer synthesized with BF_4^-, the maximum charge of 157 mC was reached after 80 cycles. For the polymer with $CF_3SO_3^-$, a maximum charge of 168 mC was obtained after 20 cycles, and for the polymer with PF_6^-, the maximum charge was 194 mC after several cycles. The decay rates of the polymer activity after the initial increase for BF_4^-, $CF_3SO_3^-$, and PF_6^- were 5.74, 5.46, and 5.14 mC/100 cycles, respectively, which are all very similar. After 1000 cycles, 47%, 44%, and 47% of the maximum were maintained for the films synthesized with BF_4^-, $CF_3SO_3^-$, and PF_6^-, respectively. However, the polymer synthesized with PF_6^- shows higher activity for all cycle numbers studied.

8.3.2 AC impedance spectroscopy

a. Impedance study on the effect of anions on p-doping of poly-PFPT

Fig. 8.8a shows the complex plane impedance plots for a poly-PFPT coated carbon paper electrode immersed in 1 M Et_4NBF_4 electrolyte solution for electrode

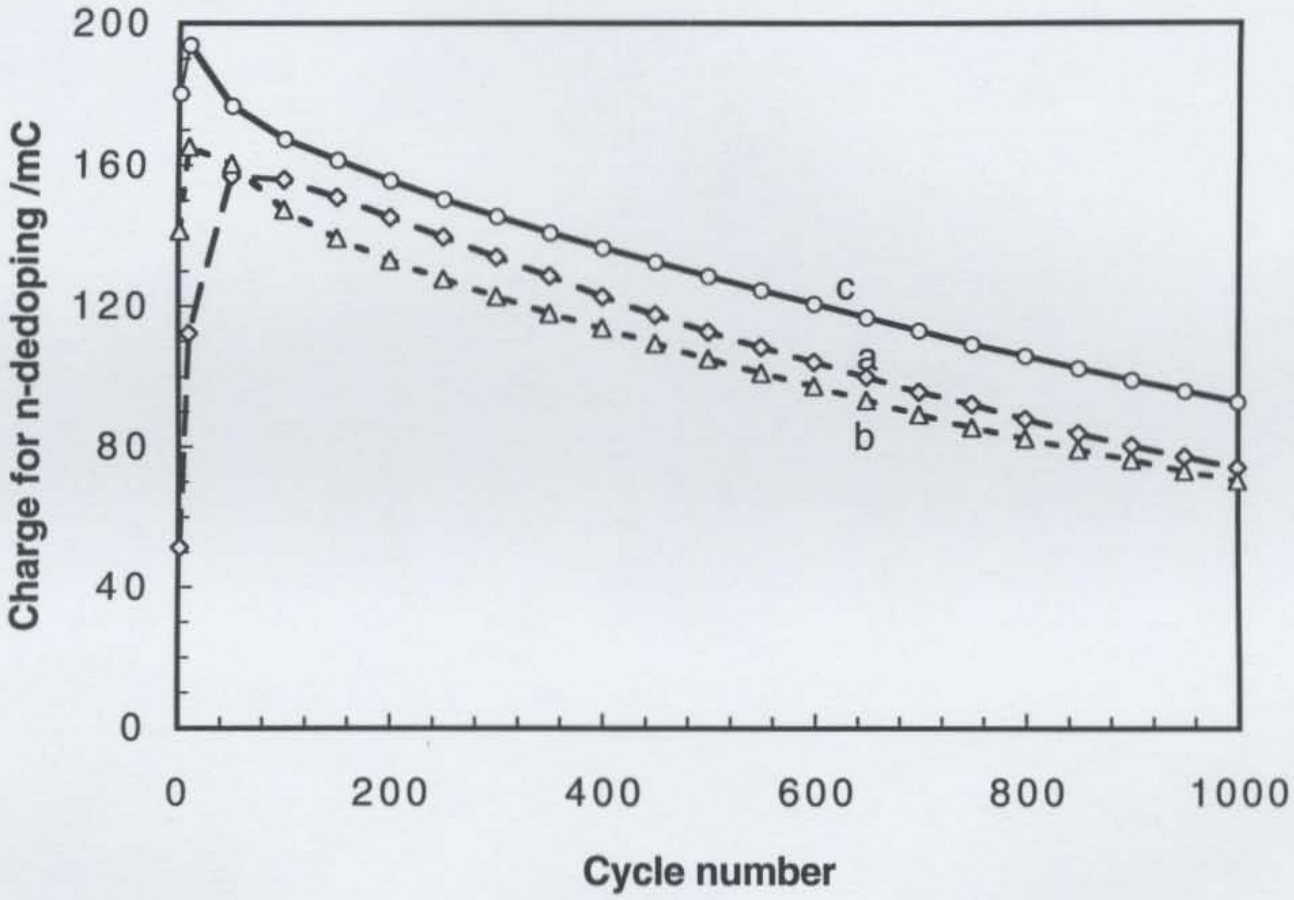

Fig. 8.7 N-type stability of poly-PFPT synthesized in 0.1 M FPT acetonitrile solution containing a) Et_4NBF_4, b) $Et_4NCF_3SO_3$, c) Et_4NPF_6. Cycling solution: 1M Et_4NBF_4 acetonitrile

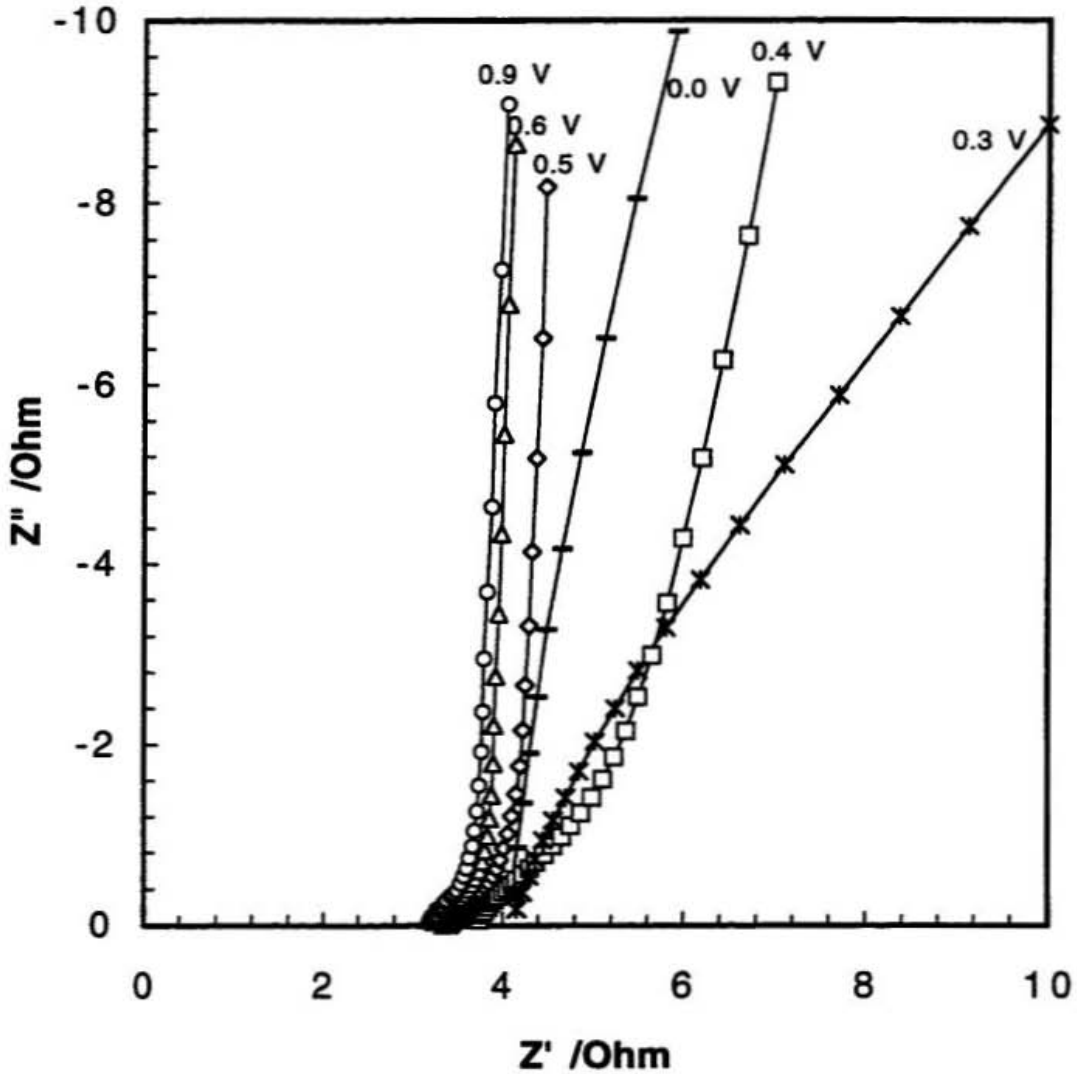

Fig. 8.8a AC complex impedance plot for p-doped poly-PFPT in 1M Et_4NBF_4 acetonitrile solution

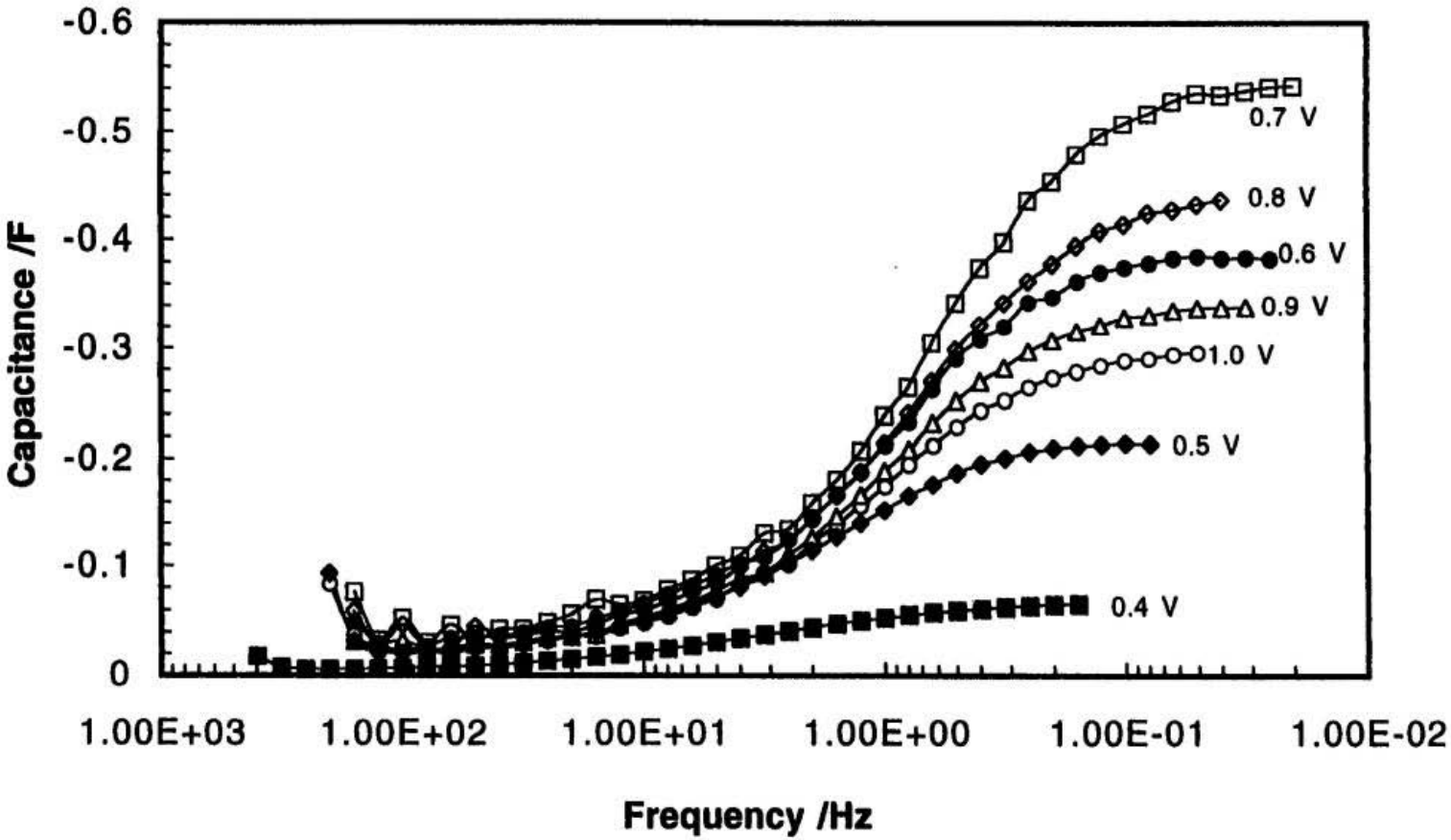

Fig. 8.8b Measurement of the p-type capacitance of poly-PFPT (5 C/cm²) grown galvanostatically on a carbon paper electrode in 1 M Et_4NBF_4 acetonitrile solution

potentials corresponding to p-doped state (0.00 to 1.00 V). From **Fig. 8.8a**, the capacitance vs. frequency (in log format) at various potentials is plotted in Fig. **8. 8b**.

When the poly-PFPT film is highly p-doped, its impedance spectra show a 45^0 Warburg-type line followed by a response vertical to the real resistance axis, which is typical for a conducting polymer [53-56]. However when the polymer is only slightly doped, a semicircle is observed at high frequencies reflecting the charge transfer process at electrode/polymer interface [53-55]. Similar impedance spectra were obtained for polymers doped with $CF_3SO_3^-$ and PF_6^-. **Table 8.2** lists the ionic and electronic resistances, and maximum capacitances at various potentials when the polymer is p-doped with BF_4^-, $CF_3SO_3^-$, and PF_6^-, respectively.

Table 8.2 Ionic and electronic resistances and maximum capacitances for poly-PFPTs doped with different anions at various potentials

	P-doped with BF_4^-			P-doped with $CF_3SO_3^-$			P-doped with PF_6^-		
Potential /V	R_I /Ω	R_E /Ω	C_{max} /F	R_I /Ω	R_E /Ω	C_{max} /F	R_I /Ω	R_E /Ω	C_{max} /F
1.0	2.19	low	0.295	2.58	low	0.291	2.58	low	0.289
0.9	2.10	low	0.338	2.37	low	0.328	2.34	low	0.326
0.8	2.01	low	0.435	2.40	low	0.432	2.25	low	0.429
0.7	2.12	<0.1	0.542	2.47	<0.1	0.527	2.28	<0.1	0.521
0.6	2.35	0.17	0.383	2.71	0.17	0.394	2.62	0.17	0.388
0.5	5.71	0.23	0.214	6.14	0.35	0.238	6.23	0.39	0.237
0.4	20.6	0.57	0.065	19.7	0.62	0.087	23.6	0.64	0.071
0.3	high	0.99		high	1.05		high	1.14	
0	high	1.04		high	1.06		high	1.09	

From the above table, the ionic resistance shows the same trend with the potential for the polymer doped with BF_4^-, $CF_3SO_3^-$, and PF_6^-. The lowest ionic resistance always occurs at 0.8 V. At higher potential, the ionic resistance increases slightly. With decreasing potential, the ionic resistance increases, more sharply after 0.5 V. The polymer doped with BF_4^- exhibits lower ionic resistances compared to the polymer doped with the other two anions, although the difference is probably not significant.

AC impedance can not reveal the electronic resistance accurately when the polymer is highly doped and has a low resistance [57] (less than 0.1 Ω in our case). Other techniques, such as two-band electrode [58], dual electrode [59] and microelectrode array [60] voltammetry have been used to measure *in situ* conductivity (normally the conductivity is high), but these techniques are difficult to apply to carbon paper electrodes. In its partially or lightly doped state, the polymer does not show significant difference in electronic resistance when doped with different anions (**Table 8.2**). When the polymer is undoped and in the neutral state (e.g., at 0 V), the ionic resistance of the electrode becomes very high, and the electronic resistance converges to a value of about $1 \sim 1.1$ Ω.

The highest capacitance is observed at 0.7 V, for all three anions used as the dopant for the polymer. The polymer film doped with BF_4^- (0.542 F at 0.7 V) has a slighly higher capacitance than the films doped with $CF_3SO_3^-$ (0.527 F at 0.7 V) or PF_6^- (0.521 F at 0.7 V). From **Fig. 8. 8b**, it is seen that most of the capacitance is only accessible at frequencies below 1 Hz.

b. Impedance study on the effect of cations on the n-doping of poly-PFPT

AC impedance spectra for poly-PFPT coated carbon paper electrodes in 1 M Bu_4NPF_6, 1 M Et_4NPF_6, and 1 M $Me_4NCF_3SO_3$ are shown in **Fig.8.9a1**, **Fig. 8.9b1 and Fig. 8.9c1** respectively for the n-doping potential range (from -2.15 to -1.50 V). **Fig. 8.9a2**, **Fig. 8.9b2** and **Fig. 8.9c2**.are the corresponding plots of capacitance vs log(frequency). Ionic and electronic resistances, and maximum capacitances obtained from these figures are summarized in **Table 8.3**.

Table 8.3 Ionic and electronic resistances and maximum capacitances for poly-PFPT doped with different cations at various potentials

	N-doped with Bu_4N^+			N-doped with Et_4N^+			N-doped with Me_4N^+		
Potential /V	R_I /Ω	R_E /Ω	C_{max} /F	R_I /Ω	R_E /Ω	C_{max} /F	R_I /Ω	R_E /Ω	C_{max} /F
-2.1	18.5	low	0.280	6.84	low	0.256	4.29	low	0.342
-2.0	9.21	low	0.310	5.13	low	0.325	3.90	low	0.385
-1.9	7.82	<0.1	0.261	4.14	<0.1	0.430	3.60	<0.1	0.469
-1.8	6.62	0.34	0.124	3.85	0.23	0.235	3.33	0.21	0.234
-1.7	8.91	0.75	0.057	4.90	0.65	0.091	6.93	0.54	0.115
-1.6	high	1.12	0.026	16.9	0.85	0.027	high	0.82	0.026
-1.5	high	1.18	0.001	high	1.16	0.001	high	1.16	0.005

For the polymer n-doped with Bu_4N^+, the lowest ionic resistance (6.62 Ω) is obtained at -1.8 V. At more negative potentials, the ionic resistance increases significantly, e.g. at -2.1 V, an ionic resistance of 18.5 Ω is obtained, and at higher potentials, the ionic resistance increases abruptly to very high values. The similar change of the ionic resistance

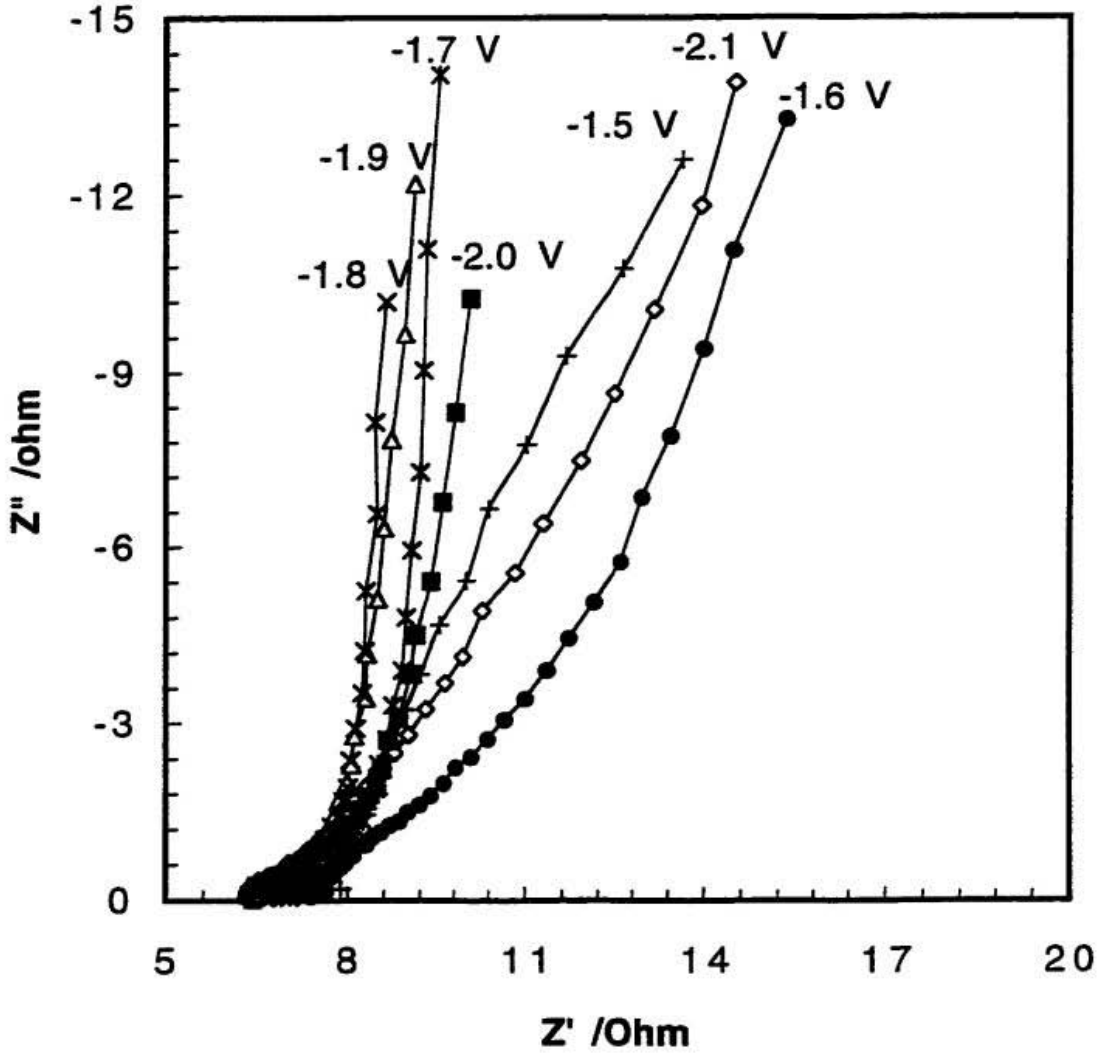

Fig 8.9 a1 AC impedance of n-doped poly-PFPT (5 C/cm^2) in 1 M Bu_4NPF_6 acetonitrile solution

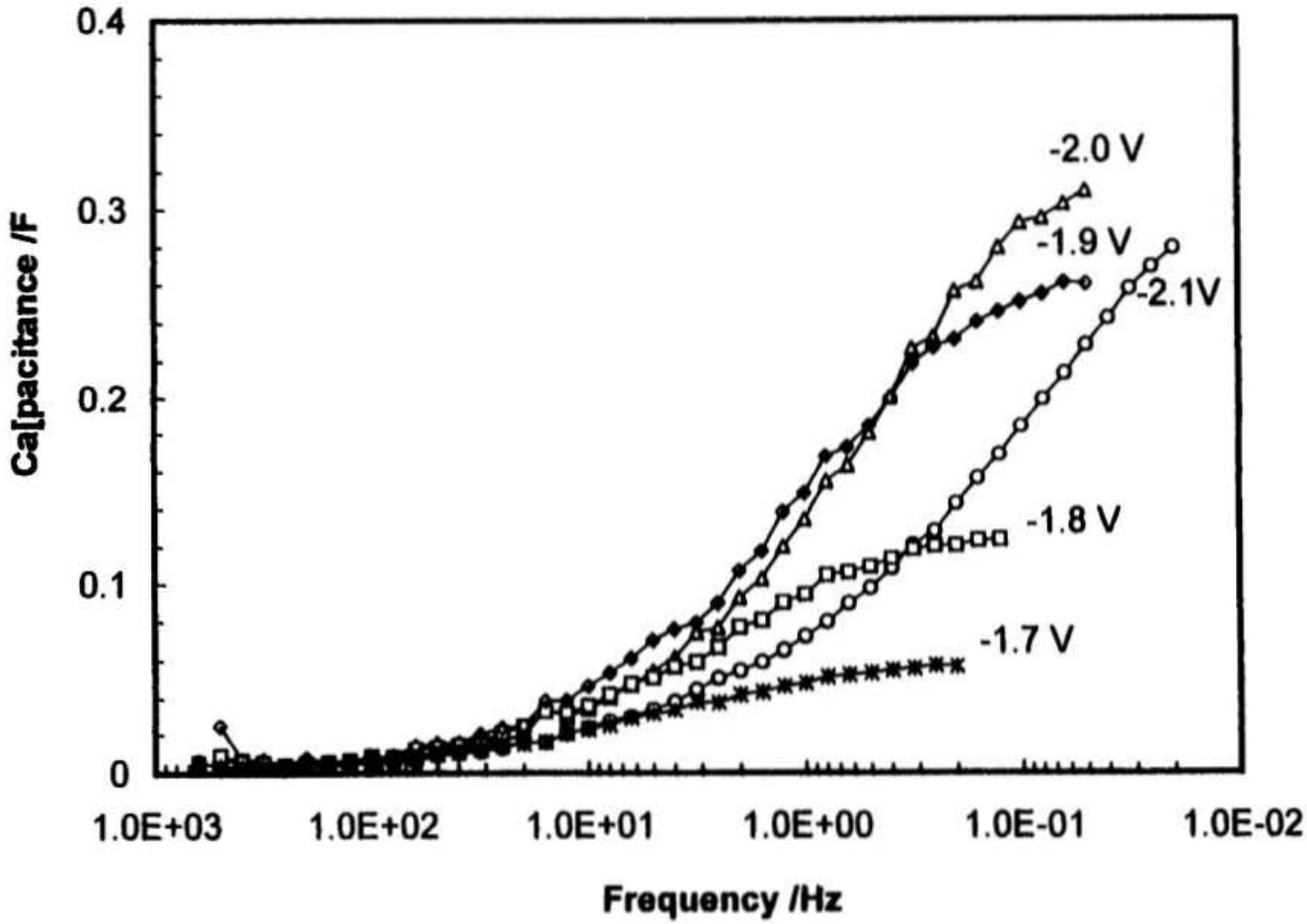

Fig 8.9 a2 N-type capacitance of poly-PFPT (5 C/cm^2) in 1 M Bu_4NPF_6

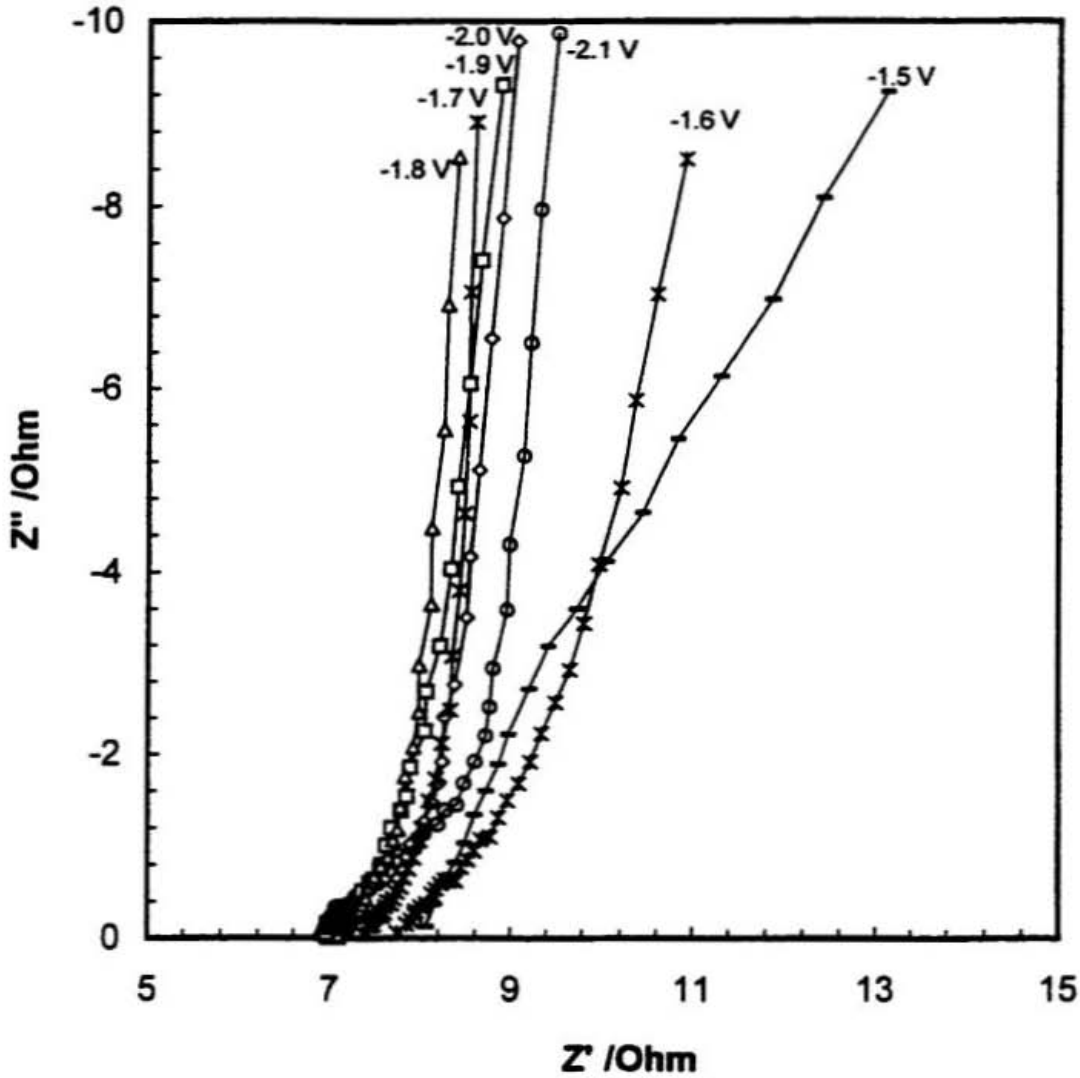

Fig. 8.9 b1 AC Impedance of n-doped poly-PFPT (5 C/cm^2) in 1 M Et_4NBF_4 acetonitrile solution

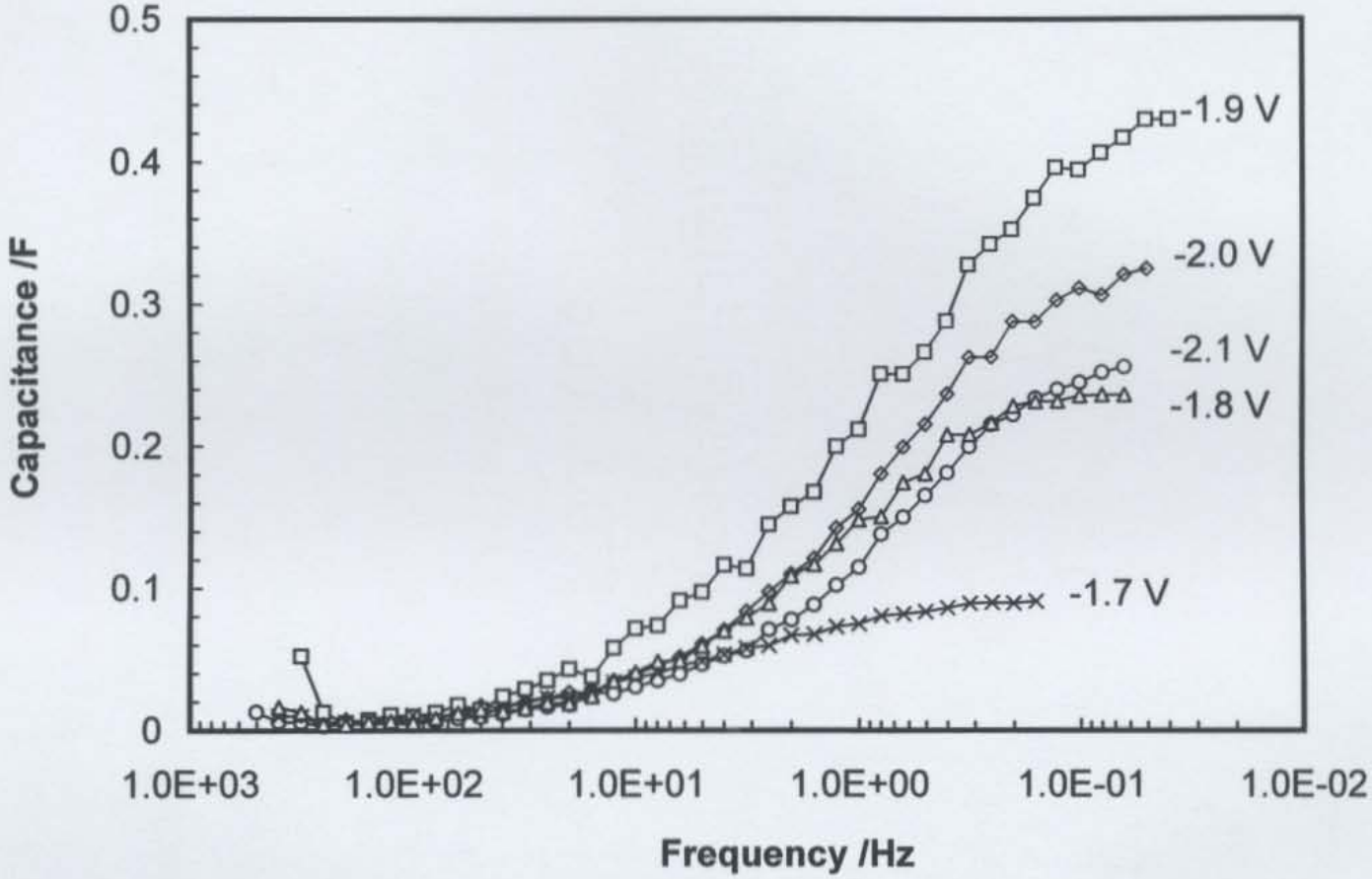

Fig. 8. 9 b2 N-type capacitance of poly-PFPT (5 C/cm^2) in 1 M Et_4NBF_4 acetonitrile solution

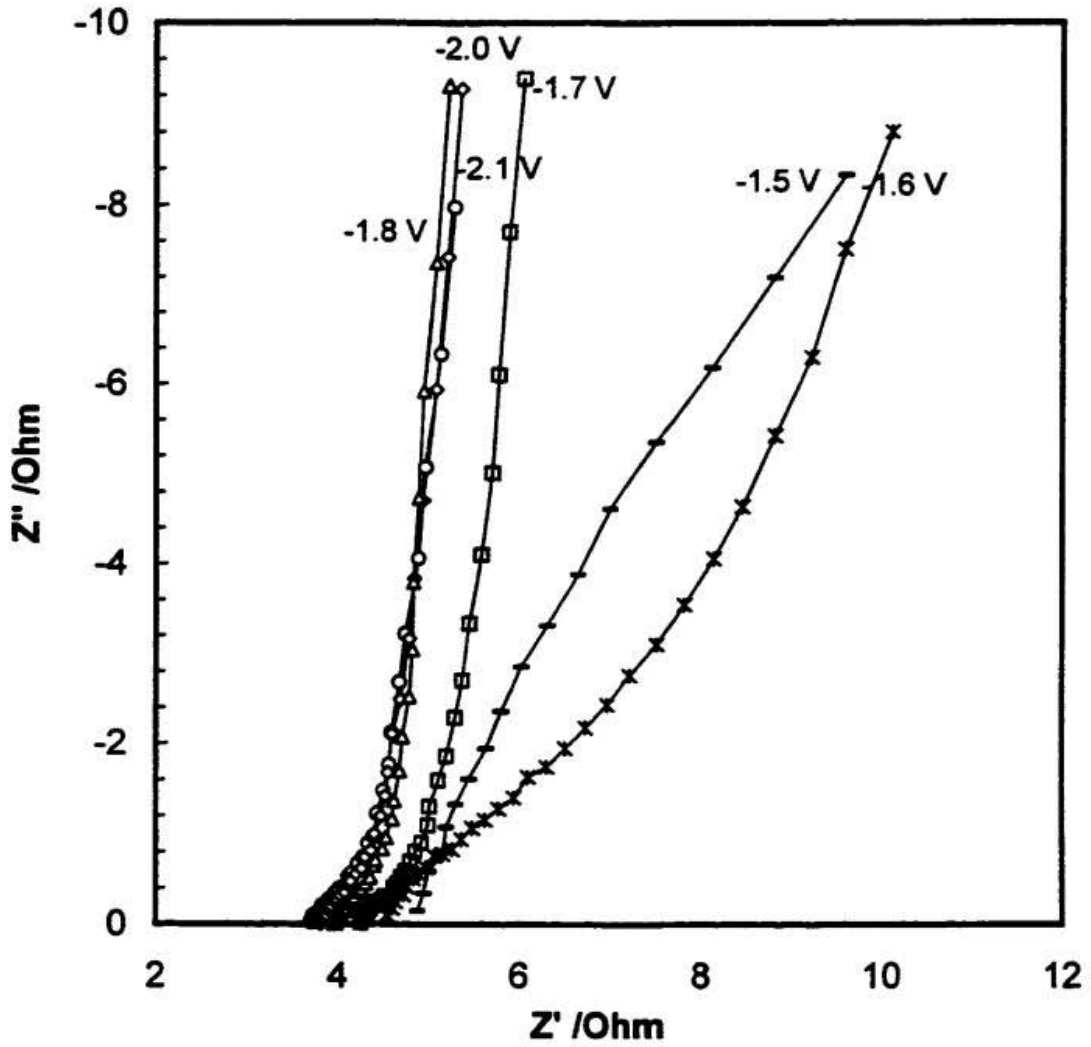

Fig 8.9 c1 AC impedance of n-doped poly-PFPT (5 C/cm^2) in 1 M $Me_4NCF_3SO_3$ acetonitrile solution

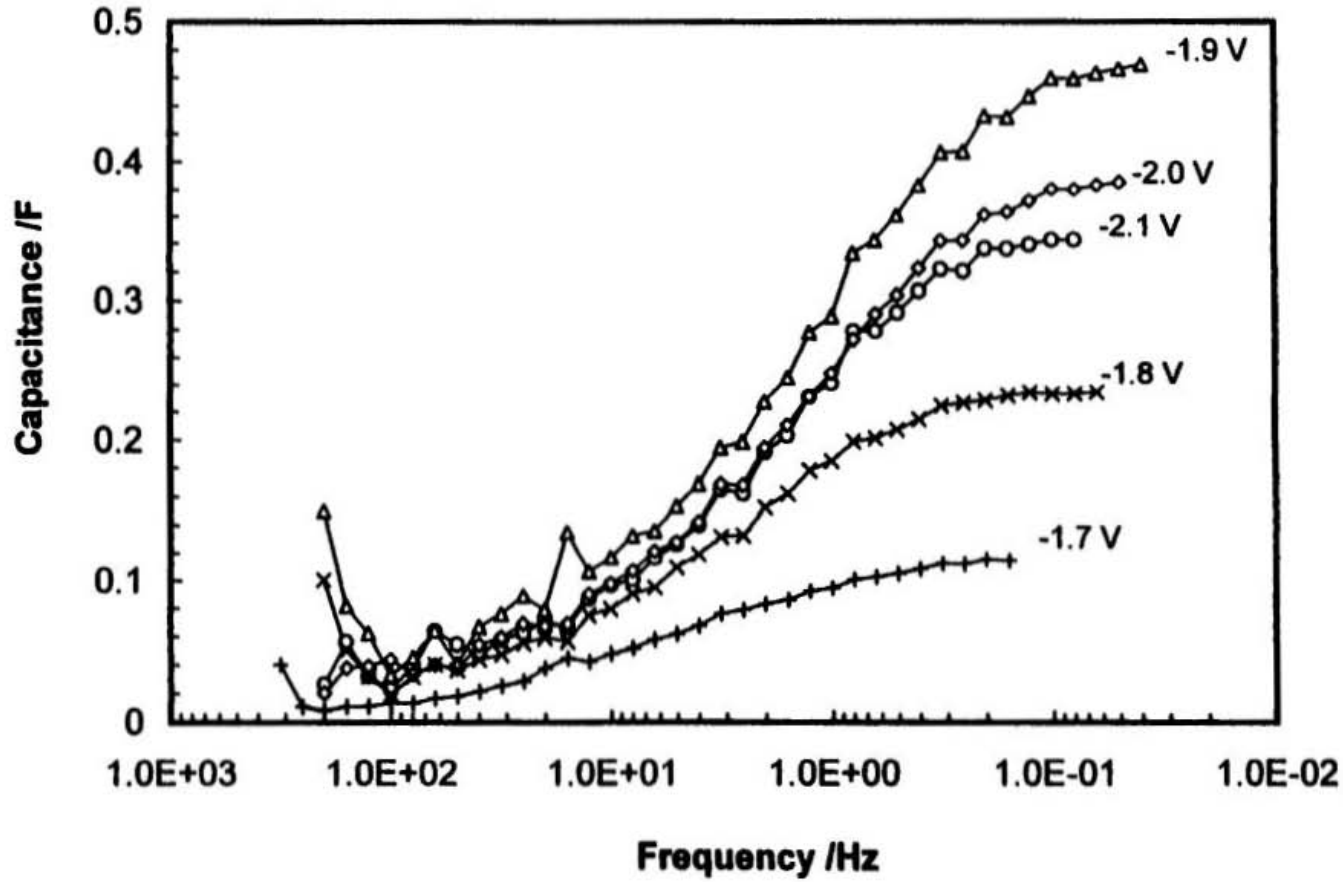

Fig. 8.9 c2 N-type capacitance of poly-PFPT (5 C/cm^2) in 1M $Me_4NCF_3SO_3$ acetonitrile solution

with potential are observed for the films doped with Et_4N^+ or Me_4N^+. The lowest ionic resistances for films doped with Et_4N^+ and Me_4N^+ are 3.85 and 3.33 Ω respectively, which are significantly lower than that for Bu_4N^+. In all cases the ionic conductivity for n-doping is lower than that for p-doping at the corresponding doping level. Comparison of the electronic resistances of the polymer electrodes when partially or lightly doped reveals the order: $Me_4N^+ > Et_4N^+ > Bu_4N^+$, the same order as the ionic resistances.

The maximum capacitance for the polymer doped with Me_4N^+ was obtained at -1.9 V as 0.469 F, which is slightly higher than that of the polymer doped with Et_4N^+ (0.430 F at -1.9 V), but much higher than that of the polymer doped with Bu_4N^+ (0.310 F at -2.0 V). At various potentials, the order of the capacitances is $Me_4N^+ > Et_4N^+ > Bu_4N^+$. From **Fig. 8.8a2**, **b2** and **c2**, most of the capacitance is available only when the frequency is less than 2 Hz.

8.4 Part II. Poly-PFPT grown using cyclic voltammetry with intervals between cycles (CV mode)

8.4.1 Poly-PFPT synthesized by CV mode

Poly-PFPT synthesized on carbon paper at constant current has been discussed extensively in section **8.3**. However, it has been found that the polymer synthesized by this technique is not distributed evenly throughout the carbon paper layer. This is attributed to hindrance of the diffusion of the monomer inside the carbon paper, making the polymer

prevalently grow on the surface layer, as observed by SEM. This is thought to lead to lower electronic conductivity and extra ionic transport resistance. To achieve polymer distributed evenly through the carbon paper, the technique of cyclic voltammetry with intervals between cycles (CV mode) was used in our later experiments. Several parameters, such as the length of the interval, the upper potential, and the sweep rate need to be optimized. In this preliminary work, the interval between cycles we adopted was 20s, which allows the diffusion of the monomer inside the carbon paper (thickness of 17mil). Suitable upper potentials for poly-PFPT growth are $1.15 \sim 1.25$ V, because at lower potentials (e.g. 1.10 V), no polymer growth occurs, when all charge is consumed for the doping of polymer, and at higher potentials (> 1.30 V), overoxidation of the polymer begins to occur, which is known to degrade on the properties of polymer. In our experiments, 1.20 V or 1.25 V was selected as the upper potential in most cases. The sweep rate was 20 mV/s. **Fig. 8.10** shows the CV mode waveform used.

Fig. 8. 11 shows a typical sequence of voltammograms for the electrogeneration of poly-PFPT on a carbon paper electrode (0.5 cm^2) from PFPT (0.05 M) in acetonitrile containing 1 M Et_4NPF_6. The upper potential was 1.25 V. The first cycle shows an electrochemically irreversible wave and the trace-crossing commonly observed in the first cycle during the synthesis of a conducting polymer. The cathodic current and anodic current at lower potentials, which increases progressively with the number of cycles, are due to the de-doping and doping of the polymer grown during the anodic processes at higher potentials. The synthesis charge for each cycle was obtained by subtracting the

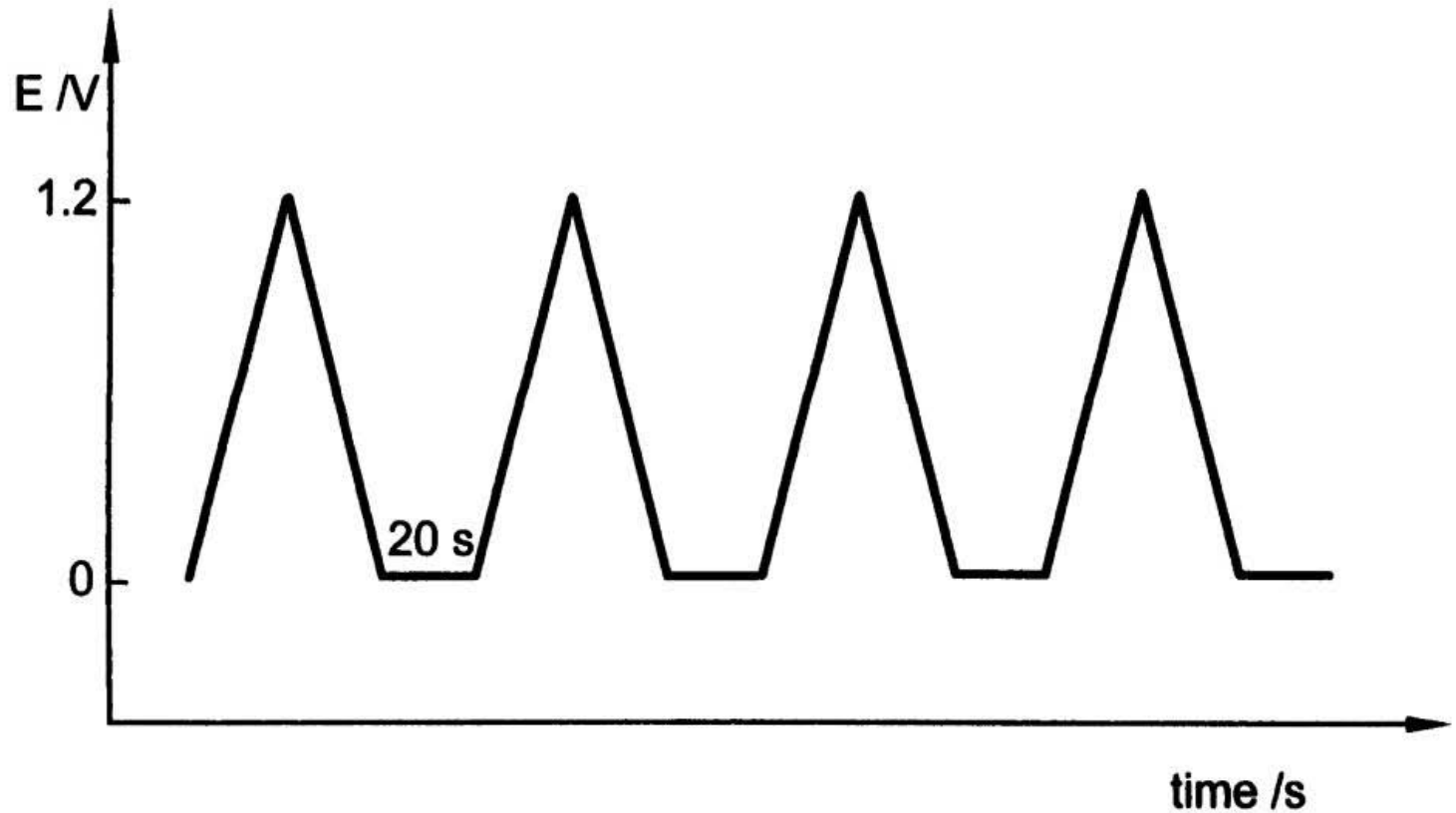

Fig. 8.10 Typical CV mode for the synthesis of poly-PFPT on carbon paper electrodes

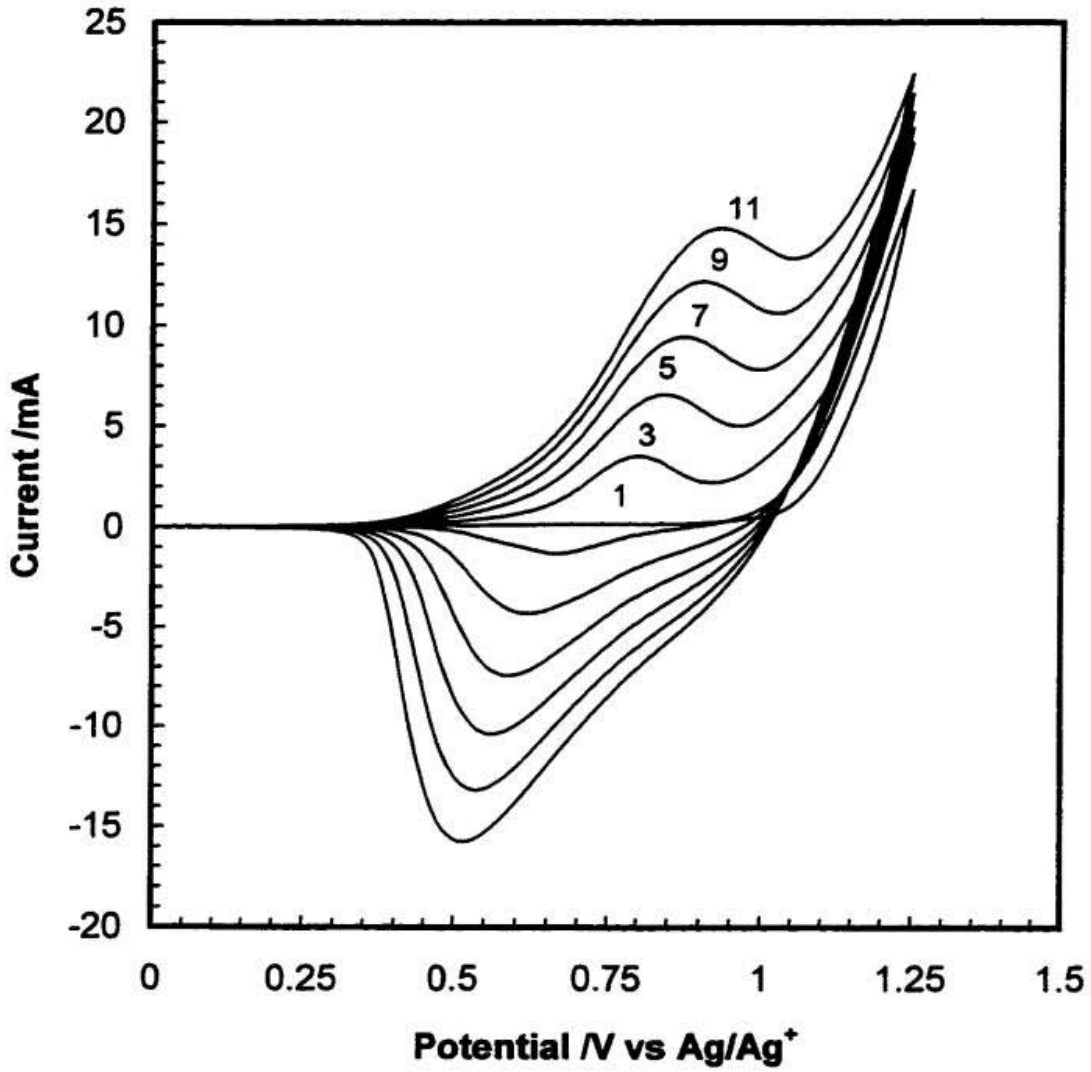

Fig. 8. 11 Typical cyclic voltammograms for poly-PFPT growth on carbon paper by CV mode

charge for doping from the total charge. After 11 cycles, 2592.7 mC, that is 5.19 C/cm^2, had been used for polymer growth. Synthesis charges of 5.1 to 5.3 C/cm^2 were typically used for polymer growth.

8.4.2 Stability test of the polymer synthesized by CV mode using different electrolytes

Fig. 8.12 (**a**), (**b**) and (**c**) are stability test results (n-dedoping charge vs. cyclic number) for the poly-PFPT carbon paper electrodes synthesized by CV mode in 0.05 M PFPT acetonitrile containing 1 M Et_4NBF_4, 1 M $Et_4NCF_3SO_3$, and 1 M Et_4NPF_6, respectively. The test was performed in 1M Et_4NBF_4 solution.

For the polymers synthesized with PF_6^- and $CF_3SO_3^-$, the initial increase in activity, which was observed when the polymers were synthesized at constant current, is absent in this case. But the initial increase of the activity is still observed when BF_4^- is used as the anion for CV synthesis, although this increase is not so significant as that for constant current synthesis. The maximum charges for BF_4^-, $CF_3SO_3^-$ and PF_6^- synthesized poly-PFPTs are 156.0, 168.2, and 183.1 mC respectively, and the decay rates of the activity are 6.44, 4.38, and 4.48 mC/100 cycles, respectively. After 1000 cycles, 58%, 67%, and 65% of the maximum charge is maintained for BF_4^-, $CF_3SO_3^-$, and PF_6^- respectively. The stability has been greatly improved compared to that obtained for constant current synthesis.

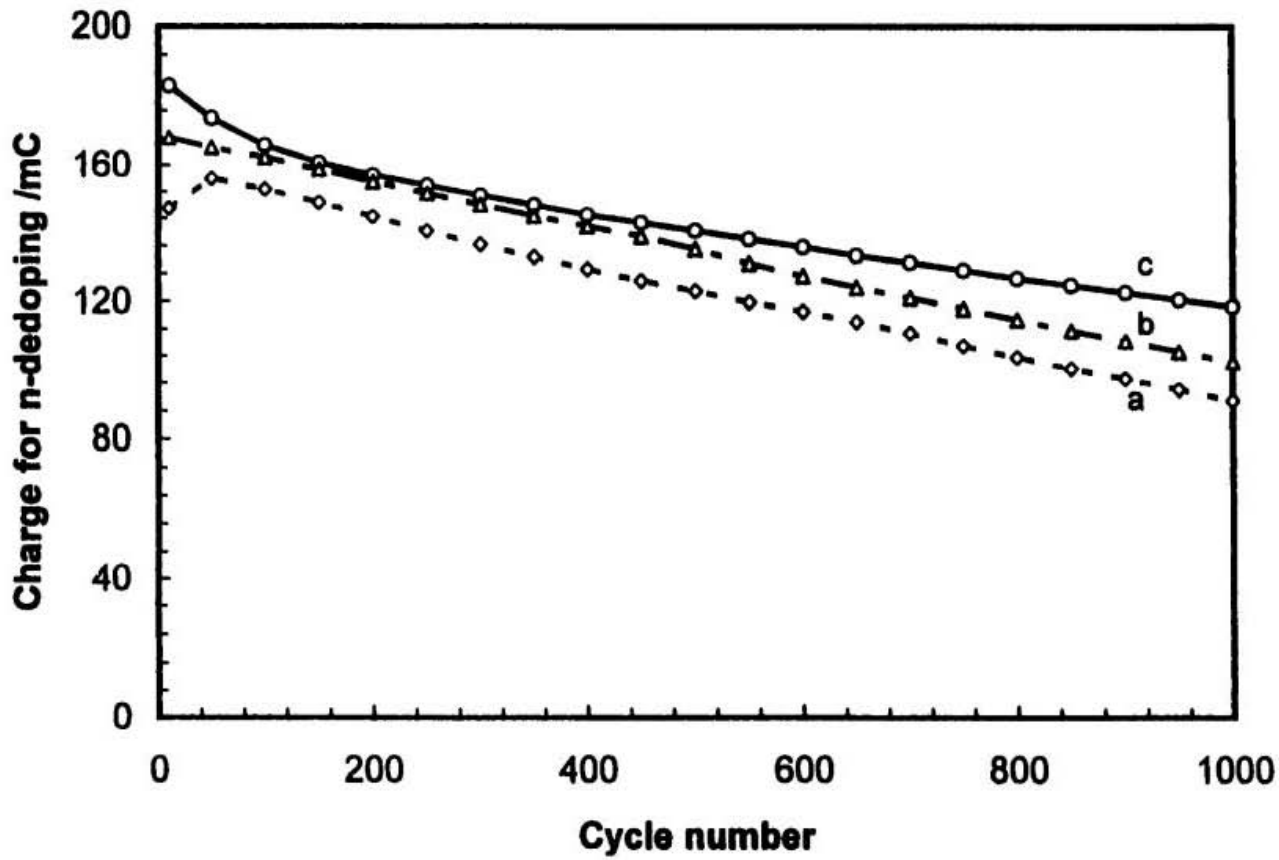

Fig. 8.12 N-type stability of poly-PFPT synthesized by CV mode in 0.05 M monomer/acetonitrile containing (a) 1 M Et_4NBF_4, (b) 1 M $Et_4NCF_3SO_3$, and (c) 1 M Et_4NPF_6

8.4.3 Impedance of the polymer synthesized by CV mode using different electrolytes

AC impedance spectra for poly-PFPT carbon paper electrodes synthesized by CV mode using Et_4NBF_4, $Et_4NCF_3SO_3$, and Et_4NPF_6 are shown in **Fig.8.13a1**, **Fig. 8.13b1** and **Fig. 8.13c1** respectively. The AC impedance measurements were performed in 1 M Et_4NBF_4. **Fig. 8.13a2**, **Fig. 8.13b2** and **Fig. 8.13c2** are the corresponding plots of capacitance vs. log(frequency). The ionic and electronic resistances and maximum capacitances are summarized in **Table 8.4.**

Table 8.4 Ionic and electronic resistances, and maximum capacitances for poly-PFPT synthesized by CV mode using different electrolytes for synthesis

	Synthesis with BF_4^-			Synthesis with $CF_3SO_3^-$			Synthesis with PF_6^-		
Potential /V	R_I /Ω	R_E /Ω	C_{max} /F	R_I /Ω	R_E /Ω	C_{max} /F	R_I /Ω	R_E /Ω	C_{max} /F
-2.1	7.77	low	0.248	7.70	low	0.228	7.14	low	0.240
-2.0	6.57	low	0.315	6.30	low	0.293	5.40	low	0.291
-1.9	5.28	<0.1	0.408	4.89	<0.1	0.426	4.17	low	0.416
-1.8	6.45	0.18	0.173	5.57	0.16	0.187	3.39	<0.1	0.325
-1.7	11.82	0.66	0.067	10.89	0.72	0.066	3.85	0.26	0.120
-1.6	high	1.03	0.024	high	1.45	0.022	9.74	1.05	0.051
-1.5	high	1.36	0.003	high	1.57	0.003	high	1.05	0.011

Of the three polymers that synthesized with PF_6^- shows the lowest ionic and electronic resistances. The polymer synthesized with BF_4^- has slightly higher ionic resistance but slightly lower electronic resistances than the polymer synthesized with $CF_3SO_3^-$. The capacitances obtained for the three polymers are all very close. Compared

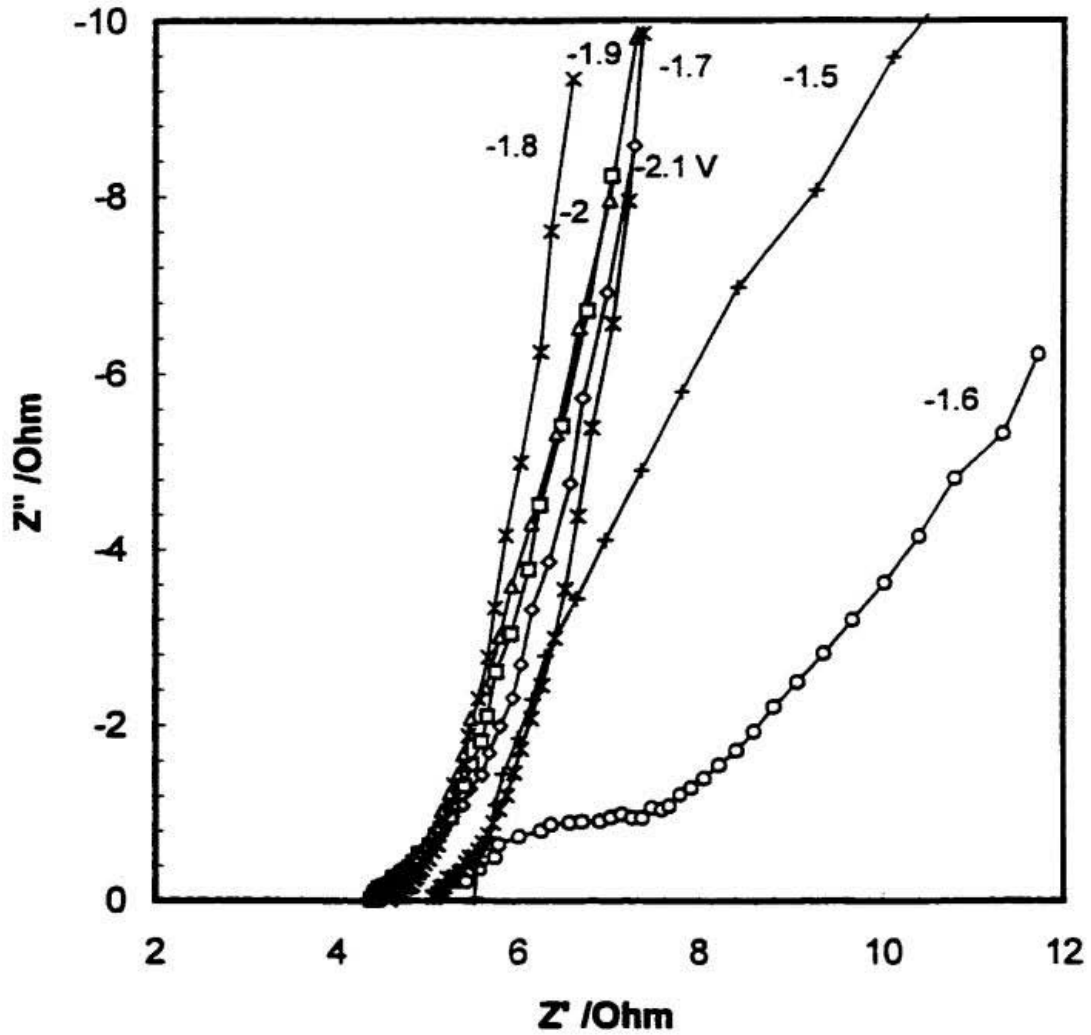

Fig 8. 13 a1 Impedance of n-doped poly-PFPT synthesized by CV mode in 1M Et_4NBF_4. Test in 1 M Et_4NBF_4

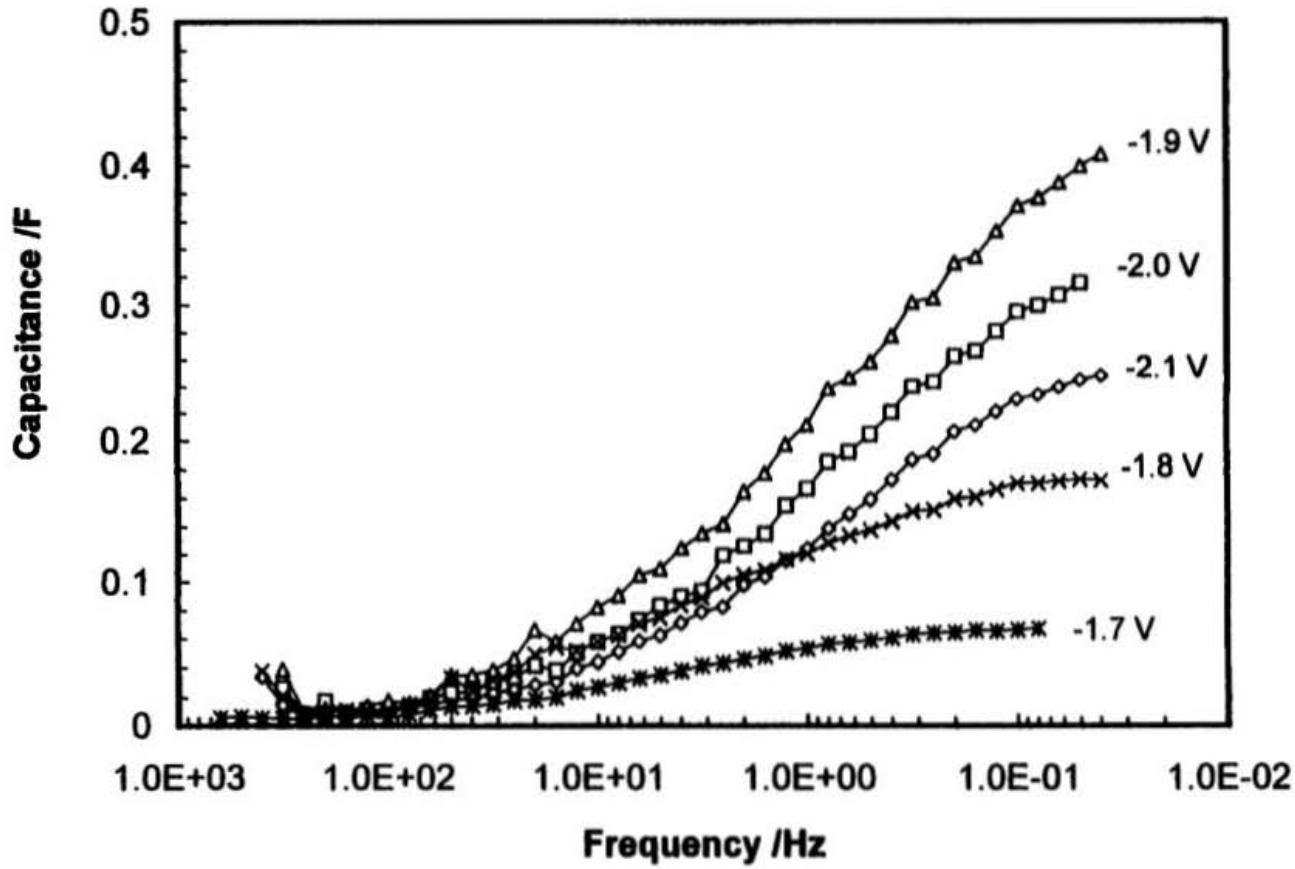

Fig. 8. 13 a2 N-type capacitance of poly-PFPT synthesized by CV mode in 1 M Et_4NBF_4. Test in 1M Et_4 NBF_4

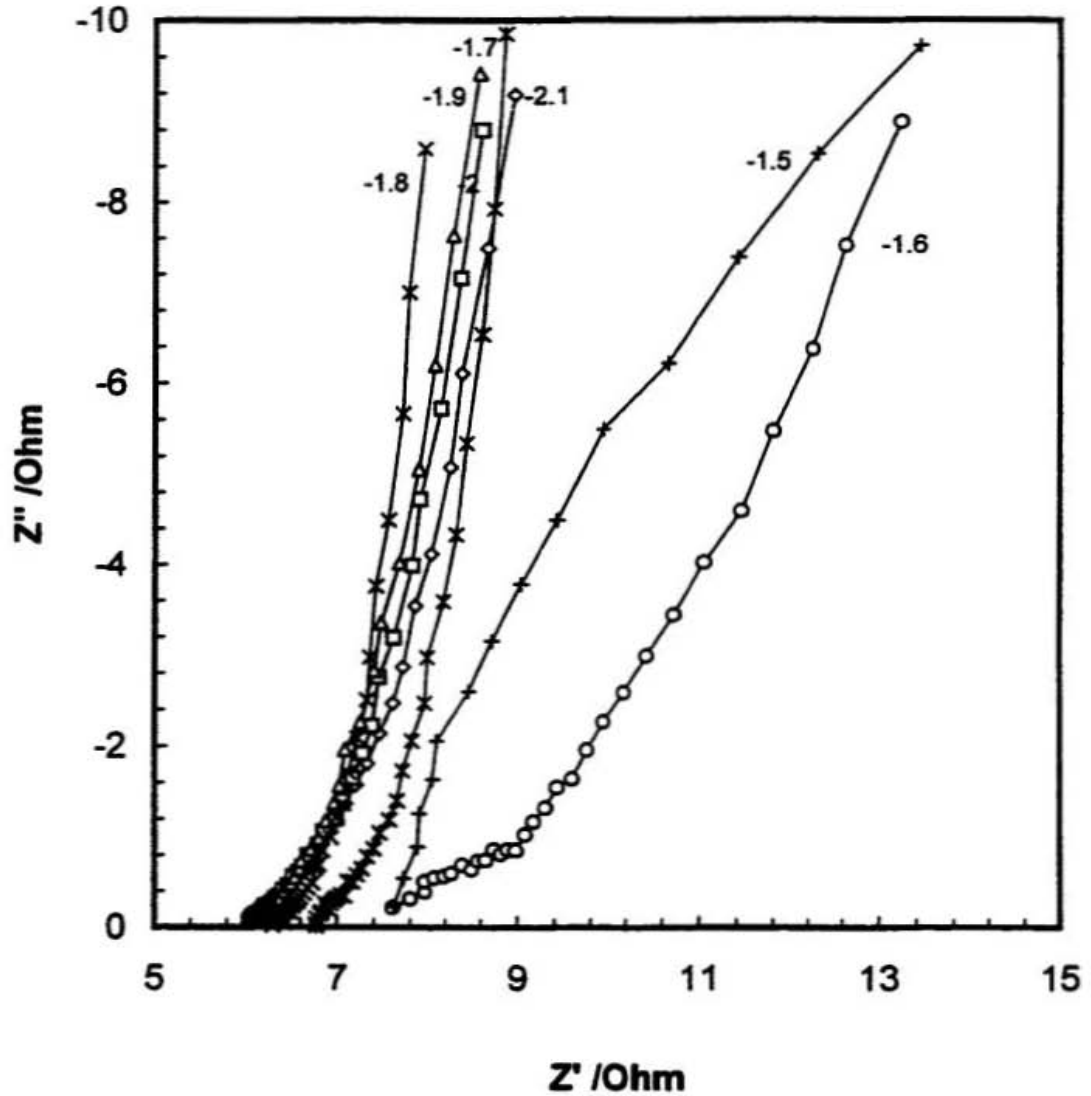

Fig. 8.13 b1 Impedance of n-doped poly-PFPT synthesized by CV mode in 1 M $Et_4NCF_3SO_3$. Test in 1 M Et_4NBF_4

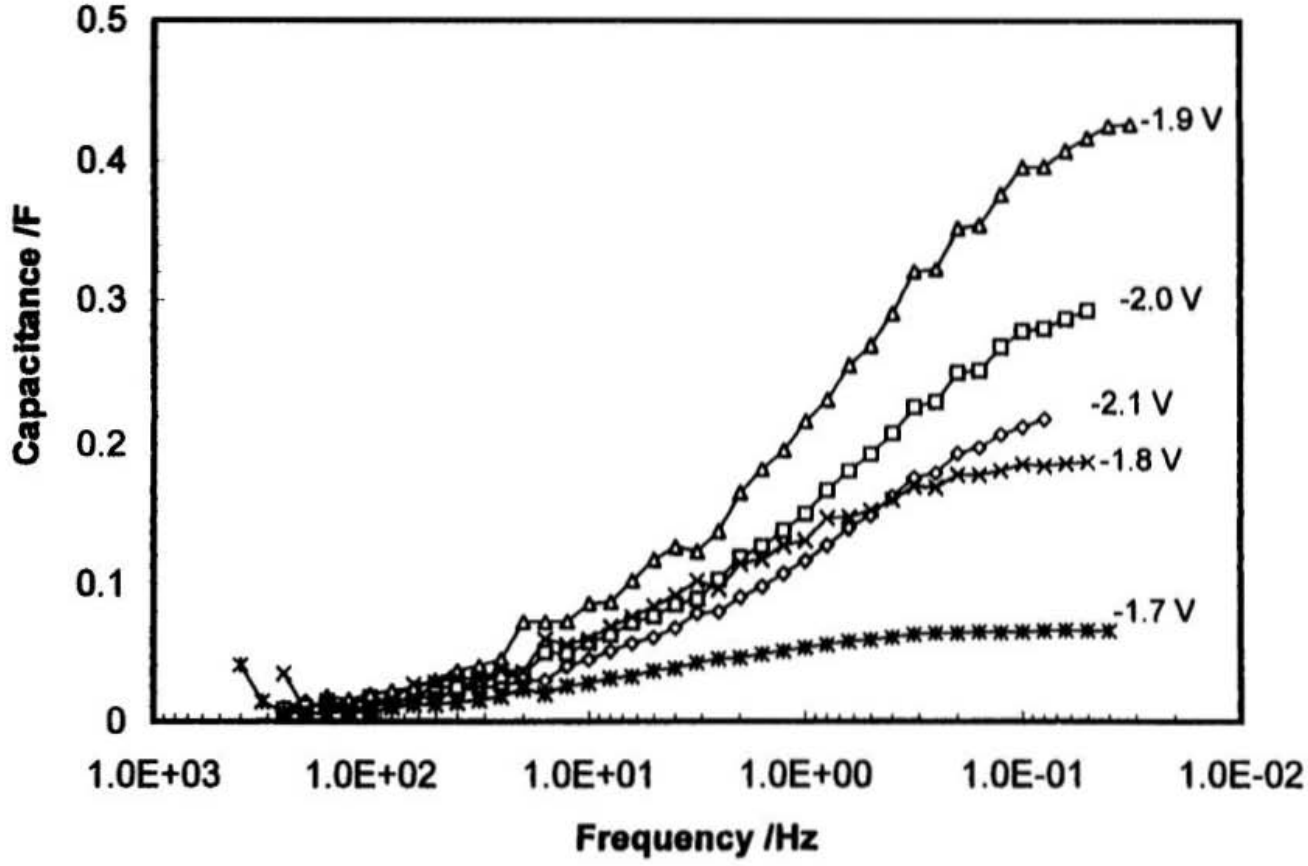

Fig. 8.13 b2 N-type capacitance of poly-PFPT synthesized by CV mode in 1 M $Et_4NCF_3SO_3$. Test in 1 M Et_4NBF_4

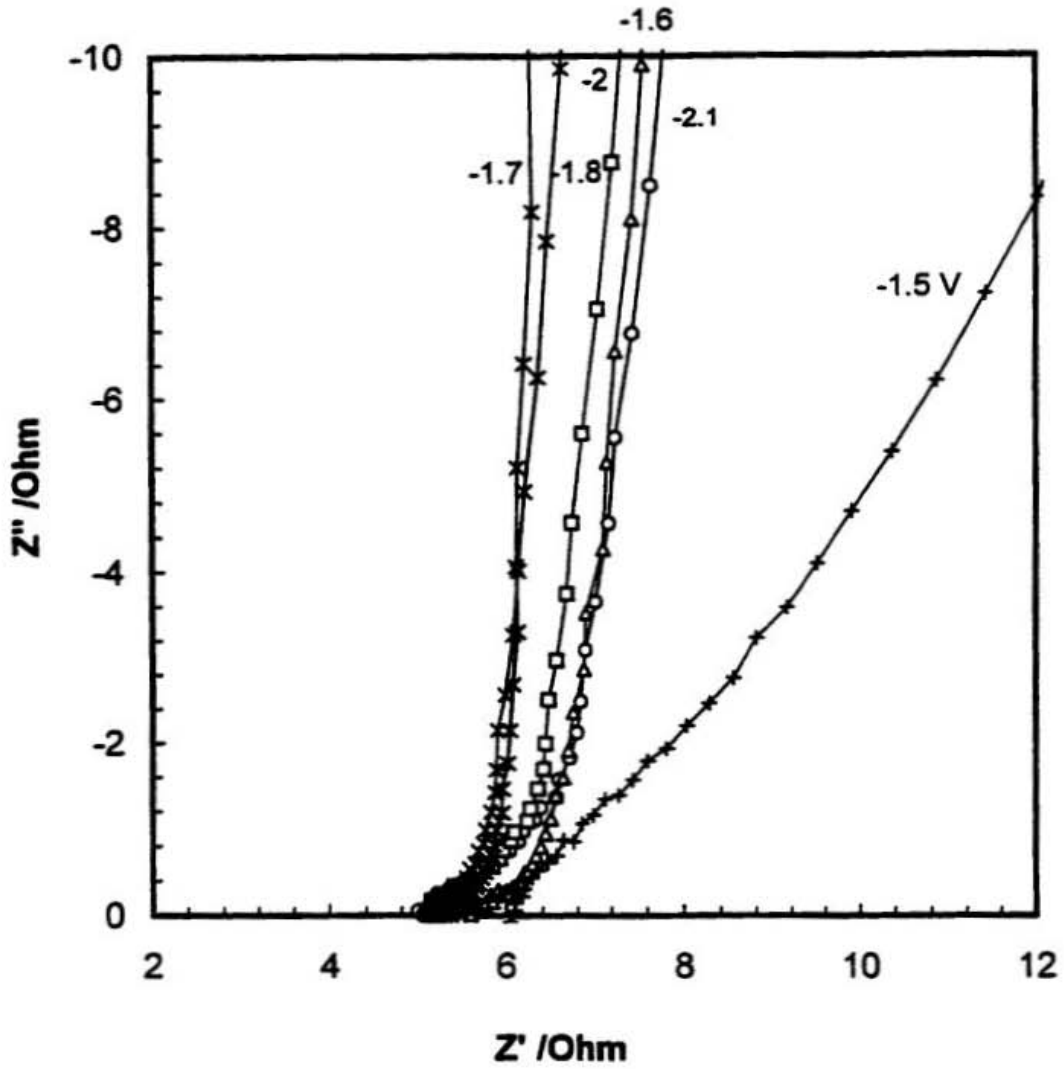

Fig.8.13 c1 Impedance of poly-PFPT synthesized by CV mode in 1 M Et_4NPF_6 acetonitrile solution. Test solution 1 M Et_4NBF_4 aceronitrile solution

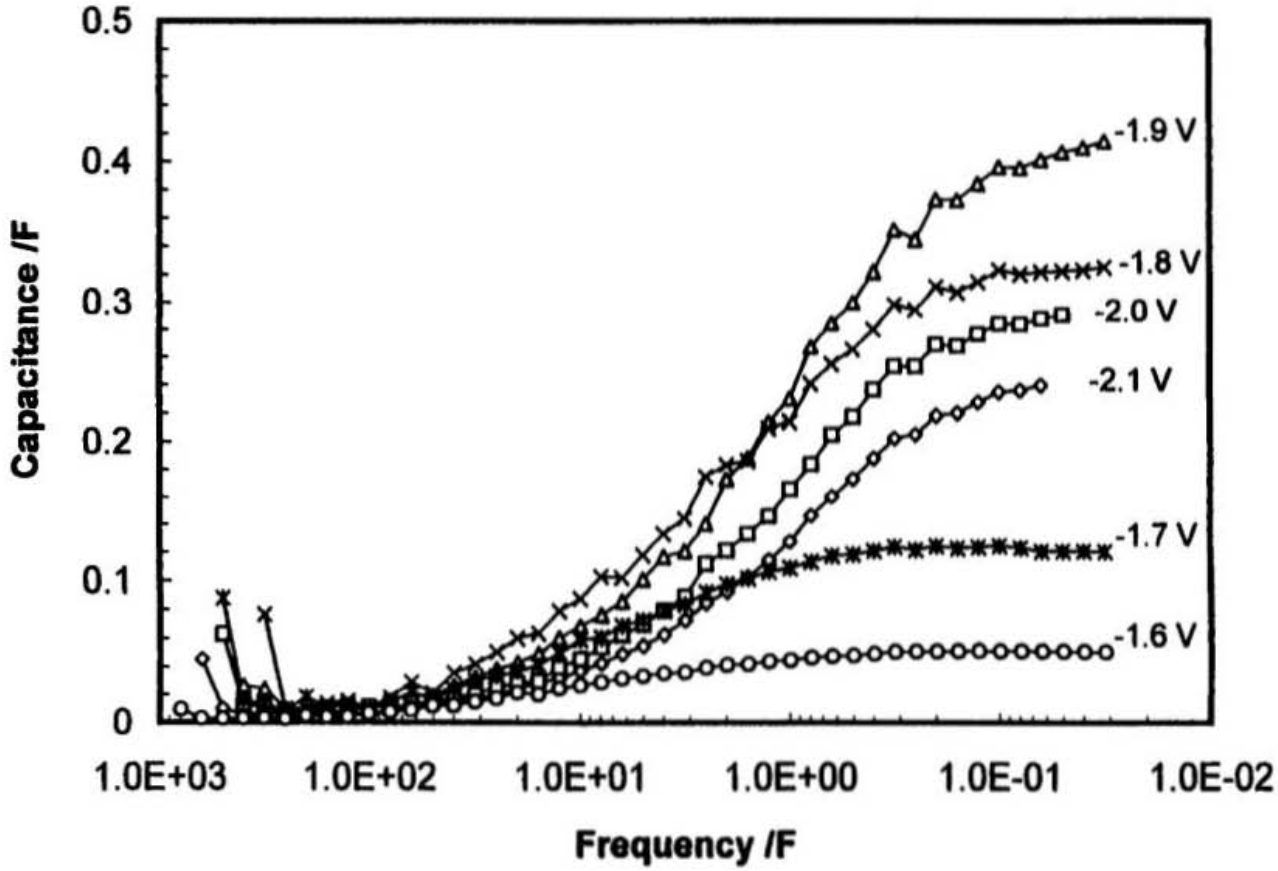

Fig. 8.13 c2 Capacitance of poly-PFPT synthesized by CV mode in 1 M Et_4NPF_6 acetronitrile solution. Test solution: 1 M Et_4NBF_4 acetonitrile solution

to the polymer synthesized at constant current with PF_6^-, the polymer synthesized by CV mode has the similar ionic conductivity, lower electronic conductivity, and slightly lower capacitance.

Fig. 8.14 a and **Fig. 8.14 b** show AC impedance spectra and a plot of capacitance vs log(frequency) after 1000 cycles for the polymer synthesized with PF_6^-. For convenience of the comparison of the polymer before and after 1000 cycles, the data are listed in **Table 8.5**.

Table 8.5 Comparison of ionic and electronic resistances and maximum capacitances of a poly-PFPT carbon paper electrode before and after 1000 cycles

	Synthesis with PF_6^-, before cycling			Synthesis with PF_6^-, after cycling		
Potential /V	R_I /Ω	R_E /Ω	C_{max} /F	R_I /Ω	R_E /Ω	C_{max} /F
-2.1	7.14	low	0.240	4.56	low	0.238
-2.0	5.40	low	0.291	4.79	<0.1	0.201
-1.9	4.17	low	0.416	4.66	0.18	0.251
-1.8	3.39	<0.1	0.325	5.38	0.33	0.167
-1.7	3.85	0.26	0.120	14.74	0.59	0.064
-1.6	9.74	1.05	0.051	high	0.90	0.022
-1.5	high	1.05	0.011	high	1.13	0.002

The above data shows that after 1000 cycles, the ionic resistance at very negative potentials (< -2.0 V) has decreased, but that it has increased at less negative potentials (≥ -1.9 V). The electronic resistance has also become larger. The highest capacitance

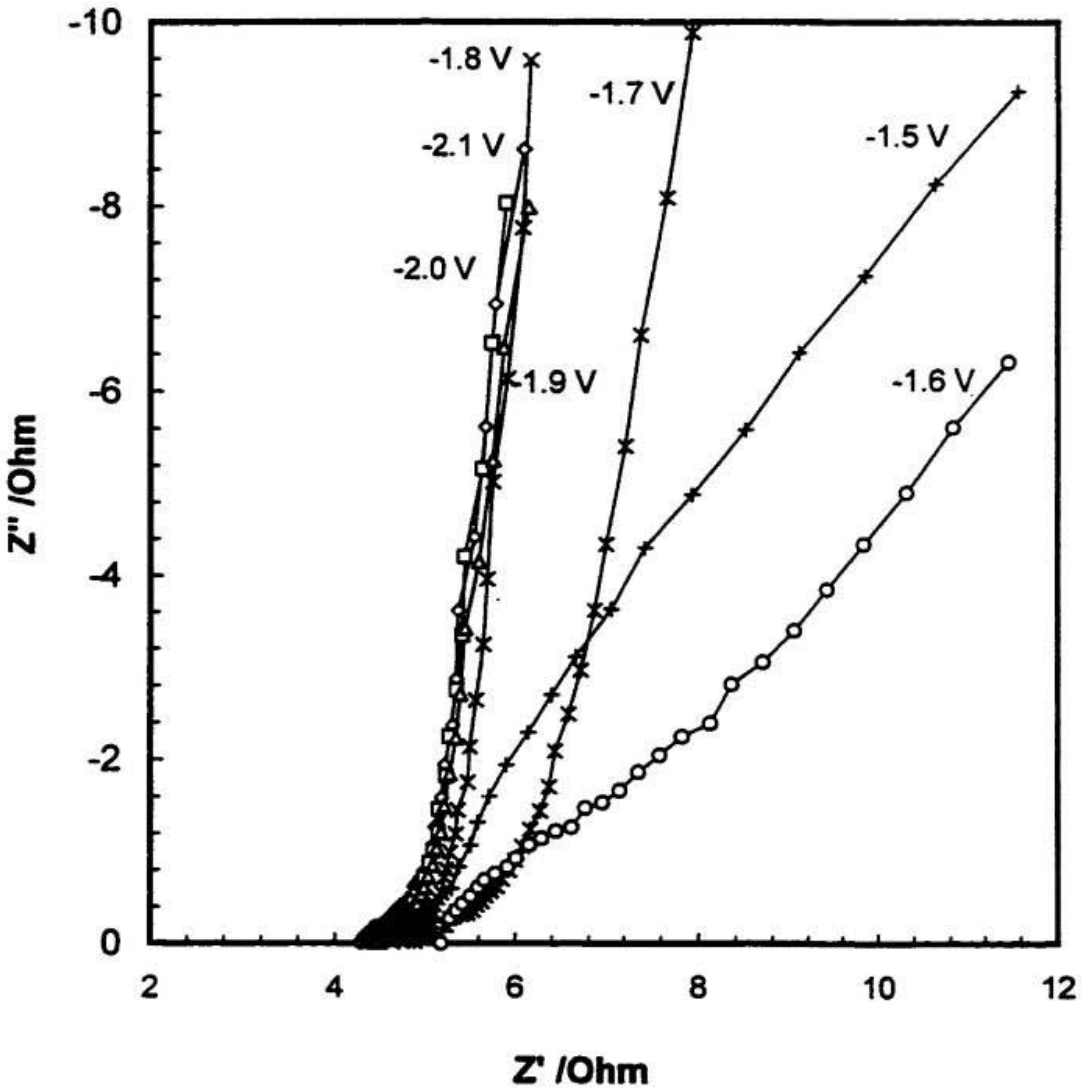

Fig. 8. 14a Impedance of poly-PFPT in 1 M Et_4NBF_4 acetonitrile solution after 1000 cycles

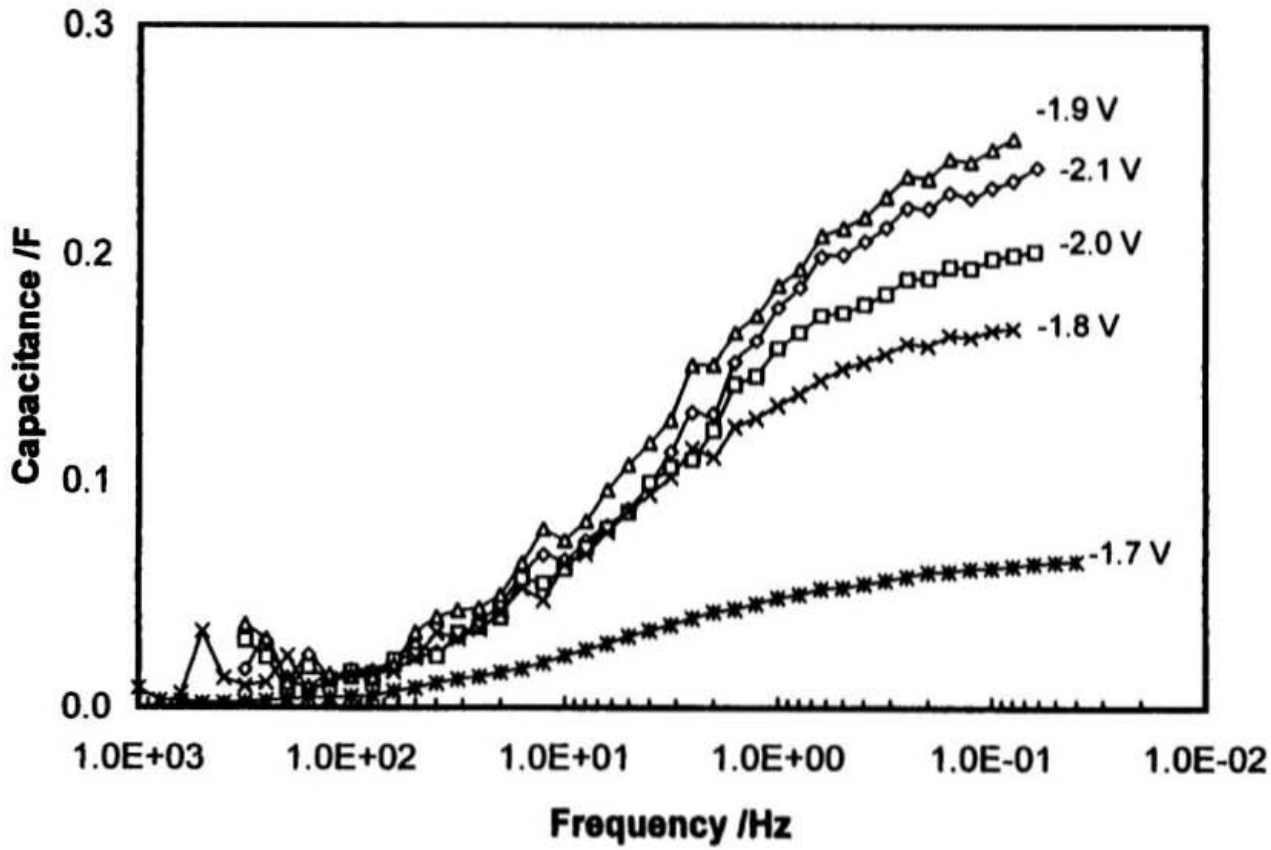

Fig. 8. 14 b N-type capacitance of poly-PFPT after 1000 cycles

obtained after 1000 cycles of deep charge/discharge is 0.251 F at -1.9 V, which is about 60% of the value before cycling, in agreement with the stability test results.

Conclusion

In our early experiments, the technique of constant current was employed to grow poly-PFPT on carbon paper electrodes. Different anions (PF_6^-, $CF_3SO_3^-$, and BF_4^-) have been used to study their effects on the p-doping performance of the polymer. Among these three p-doped polymers, the polymer doped with BF_4^- has the highest charge, the highest capacitance and the lowest ionic resistance, although the difference is not significant. After 1000 charge/discharge cycles. 79% of the initial charge is maintained for PF_6^-, 83% for $CF_3SO_3^-$, and 84% for BF_4^-.

The effect of cations on the n-type stability of poly-PFPT has been investigated using Bu_4N^+, Et_4N^+, and Me_4N^+. The n-doped polymer shows inferior stability compared to the p-doped polymer. After 1000 cycles, the percentages of the maximum charge that are maintained are 76%, 47%, and 27% for Bu_4N^+, Et_4N^+, and Me_4N^+ respectively. Although the polymer doped with Bu_4N^+ has the highest n-type stability, the charge involved is low, especially in the first 500 cycles. As expected, the ionic resistance increases with increasing the ionic size, that is, $Bu_4N^+ > Et_4N^+ > Me_4N^+$, while the capacitance is in the reverse order.

In order to improve n-doping stability of poly-PFPT, a CV mode (the technique of cyclic voltammetry with intervals between cycles) was applied to grow polymer in our later experiments. The n-type stability of the polymer synthesized by this technique has greatly

improved compared to that obtained for constant current synthesis. A polymer synthesized using Et_4NBF_4 maintains 58% of the maximum charge after 1000 cycles, while those synthesized using $Et_4NCF_3SO_3$ and Et_4NPF_6 maintains 67% and 65%, respectively. The later polymer exhibits the lowest electronic and ionic resistance. After 1000 cycles, the electronic resistance increases over the whole potential range studied, while the ionic resistance decreases in the potential range between -2.1 V and -1.9 V, but increases when potential is higher than -1.8 V.

Reference

[1] X. Andrieu and C. Rouverand, in *the 5th International Seminar on Double Layer Capacitors and Similar Energy Storage Devices*, S. P. Wolsky and N. Marincic, eds., Dec. 4-6, 1995.

[2] A. F. Burke, in *Proc. of the 36th power sources conference*, Cheery Hill, NJ, June 6-9, 1994, pp.6

[3] J. R. Miller, in *Electrochemical capacitors*, F. M. Delnick and M. Tomkiewitz, Eds., The Electrochemical Society Proc. Vol. 95-29, Pennington, NJ, 1996, pp. 246-254

[4] A. Anani, F. Eschabch, J. Howard, F. Malaspina, and V. Meadows, *Electrochim. Acta*, **40**, 211 (1995)

[5] J. R. Miller, in *the 5th International Seminar on Double Layer Capacitors and Similar Energy Storage Devices*, Deerfield Beach, FL, S. P. Wolsky and N. Marincic eds, Dec. 4-6, 1995.

[6] S. Nomoto, S. Nonaka, K. Nishida, M. Ikeda, A. Yoshida, and A. Nishino, in *Electrochemical Capacitors*, F. M. Delnick, D. Ingersoll, X. Andrieu, and K. Naoi, eds, The Electrochemical Society Proc. Vol. 96-25, Pennington, NJ, 1997, pp. 268-279

[7] D. A. Evans and J. R. Miller, in *Electrochemical Capacitors*, F. M. Delnick, D. Ingersoll, X. Andrieu, and K. Naoi eds, The Electrochemical Society Proc. Vol. 96-25, Pennington, NJ, 1997, pp. 253-257

[8] C. J. Farahmandi, in *the 3rd International Seminar on Double Layer Capacitors and Similar Energy Storage Devices*, Deerfield Beach, FL, 1993.

[9] T. Morimoto, M. Suhara, K. Hiratsuka, Y. Sanada, M. Tsushima, and T. Kawasato, in *Electrochemical Capacitors*, F. M. Delnick, D. Ingersoll, X. Andrieu, and K. Naoi eds, The Electrochemical Society Proc. Vol.96-25, Pennington, NJ, 1997, pp. 138-152

[11] A. Yoshida, K. Imoto, H. Yoneda, and A. Nishino, *IEEE Trans. Comput., Hybrids, Manuf. Technol.*, **15**, 133 (1992)

[12] S. M. Lipka, *IEEE AES Systems Magazine*, 27, July 1997

[13] A. Yoshida, S. Nonaka, I. Aoki, and A. Nishino, *J. Power Source*, **60**, 213 (1996)

[14] Y. Kibi, T. Saito, M. Kurata, J. Tabuchi, and A. Ochi, *J. Power Source*, **60**, 219 (1996)

[15] S. M. Lipka, in *Electrochemical Capacitors*, F. M. Delnick, D. Ingersoll, X. Andrieu, and K. Naoi eds, The Electrochemical Society Proc. Vol. 96-25, Pennington, NJ, 1997, pp. 244-252

[16] I. Tanahashi, A. Yoshida, and A. Nishino, *Carbon*, **29**, 1033 (1991)

[17] M. Waidhas and K. Mund, in *Electrochemical Capacitors*, F. M. Delnick, D. Ingersoll, X. Andrieu, and K. Naoi eds, The Electrochemical Society Proc. Vol. 96-25, Pennington, NJ, 1997, pp. 180-191

[18] M. G. Sullivan, M. Bartsch, R. Kotz, and O. Haas, in *Electrochemical Capacitors*, F. M. Delnick, D. Ingersoll, X. Andrieu, and K. Naoi eds, The Electrochemical Society Proc. Vol. 96-25, Pennington, NJ, 1997, pp. 192-201

[19] X. Andrieu, L. Josset, and B. Pichou, in *Electrochemical Capacitors*, F. M. Delnick, D. Ingersoll, X. Andrieu, and K. Naoi eds, The Electrochemical Society Proc. Vol. 96-25, Pennington, NJ, 1997, pp. 202-206

[20] X. Andrieu and L. Josset, in *Electrochemical Capacitors*, F. M. Delnick, T. Tomkiewicz, eds, The Electrochemical Society Proc. Vol. 95-29, Pennington, NJ, 1996, p.181

[21] S. M. Lipka, in *the 7th International Seminar on Double Layer Capacitors and Similar Energy Storage Devices*, Deerfield Beach, FL, S. P. Wolsky and N. Marincic eds, Dec. 4-6, 1997

[22] C. Niu, E. K. Sichel, R. Hoch, D. Moy, and H. Tennent, *Appl. Phys. Lett.*, **70**, 1480 (1997)

[23] M. Goodwin, in *the 5th International Seminar on Double Layer Capacitors and Similar Energy Storage Devices*, Deerfield Beach, FL, S. P. Wolsky and N. Marincic eds, Dec. 4-6, 1995

[24] D. Fianello, in *the 5th International Seminar on Double Layer Capacitors and Similar Energy Storage Devices*, Deerfield Beach, FL, S. P. Wolsky and N. Marincic eds, Dec. 4-6, 1995

[25] M. Wixom, L. Owens, J. Parker, J. Lee, and I. Song, in *Electrochemical Capacitors*, F. M. Delnick, D. Ingersoll, X. Andrieu, and K. Naoi eds, The Electrochemical Society Proc. Vol. 96-25, Pennington, NJ, 1997, pp. 63-74

[26] C. Z. Deng and K. C. Tsai, in *Electrochemical Capacitors*, F. M. Delnick, D. Ingersoll, X. Andrieu, and K. Naoi eds, The Electrochemical Society Proc. Vol. 96-25, Pennington, NJ, 1997, pp. 75-84

[27] J. P. Zheng and T. R. Jow, *J. Power Source*, **62**, 155 (1996)

[28] J. P. Zheng, P. J. Cygen, and T. R. Jow, *J. Electrochem. Soc.*, **142**, 2699 (1995)

[29] G. Mondio, F. Neri, M. Allegrini, A. Lembo, and F. Fuso, *J. Appl. Phys.*, **82**, 1730, 1997

[30] S. Trasatti and P. Kurzweil, *Plat. Met. Rev.*, **38**, 46 (1994)

[31] J. P. Zheng and T. R. Jow, *J. Electrochem. Soc.*, **142**, L6 (1995)

[32] S. Sarangapani, B. V. Tilak, and C.-P. Chen, *J. Electrochem. Soc.*, **143**, 3791 (1996)

[33] R. H. Baughman, *Makromol. Chem., Macromol. Symp.*, **51**, 193 (1991)

[34] S. Panero, E. Spila, and B. Scrosati, *J. Electroanal. Chem.*, **396**, 385 (1995)

[35] A. Rudge, J. Davey, I. Raistrick, S. Gottesfeld, and J. P. Ferraris, *J. Power Sources*, **47**, 87 (1994)

[36] Ya. L. Kogan, G. V. Gefrouch, M. I. Rudakova, and L. S. Fokeeva, *Russ. J. Electrochem.*, **31**, 750 (1995)

[37] S.-C. Huang, S.-M.Huang, H. NG, and R. B. Kaner, *Synth. Met.*, **55**, 4047 (1993)

[38] A. Rudge, J. Davey, F. Urike, J. Landeros Jr., and S. Gottesfeld, in *Proc. 3 Int. Seminar on Double-Layer Capacitors and Similar Energy Storage Devices*, Deerfield Beach, Florida, December 6-8, 1993

[39] J. C. Carlberg and O. Inganas, *J. Electrochem. Soc.*, **144**, L61 (1997)

[40] D. Naegele, *Electronic Properties of Conjugated Polymers* III, eds, H. Kuzmany, H. Mechring, and S. Roth, Berlin: Springor-Verlag, pp.428-431 (1989)

[41] M. S. Wrighton, H. S. White, and J. W. Thackeray, US Patent 4, 417, 673

[42] C. Arbizzani, M. Mastragostino, L. Meneghello, and R. Paraventi, *Adv. Mater.*, **8**, 331 (1996)

[43] A. Rudge, I. Raistrick, S. Gottesfeld, and J. Ferraris, *Electrochim. Acta*, **39**, 273 (1994)

[44] C. Arbizzani, M. Catellani, M. Mastragostino, and C. Mingazzini, *Electrochim. Acta*, **40**, 1871 (1995)

[45] C. Arbizzani, M. Mastragotino, and L. Meneghello, *Electrochim. Acta*, **40**, 2223 (1995)

[46] X. Ren, S. Gottesfeld, and J. P. Ferraris, in *Electrochemical capacitors*, F. M. Delnick and M. Tomkiewitz, Eds., The Electrochemical Society Proc. Vol. 95-29, Pennington, NJ, 1996, pp. 138-161

[47] K. Tamao, S. Kodama, I. Nakajima, and M. Kumada, *Tetrahedron*, **38**, 3347 (1982)

[48] P. G. Pickup, *J. Chem. Soc., Faraday Trans.*, **86**, 3631 (1990)

[49] J. Bobacka, M. Grzeszczuk, and A. Ivaska, *Electrochim. Acta*, **37** ,1759, 1992

[50] J. Tanguy, M. Slama, M. Hoalet, and J. L. Baudouin, *Synth. Met.*, **28**, c145 (1989)

[51] C. Gabrielli, H. Takenouti, O. Haas, and A. Tsukada, *J. Electroanal. Chem.*, **302**, 59 (1991)

[52] D. J. Guerrero, X. Ren, and J. P. Ferraris, *Chem. Mater.*, **6**, 1437 (1994)

[53] J. Bobacka, A. Ivaska, and M. Grzeszcauk, *Synth. Met.*, **44**, 21 (1991)

[54] S. Sunde, G. Hagen, and R. Φdegard, *Synth. Met.*, **55-57**, 1584 (1993)

[55] M. M. Musiani, *Electrochim. Acta*, **35**, 1665 (1990)

[56] Z. Gao, J. Bobacka, and A. Ivaska, *J. Electroanal. Chem.*, **364**, 127 (1994)

[57] P. G. Pickup, *Electrochemistry of Electronically Conducting Polymer Films*, in: *Modern Aspects of Electrochemistry* , 1997

[58] G. Schiavon, S. Sitran, and G. Zotti, *Synth. Met.*, **32**, 209 (1989)

[59] K. Wilbourn and R. W. Murray, *J. Phys. Chem.*, **92**, 3642 (1988)

[60] D. Ofer and M. S. Wrighton, *J. Am. Chem. Soc.*, **110**, 4467 (1988)

IMAGE EVALUATION
TEST TARGET (QA-3)

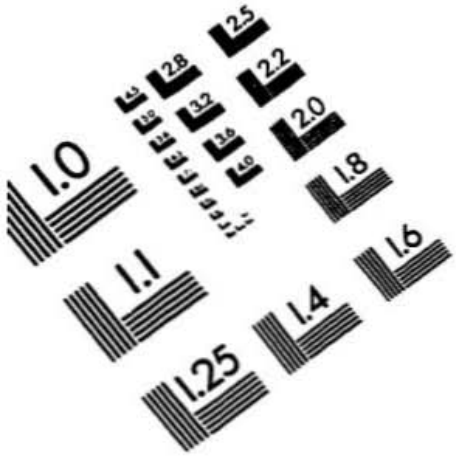

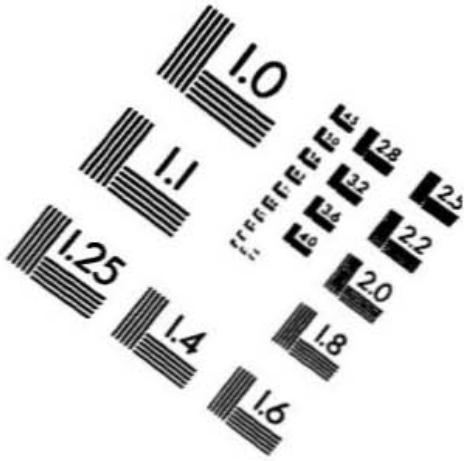

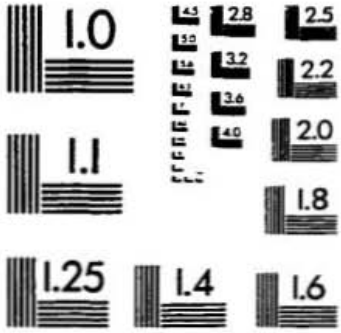

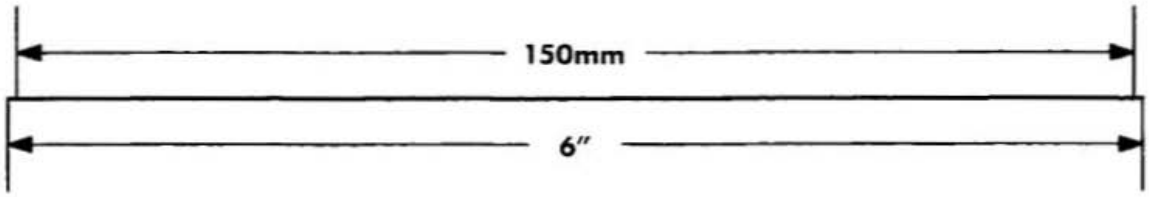

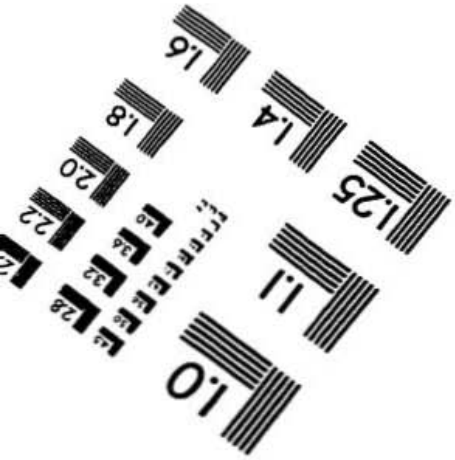

APPLIED IMAGE, Inc
1653 East Main Street
Rochester, NY 14609 USA
Phone: 716/482-0300
Fax: 716/288-5989